University of Alberta

The Foundation for Protein Targeting to Promote the Regeneration of Bone

by

Sébastien Anderson Gittens

A thesis submitted to the Faculty of Graduate Studies and Research in partial fulfillment of the requirements for the degree of *Doctor of Philosophy*

in

Pharmaceutical Sciences

Faculty of *Pharmacy and Pharmaceutical Sciences*
Medical Sciences - Biomedical Engineering

Edmonton, Alberta

Fall, 2004

Library and Archives Canada

Published Heritage Branch

395 Wellington Street
Ottawa ON K1A 0N4
Canada

Bibliothèque et Archives Canada

Direction du Patrimoine de l'édition

395, rue Wellington
Ottawa ON K1A 0N4
Canada

Your file Votre référence
ISBN: 0-612-95937-6
Our file Notre référence
ISBN: 0-612-95937-6

The author has granted a non-exclusive license allowing the Library and Archives Canada to reproduce, loan, distribute or sell copies of this thesis in microform, paper or electronic formats.

L'auteur a accordé une licence non exclusive permettant à la Bibliothèque et Archives Canada de reproduire, prêter, distribuer ou vendre des copies de cette thèse sous la forme de microfiche/film, de reproduction sur papier ou sur format électronique.

The author retains ownership of the copyright in this thesis. Neither the thesis nor substantial extracts from it may be printed or otherwise reproduced without the author's permission.

L'auteur conserve la propriété du droit d'auteur qui protège cette thèse. Ni la thèse ni des extraits substantiels de celle-ci ne doivent être imprimés ou aturement reproduits sans son autorisation.

In compliance with the Canadian Privacy Act some supporting forms may have been removed from this thesis.

Conformément à la loi canadienne sur la protection de la vie privée, quelques formulaires secondaires ont été enlevés de cette thèse.

While these forms may be included in the document page count, their removal does not represent any loss of content from the thesis.

Bien que ces formulaires aient inclus dans la pagination, il n'y aura aucun contenu manquant.

Canada

DEDICATION

This thesis is dedicated to:

My parents-- for their unwavering support throughout this entire process.

My supervisor, Dr. Hasan Uludag-- for his advice, generosity and patience.

My fiancée, Ms. C. R. Tomkinson-- for her companionship and perpetual encouragement.

My colleagues in the Uludag group, especially: Mr. A. Jalil, Ms. E. Smith, Dr. G. Bansal, Dr. G. Wohl, Dr. J. Bai.

ACKNOWLEDGMENTS

This work was financially supported by a Biomedical Engineering Grant from the Whitaker Foundation, an Operating Grant from the Canadian Institutes of Health Research and Infrastructure Grants from the Alberta Heritage Foundation for Medical Research and the Canadian Foundation for Innovation. Personally, I was primarily funded by an Izaak Walton Killam Memorial Scholarship provided by the U. of Alberta and the Killam Trust. Synthesis of the 1-amino-1,1-diphosphonate methane (i.e. aminoBP) used throughout these studies was made by Mr. L. Alverado. The Pro-Osteon 200HA® implants used were kindly donated by Dr. M. Borden from Interpore Cross International (Irvine, CA). Molecular Dynamics simulations found in **Chapter III** were performed by Dr. P. Kitov (Department of Chemistry, University of Alberta), while the micro-computed tomography data used in **Chapter VI** was collected by Dr. G. R. Wohl (Department of Chemical Engineering, University of Alberta).

Table of Contents

1. **SCOPE OF THESIS DISSERTATION** 1

2. **CHAPTER I**- Introduction to Bone Biology and the Need for Bone Targeting 6

2.1 Basic Biology of Bone Formation and Repair 7

2.2.1 Formation of Long Bones 8

2.2.2 Maintenance of Bone Integrity 9

2.2.3 Bone Remodeling 10

2.3 Osteoporosis 11

2.4 Systemic Bone Regeneration 13

2.5 Drug Targeting to Skeletal Tissue 14

2.6 Osteotropic Moieties for Drug Targeting to Bone 15

2.6.1 Conjugation of Non-BP Moieties for Drug Targeting to Bone 15

2.6.2 BP Conjugation for Drug Targeting to Bone 16

2.6.2.1 BP-steroid conjugates 17

2.6.2.2 BP-radioisotope conjugates 17

2.6.2.3 BP-anti-neoplastic conjugates 18

2.6.2.4 BP-protein conjugates 19

2.7 References 23

3. **CHAPTER II**- Imparting Bone Affinity onto Glycoproteins through the Conjugation of Bisphosphonates 36

3.1 Introduction 37

3.2 Materials and Methods 39

3.3 Results 34

3.4 Discussion and Conclusions. 39

3.5 References 63

4. **CHAPTER III**- Impact of Tether Length on Bone Mineral Affinity of Protein-Bisphosphonate Conjugates 68
   - **4.1** Introduction 69
   - **4.2** Materials and Methods 70
   - **4.3** Results 76
   - **4.4** Discussion and Conclusions 80
   - **4.5** References 92

5. **CHAPTER IV**-Assessing the Bone Mineral Affinity of Fetuin-Bisphosphonate Conjugates *In Vivo* 96
   - **5.1** Introduction 97
   - **5.2** Materials and Methods 99
   - **5.3** Results 107
   - **5.4** Discussion 111
   - **5.5** Conclusions 119
   - **5.6** References 130

6. **CHAPTER V**- Imparting Bone Mineral Affinity to Osteogenic Proteins through Heparin-Bisphosphonate Conjugates. 135
   - **6.1** Introduction 136
   - **6.2** Materials and Methods 138
   - **6.3** Results 143
   - **6.4** Discussion 147
   - **6.5** Conclusions 151
   - **6.6** References 161

7. **CHAPTER VI**- Systemic Bone Formation with Weekly PTH Administration in Ovariectomized Rats. 168
   - **7.1** Introduction 169
   - **7.2** Materials and Methods 170
   - **7.3** Results 175

7.4 Discussion 179

7.5 References 191

8. CHAPTER VI- Systemic Administration of Vascular Endothelial Growth Factor and Basic Fibroblast Growth Factor in Ovariectomized Rats. 196

8.1 Introduction 197

8.2 Materials and Methods 198

8.3 Results 203

8.4 Discussion 205

8.5 Conclusions 209

8.6 References 214

9. GENERAL DISCUSSION & FUTURE STUDIES 220

9.1 References 228

10. APPENDICES 225

10.1- Appendix A- Protein-Based Therapeutic Agents that Can Potentially Be Targeted for Diseases Affecting Bone. 226

10.1.1 Osteoporosis. 232

10.1.2 Multiple Myeloma. 233

10.1.3 Bone Metastasis 234

10.1.4 Rheumatoid Arthritis 234

10.1.5 References 240

10.2- Appendix B- Modulating Threshold on Architectural Parameter Quantification of Trabecular Bone. 255

10.2.1 Effect of Threshold on Osteopenic Bone 255

10.2.2 Effect of Threshold on Normal Bone 257

10.2.3 Comparing the Effect of Threshold on Normal and Osteopenic Bone 257

10.2.4 Analysis of the Data Using a Threshold of 214 and Subsequent Comparison to Results Generated Using a Threshold of 211 261

List of Tables

1. Protein-Based Therapeutic Agents for Treatment of Osteoporosis 21
2. Study Summary of Conjugate Targeting upon Parenteral Administration 121
3. Urinary and Blood Analysis 6, 24 and 48 h post-IV administration of aminoBP-fetuin conjugates. 127
4. Urinary and Blood Analysis 72 and 144 h post-IV administration of aminoBP-fetuin conjugates 129
5. Body and Uterus Weight, and Serum Biochemical Analysis of Bone Formation Parameters. 210
6. 3-dimensional morphometric parameters from micro-CT of the distal femora of OVX rats administered vehicle, bFGF, or VEGF 213
7. Protein-Based Therapeutic Agents for Treatment of Multiple Myeloma 236
8. Protein-Based Therapeutic Agents for Treatment of Bone Metastasis 237
9. Protein-Based Therapeutic Agents for Treatment of Rheumatoid Arthritis 238

List of Figures

1. Structures of molecules shown to exhibit a significant affinity for bone mineral 22

2. A schematic representation of the SMCC and MMCCH mediated conjugation of aminoBP onto fetuin 56

3. The conjugation efficiency and HA binding for SMCC-based fetuin conjugates 57

4. The relationship between the number of aldehyde groups introduced onto fetuin and the sodium periodate concentrations used for fetuin oxidation 58

5. The conjugation efficiency and HA binding for MMCCH-based fetuin conjugates 59

6. Correlation between the number of aminoBP's conjugated per fetuin and the conjugate binding to HA 60

7. The stability of the SMCC- and MMCCH-conjugates as a function of HA binding in 25% adult bovine serum 61

8. Binding of SMCC- and MMCCH-conjugates to various bone matrices in 50% bovine adult serum 62

9. A representation of the MANS-, MBNS-, SMCC-, LC-SMCC-, and NHS-PEG-MAL-conjugates pendant ligands. 85

10. The conjugation efficiency of aminoBP onto fetuin using MANS, MBNS, SMCC, LC-SMCC, and NHS-PEG-MAL 86

11. The probability density and the radial density distribution of the MANS-, MBNS-, SMCC-, LC-SMCC-, and NHS-PEG-MAL-conjugates 87

12. The MANS-, MBNS-, SMCC-, LC-SMCC-, and NHS-PEG-MAL-conjugates' capacity to bind to HA in 50% bovine adult serum 88

13. Binding isotherms of the MANS-, MBNS-, SMCC-, LC-SMCC-, and NHS-PEG-MAL-conjugates with HA 89

14. Modulating bovine adult serum concentrations and the MANS-, MBNS-, SMCC-, LC-SMCC-, and NHS-PEG-MAL-conjugates' capacity to bind to HA 90

15. The capacity of native fetuin, and the MBNS-, LC-SMCC-, and NHS-PEG-MAL- conjugates to bind and retention to Pro-Osteon® *in vitro* as well as *in vivo* 91

16. Gel electrophoresis of unlabeled and radiolabeled fetuin and amino BP-fetuin conjguates 122

17. Conjugate binding to Pro-Osteon and Helistat in 50% adult bovine serum *in vitro* as well as *in vivo* 123

18. The biodistribution of the SMCC- and MMCCH-fetuin conjugates 24 h after IP administration 124

19. The biodistribution of the SMCC- and MMCCH-fetuin conjugates 24 h after IV administration 125

20. The biodistribution of the SMCC-conjugates and fetuin 6 h and 48 h after IV administration 126

21. The biodistribution of the MMCCH-conjugates and fetuin 72 h and 144 h after IV administration 127

22. A schematic representation of the chemistry used to conjugate amino BP onto heparin through the use of MMCCH 153

23. The effects of modulating the concentration of $NaIO_4$ on the number of aldehydes and aminoBPs introduced onto heparin; and the linear correlation between these two parameters 154

24. The correlation between the number of aminoBPs conjugated per heparin and HA binding 155

25. The capacity of bFGF and BMP-2 to bind to HA in the absence and presence of unmodified heparin in either 200 mM or 400 mM phosphate buffer 156

26. The effect of increasing the number of aminoBPs/heparin on the conjugates' capacity to enhance the affinity of bFGF and BMP-2 in either 200 mM or 400 mM phosphate buffer 157

27. The correlation between the aminoBP-heparin conjugates' capacity to bind to HA and their ability to enhance the affinity of bFGF and BMP-2 to HA 158

28. The effect of modulating phosphate buffer concentrations on bFGF's and BMP-2's ability to bind to HA 159

29. Modulating the ratio of aminoBP-heparin conjugate and unmodified heparin to either bFGF or BMP-2 160

30. The effects of weekly PTH (1-34) administration on Tibial bone mineral content as a function of dry weight, volume and bone density 186

31. The effects of weekly PTH (1-34) administration on bone mineral density within the proximal, central, and distal regions as well as the total femur 187

32. The effect of weekly PTH (1-34) administration on femoral bone volume fraction, bone surface fraction, and trabecular thickness 188

33. The effect of weekly PTH (1-34) administration on total, trabecular, and cortical XSA within the femoral neck 189

34. The effect of weekly PTH (1-34) administration on vertebral bone volume fraction, bone surface fraction, and trabecular thickness 190

35. The effects of increasing the threshold on various architectural parameters of a bone sample from a ovariectomized rat 256

36. The effects of increasing the threshold on various architectural parameters of a bone sample from a sham-operated rat 258

37. Comparing the effects of modulating threshold on various architectural parameters on bone samples from a sham-operated rat and an ovariectomized rat 260

LIST OF ABBREVIATIONS

1. μCT; Micro-Computed Tomography
2. 2-IT; 2-Iminothiolane
3. Ab; Antibody
4. aFGF; Acidic Fibroblast Growth Factor
5. aminoBP; 1-Amino-1,1-Diphosphonate Methane
6. Apo2L; Apo2 Ligand
7. bFGF; Basic Fibroblast Growth Factor
8. BMD; Bone Mineral Density
9. BMP; Bone Morphogenetic Protein
10. BP; Bisphosphonates
11. BS/BV; Bone Surface Fraction
12. BV/TV; Bone Volume Fraction
13. BV; Bone Volume
14. DA; Degree of Anisotropy
15. DMF; N,N-Dimethylformamide
16. ET_A; Endothelin A Receptor
17. gp130; Glycoprotein 130
18. HA; Hydroxyapatite
19. ICAM; Intercellular Adhesion Molecule
20. IGF; Insulin-like Growth Factor
21. IGFBP; Insulin-like Growth Factor Binding Protein
22. IL; Interleukin
23. IV; Intravenous
24. Ixx; Moments of Area about the Horizontal Axis
25. Iyy; Moments of Area about the Vertical Axis
26. LC-SMCC; Succinimidyl-4-(N-maleimidomethyl)cyclohexane-1-carboxy-(6-amido-caproate)
27. MANS; α-Maleimidoacetic acid-N-hydroxysuccinimide
28. MBNS; Maleimidobutyric acid-N-hydroxysuccinimide

29. MD; Molecular Dynamics
30. MIP; Macrophage Inflammatory Protein
31. MMCCH; 4-(Maleimidomethyl) cyclohexane-1-carboxyl-hydrazide
32. MW; Molecular Weight
33. $NaIO_4$; Sodium Periodate
34. NHS-PEG-MAL; N-Hydroxysuccinimide-polyethylene Glycol-maleimide
35. OPG; Osteoprotegerin
36. OVX; Ovariectomized
37. PDGF; Platelet Derived Growth Factor
38. PECAM; Platelet Endothelial Cell Adhesion Molecule
39. PTH; Parathyroid Hormone
40. PTHrP; Parathyroid Hormone-Related Protein
41. RANK; Receptor Activator of Nuclear Factor Kappa B
42. RANKL; Receptor Activator of Nuclear Factor KappaB Ligand
43. SC; Subcutaneous
44. SDS; Sodium Dodecyl Sulfate
45. SMCC; Succinimidyl-4-(N-Maleimidomethyl)-Cyclohexane-1-Carboxylate
46. SMI; Structure Model Index
47. Tb.N; Trabecular Number
48. Tb.Sp; Trabecular Separation
49. Tb.Th; Mean Trabecular Thickness
50. TCA; Trichloroacetic Acid
51. TCDG; 1,3,4,6-Tetrachloro-3α,6α-diphenylglycouril
52. TGF-β; Transforming Growth Factor-β
53. TIMPs; Tissue Inhibitors of Metalloproteinases
54. TNF; Tumor Necrosis Factor
55. TNFR; Tumor Necrosis Factor Receptor
56. TRAIL; Tumor Necrosis Factor-Related Apoptosis-Inducing Ligand
57. VCAM; Vascular Cell Adhesion Molecule
58. VEGF; Vascular Endothelial Growth Factor
59. VEGFR; Vascular Endothelial Growth Factor Receptor

60. VOI; Volume of Interest

61. XSA; Cross-Sectional Area

SCOPE OF DISSERTATION

CHAPTER I serves to introduce the basic biology of bone formation and repair as well as osteoporosis, a disease which affects both the appendicular and axial skeleton. Given the clinical need to regenerate and thus restore bone lost to this disease, pre-clinical studies using growth factors to stimulate the systemic growth of bone are subsequently discussed. Because of the side-effects they elicit upon systemic administration, these osteogenic growth factors must be targeted to bone. As a prelude to bisphosphonate-mediated protein targeting to bone, previous strategies to target drugs to bone are discussed, with an emphasis on bisphosphonate-mediated drug targeting.

In response to the inherent need to deliver osteogenic growth factors to skeletal tissue, a method to conjugate 1-amino-1,1-diphosphonate methane (aminoBP) onto various proteins using succinimidyl-4-(N-maleimidomethyl)-cyclohexane-1-carboxylate (SMCC) was initially developed by Uludag and co-workers. Since these conjugates were obtained by attaching aminoBP directly onto the proteins' lysine amino acid residues, this approach *may* inadvertently alter the protein's pharmacophore and subsequently compromise the protein's inherent bioactivity. Consequently, an alternative means of conjugating aminoBP onto the carbohydrate moieties of a model glycoprotein (fetuin) using 4-(maleimidomethyl)cyclohexane-1-carboxyl-hydrazide (MMCCH) was developed and described in **CHAPTER II**. Here, the resulting bone mineral affinities of both the SMCC-based and MMCCH-based aminoBP-fetuin conjugates were compared to one another.

Based on the difference seen between aminoBPs conjugated directly onto the protein core (i.e. SMCC chemistry) and those conjugated onto carbohydrate moieties (i.e. MMCCH chemistry) in **CHAPTER II**, it was postulated that: (i) steric interference

mediated by the amino acids adjacent to the linkage site may have influenced aminoBP binding to the mineral matrices; and/or (ii) the carbohydrate moieties may have afforded the conjugated aminoBPs a greater range of motion to facilitate their interaction with HA than those conjugated directly onto the protein core. Thus, the effect of modulating tether length on protein conjugates' affinity for hydroxyapatite (HA) *in vitro* were explored. As described in **CHAPTER III**, aminoBP was conjugated onto the lysine amino acid residues of fetuin, the same glycoprotein used in **CHAPTER II**, through five crosslinkers whose lengths varied from 5.4 to ~136 Å. The capacity of the various conjugates to bind to HA *in vitro*, paralleled parameters assessed through *in silico* Molecular Dynamics simulations (i.e. radial density and probability density). These data not only revealed an inverse relationship between tether length and bone mineral affinity, but suggested the feasibility of using *in silico* simulations to predict the binding characteristics of a given conjugate.

Given the increased *in vitro* bone mineral affinity afforded to fetuin through aminoBP conjugation, **CHAPTER IV** describes the targeting efficiency of aminoBP-fetuin conjugates upon parenteral administration in rats. In addition, the retention of SMCC-based and MMCCH-based conjugates to a commercially-available coralline hydroxyapatite matrix (i.e. Pro-Osteon®) was assessed. Despite the increase in conjugate binding and retention to this HA-based matrix both *in vitro* as well as *in vivo*, aminoBP conjugation did not enhance fetuin localization to bone due to an increase in the conjugates' susceptibility to the reticuloendothelial/mononuclear phagocyte system (liver and spleen), irrespective of the conjugation chemistry. These results also suggest that the capacity of aminoBP-conjugation to enhance protein targeting to bone upon parenteral

administration might be protein-specific, since previous research demonstrating bone targeting was performed with different proteins (i.e. lysozyme and bovine serum albumin).

Based on the inherently high affinity that osteogenic proteins (e.g. basic fibroblast growth factor (bFGF) and bone morphogenetic protein-2) have for heparin, aminoBP conjugation onto this glycosaminoglycan was an initiative developed to enhance the bone mineral affinity of such heparin-binding, osteogenic growth factors without the need of directly modifying these protein through BP conjugation. As described in **CHAPTER V**, aminoBP conjugation not only enhanced heparin's affinity for HA *in vitro*, but also increased the bone mineral affinity of the aforementioned growth factors in a manner dependent on the number of aminoBPs conjugated onto the heparin. The work described in this chapter is the foundation of a novel delivery system that may enhance proteins targeting and retention to bone without the need for direct protein modification.

Prior to being able to assess the pharmacodynamic properties of aminoBP-protein conjugates, an "in-house" animal model was developed using parathyroid hormone (1-34) [PTH (1-34)], a protein whose ability to stimulate systemic bone formation has been extensively studied. Here, weekly subcutaneous administration of varying doses of PTH (1-34) was compared based on their capacity to induce the systemic formation of bone in ovariectomized rats. As described in **CHAPTER VI**, the weekly administration of 10 µg/kg led to a significant increase in bone mineral density and improved several trabecular architectural parameters assessed through the use of micro-computed tomography and dual x-ray absorptiometry. Not only do these results validate the animal

model used, the total dose of PTH (1-34) administered represents the lowest shown to induce a net anabolic effect on skeletal tissue in ovariectomized (OVX) rats.

Serving as a preliminary study to assess the pharmacodynamics of bisphosphonate-growth factor conjugates, the effects of systemic bFGF and vascular endothelial growth factor (VEGF) administration on bone were determined using the same animal model as described in **CHAPTER VI**. Although the study in **CHAPTER VII** was the first to attempt to examine the effects of exogenous VEGF administration in an OVX rat model, the results generated in this study were inconclusive as neither bFGF or VEGF elicited a significant response on bone (based on the parameters measured).

All together, the work presented herein highlights the potential of bisphosphonate-mediated protein targeting. As discussed in the **FUTURE STUDIES** chapter, this work also represents the foundation for numerous additional studies to further expand upon our knowledge in the fields of drug targeting and bone tissue engineering.

CHAPTER I

INTRODUCTION TO BONE BIOLOGY AND THE NEED FOR BONE TARGETING[1]

[1] Some of the contents of this chapter have been previously published in: Gittens SA, and Uludağ H, Growth Factor Delivery for Bone Tissue Engineering, *J. Drug Targeting*. (2001) 9(6): 407-429; and have also been accepted for publication in *Advanced Drug Delivery Reviews* as: Gittens SA, Bansal G, Zernicke RF and Uludağ H, Designing Proteins for Bone Targeting.

I. Basic Biology of Bone Formation and Repair

Consisting of a mélange of organic and inorganic constituents, bone is a highly specialized connective tissue responsible for maintaining calcium homeostasis, housing elements required for hematopoiesis, and providing an internal mechanical support system in higher vertebrates. There are two distinguishable origins of bone: intramembranous (mesenchymal, direct) and endochondral (intracartilaginous, indirect). The former, formed when mesenchymal precursor cells differentiate directly into bone-forming osteoblasts, make up the periosteal surfaces of long bones as well as some bones of the skull (cranial vault), some facial bones, and parts of the mandible and clavicle. The long bones of the appendicular skeleton and the vertebrae of the axial skeleton, on the other hand, arise from the formation of endochondral bone; a process in which mesenchymal progenitor cells condense and differentiate into chondrocytes that are responsible for forming a mineralized template which is later replaced by bone (**1**).

To maintain its integrity as well as respond to the changing demands of an organism, bone continuously undergoes a process known as remodeling. This dynamic and highly-coordinated process involves replacement of existing bone (osteolysis) with newly synthesized bone (osteogenesis). The principle cell types involved in remodeling, osteoblasts and osteoclasts, are influenced by a cascade of growth factors, cytokines, and hormones that ultimately regulate cell migration, attachment, proliferation, differentiation, and activity. Although much is known about the cellular processes involved during remodeling, the exact biochemical means through which regulation occurs have yet to be fully elucidated. Regardless of this shortcoming, it is crucial to recapitulate normal physiological events when engineering ways of promoting bone

growth; the success of which hinges on our ability to understand the underlying basic biological principles involved in the formation of bone. The following section will primarily address the cells and growth factors involved in the formation of bone as well as those responsible for maintaining its integrity.

A. Formation of Long Bones

The growing epiphyseal growth plate can be anatomically subdivided into regions where (from most distal to most proximal to the metaphysis) zones of proliferation, maturation, hypertrophy, calcification, and bone formation can be recognized. Chondrocyte proliferation and differentiation, under the influence of a complex paracrine feedback loop involving parathyroid hormone related peptide (PTHrP), Indian hedgehog (Ihh), and bone morphogenetic proteins (BMPs), and angiogenesis are attributed as the main processes that are crucial in the formation of endochondral bone (**2**). The process of chondrocyte differentiation begins when undifferentiated mesenchymal cells, which are histologically small and spherical, aggregate to form small clusters within a cartilaginous matrix primarily consisting of type II collagen and proteoglycans at the distal epiphyseal end of the growth plate. Prior to losing their ability to proliferate and differentiate into hypertrophic cells, the small, flattened chondrocytes undergo clonal expansion to form organized longitudinal columns. While actively secreting a cartilaginous matrix rich in collagen X, these cells, as they continue to enlarge as the metaphysis draws nearer, are responsible for the calcification of the matrix (**3**). Hypertrophied chondrocytes within the medullary region undergo apoptosis or differentiating into osteoblasts, remains contentious (**2**).

Subsequent resorption of the synthesized cartilaginous scaffold allows the formation of new blood vessels to enter the resorption front. This process of neovascularization, which is mediated through several angiogenic activators (i.e. transferrin, vitamin D inducible 120 kDa protein, vascular endothelial growth factor (VEGF) and basic fibroblast growth factor (bFGF)), angiogenic inhibitors (i.e. transforming growth factor-β (TGF-β), chondromodulin I), and other factors (i.e. matrix metalloproteinases (MMPs), tissue inhibitors of metalloproteinases (TIMPs), and cathepsins), allows osteoblasts to invade both the primary spongiosum and resorption front to deposit and mineralize bone matrix (**2,4,5**). The synthesis of metaphyseal trabecular bone marks the completion of the process of endochondral ossification. Among the autocrine, paracrine and endocrine factors responsible for regulating the formation of endochondral bone are growth hormone (GH), thyroid hormone (T_3), insulin-like growth factor (IGF-I), 1,25 $(OH)_2D_3$, 24,25$(OH)_2D_3$, vitamin C, calcitonin, somatomedins, insulin, and many other growth factors (**3**). Bone morphogenetic proteins (BMPs) play a critical role in this process by committing osteoprogenitor cells (mesenchymal or bone marrow-derived) into bone-depositing osteoblast phenotype. Corticosteroids, vitamin A, epidermal growth factor (EGF), androgens and estrogens are among the factors having inhibitory effect on bone growth (**2,3**).

B. Maintenance of Bone Integrity

Maintenance of bone is primarily achieved as a result of bone remodeling, a process whereby osteoclast-mediated resorbed bone is replaced by osteoblast-formed bone (as recapitulated in more detail in the following section). This process enables the

mineralized tissue to respond to the micro-damage brought about by mechanical stresses exerted during loading. In addition to being targeted to sites of microdamage, bone remodeling is integral in regulating serum mineral homeostasis, and allows bone to adapt to changes in its mechanical environment (through a process known as modeling) (**6**).

C. Bone Remodeling

The cells involved in bone remodeling are organized into basic multicellular units (BMUs) that are both spatially and temporally separated from one another (**7**). The remodeling process commences once hematopoietically-derived osteoclast precursors have proliferated and differentiated into multinucleated osteoclasts via the monocyte/macrophage intermediate (**8**). Through proteolytic MMPs, collagenases and gelatinases, lining osteoblasts are responsible for the removal of the unmineralized osteoid layer at the site; thus enabling osteoclasts to access extracellular bone matrix proteins, such as osteopontin, through the use of their integrin superfamily of adhesion receptors (**7**). Once activated, osteoclasts are then responsible for the actual resorption of bone through the production of H^+ to dissolve the mineral; and proteolytic enzymes to degrade the organic matrix (**7**). The subsequent apoptosis of osteoclasts formally terminates the resorption phase of bone remodeling. The mechanism through which osteolysis and osteogenesis are coupled is an intense area of study and traditionally accepted paradigms (i.e. osteoclast differentiating into osteoblasts; release of previously osteoblast-deposited growth factors to mediate osteoblast concentrations; biomechanical strains responsible for an increase in osteoblast concentrations; and changes in local cytokine profiles to increase preosteoblast production) are being revised by alternative

explanation(s) (e.g., capillary endothelial cells being responsible for releasing of coupling-related signals) (**9**).

Regardless of the exact mechanism through which they are activated, mesenchymally-derived pre-osteoblasts are chemotactically recruited to the site of resorption. Through the influence of autocrine and paracrine factors, such as IGF-1, IGF-II, FGFs, and platelet-derived growth factor (PDGF), they are stimulated to proliferate. Under the influence of TGF-β and BMP members, the cells are committed into osteoblastic phenotype (**10**). Once matured, osteoblasts are then responsible for filling the osteoclast-produced cavity through the synthesis of osteoid. As their production of matrix decreases, these initially stout and dynamic cells flatten and eventually differentiate into osteocytes which then become incorporated into the matrix (**11**). Approximately 13 days after the formation of the osteoid, mineralization of the matrix occurs to mark the completion of bone remodeling (**11**).

II. Osteoporosis

Due to an imbalance in bone remodeling favoring osteoclast-mediated bone resorption, osteoporosis is characterized by a generalized loss of bone mineral and an associated architectural deterioration of trabecular bone culminating in increased skeletal fragility. The increase in the susceptibility and ultimately frequency of fracture is an issue with considerable medical, social and economic implications (**12**). Typically, the types of osteoporosis can be distinguished as either primary (i.e. post-menopausal and senile osteoporosis) or secondary (e.g. glucocorticoid-induced, and immobilization-induced osteoporosis). The specific pathophysiology associated with the progression of bone loss

in each type varies significantly depending on the primary pathogenic factor. Irrespective of the etiology, however, the resulting loss of bone and increase in bone fracture susceptibility are characteristics shared by each.

The most preponderant therapeutic agents currently used in the treatment of osteoporosis are bisphosphonates (BPs), a class of pyrophosphate analog-derivatives that have an inherently high affinity for bone mineral. Based on their chemical structure, BPs have been separated into two distinct classes: amino-containing BPs and non-amino-containing BPs. The former class has been shown to induce osteoclast apoptosis by inhibiting the mevalonate intracellular pathway. This biochemical cascade is responsible for the prenylation (i.e. the transfer of farnesyl and geranylgeranyl lipid moieties onto the cysteine amino acid) of small, signaling proteins known as GTPases, which are crucial in: (i) maintaining cell morphology; (ii) regulating integrin signaling; (iii) trafficking endosomes; (iv) controlling membrane ruffling; and (v) anchoring integral proteins into cellular membranes (**13**). Non-amino-containing BPs, on the other hand, are metabolized into non-hydrolyzable analogues of ATP, which upon accumulating intracellularly, interfere with the function of numerous intracellular metabolic enzymes and culminate in adverse changes in cellular function and viability (**13**). Upon administration, BPs localize specifically to the primary mineral component of osseous tissues. Much like selective estrogen receptor modulators, and calcitonin, both of which are examples of other prescribed drugs in the treatment of osteoporosis, BP administration merely mitigates the resorption of bone. Apart from the use of parathyroid hormone (1-34), no currently prescribed agents are actually capable of promoting the systemic regeneration of bone so as to restore the lost bone to levels prior to the onset of disease. Thus developing a means

to enhance the growth of bone will help circumvent the imminent dangers associated with the diminished skeletal integrity associated with osteoporosis.

III. Systemic Bone Regeneration

As highlighted in **Table 1-1,** numerous growth factors have been shown to elicit the systemic regeneration of bone upon parenteral administration in various animal models. For example, the daily administration of bFGF was shown to stimulate both endocortical and cancellous bone formation in an ovariectomized rat model of post-menopausal osteoporosis **(19-23)**. Similarly, BMP-2 administration was shown to increase trabecular number and bone volume in murine models of post-menopausal and senile osteoporosis **(14)**. Given that their osteogenicity has been well-substantiated in the literature, growth factor-based therapeutic agents, such as the aforementioned two, are consequently ideal candidates for the basis of engineering a means to facilitate the systemic regeneration of bone.

Several limitations, however, are associated with the use of osteogenic growth factors for this purpose. Given that a relatively small fraction of the administered dose reaches skeletal tissue (< 1% is estimated for bFGF, **40**), the dose administered must be sufficiently high to elicit the desired anabolic response. This is a challenge in light of the fact that these osteogenic proteins typically do not have an innate affinity for skeletal tissue and that the half-life of these proteins in circulation is relatively short (e.g. in rats, 1.5 min for bFGF **(41)**, 16 minutes for BMP-2 **(42)**). Moreover, because many of these growth factors are expressed ubiquitously and as such are inherently pleiotropic, the dose required for osteogenesis may also elicit numerous deleterious, extra-skeletal side effects.

For example, while doses of bFGF ranging from 100-1000 μg/kg (body weight) was required to elicit an anabolic skeletal response in rats (**19-23**), the administration of 100 μg/kg was shown to result in nephropathy as a result of bFGF-mediated hypertrophy of the epithelial cells in the Bowman's capsule, in the lining of the papilla, and in the arteries supplying the glomeruli as well as podocyte distortion and hypertrophy (**43,44**). Therefore, to effectively skirt the potential toxicity associated with their systemic administration, osteogenic growth factors must specifically be targeted to bone.

IV. Drug Targeting to Skeletal Tissue

Irrespective of the desired therapeutic agent, drug targeting to skeletal tissues is expected to result in a reduction in the degree of extra-skeletal drug distribution; thus a corollary reduction in the incidence of adverse effects associated with drug administration. Furthermore, targeting would also afford a reduction in the dosage required to elicit a desired skeletal response (as a higher percentage of targeted drug would localize to bone relative to the untargeted drug). To this end, there are two distinct strategies that can be employed to target drugs to bone: the use of colloidal drug delivery systems or the conjugation of "bone-seeking" moieties directly onto a drug or drug carrier. Because this thesis does not focus on colloidal delivery systems, this means of drug targeting will not be further discussed.

V. Osteotropic Moieties for Drug Targeting to Bone:

A. Conjugation of Non-BP Moieties for Drug Targeting to Bone

Numerous osteotropic chemical moieties have been used to increase the affinity of therapeutic agents to the mineral component of bone (**Figure 1-1**). Tetracycline, for example, is a broad-spectrum antibiotic that has a high affinity for bone resulting from the formation of hydrogen bonds between its hydroxyl- and keto-oxygens and the surface of hydroxyapatite (HA), which is hydrated by 1.5 layers of physisorbed water *in vivo* (**45**). Taking advantage of this affinity, conjugation of tetracycline onto β-estradiol-3-benzoate yielded a conjugate with an enhanced affinity for HA over the unmodified estradiol derivative (**46**). Using another "bone seeking" moiety, Willson *et al.* markedly enhanced estrogen's affinity for HA by conjugating 4-carboxy-3-hydroxy-1,2-pyrazole, one of several heterocycles exhibiting bone affinity, directly onto it (**47**). Although they have yet to be used as targeting moieties, additional heterocyclic, thiadiazole derivitives can potentially be used as targeting agents as their capacity to bind to HA is comparable to that of tetracycline (**48**).

Other osteotropic moieties include small polyelectrolytic peptides. Based on their dense negative charges, polycarboxylate peptide sequences (i.e. poly(aspartic) and poly(glutamic) acid) have an inherent affinity for HA (**49**). Consequently, these sequences, which are believed to be responsible for imparting bone sialoprotein and osteopontin's ability to bind to bone endogenously (**49**), are suitable moieties that can be used for drug targeting. Using this approach, Kasugai *et al.* demonstrated that the conjugation of hexameric poly(aspartic acid) onto fluorescein isothiocyanate (FITC) increased FITC's affinity for bone both *in vitro* as well as upon intravenous and

subcutaneous administration in mice (**50**). Similarly, conjugation of poly(aspartic acid)-poly(ethylene glycol) moieties onto FITC significantly increased this fluorescent molecule's binding capacity for HA *in vitro* and resulted in an increase in bone (specifically, endosteal and metaphyseal) targeting upon its intravenous administration in mice (**51**). The administration of estradiol-aspartic acid hexapeptide conjugate not only increased estradiol's affinity for bone *in vivo* but also increased the bone mineral density of ovariectomized mice in a dose-dependent manner without adversely affecting uterine weight (**52**). In another study, decameric poly(glutamic acid) was conjugated onto both biotin and methotrexate. As bone-seeking drug carriers, these molecules significantly enhanced the *in vitro* affinity of avidin and dihydrofolate reductase for HA, respectively (**53**). It should be noted that this is one of the first reports describing the conjugation of a "bone-seeking" moiety onto a carrier to enhance the affinity of a desired ligand without the need of directly modifying it. Demonstrating the feasibility of conjugating an array of phosphate-containing moieties, such as phosphonomethylphosphonylate, Sawyer *et al.* improved the HA affinity of small organic Src tyrosine kinase inhibitors, agents that can effectively abrogate osteoclast-mediated bone resorption (**54-59**). Other examples of phosphate-containing molecules which can be used for bone targeting are the pyrophosphate analog-derivatives collectively known as BPs.

B. <u>BP Conjugation for Drug Targeting to Bone</u>

As aforementioned, BPs have an exceptionally high affinity for mineralized tissues resulting from strong electrostatic interactions between their negatively charged phosphate moieties and HA. Based on this affinity, BP conjugation has been the most

prevalent approach used in the literature to impart bone affinity onto therapeutic agents. To improve their targeting efficiency to skeletal tissue, BPs have been conjugated onto a variety of chemical entities ranging from steroids, anti-neoplastic agents, and radioisotopes, to proteins.

BP-steroid conjugates: To circumvent the numerous adverse effects associated with their pleiotropic nature, various bisphosphonate-containing estrogenic molecules have been synthesized to enhance this steroid's affinity for skeletal tissue **(60-65)**. While the BP-conjugated estrogens used by Fujisaki *et al.*, and Tsushima *et al.* successfully prevented bone loss associated with ovariectomization in rats, those used in Bauss *et al.* conferred little or no benefits over unmodified 17β-estradiol, irrespective of whether the linkage between the estrogen and BP was cleavage-resistant or not **(62)**. Based on these findings, further studies are required to determine the feasibility of BP conjugation for the delivery of estrogen derivatives *in vivo*.

BP-radioisotope conjugates: Primarily intended for the diagnosis of osseous neoplastic lesions and their treatment, a multitude of radioisotopes have been targeted to bone through BP conjugation. Bisphosphonate-radioisotope conjugates which have been used in a clinical setting include: ^{188}rhenium-hydroxyethylidenediphosphonate (HEDP) **(67,68)**, ^{186}rhenium-HEDP **(68,69)**, ^{99m}technetium-methylene diphosphonate **(70,71)**, ^{99m}technetium-hydroxymethylene diphosphonate **(72,73)** ^{153}samarium-ethylenediaminetetramethylene phosphonate **(74,75)** and ^{131}iodine-amino-(4-hydroxybenzylidene)-diphosphonate **(76)**. Numerous other bisphosphonate-radioisotope

conjugates are currently under development for bone imaging and chemotherapeutic purposes.

BP-anti-neoplastic conjugates: Given that toxic effects limit their therapeutic window, anti-neoplastic agents are suitable candidates for bone targeting—as an increase in their localization is expected to result in a reduction in their systemic toxicity. Although several BPs are now being recognized as being inherently anti-neoplastic themselves **(77,78)**, BPs have been conjugated onto three well-established chemotherapeutic agents: cisplatin; doxorubicin; and methotrexate. Bisphosphonic derivatives of cisplatin include *cis*-diammine[(bis(phosphonatomethyl)amino)acetato(2-)-O^1,N^1]platinum(II) **(79,80)**, as well as numerous other platinum-containing derivatives such as *cis*-$Pt(NH_3)_2$(bmpaa), *cis*-$Pt(NH_3)_2$ (ntmp), and Pt(*R,S* dach) (ntmp) **(80, 81)**, *cis*-$PtCl_2$(4-pmpe)$_2$ **(82)** and Pt(II)- quinolylmethylphosphonate complexes **(83)**. On the other hand, four different gem-bisphosphonic moieties (i.e. 3,3-bis(diethylphosphono)propanoic acid 2, 4,4-bis(diethylphosphono)butanoic acid 3, and (R + S)-N-(9-fluorenylmethyloxycarbonyl)-2-amino-4,4-bis(diethylphosphono)butanoic acid) have previously been coupled onto doxorubicin **(84)**. The process of conjugating these moieties onto this agent, however, resulted in a decrease in doxorubicin's native bioactivity as no effect was observed against human tumor xenografts **(84)**. Methotrexate-bisphosphonate conjugates, however, were either as or more cytotoxic than unmodified methotrexate in murine model of osteosarcoma **(85)**. Subsequent pharmacokinetic analysis of one of these conjugates (labeled with ^{99m}technetium) suggested that its affinity for bone upon intravenous

administration was equivalent to that seen with bone-seeking agents such as ^{99m}technetium-diphosphonates (**86**).

BP-protein conjugates: BP conjugation may be a means to address some of the previously mentioned issues regarding the administration of growth factors for the intent of promoting bone regeneration (i.e. short systemic half-life and induction of extra-skeletal side effects). To this end, conjugation of 1-amino-1,1-diphosphonate methane (aminoBP) onto the lysine amino acid residues of bovine serum albumin (BSA) using succinimidyl-4-(N-maleimidomethyl)-cyclohexane-1-carboxylate was originally reported by Uludag *et al.* (**87**). AminoBP-modification significantly enhanced BSA's affinity for synthetic HA, and various other bone matrices over unmodified protein *in vitro*. Subsequent studies demonstrated that the conjugation of 4.9 aminoBP per BSA increased the protein retention's to bone upon intramedullary administration by 8- and 12-fold in the tibiae of normal and ovariectomized rats, respectively (**88**). Upon intravenous administration, BSA conjugates containing 11.0 aminoBPs/BSA exhibited a significant increase in targeting to skeletal tissue (i.e. femora, tibiae, and sternum) as well as a significant decrease in kidneys, liver and spleen over unmodified BSA (**89**).

In addition to enhancing bone targeting, aminoBP conjugation increased protein retention at the mineralized sites of localization, and afforded a reduction in the extra-skeletal distribution (to aforementioned clearance organs) upon parenteral administration. Altered growth factor pharmacokinetics mediated by BP conjugation is expected to enhance the feasibility of using these osteogenic molecules for clinical indications such as osteoporosis. This concept of BP-proteins conjugation ultimately formed the foundation

on which the work presented in this thesis is based. (Although this approach was initially designed for promoting the systemic growth of bone for clinical indications such as osteoporosis, see **APPENDIX A** for musculoskeletal diseases and appropriate protein-based therapeutic options suitable for BP-mediated targeting to bone).

Table 1-1. Protein-Based Therapeutic Agents for Treatment of Osteoporosis

Protein	Rationale	Reference
BMP-2	BMP-2 is a potent promoter of osteoblastogenesis. Its intra-peritoneal administration enhanced bone mineral density and architecture in a murine model of osteopenia.	14
TGF-β	TGF-β is a pleiotropic growth factor shown to induce the proliferation of osteoblasts. TGF-β administration resulted in the promotion of bone regeneration in several rat models of osteopenia.	15-18
bFGF	bFGF is a potent mitogen for osteoblasts. Parenteral administration of bFGF resulted in an anabolic effect on skeletal tissue in rat and murine models of osteopenia.	19-28
IGF-1 and IGF-1/IGFBP-3	IGF-1 was shown to promote osteoblastic cell proliferation and differentiation. IGF-1 and IGF-1/IGFBP-3 administration increased bone mineral density in several clinical trials.	29-31
Activin	Activin promotes osteoblast proliferation and matrix synthesis *in vitro*. Its intramuscular administration increased bone mineral density and strength systemically in an ovariectomized rat model of osteopenia.	32,33
PDGF	PDGF is a mitogen for osteoblasts. In an ovariectomized rat model, its administration led to an increase in bone mineral density and strength.	34
PTH (1-34)	Through an increase in remodeling frequency favoring bone apposition, intermittent PTH administration improves bone mineral density, strength and micro-architecture. It is currently prescribed as an anti-osteoporotic agent.	35-38
aFGF	aFGF acts as a mitogen on osteoblasts and increase bone nodule formation *in vitro*. Parenteral administration of aFGF generated woven bone and new trabeculae in both rat and murine models of osteoporosis.	39

Abbreviations: Acidic Fibroblast Growth Factor (aFGF); Basic Fibroblast Growth Factor (bFGF); Bone Morphogenetic Protein (BMP); Insulin-like Growth Factor (IGF); Insulin-like Growth Factor Binding Protein (IGFBP); Osteoprotegerin (OPG); Parathyroid Hormone (PTH); Parathyroid Hormone-Related Protein (PTHrP); Platelet-Derived Growth Factor (PDGF); Receptor Activator of Nuclear Factor Kappa B (RANK); Transforming Growth Factor (TGF).

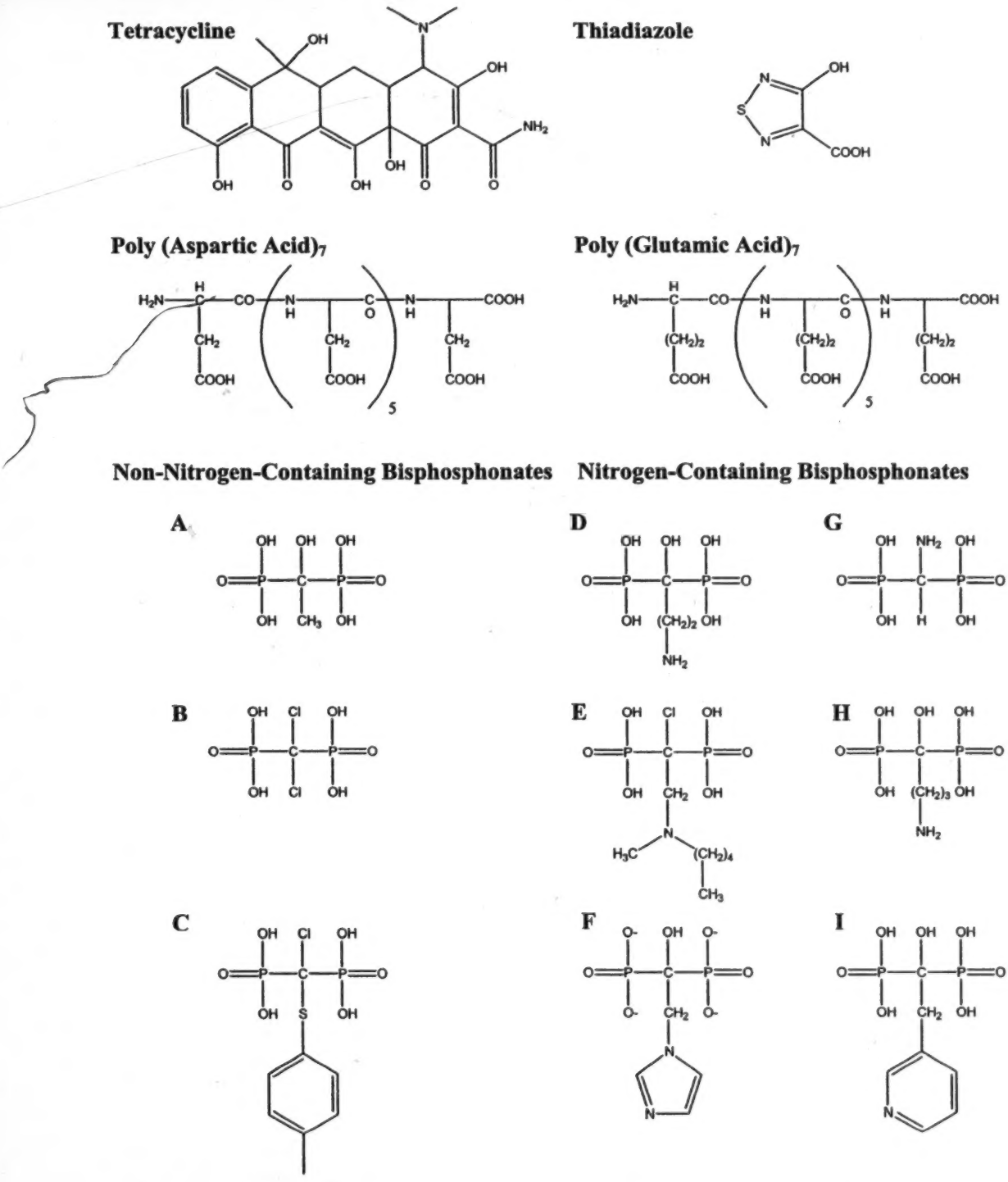

Figure 1-1: Structures of molecules shown to exhibit a significant affinity for bone mineral, including non-nitrogen-containing bisphosphonates such as: etidronate (**A**); clodronate (**B**); and tiludronate (**C**); as well as nitrogen-containing bisphosphonates such as: pamidronate (**D**); ibandronate (**E**); zolendronate (**F**); aminoBP (**G**); alendronate (**H**); and residronate (**I**).

References

1. A. Erlebacher, E.H. Filvaroff, S.E. Gitelman, R. Derynck. Towards a molecular understanding of skeletal development, *Cell*. 80 (1995) 371-378.

2. D.A. Stevens, G.R. Williams, Hormone regulation of chondrocyte and endochondral bone formation, *Mol. Cell. Endo.* 151 (1999) 195-204.

3. J.P. Iannotti, S. Goldstein, J. Kuhn, L. Lipiello, F.S. Kaplan, D.J. Zaleske The formation of growth and skeletal tissues. In Buckwater, J.A., Einhorn T.A., Simon, S.R. (eds). Orthopaedic Basic Science, 2nd edition. (2000) American Academy of Orthopaedic Surgeons, pp.78-109.

4. U.I. Sires, T.M. Schmid, C.J. Fliszar, Z.Q. Wang, S.L. Gluck, H.G. Welgus, Complete degradation of type X collagen requires the combined action of interstitial collagenase and osteoclast-derived cathepsin-B, *J. Clin. Invest.* 95 (1995) 2089-2095.

5. M. Soderstrom, H. Salminen, V. Glumoff, H. Kirschke, H. Aro, E. Vuorio, Cathepsin expression during skeletal development, *Biochim. Biophys. Acta*. 1446 (1999) 35-46.

6. D.B. Burr, Targeted and nontargeted remodeling, *Bone*. 30 (2002) 2-4.

7. P.A. Hill, Bone remodelling, *Br. J. Orthodont*. 25 (1998) 101-107.

8. S.L. Teitelbaum. Bone resorption by osteoclasts, *Science*. 289 (2000) 1504-1508.

9. A.M. Parfitt, The mechanism of coupling: A role for the vasculature, *Bone*. 26 (2000) 319-323.

10. P. Ducy, T. Schinke, G. Karsenty, The osteoblast: a sophisticated fibroblast under central surveillance, *Science*. 289 (2000) 1501-1504.

11. S. Ott, Theoretical and methodological approach. In Blezikian J.P., Raisz L.G., Rodan G.A. (eds.) Principles of Bone Biology (1996) Academic Press, pp. 231-241.

12. J.P. Brown, R.G. Josse, Scientific Advisory Council of the Osteoporosis Society of Canada, 2002 Clinical practice guidelines for the diagnosis and management of osteoporosis in Canada, *CMAJ*. 167 (2002) S1-S34.

13. M.J. Rogers, S. Gordon, H.L. Benford, F.P. Coxon, S.P. Luckman, J. Monkkonen, J.C. Frith, Cellular and molecular mechanisms of action of bisphosphonates, Cancer. 88 (2000) 2961-2978.

14. G. Turgeman, Y. Zilberman, S. Zhou, P. Kelly, I.K. Moutsatsos, Y.P. Kharode, L.E. Borella, F.J. Bex, B.S. Komm, P.V. Bodine, D. Gazit, Systemically administered rhBMP-2 promotes MSC activity and reverses bone and cartilage loss in osteopenic mice, *J. Cell. Biochem*. 86 (2002) 461-474.

15. D. Gazit, Y. Zilberman, G. Turgeman, S. Zhou, A. Kahn, Recombinant TGF-beta1 stimulates bone marrow osteoprogenitor cell activity and bone matrix synthesis in osteopenic, old male mice, *J. Cell. Biochem*. 73 (1999) 379-389.

16. J. Beaudreuil, G. Mbalaviele, M. Cohen-Solal, C. Morieux, M.C. De Vernejoul, P. Orcel, Short-term local injections of transforming growth factor-beta 1 decrease ovariectomy-stimulated osteoclastic resorption in vivo in rats, J. *Bone Miner. Res*. 10 (1995) 971-977.

17. M. Machwate, E. Zerath, X. Holy, M. Hott, D. Godet, A. Lomri, P.J. Marie, Systemic administration of transforming growth factor-beta 2 prevents the

impaired bone formation and osteopenia induced by unloading in rats, *J. Clin. Invest.* 96 (1995) 1245-1253.

18. S. Ahdjoudj, F. Lasmoles, X. Holy, E. Zerath, P.J. Marie, Transforming growth factor beta2 inhibits adipocyte differentiation induced by skeletal unloading in rat bone marrow stroma, *J. Bone Miner. Res.* 17 (2002) 668-677.

19. U.T. Iwaniec, K.A. Magee, N.G. Mitova-Caneva, T.J. Wronski, Bone anabolic effects of subcutaneous treatment with basic fibroblast growth factor alone and in combination with estrogen in osteopenic ovariectomized rats, *Bone.* 33 (2003) 380-386.

20. T.J. Wronski, A.M. Ratkus, J.S. Thomsen, Q. Vulcan, L. Mosekilde, Sequential treatment with basic fibroblast growth factor and parathyroid hormone restores lost cancellous bone mass and strength in the proximal tibia of aged ovariectomized rats, *J. Bone Miner. Res.* 16 (2001) 1399-1407.

21. R.A. Power, U.T. Iwaniec, T.J. Wronski, Changes in gene expression associated with the bone anabolic effects of basic fibroblast growth factor in aged ovariectomized rats, *Bone.* 31 (2002) 143-148.

22. S. Pun, R.L. Dearden, A.M. Ratkus, H. Liang, T.J. Wronski, Decreased bone anabolic effect of basic fibroblast growth factor at fatty marrow sites in ovariectomized rats, *Bone.* 28 (2001) 220-226.

23. H. Liang, S. Pun, T.J. Wronski, Bone anabolic effects of basic fibroblast growth factor in ovariectomized rats, *Endocrinology.* 140 (1999) 5780-5788.

24. U.T. Iwaniec, L. Mosekilde, N.G. Mitova-Caneva, J.S. Thomsen, T.J. Wronski, Sequential treatment with basic fibroblast growth factor and PTH is more efficacious than treatment with PTH alone for increasing vertebral bone mass and

strength in osteopenic ovariectomized rats, *Endocrinology*. 143 (2002) 2515-2526.

25. N.E. Lane, J. Kumer, W. Yao, T. Breunig, T. Wronski, G. Modin, J.H. Kinney, Basic fibroblast growth factor forms new trabeculae that physically connect with pre-existing trabeculae, and this new bone is maintained with an anti-resorptive agent and enhanced with an anabolic agent in an osteopenic rat model, *Osteoporos. Int.* 14 (2003) 374-382.

26. S. Pun, C.L. Florio, T.J. Wronski, Anabolic effects of basic fibroblast growth factor in the tibial diaphysis of ovariectomized rats, *Bone*. 27 (2000) 197-202.

27. H. Nagai, R. Tsukuda, H. Yamasaki, H. Mayahara, Systemic injection of FGF-2 stimulates endocortical bone modelling in SAMP6, a murine model of low turnover osteopenia, *J. Vet. Med. Sci.* 61 (1999) 869-875.

28. T. Nakamura, K. Hanada, M. Tamura, T. Shibanushi, H. Nigi, M. Tagawa, S. Fukumoto, T. Matsumoto, Stimulation of endosteal bone formation by systemic injections of recombinant basic fibroblast growth factor in rats, *Endocrinology*. 136 (1995) 1276-1284.

29. S. Boonen, C. Rosen, R. Bouillon, A. Sommer, M. McKay, D. Rosen, S. Adams, P. Broos, J. Lenaerts, J. Raus, D. Vanderschueren, P. Geusens, Musculoskeletal effects of the recombinant human IGF-I/IGF binding protein-3 complex in osteoporotic patients with proximal femoral fracture: a double-blind, placebo-controlled pilot study, *J. Clin. Endocrinol. Metab.* 87 (2002) 1593-1599.

30. S. Grinspoon, L. Thomas, K. Miller, D. Herzog, A. Klibanski, Effects of recombinant human IGF-I and oral contraceptive administration on bone density in anorexia nervosa, *J. Clin. Endocrinol. Metab.* 87 (2002) 2883-2891.

31. L.J. Ghiron, J.L. Thompson, L. Holloway, R.L. Hintz, G.E. Butterfield, A.R. Hoffman, R. Marcus, Effects of recombinant insulin-like growth factor-I and growth hormone on bone turnover in elderly women, *J. Bone Miner. Res.* 10 (1995) 1844-1852.

32. R. Sakai, Y. Eto, Involvement of activin in the regulation of bone metabolism. *Mol. Cell. Endocrinol.* 180 (2001) 183-188.

33. R. Sakai, S. Fujita, T. Horie, T. Ohyama, K. Miwa, T. Maki, N. Okimoto, T. Nakamura, Y. Eto, Activin increases bone mass and mechanical strength of lumbar vertebrae in aged ovariectomized rats, *Bone.* 27 (2000) 91-96.

34. B.H. Mitlak, R.D. Finkelman, E.L. Hill, J. Li, B. Martin, T. Smith, M. D'Andrea, H.N. Antoniades, S.E. Lynch, The effect of systemically administered PDGF-BB on the rodent skeleton, *J. Bone Miner. Res.* 11 (1996) 238-247.

35. R. Marcus, O. Wang, J. Satterwhite, B. Mitlak, The skeletal response to teriparatide is largely independent of age, initial bone mineral density, and prevalent vertebral fractures in postmenopausal women with osteoporosis, *J. Bone Miner. Res.* 18 (2003) 18-23.

36. E.S. Orwoll, W.H. Scheele, S. Paul, S. Adami, U. Syversen, A. Diez-Perez, J.M. Kaufman, A.D. Clancy, G.A. Gaich, The effect of teriparatide [human parathyroid hormone (1-34)] therapy on bone density in men with osteoporosis, *J. Bone Miner. Res.* 18 (2003) 9-17.

37. P. Morley, J.F. Whitfield, G.E. Willick, Design and applications of parathyroid hormone analogues, *Curr. Med. Chem.* 6 (1999) 1095-1106.

38. A.H. Tashjian Jr, B.A. Chabner, Commentary on clinical safety of recombinant human parathyroid hormone 1-34 in the treatment of osteoporosis in men and postmenopausal women, *J. Bone Miner. Res.* 17 (2002) 1151-1161.

39. C.R. Dunstan, R. Boyce, B.F. Boyce, I.R. Garrett, E. Izbicka, W.H. Burgess, G.R. Mundy, Systemic administration of acidic fibroblast growth factor (FGF-1) prevents bone loss and increases new bone formation in ovariectomized rats, *J. Bone Miner. Res.* 14 (1999) 953-959.

40. S.A. Gittens, H. Uludag, Growth factor delivery for bone tissue engineering, *J. Drug Targeting.* 9 (2001) 407-429.

41. G.F. Whalen, Y. Shing, J. Folkman, The fate of intravenously administered bFGF and the effect of heparin, *Growth Factors.* 1 (1989) 157-164.

42. A.R. Poynton, J.M. Lane, Safety profile for the clinical use of bone morphogenetic proteins in the spine, *Spine.* 27 (2002) S40-S48.

43. G. Mazue, A.J. Newman, G. Scampini, P. Della Torre, G.C. Hard, M.J. Iatropoulos, G.M. Williams, S.M. Bagnasco, The histopathology of kidney changes in rats and monkeys following intravenous administration of massive doses of FCE 26184, human basic fibroblast growth factor, *Toxicol. Pathol.* 21 (1993) 490-501.

44. G. Mazue, F. Bertolero, L. Garofano, M. Brughera, P. Carminati, Experience with the preclinical assessment of basic fibroblast growth factor (bFGF), *Toxicol. Lett.* 64-65 (1992) 329-338.

45. D.N. Misra, Adsorption and orientation of tetracycline on hydroxyapatite, *Calcif. Tissue Int.* 48 (1991) 362-367.

46. M.W. Orme, V.M. Labroo, Synthesis of beta-estradiol-3-benzoate-17-(succinyl-12a-tetracycline)-A potential bone-seeking estrogen, *Bioorg. Med. Chem. Lett.* 4 (1994) 1375-1380.

47. T.M. Willson, B.R. Henke, T.M. Momtahen, D.T. Garrison, L.B. Moore, N.G. Geddie, P.G. Baer, Bone targeted drugs. 2. Synthesis of estrogens with hydroxyapatite affinity. *Bioorg. Med. Chem. Lett.* 6 (1996) 1047-1050.

48. T.M. Willson, P.S. Charifson, A.D. Baxter, N.G. Geddie, Bone targeted drugs. 1. Identification of heterocycles with hydroxyapatite affinity, *Bioorg. Med. Chem. Lett.* 6 (1996) 1043-1046

49. H.A. Goldberg, K.J. Warner, M.C. Li, G.K. Hunter, Binding of bone sialoprotein, osteopontin and synthetic polypeptides to hydroxyapatite, *Conn. Tissue Res.* 42 (2001) 25-37.

50. S. Kasugai, R. Fujisawa, Y. Waki, K. Miyamoto, K. Ohya, Selective drug delivery system to bone: small peptide (Asp)6 conjugation, *J. Bone Miner. Res.* 15 (2000) 936-943.

51. D. Wang, S. Miller, M. Sima, P. Kopeckova, J. Kopecek, Synthesis and evaluation of water-soluble polymeric bone-targeted drug delivery systems, *Bioconjug. Chem.* 14 (2003) 853-859.

52. K. Yokogawa, K. Miya, T. Sekido, Y. Higashi, M. Nomura, R. Fujisawa, K. Morito, Y. Masamune, Y. Waki, S. Kasugai, K. Miyamoto, Selective delivery of estradiol to bone by aspartic acid oligopeptide and its effects on ovariectomized mice, *Endocrinology*. 142 (2001) 1228-1233.

53. B.C. Chu, L.E. Orgel, Presentation of ligands on hydroxylapatite, *Bioconjug. Chem.* 8 (1997) 103-105.

54. C.B. Vu, G.P. Luke, N. Kawahata, W.C. Shakespeare, Y. Wang, R. Sundaramoorthi, C.A. Metcalf 3rd, T.P. Keenan, S. Pradeepan, E. Corpuz, T. Merry, R.S. Bohacek, D.C. Dalgarno, S.S. Narula, M.R. van Schravendijk, M.K.

Ram, S. Adams, S. Liou, J.A. Keats, S.M. Violette, W. Guan, M. Weigele, T.K. Sawyer, Bone-targeted pyrido[2,3-d]pyrimidin-7-ones: potent inhibitors of Src tyrosine kinase as novel antiresorptive agents, *Bioorg. Med. Chem. Lett.* 13 (2003) 3071-3074.

55. Y. Wang, C.A. Metcalf 3rd, W.C. Shakespeare, R. Sundaramoorthi, T.P. Keenan, R.S. Bohacek, M.R. van Schravendijk, S.M. Violette, S.S. Narula, D.C. Dalgarno, C. Haraldson, J. Keats, S. Liou, U. Mani, S. Pradeepan, M. Ram, S. Adams, M. Weigele, T.K. Sawyer, Bone-targeted 2,6,9-trisubstituted purines: novel inhibitors of Src tyrosine kinase for the treatment of bone diseases, *Bioorg. Med. Chem. Lett.* 13(2003) 3067-3070.

56. R. Sundaramoorthi, W.C. Shakespeare, T.P. Keenan, C.A. Metcalf 3rd, Y. Wang, U. Mani, M. Taylor, S. Liu, R.S. Bohacek, S.S. Narula, D.C. Dalgarno, M.R. van Schravandijk, S.M. Violette, S. Liou, S. Adams, M.K. Ram, J.A. Keats, M. Weigele, T.K. Sawyer, Bone-targeted Src kinase inhibitors: novel pyrrolo- and pyrazolopyrimidine analogues, *Bioorg. Med. Chem. Lett.* 13 (2003) 3063-3066.

57. W.C. Shakespeare, C.A. Metcalf 3rd, Y. Wang, R. Sundaramoorthi, T. Keenan, M. Weigele, R.S. Bohacek, D.C. Dalgarno, T.K. Sawyer, Novel bone-targeted Src tyrosine kinase inhibitor drug discovery, *Curr. Opin. Drug. Discov Devel.* 6 (2003) 729-741.

58. C.A. Metcalf 3rd, M.R. van Schravendijk, D.C. Dalgarno, T.K. Sawyer, Targeting protein kinases for bone disease: discovery and development of Src inhibitors, *Curr. Pharm. Des.* 8 (2002) 2049-2075.

59. W. Shakespeare, M. Yang, R. Bohacek, F. Cerasoli, K. Stebbins, R. Sundaramoorthi, M. Azimioara, C. Vu, S. Pradeepan, C. Metcalf 3rd, C. Haraldson, T. Merry, D. Dalgarno, S. Narula, M. Hatada, X. Lu, M.R. van Schravendijk, S. Adams, S. Violette, J. Smith, W. Guan, C. Bartlett, J. Herson, J. Iuliucci, M. Weigele, T. Sawyer, Structure-based design of an osteoclast-

selective, nonpeptide src homology 2 inhibitor with in vivo antiresorptive activity, *Proc. Natl. Acad. Sci. U. S. A.* 97 (2000) 9373-9378.

60. J. Fujisaki, Y. Tokunaga, T. Takahashi, F. Shimojo, S. Kimura, T. Hata, Osteotropic drug delivery system (ODDS) based on bisphosphonic prodrug. I.v. effects of osteotropic estradiol on bone mineral density and uterine weight in ovariectomized rats, *J. Drug Target.* 5 (1998) 129-138.

61. J. Fujisaki, Y. Tokunaga, T. Takahashi, S. Kimura, F. Shimojo, T. Hata, Osteotropic drug delivery system (ODDS) based on bisphosphonic prodrug. V. Biological disposition and targeting characteristics of osteotropic estradiol, *Biol. Pharm. Bull.* 20 (1997) 1183-1187.

62. F. Bauss, A. Esswein, K. Reiff, G. Sponer, B. Muller-Beckmann, Effect of 17beta-estradiol-bisphosphonate conjugates, potential bone-seeking estrogen pro-drugs, on 17beta-estradiol serum kinetics and bone mass in rats, *Calcif. Tissue Int.* 59 (1996) 168-173.

63. N. Tsushima, M. Yabuki, H. Harada, T. Katsumata, H. Kanamaru, I. Nakatsuka, M. Yamamoto, M. Nakatsuka, Tissue distribution and pharmacological potential of SM-16896, a novel oestrogen-bisphosphonate hybrid compound, *J. Pharm. Pharmacol.* 52 (2000) 27-37.

64. P.C.B. Page, J.P.G. Moore, Mansfield, M.J. McKenzie, W.B. Bowler, J.A. Gallagher, Synthesis of bone-targeted oestrogenic compounds for the inhibition of bone resorption, *Tetrahedron.* 57 (2001) 1837-1847

65. P.C. Page, M.J. McKenzie, J.A. Gallagher, Novel synthesis of bis(phosphonic acid)-steroid conjugates, *J. Org. Chem.* 66 (2001) 3704-3708.

66. K. Liepe, J. Kropp, R. Runge, J. Kotzerke, Therapeutic efficiency of rhenium-188-HEDP in human prostate cancer skeletal metastases, *Br. J. Cancer*. 89 (2003) 625-629.

67. H. Palmedo, A. Manka-Waluch, P. Albers, I.G. Schmidt-Wolf, M. Reinhardt, S. Ezziddin, A. Joe, R. Roedel, R. Fimmers, F.F. Knapp Jr., S. Guhlke, H.J. Biersack, Repeated bone-targeted therapy for hormone-refractory prostate carcinoma: tandomized phase II trial with the new, high-energy radiopharmaceutical rhenium-188 hydroxyethylidenediphosphonate, *J. Clin. Oncol.* 21 (2003) 2869-2875.

68. J.M. O'Sullivan, V.R. McCready, G. Flux, A.R. Norman, F.M. Buffa, S. Chittenden, M. Guy, K. Pomeroy, G. Cook, J. Gadd, J. Treleaven, A. Al-Deen, A. Horwich, R.A. Huddart, D.P. Dearnaley, High activity Rhenium-186 HEDP with autologous peripheral blood stem cell rescue: a phase I study in progressive hormone refractory prostate cancer metastatic to bone, *Br. J. Cancer*. 86 (2002) 1715-1720.

69. N.O. Kucuk, E. Ibis, G. Aras, S. Baltaci, G. Ozalp, Y. Beduk, N. Canakci, A. Soylu, Palliative analgesic effect of Re-186 HEDP in various cancer patients with bone metastases, *Ann. Nucl. Med.* 14 (2000) 239-245.

70. C. Franzius, S. Bielack, S. Flege, J. Sciuk, H. Jurgens, O. Schober, Prognostic significance of (18)F-FDG and (99m)Tc-methylene diphosphonate uptake in primary osteosarcoma, *J. Nucl. Med.* 43 (2002) 1012-1017.

71. J. Yahara, M. Noguchi, S. Noda, Quantitative evaluation of bone metastases in patients with advanced prostate cancer during systemic treatment, *B.J.U. Int.* 92 (2003) 379-384.

72. W. Brenner, K.H. Bohuslavizki, N. Sieweke, S. Tinnemeyer, M. Clausen, E Henze, Quantification of diphosphonate uptake based on conventional bone scanning, *Eur. J. Nucl. Med.* 24 (1997) 1284-1290.

73. T. Nishimura, T. Iizuka, Evaluation of the pathophysiology of odontogenic maxillary sinusitis using bone scintigraphy, *Int. J. Oral. Maxillofac. Surg.* 31 (2002) 389-396.

74. J.H. Turner, P.G. Claringbold, E.L. Hetherington, P. Sorby, A.A. Martindale, A phase I study of samarium-153 ethylenediaminetetramethylene phosphonate therapy for disseminated skeletal metastases, *J. Clin. Oncol.* 7 (1989) 1926-1931.

75. A. Ahonen, H. Joensuu, J. Hiltunen, M. Hannelin, J. Heikkila, M. Jakobsson, J. Jurvelin, K. Kairemo, E. Kumpulainen, J. Kulmala, Samarium-153-EDTMP in bone metastases, *J. Nucl. Biol. Med.* 38 (1994) 123-127.

76. M. Eisenhut, R. Berberich, B. Kimmig, E. Oberhausen, Iodine-131-labeled diphosphonates for palliative treatment of bone metastases: II. Preliminary clinical results with iodine-131 BDP3, *J. Nucl. Med.* 27 (1986) 1255-1261.

77. C.L. Eaton, R.E. Coleman, Pathophysiology of bone metastases from prostate cancer and the role of bisphosphonates in treatment, *Cancer Treat. Rev.* 29 (2003) 189-198.

78. P.I. Croucher, C.M. Shipman, B. Van Camp, K. Vanderkerken, Bisphosphonates and osteoprotegerin as inhibitors of myeloma bone disease, *Cancer*. 97(2003) 818-824.

79. L. Trynda-Lemiesz, H. Kozlowski, B.K. Keppler, Effect of cis-, trans-diamminedichloroplatinum(II) and DBP on human serum albumin, *J. Inorg. Biochem.* 77 (1999) 141-146.

80. M.J. Bloemink, J.J.H. Diederen, J.P. Dorenbos, R.J. Heetebrij, B.K Keppler, J. Reedijk, Calcium ions do accelerate the DNA binding of new antitumor-active platinum aminophosphonate complexes, *Eur. J. Inorg. Chem.* 10 (1999) 1655-1657.

81. M. Galanski, S. Slaby, M.A. Jakupec, B.K. Keppler, Synthesis, characterization, and in vitro antitumor activity of osteotropic diam(m)ineplatinum(II) complexes bearing a N,N-bis(phosphonomethyl)glycine ligand, *J. Med. Chem.* 46 (2003) 4946-4951.

82. E. Brzezinska-Blaszczyk, M. Mincikiewicz, J. Ochocki, Effect of cisplatin and cis-platinum (II) phosphonate complex on murine mast cells, *Eur. J. Pharmacol.* 298 (1996) 155-158.

83. L. Tusek-Bozic, F. Frausin, V. Scarcia, A. Furlani, Synthesis, characterization and antitumor activity of platinum(II) complexes with diethyl and monoethyl 2-quinolylmethylphosphonates, *J. Inorg. Biochem.* 95 (2003) 259-269.

84. O. Fabulet, G. Sturtz, Synthesis of gem-bisphosphonic doxorubicin conjugates, *Phosph. Sul. Sili. Rel. Elem.* 101 (1995) 225-234.

85. G. Sturtz, G. Appere, K. Breistol, O. Fodstad, G. Schwartsmann, H.R.A. Hendriks, Study of the delivery-targeting concept applied to antineoplastic drugs active on human osteosarcoma. 1. Synthesis and biological-activity in nude-mice carrying human osteosarcoma xenografts of gem-bisphosphonic methotrexate analogs, *Eur. J. Med. Chem.* 27 (1992) 825-833.

86. F. Hosain, R.P. Spencer, H.M. Couthon, G.L. Sturtz, Targeted delivery of antineoplastic agent to bone: biodistribution studies of technetium-99m-labeled gem-bisphosphonate conjugate of methotrexate, *J. Nucl. Med.* 37 (1996) 105-107.

87. H. Uludag, N. Kousinioris, T. Gao, D. Kantoci, Bisphosphonate conjugation to proteins as a means to impart bone affinity, *Biotechnol. Prog.* 16 (2000) 258-267.

88. H. Uludag, T. Gao, G.R. Wohl, D. Kantoci, R.F. Zernicke, Bone affinity of a bisphosphonate-conjugated protein in vivo, *Biotechnol. Prog.* 16 (2000) 1115-1118.

89. H. Uludag, J. Yang, Targeting systemically administered proteins to bone by bisphosphonate conjugation, *Biotechnol. Prog.* 18 (2002) 604-611.

CHAPTER II

IMPARTING BONE AFFINITY ONTO GLYCOPROTEINS THROUGH THE CONJUGATION OF BISPHOSPHONATES[1]

[1] The contents of this chapter have been previously published in: Gittens SA, Matyas JR, Zernicke RF and Uludağ H. Imparting Bone Affinity onto Glycoproteins through the Conjugation of Bisphosphonates. *Pharmaceutical Research*, (2003) 20(7): 978-987.

INTRODUCTION

Currently prescribed agents for the treatment of osteoporosis include estrogens, selective estrogen receptor modulators, such as tamoxifene and raloxifene, in addition to the bisphosphonates class of molecules (**1**). The usefulness of these agents, however, is rather limited as they merely halt the resorption of bone, and as such, fail to reverse the progressive loss of bone mineral density associated with the disease to levels seen prior to its onset. One emerging prospect in the treatment of osteoporosis is the use of growth factors that are capable of stimulating deposition of new bone upon their systemic administration (reviewed in **2**). Typically, these ubiquitous growth factors mediate their bone formation effects by promoting the mitogenesis and morphogenesis of cells residing at skeletal tissues. Given their pleiotropic nature, however, their exogenous administration is often associated with various unwanted side effects at extraskeletal sites (**2**). For example, the intravenous administration of an optimal dose of basic fibroblast growth factor (bFGF) has been shown to result in deleterious anatomical changes in both the kidney and lung (**3, 4**). To minimize such adverse effects, which arise as a result of their non-specific distribution throughout the body, a means of delivering these osteogenic growth factors to bone is required.

To this end, we have previously shown that direct conjugation of 1-amino-1,1-diphosphonate methane (aminoBP) onto the lysine amino acid residues of bovine serum albumin using sulfo-succinimidyl-4-(N-maleimidomethyl)-cyclohexane-1-carboxylate (sulfo-SMCC), resulted in an increased affinity for various bone matrices *in vitro* (**5**). Subsequent studies have shown that these conjugates exhibited an enhanced retention when administered intra-osseously to femurs (**6**); as well as an increased localization to

bones (i.e. femur and tibia) when administered either intravenously or subcutaneously (7). Since the conjugates were obtained by attaching aminoBP onto the protein's core, there is a possibility that this means of conjugation *may* inadvertently alter the protein's pharmacophore and compromise the protein's inherent bioactivity. As a result, we sought to develop an alternative means that might circumvent any difficulties that this particular means of conjugating bisphosphonate may elicit.

In delineating an alternative method, we decided to take advantage of the fact that the vast majority of mammalian proteins undergo some degree of post-translational glycosylation (between <1% to >99% by molecular weight) (**8, 9**). Although these carbohydrate groups mediate a variety of functions, some appear to have no biologically relevant significance (**9**). It was previously shown that the oxidation of carbohydrate diols yields functional aldehyde groups which can serve as the basis for subsequent chemical modifications (**10**). This approach has been used for antibody modifications, such as immobilization onto surfaces and radioactive / fluorescent labeling (**10, 11**), derivatization of cell-surface glycoproteins (**12**) and conjugation of targeting moieties onto bioactive proteins (**13, 14**). As such, it was our intent to develop a chemistry that would use the oxidation of carbohydrate groups as a means through which bisphosphonates (BPs) could be conjugated onto glycoproteins. Bovine fetuin was chosen as a model glycoprotein for this study due to its relative abundance of carbohydrate groups (22% of its molecular weight (**15**)). In addition, its 23 lysine amino acid residues also make it a suitable candidate for aminoBP-conjugation via the SMCC conjugation.

Described herein is a novel method to conjugate aminoBP onto fetuin's carbohydrate moieties as a means of enhancing its bone affinity. The conjugate affinity

for various bone matrices was assessed and compared to conjugates obtained from the previously established SMCC conjugation.

MATERIALS AND METHODS

Materials

4-(maleimidomethyl)cyclohexane-1-carboxyl-hydrazide (MMCCH), succinimidyl-4-(N-maleimidomethyl)-cyclohexane-1-carboxylate (SMCC) and sulfo-SMCC were acquired from Molecular Biosciences (Boulder, CO). Bovine fetuin (lot #59H7616), 2-iminothiolane (2-IT), bovine adult serum, sodium m-periodate ($NaIO_4$), trichloroacetic acid (TCA), 1,3,4,6-tetrachloro-3α,6α-diphenylglycouril (TCDG) and pre-cast mini-polyacrylamide, 4-20% Tris-HCl gels were obtained from Sigma Aldrich (St. Louis, MO). $Na^{125}I$ (in 0.1M NaOH) was obtained from Perkin Elmer (Wellesley, MA). 0.9% NaCl was from Baxter Corporation (Toronto, ON). Piperazine was acquired from General Intermediates of Canada (Edmonton, AB). 2,4-dinitrophenylhydrazine (DNP) was from Kodak (Rochester, NY). N,N-dimethylformamide (DMF) was from Caledon Laboratories (Georgetown, ON). The Spectra/Por dialysis tubing with MW cutoff of 12-14,000 Da was acquired from Spectrum Laboratories (Rancho Dominguez, CA). Sodium dodecylsulfate (SDS) and Coomassie Blue R-250 were acquired from Bio-Rad (Hercules, CA). Bromophenol blue was from Serva Feinbiochemica (Heidelberg, Germany). The hydroxyapatite (HA) and aminoBP were prepared as described in (**16**) and (**5**), respectively. The piperazine buffer (pH 5, 7 and 9) was prepared by mixing 0.1 M piperazine with desired amounts of 10 mM HCl. 0.1 M phosphate (pH 7.4), and 0.1 M carbonate (pH 10) buffers were prepared as described (**5**), whereas the 0.1 M sodium

acetate buffer was prepared as described in (**14**). The SDS-glycine sample buffer for electrophoresis was prepared by adding 10% (w/v) SDS, glycerol, 0.1% (w/v) bromophenol blue, 0.5 M Tris-HCl (pH 6.8), and dH_2O in a 4:2:1:2.5:10 fashion. The SDS-PAGE running buffer was prepared by the addition of 2.9% (w/v) Trizma Base, 14.4% (w/v) glycine, and 1.0% (w/v) SDS in dH_2O.

AminoBP Conjugation onto Fetuin

Fetuin-AminoBP Conjugation Using SMCC ***(Figure 2-1a)***: Conjugation by SMCC was performed according to a previously published procedure (**5**). Fetuin (15 mg/ml in 0.1 M phosphate buffer) was incubated for 2.5 h with 10 mM of either sulfo-SMCC or SMCC, two heterobifunctional crosslinkers with $-NH_2$ and –SH reactive groups. Separately, aminoBP was thiolated by incubating equal volumes of aminoBP (80 mM in 0.1 M phosphate buffer) with 2-IT solution (40 mM in 0.1 mM phosphate buffer) for 2.5 h. The product from this reaction was then directly added to SMCC-reacted fetuin in equal volumes for 1.5 h. In order to remove the unreacted reagents, the final conjugate was thoroughly dialyzed against 0.1 M carbonate buffer (x 3) and dH_2O (x2).

Fetuin-AminoBP Conjugation Using MMCCH ***(Figure 2-1b)***: The vicinal hydroxide groups within fetuin's carbohydrate moieties were selectively oxidized (**14**) by treating fetuin (15.5 mg/ml in 0.1 M acetate buffer) with 4 mM of $NaIO_4$. Following a 2.5 h incubation, oxidization was halted by extensive dialysis against dH_2O and subsequently against 0.1 M acetate buffer. The oxidized fetuin was then reacted for 2.5 h with 10 mM MMCCH (stock solution dissolved as 150 mM in DMF), a heterobifunctional crosslinker

whose nucleophilic hydrazine and electrophilic maleimide moieties react with aldehyde and -SH groups, respectively. Thiolated aminoBP, which had been prepared as described above, was then added to the MMCCH-reacted fetuin product at equal volumes. After 1.5 h incubation, the conjugate was dialyzed extensively against 0.1 M carbonate buffer and subsequently dH_2O to remove unreacted starting material.

Analysis of the Conjugates

Bradford Protein Assay **(17)**: The protein reagent used consisted of 0.01% (w/v) Coomassie Blue R-250, 4.7% (w/v) ethanol, and 8.5% (w/v) phosphoric acid. A 50 µl sample was added to 1 ml of the protein reagent and the absorbance was determined at 595 nm. Serially diluted bovine fetuin in dH_2O was used for the calibration curve.

DNP Assay for Aldehydes **(18)**: 2.5 ml of 0.2 mM DNP (in 1 M HCl) was added to 50 µl of oxidized protein, incubated for 1 h at 37 °C and the absorbance of the samples was determined at 370 nm. Serially diluted formaldehyde (in dH_2O) was used for the calibration curve. Once the aldehyde and protein concentrations were quantified, the number of aldehyde groups per fetuin was calculated (mol:mol ratio).

Phosphate Assay: The phosphate assay was modified from the original procedure of Ames **(19)** and was previously described **(5)**. A calibration curve consisting of known concentrations of aminoBP dissolved in dH_2O was utilized. The phosphate concentrations generated here were used in combination with the results from the protein assay to yield the number of aminoBPs conjugated onto fetuin (mol:mol ratio).

SDS-PAGE: Approximately 10 μg of protein sample was mixed with an SDS-glycine sample buffer and loaded onto a 4-20% Tris-HCl polyacrylamide gel. The samples were run at 150V for 1.5 h in an SDS-glycine running buffer. The gels were then stained overnight using a Coomassie Blue R-250 (0.1% w/v Coomassie Blue R-250 in 10:10:80 = methanol:acetic acid:dH_20) and scanned on a flat-bed scanner.

Assessment of Mineral Affinity

HA Binding: The details of the HA binding assay were described previously (5). Briefly, an aliquot of sample (~25 μg) was added to a microcentrifuge tube containing 10 mg of HA with 150 mM phosphate buffer (pH 7.4). This phosphate molarity had been previously determined to provide the optimal conditions for differentiating HA binding between the conjugate and unmodified glycoprotein. The samples were shaken for 2.5 h at room temperature, centrifuged, and the protein concentration in the supernatant was subsequently determined using the Bradford assay. HA affinity (expressed as %binding) was calculated as follows: 100% x {(protein concentration without HA) – (protein concentration with HA)} ÷ (protein concentration without HA). All binding was assessed in duplicate.

Bone Matrix Binding: The preparation of untreated, demineralized, and ashed bone was as follows. The marrow was purged from the diaphyses of 6-month-old male rat tibiae and femurs and the bones were subjected to multiple freeze-thaw cycles to ensure the non-viability of the cellular content. The samples were subsequently crushed into small fragments and thoroughly washed in dH_2O and absolute ethanol. The bones were either

not processed any further (untreated bone), demineralized in 0.6 M HCl for 72 h (demineralized bone matrix), or ashed at 800°C for 48 h (ashed bone). The samples were stored at 4°C until needed.

The binding was assessed by using ^{125}I-labeled proteins. In tubes previously coated with TCDG (200 µl of 20 µg/ml TCDG in choloroform), 10 µg of protein was added to 50 µl of 0.1 M phosphate buffer (pH 7.4), and 10 µl of 0.01 mCi of Na^{125}I (in 0.1 M NaOH). After reacting for 20 minutes, free ^{125}I was separated from the radiolabeled protein by elution on a NAP-5 column with 0.1 M phosphate buffer (pH 7.4). The use of the NAP column was not suitable for the radiolabeled-MMCCH conjugates. Consequently, these conjugates were dialyzed against 0.05 M phosphate buffer after iodination. After precipitating an aliquot of the samples with 20% TCA, it was confirmed that all iodinated samples contained <5% free ^{125}I. The labeled proteins were added to cold protein to give a radioactive count of 50,000 cpm at 0.1 mg/ml protein concentration. Along with 350 µl of media (refer to Legends for media content), the amount of binding matrix added to microcentrifuge tubes was: 50 mg of untreated bone; 50 mg of ashed bone; 10 mg of demineralized bone matrix; and 8 mg of HA. After periodical shaking over a 3 h period, the samples were centrifuged. The supernatant was collected and the pellet, consisting of the bone matrix, was washed with the binding buffer, and re-centrifuged. This washing procedure was then repeated (x2) and the collected supernatant from each of these steps was subsequently measured separately. Quantification of the radioactivity was then determined using a γ-counter (Wallac Wizard 1470, Turku, Finland). Matrix affinity, expressed as %matrix binding, was calculated as

follows: 100% x (counts in matrix pellet) ÷ { (counts in matrix pellet) + (counts in supernatants) }. All binding was assessed in duplicate.

Conjugate Stability

To investigate the influence of pH on conjugate stability, the conjugates were dialyzed against a 0.1 M piperazine, a universal buffer, at either a pH of 5, 7 or 9. At various time points over the course of one week, aliquots of the dialyzing samples were analyzed to assess the conjugates' affinity for HA. To determine the rate of conjugate degradation, the conjugates were prepared as described before, labeled radioactively, and subsequently dialyzed in 25% serum in saline. At various time points, aliquots were taken and the conjugates' binding affinity for HA was determined. Binding was assessed in duplicate.

Statistical Analysis

Significant differences ($p < 0.05$) within the data were determined by student *t*-test or linear regression analysis. Statistical analysis was performed by S-PLUS Student Ed. 6.0 (Insightful Corp, Seattle, WA).

RESULTS

SMCC-Based Conjugation

Conjugation of aminoBP onto fetuin was initially attempted using sulfo-SMCC. The results had indicated that by independently augmenting the concentrations of either sulfo-SMCC (**Figure 2-2A**) or thiolated aminoBP (**Figure 2-2B**), the number of

aminoBPs conjugated onto fetuin increased proportionally to a maximum of 17.0 aminoBPs/fetuin and 15.2 aminoBPs/fetuin when sulfo-SMCC and thiolated aminoBP concentrations were raised to 20 mM, respectively. The control samples (i.e. reactions with non-thiolated aminoBP in the case when sulfo-SMCC concentration was changed, and reaction with 0 mM sulfo-SMCC in the case when thiolated aminoBP concentration was changed), had less than 2 aminoBPs/fetuin, indicating some degree of aminoBP retention after dialysis, albeit significantly lower than the corresponding conjugates. Using the same samples, an increase in the conjugates' capacity to bind to HA was observed as the number of aminoBPs conjugated to fetuin was increased (**Figures 2-2C** and **2-2D**). All control samples, however, exhibited significantly lower binding irrespective of the concentration of thiolated aminoBP or sulfo-SMCC used in conjugations. Since the control samples in **Figure 2-2B**, which were reacted with sulfo-SMCC, did not exhibit an HA affinity, sulfo-SMCC reaction with fetuin's amine groups did not appear to influence the HA binding of the glycoprotein. Due to cost considerations, all subsequent studies utilized SMCC instead of sulfo-SMCC. As the final conjugation products from both crosslinkers were identical, the substitution of sulfo-SMCC with SMCC was considered inconsequential.

MMCCH-Based Conjugation

Fetuin's intrinsic aldehyde content (i.e. 7.3 aldehydes per fetuin) was initially found to be insufficient for aminoBP conjugation. As a result, the first step in MMCCH-based conjugation was the $NaIO_4$-mediated introduction of aldehyde groups onto fetuin's carbohydrate groups. Results from this process gave a linear relationship between $NaIO_4$

concentration and the number of aldehydes introduced per fetuin (**Figure 2-3**). Given that a concentration of 4 mM $NaIO_4$ not only yielded an adequate number of aldehyde groups (~30 aldehyde groups/molecule of fetuin) but was also considered mild enough to circumvent the complete destruction of fetuin's carbohydrate groups (**19**), this concentration was typically chosen for subsequent reactions. It was found that the product of this oxidation process was stable at 4°C for in excess of a month, as determined by the DNP and Bradford protein assays.

The conjugation of aminoBP to fetuin was initially attempted by reacting its $-NH_2$ directly with the aldehyde moieties of oxidized fetuin via the formation of a Schiff base. No effective conjugation was noted by this approach (data not shown). As a result, MMCCH was then used to facilitate the chemical conjugation of aminoBPs onto fetuin's aldehyde moieties. Increasing $NaIO_4$ concentrations to modulate the number of aldehydes introduced onto each molecule of fetuin as well as thiolated aminoBP concentrations, led to an increase in the number of aminoBPs conjugated onto fetuin (**Figures 2-4A** and **2-4B**, respectively). Similar to the SMCC-based chemistry, increasing MMCCH concentrations led to an increase in the number of aminoBPs conjugated onto fetuin, which corresponded to an increase in the conjugate's ability to bind to HA (data not shown). A maximum of 7.0 aminoBPs per fetuin was achieved under the experimental conditions for MMCCH-conjugation. The propensity for these samples to bind to HA was then determined. As expected, the results indicated that increasing the number of conjugated aminoBPs resulted in a proportionally linear increase in the conjugates' affinity for HA (**Figures 2-4C** and **2-4D**). Typically, the number of aminoBPs conjugated per fetuin for these controls, which exhibited nominal binding to

HA, was < 1. As seen in **Figure 2-4C**, the degree of oxidation did not affect the glycoprotein's intrinsic affinity for HA. Since control samples in **Figures 2-4D**, which were reacted with MCCHH, did not exhibit an HA affinity, MMCCH reaction with the fetuin's glycan groups did not appear to influence the HA binding of the glycoprotein.

Protein Purity by SDS-PAGE

Gel electrophoresis was employed to determine whether inadvertent protein-protein crosslinking was occurring as a result of using either crosslinker or through the formation of a Schiff base between fetuin $-NH_2$ and aldehyde groups (**21**). Given that the molecular weight of fetuin is 48.4 kDa, protein-protein crosslinking would have manifested itself as ≥100 kDa protein bands on the gels. Our results indicated that there were no visible changes in the intensity of native fetuin's band of 48.4 kDa and no visible increase in the higher molecular weight bands as the concentrations of SMCC and MMCCH was increased to 10 mM and 20 mM, respectively, while thiolated aminoBP concentration used was 20 mM (data not shown). As such, any protein:protein crosslinking was deemed negligible.

Comparison of the Mineral Affinity of MMCCH and SMCC Conjugates

To compare the ability of two types of conjugates to bind to HA, each conjugate's capacity to bind to HA was plotted as a function of the number of conjugated aminoBPs (**Figure 2-5**). The observed trend suggested that increasing the number of conjugated aminoBPs resulted in a linear increase in conjugate's affinity for HA, regardless of the crosslinker used. The MMCCH-conjugates' binding to HA rose to a maximum of ~77%

when a maximal number of ~7.0 aminoBPs were conjugated onto fetuin. Similarly, a binding of ~86% was achieved when ~9.0 aminoBPs were conjugated via SMCC. Increasing the number of conjugated aminoBPs past this threshold, however, did not enhance mineral affinity for the SMCC conjugates. The HA binding of the MMCCH-based conjugates could not be tested in this region since this crosslinker did not give any conjugates in this range. A comparison between the slopes in the linear regions (i.e. < 8 aminoBPs/fetuin) for each conjugate revealed no significant differences between the two conjugation approaches.

To investigate conjugate stability, the effect of pH on the conjugates' affinity to HA was determined. A comparison of the slopes (from % HA binding vs. times curves) revealed no significant differences in either of the conjugates' affinity for HA when in a basic, neutral or acidic piperazine buffered environment (data not shown). These results suggest that the conjugates' stability, as determined by its affinity for HA, was not adversely affected by the pH of the incubating medium. To assess conjugate stability, conjugate binding to HA in 25% adult bovine serum was determined over a one week time period. As shown in **Figure 2-6**, the binding of the SMCC and MMCCH conjugates were initially ~71% and ~58%, respectively. The control samples (i.e. control for SMCC-based chemistry: fetuin incubated with thiolated aminoBP without SMCC; and for the MMCCH-based chemistry: oxidized fetuin incubated with the crosslinker without aminoBP), did not exhibit a change in HA binding over time. The conjugates' binding to HA, on the other hand, decreased gradually with time (~3% per day for both types of conjugates). Comparing the two slopes for parallelism revealed no statistically significant differences between the two conjugates' rate of degradation.

The relative stability of the conjugates in serum led us to explore their bone mineral affinity in serum, a medium that better represents *in vivo* conditions than the phosphate buffer previously used. The matrices utilized were untreated, ashed, demineralized rat bone and synthetic HA in 50% bovine adult serum (**Figure 2-7**). With the exception of demineralized bone matrix, the conjugates' binding to various bone matrices increased in response to increasing number of conjugated aminoBPs per fetuin. With demineralized bone matrix, however, MMCCH-conjugates, but not SMCC-conjugates, gave significant binding. For all matrices, as the number of aminoBPs/fetuin increased, it was found that the MMCCH-conjugate's had a statistically significantly higher affinity over the SMCC conjugate. By dividing the maximum binding capacity that the MMCCH-conjugate had for a given matrix by the maximum binding capacity that the SMCC-conjugate had for the same matrix, a 2.6, 2.0, 30.5, and 1.84-fold difference in the conjugates' ability to bind to untreated, ashed, demineralized bone and HA, respectively, was revealed.

DISCUSSION AND CONCLUSIONS

As part of the initial phase of developing a general approach for systemic delivery of any glycosylated protein capable of eliciting a desired pharmacological response at skeletal sites, it was the goal of this study to develop a means of conjugating bisphosphonates onto the carbohydrate moieties of a model protein, fetuin. The proposed method was designed as an alternative to the previously established SMCC-based conjugation where aminoBP was conjugated onto the protein through the direct chemical modification of the lysine amino acid residues. As a result, we were concerned that such

a modification of the protein backbone may inadvertently lead to an adverse change in the protein's tertiary structure and/or interfere with its receptor binding/activation, which might culminate in the loss of the protein's desired pharmacological activity on skeletal tissues. Most non-cytosolic proteins undergo some degree of post-translational glycosylation endogenously. Much like the notorious heterogeneity associated with their chemical structure, the function of these covalently attached carbohydrate groups vary widely. Some of the physicochemical and biological roles the carbohydrates mediate include: protein folding, stability and solubility; regulation of glycoprotein intracellular trafficking and localization, as well as modulation of enzyme and hormone activity (**22**). Based on the observed bioactivity of recombinant proteins expressed in prokaryotic systems, which are inherently incapable of performing post-translational glycosylation, it is apparent that the absence of carbohydrate residues does not have any adverse ramifications on their ability to elicit a biological response (**9**). In fact, the non-glycosylated forms of numerous osteogenic proteins such as bone morphogenetic protein (BMP)-2 (**23**), BMP-4 (**24**), BMP-7 (**25**), BMP-14 (also known as Growth and Differentiation Factor-5, GDF-5) (**26**), BMP-13, (GDF-6) (**26**), and BMP-12 (GDF-7) (**26**) have either been shown to induce effective bone formation or elicit other musculoskeletal effects typical of the protein's normal biological function. bFGF produced in a prokaryotic system has also retained its characteristic mitogenic activity (**27**). Given the biologically non-essential nature of the carbohydrate moieties of these musculoskeletally-active proteins, the conjugation of aminoBP onto their carbohydrate groups should not affect the proteins' inherent bioactivity.

The results described herein demonstrated that fetuin, a glycoprotein chosen for its relatively high degree of glycosylation, was an appropriate candidate to undergo SMCC-based aminoBP conjugation onto its proteinaceous backbone, as well as MMCCH-based aminoBP conjugation, to its carbohydrate moieties. It was shown that the conjugation efficiency (i.e., number of conjugated aminoBPs per protein) was varied by the reagent concentrations used in either conjugation procedures. The aminoBP was utilized as a prototypical BP for our purposes since it is one of the simplest BPs synthesized, contains a functional $-NH_2$ group for the necessary conjugations, and acts as a model for a range of other $-NH_2$ containing BPs currently studied in the context of bone biology (e.g., pamidronate, alendronate, risedronate, and ibandronate) **(5,28)**. Despite our desire, we were unable to use this functional group for direct conjugation with the introduced aldehyde groups on fetuin (as well as direct conjugation with succinimide ester of SMCC). Using a simple HA-binding assay that was previously shown to correlate with *in vivo* bone affinity **(5, 7)**, it was ascertained that an increase in the number of conjugated aminoBPs led to an increase in conjugate binding to HA. This was assessed under conditions (150 mM phosphate) that were not conducive for the electrostatic binding of the unmodified protein to HA. Nevertheless, a nominal degree of HA binding was noted, presumably due to protein carboxyl groups forming weak complexes with the fixed Ca^{2+} on the mineral surface **(29, 30)**. As was evident using the SMCC-mediated conjugation, an upper limit of HA binding (~95% under the experimental conditions) was reached once >9 aminoBPs were conjugated onto fetuin. It was not possible to assess whether a similar behavior was exhibited with MMCCH-mediated conjugation, since it was not experimentally possible to obtain conjugates with

>7 aminoBPs per protein. This was unexpected since an abundant (>30) number of aldehyde groups was introduced onto the glycoprotein, suggesting that MMCCH conjugation utilized only a small fraction of the available groups. A saturable binding kinetics was observed for both conjugates under serum conditions for HA and bone-derived matrices (40-60% for MMCCH and 10-40% for SMCC mediated conjugations, depending on the choice of the matrix). Taken all together, this data suggests that the conjugation of aminoBPs onto fetuin was indeed responsible for imparting the observed bone mineral affinity and that modification beyond a certain threshold did not enhance the bone affinity any further.

Bone matrix binding was also dependent on the conjugation efficiency for both conjugation approaches when the binding was assessed under serum conditions. These conditions, consisting of anions, cations, and other proteins, were believed to offer a more stringent (competitive) environment for protein binding. Unlike HA-binding in phosphate buffer, the MMCCH-conjugate exhibited a significantly higher affinity for the bone matrices than that of the SMCC-conjugate under these conditions. To explain the difference between the binding capacity of the two conjugates, it was postulated that by being conjugated onto the carbohydrate residues, the aminoBPs were further distanced from the glycoproteins' protein core where the conjugated aminoBPs would be subjected to steric interference. Furthermore, conjugation via the flexible carbohydrate moieties may afford the aminoBP molecules an increased range of motion that would enable them to access a mineral matrix more effectively. An unexpected observation was the aminoBP-dependent binding of the MMCCH-conjugates to demineralized bone matrix, to which the SMCC-conjugates did not bind. Although the latter observation suggested that

the mineral content of the bone was minimal, the fact that the MMCCH-conjugates bound to the demineralized bone in an aminoBP-dependent manner indicated that a residual bone mineral might have been left in bone matrix preparations. As with the other matrices, conjugates from the MMCCH-chemistry exhibited a superior affinity for the demineralized matrix compared to the SMCC-mediated conjugation. It is also possible that the binding might be mediated by an alternative mechanism (e.g. a serum mediated process affecting the binding of the 2 types of conjugates differently) which is not clear to us yet. We intend on addressing this issue in future studies by exploring the role of varying the linkage spacing between the BP and the protein molecules, so as to elucidate the role of steric interference on BP-mediated protein binding to bone mineral.

Numerous studies have shown that SMCC conjugates were non-degradable in a variety of environments, including serum-containing media *in vitro*, as well as in *in vivo* models (**31, 32**). MMCCH has been previously used to conjugate STn, a mucin-associated disaccharide epitope over-expressed in human carcinomas, to keyhole limpet hemocyanin, an anti-neoplastic agent (**33, 34**). Unfortunately, the stability of these conjugates was never determined (**33, 34**). It has been shown, however, that hydrazone and thioether bonds, i.e., the linkages formed by the reactive groups of the MMCCH, were inherently stable under aqueous conditions (**14**). Consequently, we expected our conjugates to be stable under the experimental binding conditions, regardless of the conjugation approach. Supporting this hypothesis, the results presented herein suggest that the conjugates' mineral affinity was not influenced by the pH of the medium. Some loss of protein affinity (3% per day) was seen in 25% bovine adult serum over the course of a week but this was similar for both proteins and was likely not to be due to the

differences in the conjugation linkages. Our studies were performed for a longer duration than the previously reported studies (**33, 34**) and may explain the discrepancy. Nevertheless, the two conjugation approaches were considered to have a similar stability when used to impart an aminoBP-mediated bone affinity.

The extent of periodate-mediated carbohydrate oxidation was dependent on the medium pH, the reaction time, the periodate concentration and the temperature (**35**). As a side-reaction, the process of oxidation was found to result in modification of some amino acids, such as cysteine, methionine, tryptophan, and tyrosine (**10**). According to a published review of the literature (**10**), the conditions required to attain this undesirable oxidation of amino acids (120 mM periodate for >6 hours) far exceeds those used in this study (<10 mM for 2 hours). In fact, using periodate concentrations similar to our own, independent investigators have shown no or nominal abrogation of bioactivity for several proteins, such as horse radish peroxidase (**36**), gelonin (**13**), soluble CD4 (**14**), and immunoglobulin G (**35**). As fetuin only served as a model glycoprotein in our studies, its bioactivity was not of interest. Studies, which have examined the effects of deleting the fetuin gene in a mouse model, have shown that the glycoprotein plays a role in the prevention of ectopic microcalcifications (**37**), and affects the process of endochondral bone formation by binding to members of TGF-beta family (including BMPs) and inhibiting their bone-formation activity (**38**). Our long term goal is to apply the described MMCCH approach to glycoproteins such as BMP-2, whose bone forming activity has been unequivocally established. Although the *in vivo* targeting capability of the conjugates was not assessed in this study, it was previously shown that SMCC conjugates with increased affinity to HA also enhanced protein targeting to bone: intravenous

administration of aminoBP-conjugated albumin (SMCC as the linker) led to a 2.0-3.7-fold and 2.2-7.5-fold increase in bone delivery compared to unmodified albumin in normal and osteopenic rats, respectively (7). Similar results were obtained for lysozyme in the same animal models as well (7). Consequently, it is anticipated that the conjugation of aminoBP onto fetuin via the MMCCH approach will enhance the glycoprotein's *in vivo* delivery to bone in a manner similar to previous SMCC-conjugates (5).

In summary, this study described the first attempt to impart a bone mineral affinity onto proteins via the modification of carbohydrate moieties. It is expected that the protein bioactivity will be better preserved by the proposed approach as compared to our previously described approach where the BPs were directed conjugated to the protein core. Based on the results presented in this study, it is also likely that aminoBP conjugation via carbohydrate moieties might exhibit a superior mineral affinity as compared to aminoBP conjugation to the protein core. Previous efforts to conjugate BPs as a means to localize molecules to bone have not been limited to proteins (39). BPs have been conjugated onto radionucleotides and bioactive drugs such as estrogen, anti-neoplastic and anti-inflammatory agents, and the proposed approach could find applications beyond the protein class of therapeutic agents.

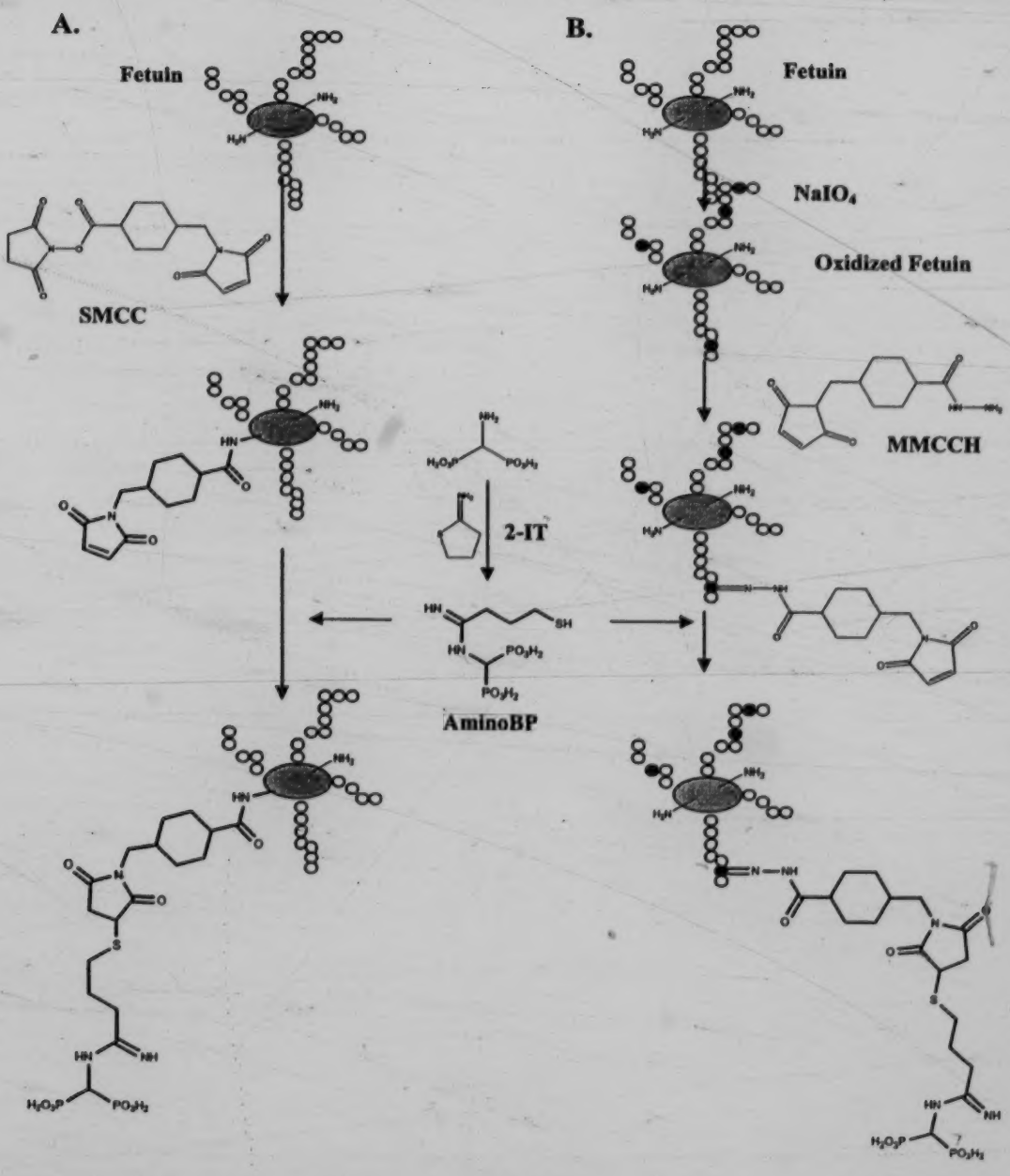

Figure 2-1. A schematic representation of the SMCC (A) and MMCCH (B) mediated conjugation of aminoBP onto fetuin. The former crosslinker used reactive amine groups to facilitate the conjugation of aminoBP directly onto the fetuin's protein backbone whereas the latter crosslinker used the fetuin's carbohydrate groups for conjugation.

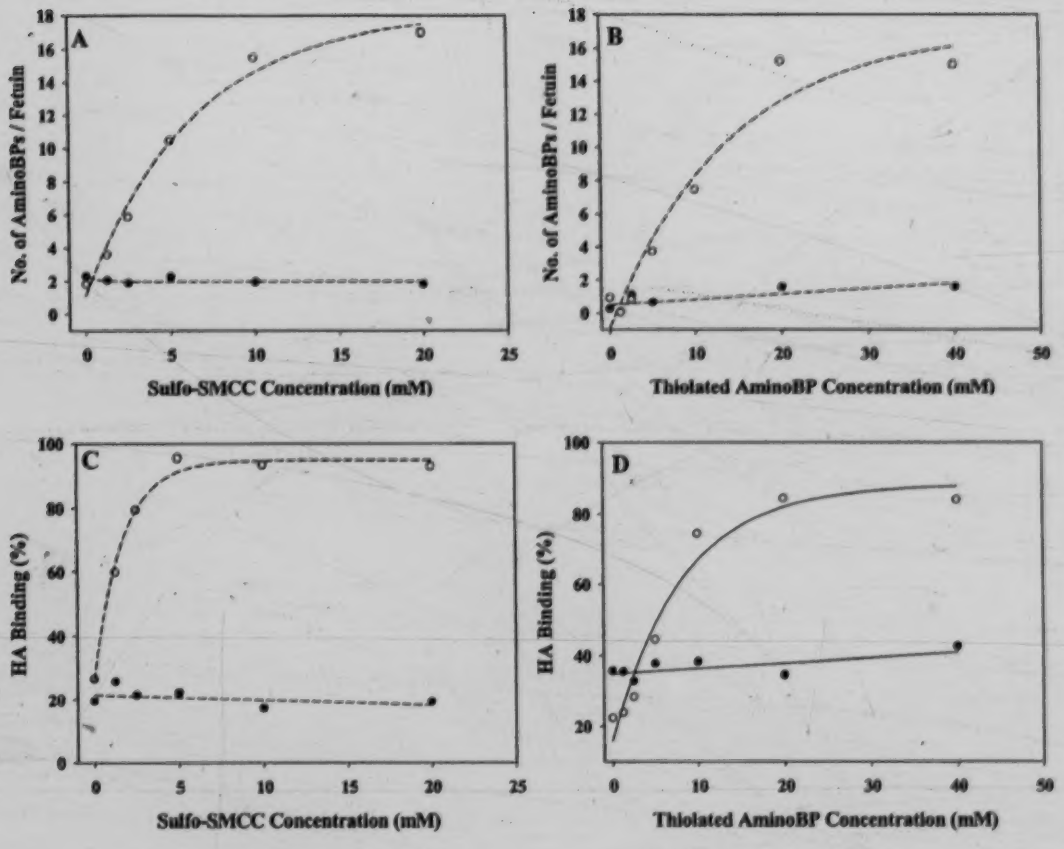

Figure 2-2. The conjugation efficiency (**A** and **B**) and HA binding (**C** and **D**) for fetuin incubated with either un-thiolated aminoBP (•) or thiolated aminoBP (○). The 2-IT/aminoBP concentration was maintained at 10/20 mM in **A** and **C**, whereas sulfo-SMCC concentration was maintained at 10 mM in **B** and **D**. Increasing the sulfo-SMCC concentration increased the number of aminoBP conjugated onto fetuin (**A**), as well as increasing the thiolated aminoBP concentration (**B**). Corresponding increases in the conjugates' affinity for HA was noted for increasing sulfo-SMCC (**C**), and thiolated aminoBP concentrations (**D**).

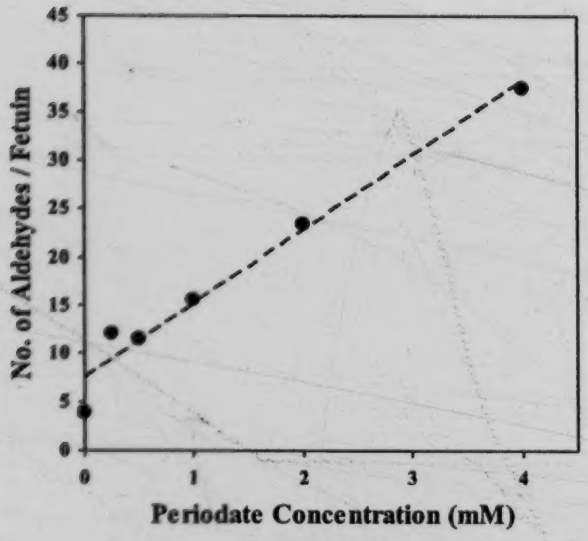

Figure 2-3. Increasing the number of aldehyde groups introduced onto fetuin in a linear fashion ($r^2 = 0.969$) by increasing sodium periodate concentrations used for oxidation.

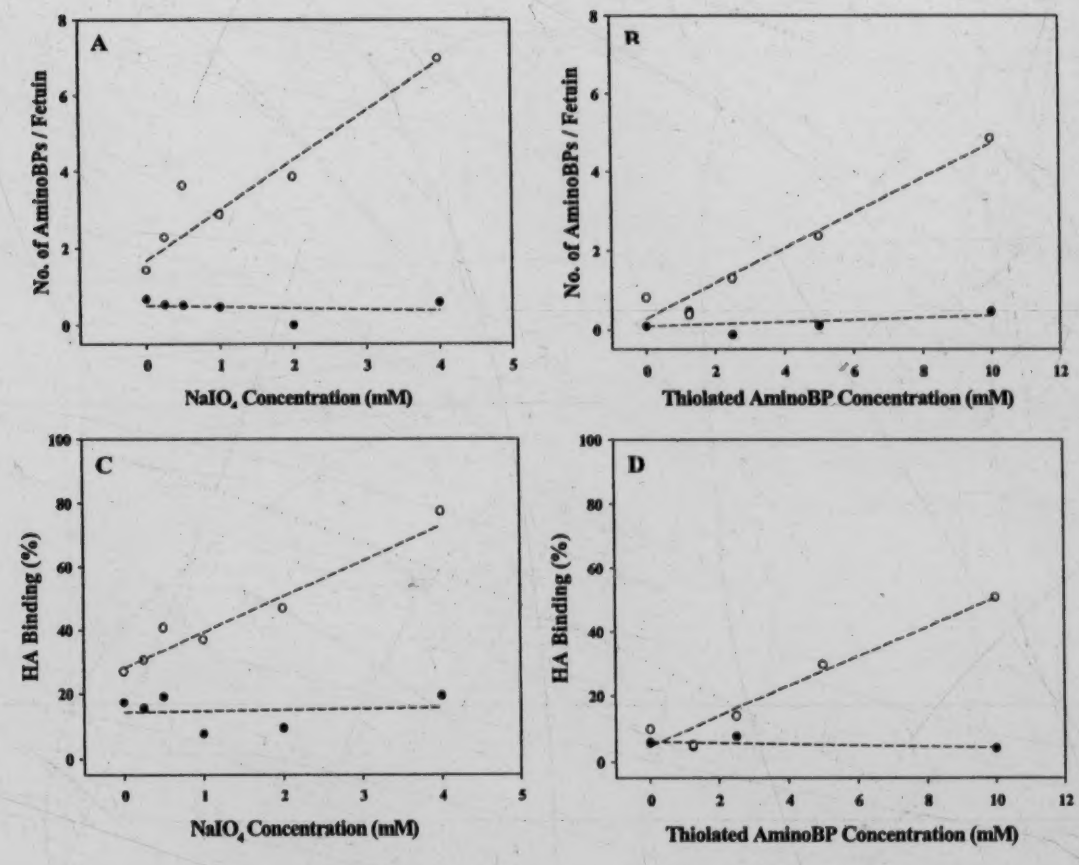

Figure 2-4. The conjugation efficinecy (**A** and **B**) and HA binding (**C** and **D**) for fetuin incubated with either non-thiolated aminoBP (●) or thiolated aminoBP (○). The MMCCH concentration was 10 mM for all samples. The thiolated aminoBP concentration was 10 mM for samples in **A** and **C**, whereas the samples in **B** and **D** were oxidized with 4 mM $NaIO_4$. Increasing the $NaIO_4$ concentration increased the number of aminoBP conjugated onto fetuin (**A**), as well as increasing the thiolated aminoBP concentration (**B**). Corresponding increases in the conjugates' affinity for HA was noted for increasing $NaIO_4$ (**C**), and thiolated aminoBP concentrations (**D**).

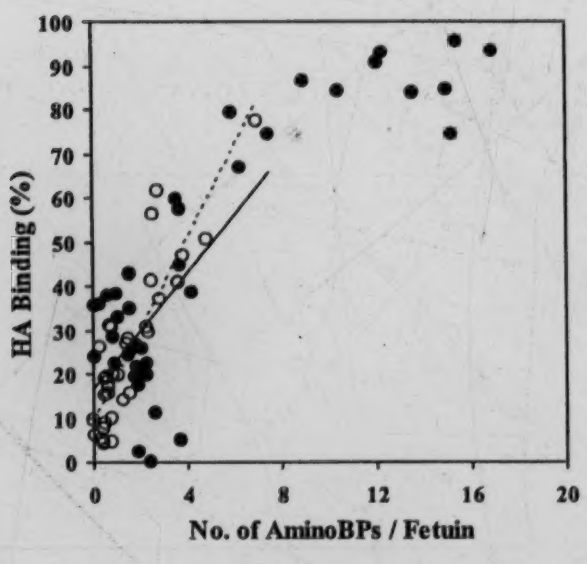

Figure 2-5. Correlation between the number of aminoBP's conjugated per fetuin and the conjugate binding to HA. The MMCCH-conjugates' (○) binding to HA increased in a linear fashion as the number of conjugated aminoBPs increased. While sharing a similar linear trend, the conjugation of more than 9 aminoBP/fetuin did not enhance the sulfo-SMCC-conjugates' (●) capacity to bind to HA. There was no significant difference in the slopes observed in the linear region (<8 aminoBP/fetuin) for the MMCCH- and the SMCC-conjugates (hashed and solid trend lines, respectively).

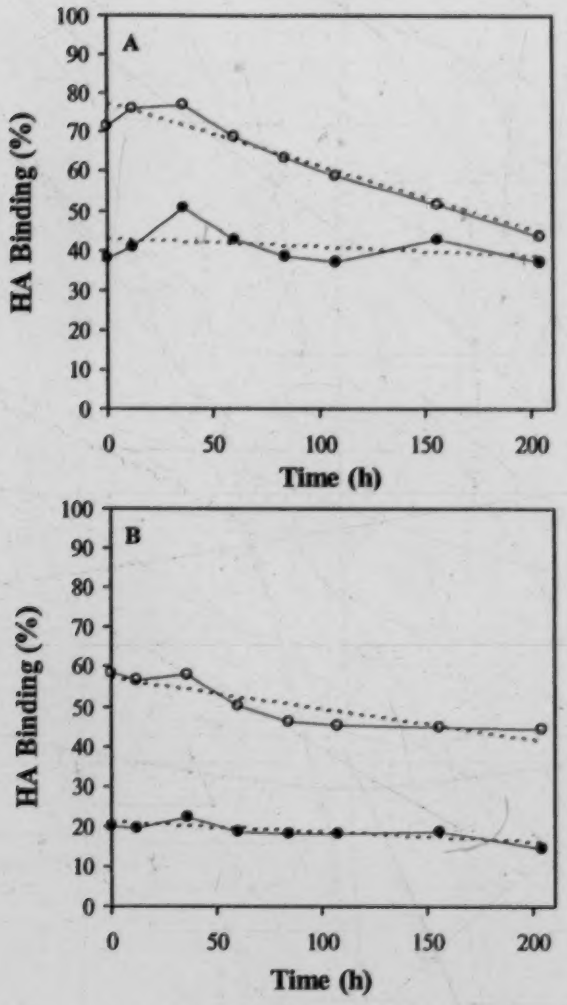

Figure 2-6. The stability of the SMCC- (A) and MMCCH- (B) conjugates was determined as a function of their capacity to bind to HA in 25% adult bovine serum over the course of one week. As time progressed, the binding affinity for the SMCC- and MMCCH- conjugates (○) decreased in a linear fashion (r^2 = 0.95 and 0.77, respectively) while their respective controls (●) remained relatively constant. No significant difference was observed between the two conjugates' decreasing ability to bind to HA.

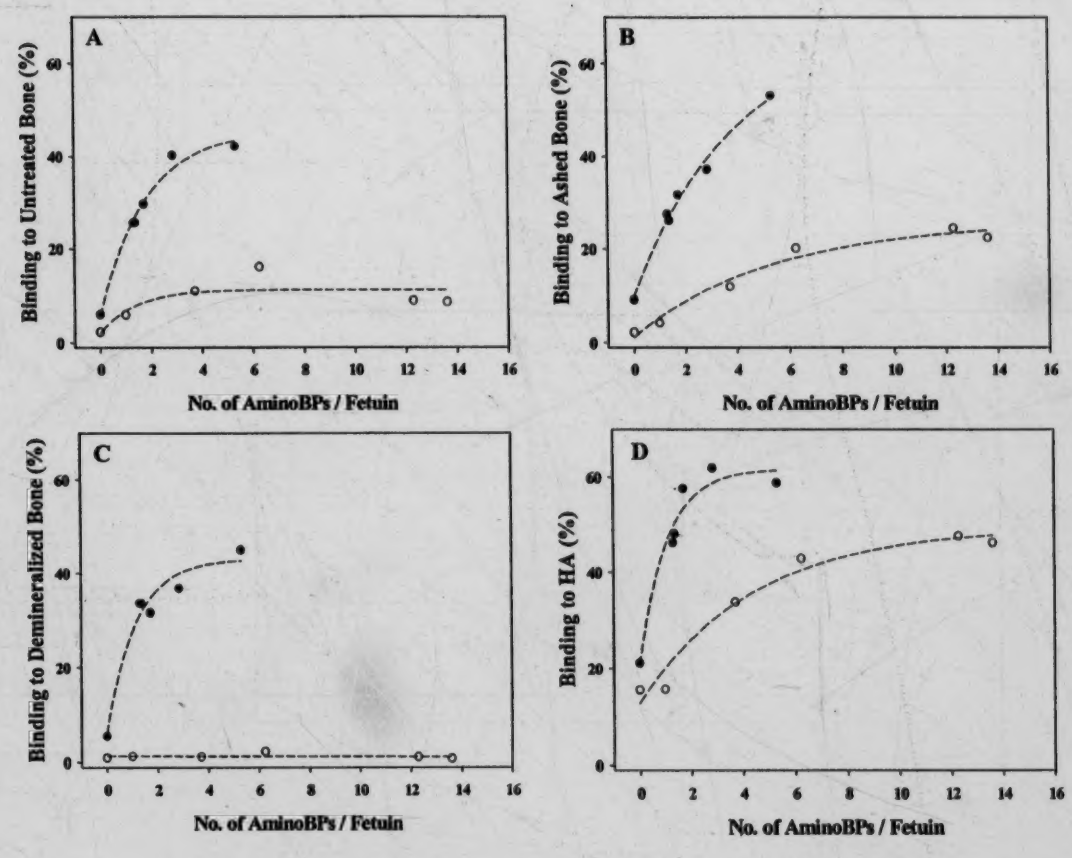

Figure 2-7. Binding of SMCC- (○) and MMCCH- (●) conjugates to various bone matrices in 50% bovine adult serum to untreated bone (**A**), ashed bone (**B**), demineralized bone matrix (**C**) and HA (**D**). In all instances, the matrix binding of the MMCCH-conjugates exceeded to that of SMCC-conjugates.

REFERENCES

1. S. Sherman, Preventing and treating osteoporosis: strategies at the millennium, *Ann. N. Y. Acad. Sci.* 949 (2001) 188-197.

2. S.A. Gittens, H. Uludag, Growth factor delivery for bone tissue engineering, *J. Drug Targeting.* 9 (2001) 407-429.

3. H. Nagai, R. Tsukuda, H. Mayahara, Effects of basic fibroblast growth factor (bFGF) on bone formation in growing rats, *Bone.* 16 (1995) 367-373.

4. G. Mazue, A.J. Newman, G. Scampini, P. Della Torre, G.C. Hard, M.J. Iatropoulos, G.M. Williams, S.M. Bagnasco, The histopathology of kidney changes in rats and monkeys following intravenous administration of massive doses of FCE 26184, human basic fibroblast growth factor, *Toxicol. Pathol.* 21 (1993) 490-501.

5. H. Uludag, N. Kousinioris, T. Gao, D. Kantoci, Bisphosphonate conjugation to proteins as a means to impart bone affinity, *Biotechnol. Prog.* 16:258-267 (2000).

6. H. Uludag, T. Gao, G.R. Wohl, D. Kantoci, R.F. Zernicke, Bone affinity of a bisphosphonate-conjugated protein in vivo, *Biotechnol. Prog.* 16 (2000) 1115-1118.

7. H. Uludag, J. Yang, Targeting systemically administered proteins to bone by bisphosphonate conjugation, *Biotechnol. Prog.* 18 (2002) 604-611.

8. D. Voet J.G. Voet, *Biochemistry*, John Wiley & Sons, New York, 1995.

9. D.F. Wyss, G. Wagner, The structural role of sugars in glycoproteins, *Curr. Opin. Biotechnol.* 7 (1996) 409-416.

10. D.J. O'Shannessy, R.H. Quarles, Labeling of the oligosaccharide moieties of immunoglobulins, *J. Immunol. Methods*. 99 (1987) 153-161.

11. T.O. Harasym, M.B. Bally, P. Tardi, Clearance properties of liposomes involving conjugated proteins for targeting, *Adv. Drug Deliv. Rev.* 32 (1998) 99-118.

12. P.A. De Bank, B. Kellam, D.A. Kendall, K.M. Shakesheff, Surface engineering of living myoblasts via selective periodate oxidation, *Biotechnol. Bioeng.* 81 (2003) 800-808.

13. S.F. Atkinson, T. Bettinger, L.W. Seymour, J.P. Behr, C.M. Ward, Conjugation of folate via gelonin carbohydrate residues retains ribosomal-inactivating properties of the toxin and permits targeting to folate receptor positive cells, *J. Biol. Chem.* 276 (2001) 27930-27935.

14. S.M. Chamow, T.P. Kogan, D.H. Peers, R.C. Hastings, R.A. Byrn, A. Ashkenazi, Conjugation of soluble CD4 without loss of biological activity via a novel carbohydrate-directed cross-linking reagent, *J. Biol. Chem.* 267 (1992) 15916-15922.

15. R.G. Spiro, V.D. Bhoyroo, Structure of the O-glycosidically linked carbohydrate units of fetuin, *J. Biol. Chem.* 249 (1974) 5704-5717.

16. D. Kantoci, J.K. Denike, W.J. Wechter, Synthesis of Aminobisphosphonate, *Synth. Comm.* 26 (1996) 2037-2043.

17. M.M. Bradford, A rapid and sensitive method for the quantitation of microgram quantities of protein utilizing the principle of protein-dye binding, *Anal. Biochem.* 72 (1976) 248-254.

18. R. Fields, H.B. Dixon, Micro method for determination of reactive carbonyl groups in proteins and peptides, using 2,4-dinitrophenylhydrazine, *Biochem. J.* 121 (1971) 587-589.

19. B.N. Ames, Assay of inorganic phosphate, total phosphate, and phosphatases. In E.F. Neufield, and V. Ginsburg (eds.), *Methods in Enzymology, Volume VIII, Complex Carbohydrates*, Academic Press, New York, (1966), pp. 115-117.

20. R.G. Spiro, Periodate Oxidation of the Glycoprotein Fetuin, *J. Biol. Chem.* 239 (1964) 567-573.

21. I. Bouchez-Mahiout, C. Doyen, M. Lauriere, Accurate detection of both glycoproteins and total proteins on blots: control of side reactions occurring after periodate oxidation of proteins, *Electrophoresis*. 20 (1999) 1412-1417.

22. H. Lis, N. Sharon, Protein glycosylation. Structural and functional aspects, *Eur. J. Biochem.* 218 (1993) 1-27.

23. K. Bessho, Y. Konishi, S. Kaihara, K. Fujimura, Y. Okubo, T. Iizuka, Bone induction by Escherichia coli -derived recombinant human bone morphogenetic protein-2 compared with Chinese hamster ovary cell-derived recombinant human bone morphogenetic protein-2, *Br. J. Oral. Maxillofac. Surg.* 38 (2000) 645-649.

24. N.R. Kubler, M. Moser, K. Berr, G. Faller, T. Kirchner, W. Sebald, J.F. Reuther, Biological activity of E. coli expressed BMP-4, *Mund. Kiefer. Gesichtschir.* 2 (1998) S149-S152.

25. T.K. Sampath, J.E Coughlin, R.M. Whetstone, D. Banach, C. Corbett, R.J Ridge, E. Ozkaynak, H. Oppermann, D.C. Rueger, Bovine osteogenic protein is composed of dimers of OP-1 and BMP-2A, two members of the transforming growth factor-beta superfamily, *J. Bio.l Chem.* 265 (1990) 13198-13205.

26. N.M. Wolfman, G. Hattersley, K. Cox, A.J. Celeste, R. Nelson, N. Yamaji, J.L. Dube, E. DiBlasio-Smith, J. Nove, J.J. Song, J.M. Wozney, V. Rosen, Ectopic induction of tendon and ligament in rats by growth and differentiation factors 5, 6, and 7, members of the TGF-beta gene family, *J. Clin. Invest.* 100 (1997) 321-330.

27. G. Garke, W.D. Deckwer, F.B. Anspach, Preparative two-step purification of recombinant human basic fibroblast growth factor from high-cell-density cultivation of Escherichia coli, *J. Chromatogr. B. Biomed. Sci. Appl.* 737 (2000) 25-38.

28. K. Thompson, J.E. Dunford, F.H. Ebetino, M.J. Rogers. Identification of a bisphosphonate that inhibits isopentenyl diphosphate isomerase and farnesyl diphosphate synthase, *Biochem. Biophys. Res. Commun.* 290 (2002) 869-873.

29. M.J. Gorbunoff, The interaction of proteins with hydroxyapatite. II. Role of acidic and basic groups, *Anal. Biochem.* 136 (1984) 433-439.

30. M. Suzuki, H. Shimokawa, Y. Takagi, S. Sasaki, Calcium-binding properties of fetuin in fetal bovine serum, *J. Exp. Zool.* 270 (1994) 501-507.

31. C.F. Foulon, D.D. Bigner, M.R. Zalutsky, Preparation and characterization of anti-tenascin monoclonal antibody-streptavidin conjugates for pretargeting applications, *Bioconjug. Chem.* 10 (1999) 867-876.

32. H. Karacay, R.M. Sharkey, S.V. Govindan, W.J. McBride, D.M. Goldenberg, H.J. Hansen, G.L. Griffiths, Development of a streptavidin-anti-carcinoembryonic antigen antibody, radiolabeled biotin pretargeting method for radioimmunotherapy of colorectal cancer. Reagent development, *Bioconjug. Chem.* 8 (1997) 585-594.

33. G. Ragupathi, R.R. Koganty, D. Qiu, K.O. Lloyd, P.O. Livingston, A novel and efficient method for synthetic carbohydrate conjugate vaccine preparation: synthesis of sialyl Tn-KLH conjugate using a 4-(4-N-maleimidomethyl) cyclohexane-1-carboxyl hydrazide (MMCCH) linker arm, *Glycoconj. J.* 15 (1998) 217-221.

34. G. Ragupathi, L. Howard, S. Cappello, R.R. Koganty, D. Qiu, B.M. Longenecker, M.A. Reddish, K.O. Lloyd, P.O. Livingston, Vaccines prepared with sialyl-Tn and sialyl-Tn trimers using the 4-(4-maleimidomethyl)cyclohexane-1-carboxyl hydrazide linker group result in optimal antibody titers against ovine submaxillary mucin and sialyl-Tn-positive tumor cells, *Cancer Immunol. Immunother.* 48 (1999) 1-8.

35. C.A. Wolfe, and D.S. Hage, Studies on the rate and control of antibody oxidation by periodate, *Anal. Biochem.* 231 (1995) 123-130.

36. D. Horak, M. Karpisek, J. Turkova, M. Benes, Hydrazide-functionalized poly(2-hydroxyethyl methacrylate) microspheres for immobilization of horseradish peroxidase. *Biotechnol. Prog.* 15 (1999) 208-215.

37. W. Jahnen-Dechent, T. Schinke, A. Trindl, W. Muller-Esterl, F. Sablitzky, S. Kaiser, M. Blessing, Cloning and targeted deletion of the mouse fetuin gene, *J. Biol. Chem.* 272 (1997) 31496-31503.

38. M. Szweras, D. Liu, E.A. Partridge, J. Pawling, B. Sukhu, C. Clokie, W. Jahnen-Dechent, H.C. Tenenbaum, C.J. Swallow, M.D. Grynpas, J.W. Dennis, alpha 2-HS glycoprotein/fetuin, a transforming growth factor-beta/bone morphogenetic protein antagonist, regulates postnatal bone growth and remodeling, *J. Biol. Chem.* 277 (2002) 19991-19997.

39. H. Uludag, Bisphosphonates as a foundation of drug delivery to bone, *Curr. Pharm. Des.* 8 (2002) 1929-1944.

CHAPTER III

IMPACT OF TETHER LENGTH ON BONE MINERAL AFFINITY OF PROTEIN-BISPHOSPHONATE CONJUGATES[1]

[1] The contents of this chapter have been previously published in: Gittens SA, Kitov PI, Matyas JR, Löbenberg R, and Uludağ H. Impact of Crosslinker Length on the Bone Mineral Affinity of Protein-Bisphosphonate Conjugates. Pharm. Res. 21 (2004) 608-616.

INTRODUCTION

To enable the use of osteogenic growth factors to systemically promote the regeneration of bone for clinical indications such as osteoporosis, these proteins must be targeted to skeletal tissues in order to circumvent the extra-skeletal effects they may elicit upon parenteral administration (1). A promising approach to delivering these proteins to bone is by conjugating bisphosphonates (BPs), pyrophosphate analogs with an inherently high affinity for the hydroxyapatite mineral content of bone, directly onto them via a tether (2-5). In designing BP-protein conjugates, the inherent affinity of the BP to bone mineral, as well as the nature (i.e. size and molecular structure) of the BP and tether are expected to influence the bone affinity ultimately imparted onto the conjugate (6). We have previously shown that the conjugation of 1-amino-1,1-diphosphonate methane (aminoBP) onto bovine fetuin's carbohydrate moieties using 4-(maleimidomethyl) cyclohexane-1-carboxyl-hydrazide (MMCCH) was feasible. This process of conjugation enhanced protein affinity for various bone matrices *in vitro* (7). When compared to conjugates that have aminoBP covalently attached onto fetuin's lysine residues using succinimidyl-4-(N-maleimidomethyl)-cyclohexane-1-carboxylate (SMCC), however, the affinity of the MMCCH-conjugates was found to be superior than that of the SMCC-conjugates. We postulated that the steric interference mediated by the amino acids adjacent to the linkage site may have accounted for the difference in the SMCC conjugates' capacity to bind to various mineral matrices. Alternatively, the carbohydrate moieties may have afforded a greater range of motion to facilitate the interaction between the conjugated aminoBPs and mineral matrices (7). Indeed, these observations were consistent with theoretical models, in which binding between receptor-ligand pairs

hindered by steric interference are improved by increasing tether length (**6, 8**), as well as experimental observations in liposomal targeting (**9-13**), gene delivery (**14, 15**), immunosorbent assays (**16, 17**), and the functionalization of cell-adhesive surfaces (**18**). As a result, it was expected that increasing the tether length of the BP conjugates would enhance aminoBP-mediated conjugate binding to mineralized matrices.

This study was performed in order to explore the influence of the tether on the mineral affinity of the BP-conjugates. Several conjugates with varying tether lengths have been prepared and their mineral affinity was explored in binding assays *in vitro* and in an *in vivo* implant model. The results presented herein are expected to improve the design of future aminoBP-protein conjugates by providing insight into ways of optimizing the conjugate affinity to bone.

MATERIALS AND METHODS

Materials

Succinimidyl-4-(N-maleimidomethyl)cyclohexane-1-carboxylate (SMCC), succinimidyl-4-(N-maleimidomethyl)cyclohexane-1-carboxy-(6-amido-caproate) (LC-SMCC), α-maleimidoacetic acid-N-hydroxysuccinimide (MANS), and maleimidobutyric acid-N-hydroxysuccinimide (MBNS) were acquired from Molecular Biosciences (Boulder, CO). N-hydroxysuccinimide-polyethylene glycol-maleimide (NHS-PEG-MAL) with molecular weight (MW) was 2300 Da, was from Nektar Therapeutics (Huntsville, AL). Bovine fetuin (lot #59H7616), 2-iminothiolane (2-IT), bovine adult serum, trichloroacetic acid (TCA), and 1,3,4,6-tetrachloro-3α,6α-diphenylglycouril (TCDG) were obtained from Sigma Aldrich (St. Louis, MO). Pre-cast 4-20% LongLife

polyacrylamide gels were from Gradipore (Frenchs Forest, NSW), whereas $Na^{125}I$ (in 0.1 M NaOH) was obtained from Perkin Elmer (Wellesley, MA). 0.9% NaCl was from Baxter Corporation (Toronto, ON). N,N-dimethylformamide (DMF) was from Caledon Laboratories (Georgetown, ON). The Spectra/Por dialysis tubing with MW cutoff of 12-14,000 Da was acquired from Spectrum Laboratories (Rancho Dominguez, CA). The SDS-glycine sample buffer for electrophoresis was prepared as previously described (7). The SDS-PAGE running buffer was prepared by the addition of 2.9% (w/v) Trizma Base, 14.4% (w/v) glycine, and 1.0% (w/v) SDS in deionized water. Metofane® (methoxyflurane) was obtained from Janssen Inc. (Toronto, ON). The Pro-Osteon 200HA® implants, which were coralline hydroxyapatite discs (10 mm in diameter x 4 mm in thickness) with porous three-dimensional micro-architecture similar to that of cortical bone (19), were kindly donated by Interpore Cross International (Irvine, CA).

AminoBP Conjugation onto Fetuin

Conjugations by SMCC, LC-SMCC, MANS, MBNS, and NHS-PEG-MAL, heterobifunctional crosslinkers with $-NH_2$ and –SH reactive groups, were performed according to a previously published procedure (7). Briefly, fetuin (15 mg/ml in 0.1 M phosphate buffer) was incubated for 2.5 h with up to 15 mM of one of the crosslinkers, which was initially dissolved in DMF at a concentration of 45 mM. Separately, aminoBP was thiolated by incubating equal volumes of aminoBP (80 mM in 0.1 M phosphate buffer) with 2-IT solution (40 mM in 0.1 mM phosphate buffer) for 2.5 h. The product from this reaction was then directly added to crosslinker-reacted fetuin in equal volumes and incubated for 2.5 h at room temperature. To remove the unreacted reagents (i.e.

aminoBP, 2-IT, and crosslinker), the conjugates were thoroughly dialyzed against 0.1 M carbonate buffer (x3) and deionized water (x2).

Analysis of the Conjugates

After dialysis, protein concentrations were determined using the Bradford Protein Assay (**20**) as follows: a 50 µl sample was added to 1 ml of the protein reagent, which consisted of 0.01% (w/v) Coomassie Blue R-250, 4.7% (w/v) ethanol, and 8.5% (w/v) phosphoric acid. The sample's absorbance was subsequently determined at 595 nm. A phosphate assay, which was modified from that described by Ames (**21**), was then used to determine aminoBP concentration of the samples (**7**). The aminoBP concentrations of the protein samples were used in combination with the results from the protein assay to yield the number of aminoBPs conjugated onto fetuin (mol:mol ratio). Gel electrophoresis was employed to determine whether inadvertent protein-protein crosslinking occurred during the process of conjugation. As the molecular weight of fetuin is 48.4 kDa, protein-protein crosslinking would have manifested itself as ≥100 kDa protein bands on the gels. Approximately 10 µg of protein sample was mixed with an SDS-glycine sample buffer and loaded onto a 4-20% Tris-HCl polyacrylamide gel. The samples were run at 150V for 1.5 h in an SDS-glycine running buffer. The gels were then stained overnight using a Coomassie Blue R-250 (0.1% w/v Coomassie Blue R-250 in 10:10:80 = methanol:acetic acid: deionized water), destained, and scanned on a flat-bed scanner.

Molecular Dynamics Modeling of the Conjugates

Molecular dynamics (MD) modeling of the products from the process of conjugations was performed using *Insight-II* suite of software programs (Molecular Simulations Inc, San Diego, CA) on a Silicon Graphics Octane-2 workstation. The structures to be modeled (**Figure 3-1**) were generated using standard fragment library in *Biopolymer* block; aminoBP ligands (which are subsequently referred to as pendant ligands) were uncharged. Consistent Valence Forcefield (CVFF) potentials were automatically assigned followed by manual correction where necessarily; after the formal charges for all atoms were set to zero, the partial charges were automatically generated. Free energies for all structures were sufficiently minimized prior to the initiation of MD modeling. The dielectric constant was set to 80 and the temperature to 1000 K (a temperature selected for simulation in order to accelerate collection of the representative set of configurations). Each MD experiment, except for the NHS-PEG-MAL crosslinker, was conducted for 2.5 ns (with a step of 1 fs), trajectories being sampled after every 250 steps. In case of NHS-PEG-MAL, the configurational space was explored for 10 ns and every 1000-th frame was sampled. The distances (also known as the end-to-end separation) between lysine's α-carbon and the aminoBP's central carbon (separating the two phosphonate moieties) were measured from each of the 10,000 frames obtained from the simulations. Histograms with a step of 0.5 Å were subsequently generated to determine probability density. The radial density distribution was calculated by normalizing the probability density by the volume enclosed by two hemispheres with the center in the attachment point and radii R and R-0.5 Å (as described in **23**).

Assessment of Conjugate Mineral Affinity

Preparation of Radioiodinated Conjugates: Binding was assessed by using ^{125}I-labeled proteins. In tubes previously coated with TCDG (200 µl of 20 µg/ml TCDG in chloroform), 10 µg of protein was added to 50 µl of 0.1 M phosphate buffer (pH 7.4), and 10 µl of 0.01 mCi of Na^{125}I (in 0.1 M NaOH). After reacting for 20 minutes, free ^{125}I was separated from the radiolabeled protein via dialysis against 0.05 M phosphate buffer. After precipitating an aliquot of the samples with 20% TCA, it was confirmed that all iodinated samples contained <5% free ^{125}I.

In Vitro Mineral Binding: The preparation of HA has been previously described (2). The radiolabeled proteins were added to cold protein to give a radioactive count of 10^6 cpm at 0.1 mg/ml protein concentration. Along with 175 µl of 50% bovine adult serum (diluted with 0.9% saline), 25 mg of normal bone or 5 mg of HA was added the microcentrifuge tubes. This serum-containing binding medium was used because it better represented physiological conditions than phosphate buffers (7). After periodical shaking over a 3 h period, the samples were centrifuged. The supernatant was collected and the pellet, consisting of the mineral matrix, was washed with the binding buffer used, and re-centrifuged. This washing procedure was then repeated twice more and the collected supernatant from each of these steps was subsequently counted separately by a γ-counter (Wallac Wizard 1470, Turku, Finland). Matrix affinity, expressed as percentage matrix binding, was calculated as follows: 100% x (counts in matrix pellet) ÷ { (counts in matrix pellet) + (counts in supernatants) }. All binding was assessed in duplicate.

The affinity of the conjugates to the mineral matrix used for implantation (i.e. Pro-Osteon®) was also determined *in vitro*. A 50 µl aliquot, containing 2.5 x 10^5 cpm of radiolabeled conjugate along with 0.1 mg/ml cold protein, was initially applied to each autoclaved Pro-Osteon® disc. Following a 10 minute-incubation period, the discs (two per group) were washed thoroughly (5x) using 50% bovine adult serum in saline. The supernatants collected from each of the washes, along with the implants themselves, were quantified separately using a γ-counter. The affinities that the conjugates exhibited for the implants were calculated using the "matrix affinity" formula described above.

In Vivo HA-based Matrix Binding: Two month-old female Sprague-Dawley rats were purchased from Charles River Laboratories (Quebec City, PQ). Rats were acclimated until 3 months of age under standard laboratory conditions (23°C, 12 h of light/day) prior to the beginning of the study. While maintained in pairs in sterilized cages, rats were provided standard commercial rat chow and tap water *ad libitum* for the duration of the study. All procedures involving the rats were approved by the Animal Welfare Committee at the University of Alberta (Edmonton, Alberta).

For assessing conjugate affinity to bone *in vivo*, powdered HA was considered unsuitable due to the difficulty associated with recovering the particulate HA matrix following implantation. Consequently, Pro-Osteon® discs, which are clinically used for bone implantation, were used. The discs used for *in vivo* implantation were prepared essentially as described above. The initial counts in the implant were determined before implantation. Once rats were anaesthetized with Metofane®, two Pro-Osteon® discs were implanted subcutaneously into bilateral ventral pouches in each rat (n = 2 rats per

conjugate group). Three days following implantation, the rats were asphyxiated with CO_2. The radioactivity associated with the excised implants and the soft tissue surrounding the implant was quantified separately using a γ-counter. The degree of protein retention, expressed as a percentage of the implanted dose, was calculated as follows: 100% x { (initial counts in implant) – (final counts in implant) } ÷ (initial counts in implant).

Statistics

Significant differences ($p < 0.05$) in conjugate binding to the Pro-Osteon® discs were determined by Tukey post-hoc comparison. Linear regression was also used in the analysis of the data. All statistics was done using SPSS for Windows 11.0.1, SPSS Inc., Chicago, IL.

RESULTS

AminoBP-Conjugation to Fetuin:

Conjugation of aminoBP onto the lysine –NH_2 moieties of fetuin was carried out using MANS, MBNS, SMCC, LC-SMCC, and NHS-PEG-MAL. While keeping thiolated aminoBP concentrations at 20 mM, increasing the concentration of crosslinker during the process of conjugation led to a concentration-dependent increase in the number of aminoBPs attached onto fetuin (**Figure 3-2**). The maximal conjugation efficiency using MANS, MBNS, SMCC, LC-SMCC, and NHS-PEG-MAL were: 9.7, 15.0, 23.0, 17.8, and 22.1 aminoBPs/fetuin, respectively. These were significantly higher than their respective controls (i.e. fetuin reacted with 0 mM crosslinker and 20 mM thiolated

aminoBP prepared for each conjugate), which had an average of 1.8±0.5 aminoBPs/fetuin. Each crosslinker used, regardless of its length, successfully facilitated the conjugation of aminoBP onto fetuin.

Corresponding to the degree of conjugation, gel electrophoresis indicated that there were slight upward shifts in the intensity of conjugates' bands relative to native fetuin's band at 48.4 kDa—especially with the larger molecular weight crosslinked conjugates such as LC-SMCC and NHS-PEG-MAL. No visible bands at the ~100 kDa region, however, presented themselves (**data not shown**). These results confirmed that aminoBP conjugation had indeed occurred (as was especially evident with the use of the larger molecular weight crosslinkers) and that the occurrence of protein:protein crosslinking was insignificant for all crosslinkers.

Molecular Dynamics Modeling of the Conjugates

MD modeling was used to characterize the conformational behavior of linker structures containing pendant aminoBP ligand moieties. As illustrated in **Figures 3-3,** the calculated maximal probability densities as well as the radial distribution profiles were inversely related to the length of crosslinkers used. Possessing fewer potential structural permutations, aminoBPs tethered onto fetuin using shorter crosslinkers (i.e. MANS, MBNS and SMCC) were more likely to be within a shorter distance of the protein core, which consequently induced a greater density of the pendant ligand than those tethered using longer crosslinker (i.e. LC-SMCC and NHS-PEG-MAL).

Conjugate Binding to Bone and HA Matrices *In Vitro*:

The MANS, MBNS, SMCC and LC-SMCC conjugates exhibited a binding to HA that was aminoBP-dependent: samples with low conjugation efficiency had ~20% binding, whereas samples with high conjugation efficiency had >50% binding (**Figure 3-4**). The binding efficiency for each group of conjugates differed significantly, however, as the conjugates whose aminoBPs were tethered onto fetuin via shorter crosslinkers, namely the MANS, MBNS and SMCC, bound to the synthetic mineral matrix more tenaciously (with a maximum binding of 63.8%, 66.1%, and 74.0%, respectively) than the longer LC-SMCC conjugates, which exhibited reduced binding (maximum binding of 45.6%). Despite its relatively high conjugation efficiency, the NHS-PEG-MAL conjugate binding to HA diminished significantly in a manner proportional to the number of aminoBPs conjugated onto fetuin. These conjugates exhibited the weakest capacity to bind to HA relative to any of the other conjugation products. In comparison, binding of control fetuin to HA was significantly lower (averaging 13.3±4.8 %). These results also corroborated the fact that HA binding was mediated by the conjugated aminoBP.

To further characterize conjugate binding to HA, binding isotherms for each group of conjugates were generated. The conjugate samples chosen for these studies were those containing ~10 aminoBPs/fetuin. As previously observed, the MANS, MBNS, and SMCC conjugates exhibited superior binding to HA, followed by the LC-SMCC conjugates, and the NHS-PEG-MAL conjugates (**Figure 3-5**).

Using the same conjugates as above (i.e. ~10 aminoBPs/fetuin), the effect of modulating bovine adult serum concentration on conjugate binding to HA was subsequently determined. As shown in **Figure 3-6**, all conjugates, even the NHS-PEG-

MAL conjugates, exhibited exceptional binding to HA in the absence of serum (in saline). As the concentration of adult bovine serum increased, the propensity of all conjugates' to bind to HA decreased. This reduction in binding, however, was not uniform as the conjugates with the longest crosslinkers (i.e. LC-SMCC and NHS-PEG-MAL) were more adversely affected by the increasing competitive-nature of the binding media. These results reflected trends found in the previous binding results: aminoBPs tethered onto fetuin via longer crosslinkers afforded the poorest conjugate binding to HA.

Conjugate Retention to HA-Implants *In Vivo*:

Given the similar binding profiles of the MANS, MBNS, and SMCC conjugates, the MBNS conjugate was chosen to represent the group of shorter crosslinkers in the *in vivo* experiments. Using 50% bovine adult serum, the *in vitro* affinity that native fetuin had for the Pro-Osteon® implants (26.0±5.9%) was lower than the MBNS, LC-SMCC and NHS-PEG-MAL conjugates (82.5±1.9%, 83.2±3.5%, and 46.7±1.7%, respectively, **Figure 3-7A**). In contrast to the HA binding results, the MBNS conjugate's mineral affinity was not different to that of the LC-SMCC conjugate. Following three days of implantation, all conjugates exhibited higher affinity to the Pro-Osteon® matrix compared to unconjugated fetuin ($p<0.02$). Conjugate retention to the soft tissue surrounding the implant, however, was negligible (<0.2% of the dose implanted on average). This was indicative of rapid clearance of the released protein from the site of implantation. The affinity of the NHS-PEG-MAL conjugate was lower than both the MANS and LC-SMCC conjugates. Following their *in vitro* binding profiles to Pro-Osteon®, the MBNS and LC-SMCC conjugate retention in Pro-Osteon® discs were significantly greater than

unconjugated fetuin or the NHS-PEG-MAL conjugates ($p < 0.0005$, and $p < 0.0005$, respectively) (**Figure 3-7B**). A plot of conjugate binding to Pro-Osteon® *in vitro* vs. *in vivo* (**not shown**) gave a good correlation ($r^2 = 0.999$) that was statistically significant ($p < 0.0005$).

DISCUSSION and CONCLUSIONS

It was the goal of this study to elucidate the effect of tether length on aminoBP-fetuin conjugate affinity for various mineral matrices. Here, we elected to conjugate aminoBP onto fetuin's protein core so that by varying tether length, the resulting conjugates could meet, if not exceed, the aforementioned superior affinity imparted by aminoBP conjugation onto fetuin's carbohydrate groups (**7**). Consequently, the five crosslinkers utilized (i.e. MANS, MBNS, SMCC, LC-SMCC and NHS-PEG-MAL) were chosen primarily on their varying lengths.

The results described suggest that irrespective of the crosslinker's length, each was capable of facilitating the conjugation of aminoBP directly onto fetuin in a concentration-dependent manner. Conjugation efficiency, however, appeared to be dependent on the crosslinker length as the shorter tethers (namely MANS and MBNS) were less efficient in conjugating aminoBPs onto fetuin than the longer counterparts. As previously shown (**2-4, 7**), the data presented herein suggests that the mineral binding was indeed mediated by aminoBP. Similar to previous observations with the SMCC conjugates (**7**), a saturable binding kinetics was observed with the MANS, MBNS, SMCC and LC-SMCC conjugates. At low conjugation efficiencies (i.e., <4 aminoBPs/fetuin), the extent of HA binding was proportional to the number of

conjugated aminoBPs. As the conjugation efficiency was increased, however, the aminoBPs tethered onto fetuin using the shorter crosslinkers (i.e. MANS, MBNS and SMCC) imparted a higher HA affinity than those tethered using the longer crosslinkers (i.e. LC-SMCC and NHS-PEG-MAL). In addition to these results, a similar pattern emerged from the experiments that explored the effects of modulating conjugate (**Figure 3-5**) and competing serum concentrations (**Figure 3-6**) on HA binding. Unlike HA, however, Pro-Osteon® did not reveal any differences in affinity between the conjugates derived from MBNS and LC-SMCC. The PEG-linked conjugates, however, were again inferior in mineral binding. We do not currently know which matrix properties were responsible for the binding differences between the HA synthesized in-house and the commercially-available Pro-Osteon®, but the binding pattern to the latter matrix was consistent both *in vitro* and *in vivo*.

Similar to our findings, Hirabayashi *et al.* had observed that an increase in tether length from 1 to 10 methylene groups between carboxyfluorescein (an organic molecule much smaller than proteins) and a BP resulted in a nearly 10-fold *decrease* in skeletal targeting upon the compounds' intravenous administration (**22**). They postulated that this decrease in targeting was due to a corresponding increase the molecules' hydrophobicity, as determined through theoretical calculations of the compounds' octanol/water partition coefficient (it should be noted that the mineral affinities of their conjugates were not assessed *in vitro*). The NHS-PEG-MAL tether used in this study, which is significantly more hydrophilic that the methylene-based tethers used in the study of Hirabayachi *et al.*, resulted in a reduction in conjugate mineral affinity. Consequently, it is postulated that

tether hydrophobicity is unlikely to be the underlying factor responsible for the reduction in mineral affinity associated with increased tether lengths.

The strength of tethered aminoBP-HA binding is expected to depend primarily on number of aminoBP ligands incorporated onto the conjugate, the strength of the individual aminoBP-HA interactions, and the surface area of HA available for the interactions (**6**). Since the amount of mineral matrix (and thus the interacting surface) remained constant throughout each experiment, binding of conjugates with comparable degree of conjugation efficiency to HA should primarily rely on the strength of individual interactions. Since the same ligand was used throughout this study (i.e. aminoBP), it is reasonable to assume that the intrinsic binding energies do not vary among conjugates. On the other hand, the probabilities of aminoBP-HA interaction and the corresponding entropic terms should differ according to the effective concentration (i.e. radial density) of aminoBP at the HA surface. Therefore, the end-to-end separation between pendant ligand and protein at the maximum radial density corresponds to the distance most favorable for conjugate-HA interaction and represents the equilibrium distance between the pendant ligand and the attachment point in the bound state. As the magnitude of the density at the equilibrium distance is directly proportional to binding constant of the interaction (**23**), this method can be used to rank the various tethers according to their apparent binding efficiencies. These MD results were in agreement with our experimental observations of the conjugates' capacity to bind to bone mineral. As an increase in tether length would enable a ligand to escape the adverse effects of steric hindrance exerted from neighboring amino acids, it can be inferred from these data that steric effects did not influence aminoBP binding onto HA. Consequently, we postulate that steric hindrance

was probably not the likely reason for the significant difference observed between aminoBP conjugated onto fetuin's protein core and its carbohydrate residues. Perhaps other interactions between HA and the protein's functional groups (as suggested by **24** and **25**) contributed to additional binding that helped stabilize and/or improve aminoBP-mediated conjugate binding. Since longer tethers retain the protein at a distance from the surface of HA, this might be one reason why longer tether length are less effective in facilitating conjugate-HA binding.

The results from the Pro-Osteon® implantation study, suggest that the mineral affinity imparted by the conjugation of aminoBP onto fetuin leads to a significant degree of protein retention to the HA-based biomaterial over non-conjugated protein. Given that the retention of the osteogenic proteins (i.e. those capable of inducing bone formation such as several members of the BMP family (**1**)) correlates directly with the degree of bone formation they elicit (**26**), these implications are significant as they suggest that HA-based implants, which are used in numerous clinical applications, may be applied with BP-conjugated osteogenic proteins. Furthermore, these results are of clinical relevance as Pro-Osteon®, itself, has been used as a bone substitute in numerous orthopaedic, ophthalmologic, and maxillofacial applications (**19**). It is thought that this BP-based delivery system may improve the performance of such biomaterials by improving their osteoconductivity as well as afford some degree of osteoinductivity. As previously discussed (**7**), however, the potential use of BP-protein conjugates is not limited to HA-based implants. In fact, we have previously shown that aminoBP-albumin conjugates exhibit an improved retention when administered intraosseously in a tibial injection animal model—suggesting that our approach may be applicable to promote the

regeneration of bone in local defects that do not necessarily require the use of an implant (3).

In summary, this study has shown that a range of crosslinkers could facilitate the conjugation of aminoBP onto fetuin, but the resulting bone mineral affinity for each of these conjugates differed significantly. AminoBPs tethered onto fetuin using the shorter crosslinkers (i.e. MANS, MBNS and SMCC) imparted a higher affinity than those tethered using the longer crosslinkers (i.e. LC-SMCC and NHS-PEG-MAL). This is the first study to report that the mineral affinity imparted by BP conjugation enhances a protein's retention once implanted by a HA-based biomaterial *in vivo*. The results presented in this report will facilitate improvements in the design of aminoBP-protein conjugates to maximize bone mineral affinity.

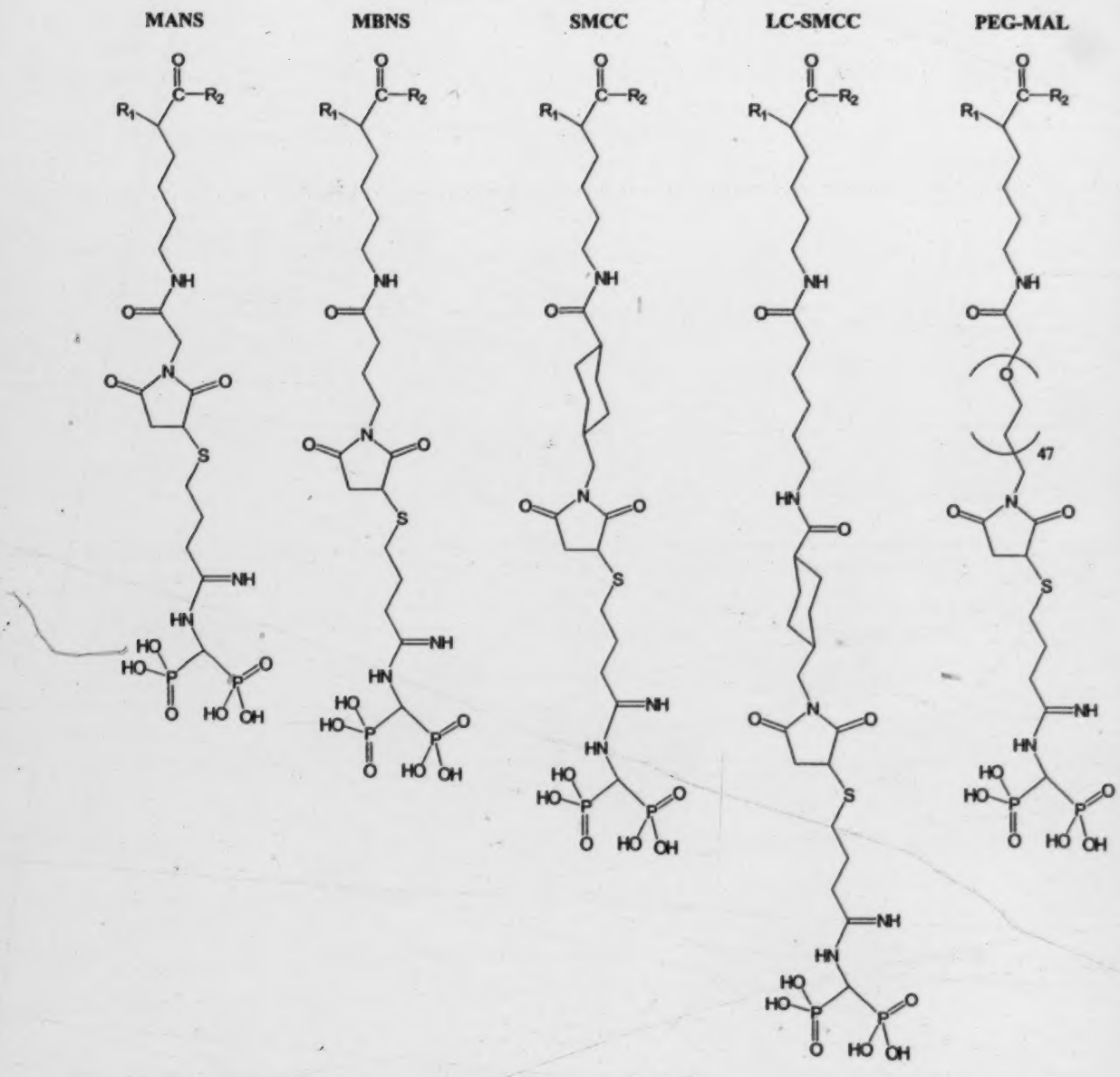

Figure 3-1: A representation of the MANS-, MBNS-, SMCC-, LC-SMCC-, and NHS-PEG-MAL-conjugates pendant ligands. The substituents R_1 and R_2 at the lysine moiety represent preceding and following residues in the peptide chain. In the structures that were used in MD simulations R_1 = -NH_2 and R_2 = -H. The length of listed heterobifunctional crosslinkers themselves, from the maleimide moiety up to but excluding the succinimide moiety were: 5.7, 10.2, 11.6, 16.1 and ~136 Å (**6**), respectively.

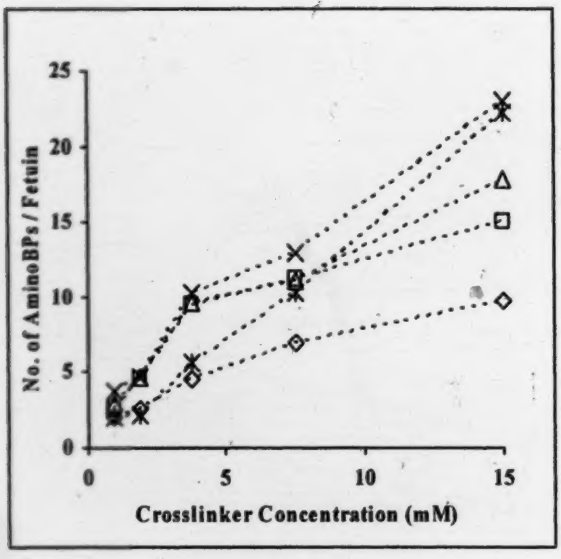

Figure 3-2: The conjugation efficiency of aminoBP onto fetuin. As the concentrations of MANS (◊), MBNS (□), SMCC (X), LC-SMCC (Δ), and NHS-PEG-MAL (*) increased, the subsequent number of conjugated aminoBPs rose linearly (r^2 = 0.961, 0.859, 0.975, 0.987, and 0.996, respectively).

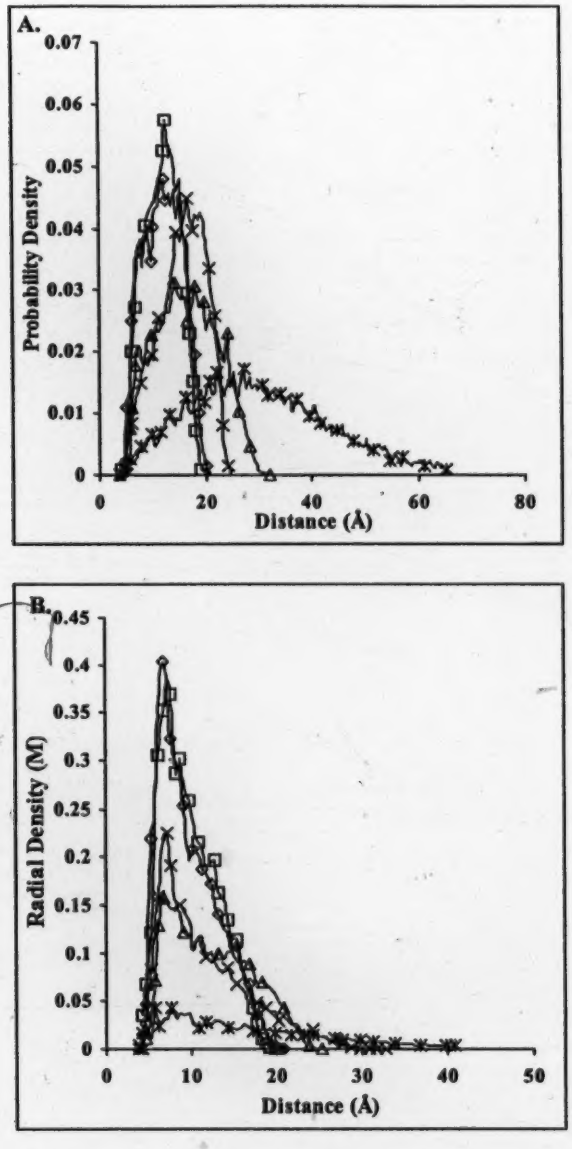

Figure 3-3: The probability density **(A)** and the radial density distribution **(B)** of the MANS- (◊), MBNS- (□), SMCC- (X), LC-SMCC- (Δ), and NHS-PEG-MAL- (*) conjugates. In each case, maximal probability density and radial density were inversely proportional to the size of the tether used.

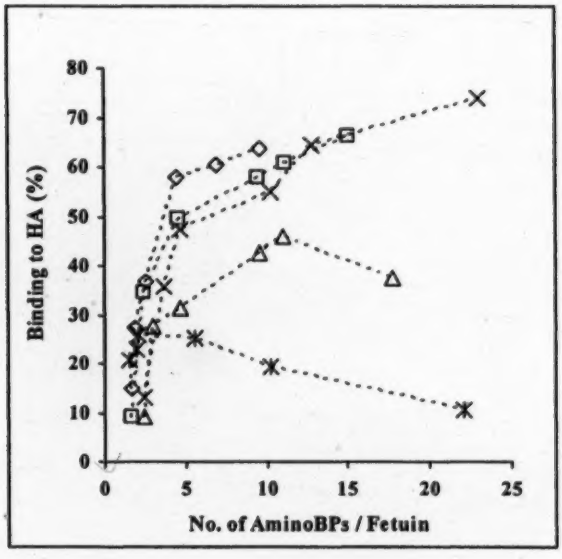

Figure 3-4: The MANS (◊), MBNS (□), SMCC (x), LC-SMCC (Δ), and NHS-PEG-MAL (*) conjugates' capacity to bind to HA in 50% bovine adult serum. The conjugates synthesized using the MANS, MBNS and SMCC tethers bound to HA more extensively than those synthesized with LC-SMCC and NHS-PEG-MAL.

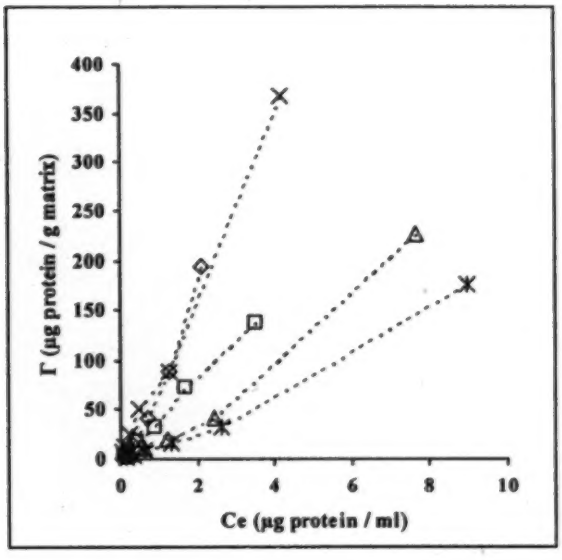

Figure 3-5: Binding isotherms of the MANS (◊), MBNS (□), SMCC (x), LC-SMCC (Δ), and NHS-PEG-MAL (•) conjugates with HA. Conjugate concentrations were serially diluted two-fold from a maximum 10^6 cpm at 0.1 mg/ml and the resulting conjugate binding was expressed as C_e (the equilibrium concentration after the 3 h binding period) versus Γ (the amount of bound protein per gram of HA). The slopes and corresponding correlation coefficient (r^2) values for the each of the conjugates are: 91.7, 0.976; 39.5, 0.997; 86.0, 0.992; 30.0, 0.981; and 19.7, 0.989, respectively.

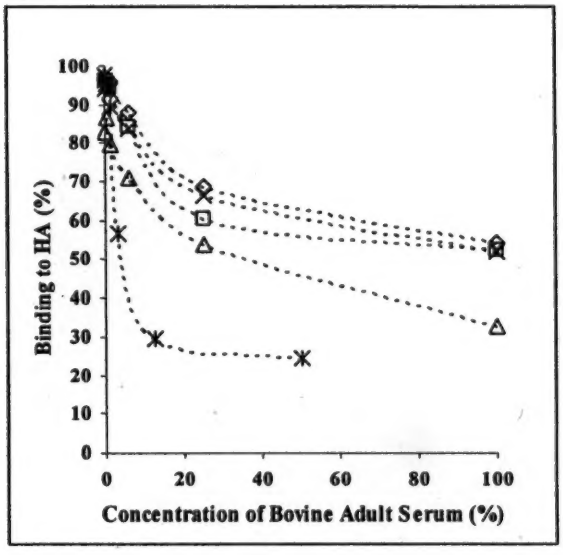

Figure 3-6: Modulating bovine adult serum concentration affects the MANS (◊), MBNS (□), SMCC (x), LC-SMCC (Δ), and NHS-PEG-MAL (*) conjugates' capacity to bind to HA. Binding of the LC-SMCC and NHS-PEG-MAL conjugates were most adversely affected by the increasing serum concentrations than the MANS, MBNS and SMCC conjugates.

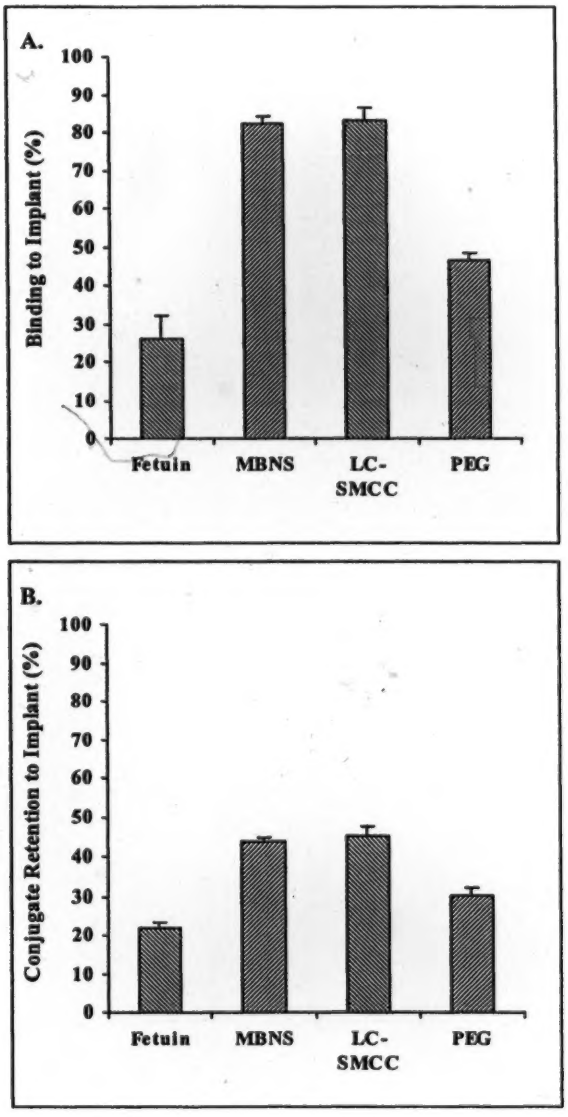

Figure 3-7: Mean ± SD of the capacity of native fetuin, and the MBNS, LC-SMCC, and NHS-PEG-MAL conjugates to bind to Pro-Osteon® in vitro (**A**) as well as their retention in the biomaterial 3 days after implantation in vivo (**B**). In both cases, the binding of the MBNS, and LC-SMCC conjugates was superior to that of the NHS-PEG-MAL conjugates and even more so the native fetuin.

REFERENCES

1. S.A. Gittens, H. Uludag, Growth factor delivery for bone tissue engineering, *J. Drug Targeting.* 9 (2001)407-429.

2. H. Uludag, N. Kousinioris, T. Gao, D. Kantoci, Bisphosphonate conjugation to proteins as a means to impart bone affinity, *Biotechnol. Prog.* 16 (2000)258-267.

3. H. Uludag, T. Gao, G.R. Wohl, D. Kantoci, R.F. Zernicke, Bone affinity of a bisphosphonate-conjugated protein in vivo, *Biotechnol. Prog.* 16 (2000) 1115-1118.

4. H. Uludag, J. Yang, Targeting systemically administered proteins to bone by bisphosphonate conjugation, *Biotechnol. Prog.* 18 (2002) 604-611.

5. H. Uludag, Bisphosphonates as a foundation of drug delivery to bone, Curr. Pharm. Des. 8 (2002) 1929-1944.

6. C. Jeppesen, J.Y. Wong, T.L. Kuhl, J.N. Israelachvili, N. Mullah, S. Zalipsky, C.M. Marques, Impact of polymer tether length on multiple ligand-receptor bond formation, *Science.* 293 (2001) 465-468.

7. S.A. Gittens, J.R. Matyas, R.F. Zernicke, H. Uludag, Imparting bone affinity to glycoproteins through the conjugation of bisphosphonates, *Pharm. Res.* 20 (2003) 978-987.

8. J.Y. Wong, T.L. Kuhl, J.N. Israelachvili, N. Mullah, S. Zalipsky, Direct measurement of a tethered ligand-receptor interaction potential, *Science.* 275 (1997) 820-822.

9. R.J. Lee, P.S. Low, Delivery of liposomes into cultured KB cells via folate receptor-mediated endocytosis, *J. Biol. Chem.* 269 (1994) 3198-3204.

10. A. Engel, S.K. Chatterjee, A. Al-arifi, D. Riemann, J. Langner, P. Nuhn, Influence of spacer length on interaction of mannosylated liposomes with human phagocytic cells, *Pharm. Res.* 20 (2003) 51-57.

11. J. Salord, C. Tarnus, C.D. Muller, F. Schuber, Targeting of liposomes by covalent coupling with ecto-NAD+-glycohydrolase ligands, *Biochim. Biophys. Acta.* 886 (1986) 64-75.

12. C.P. Leamon, D. Weigl, R.W. Hendren, Folate copolymer-mediated transfection of cultured cells, *Bioconjug. Chem.* 10 (1999) 947-957.

13. C.P. Leamon, S.R. Cooper, G.E. Hardee, Folate-liposome-mediated antisense oligodeoxynucleotide targeting to cancer cells: evaluation in vitro and in vivo, *Bioconjug. Chem.* 14 (2003) 738-747.

14. C.M. Ward, M. Pechar, D. Oupicky, K. Ulbrich, L.W. Seymour, Modification of pLL/DNA complexes with a multivalent hydrophilic polymer permits folate-mediated targeting in vitro and prolonged plasma circulation in vivo, *J. Gene Med.* 4 (2002) 536-547.

15. D.V. Schaffer, D.A. Lauffenburger, Optimization of cell surface binding enhances efficiency and specificity of molecular conjugate gene delivery, *J. Biol. Chem.* 273 (1998) 28004-28009.

16. P. Luppa, C. Bruckner, I. Schwab, S. Hauck, S. Schmidmayr, C. Birkmayer, B. Paulus, H. Hauptmann, 7 alpha-Biotinylated testosterone derivatives as tracers for a competitive chemiluminescence immunoassay of testosterone in serum, *Clin. Chem.* 43 (1997) 2345-2352.

17. C. Bieniarz, M. Husain, G. Barnes, C.A. King, C.J. Welch, Extended length heterobifunctional coupling agents for protein conjugations, *Bioconjug. Chem.* 7 (1996) 88-95.

18. L.G. Griffith, S. Lopina. Microdistribution of substratum-bound ligands affects cell function: hepatocyte spreading on PEO-tethered galactose, *Biomaterials*. 19 (1998) 979-986.

19. J.S. Thalgott, Z. Klezl, M. Timlin, J.M. Giuffre. Anterior lumbar interbody fusion with processed sea coral (coralline hydroxyapatite) as part of a circumferential fusion, *Spine*. 27 (2002) E518-E527.

20. M.M. Bradford, A rapid and sensitive method for the quantitation of microgram quantities of protein utilizing the principle of protein-dye binding, *Anal. Biochem.* 72 (1976) 248-254.

21. B.N. Ames, Assay of Inorganic Phosphate, Total Phosphate, and Phosphatases. In E.F. Neufield, and V. Ginsburg (eds.), *Methods in Enzymology, Volume VIII, Complex Carbohydrates*, Academic Press, New York, (1966), pp. 115-117.

22. H. Hirabayashi, T. Sawamoto, J. Fujisaki, Y. Tokunaga, S. Kimura, T. Hata, Dose-dependent pharmacokinetics and disposition of bisphosphonic prodrug of diclofenac based on osteotropic drug delivery system (ODDS), *Biopharm. Drug. Dispos.* 23 (2002) 307-315.

23. P.I. Kitov, H. Shimizu, S.W. Homans, D.R. Bundle, Optimization of tether length in nonglycosidically linked bivalent ligands that target sites 2 and 1 of a Shiga-like toxin, *J. Am. Chem. Soc.* 125 (2003) 3284-3294.

24. H. Chen, M. Banaszak Holl, B.G. Orr, I. Majoros, B.H. Clarkson, Interaction of dendrimers (artificial proteins) with biological hydroxyapatite crystals, *J. Dent. Res.* 82 (2003) 443-448.

25. M.J. Gorbunoff, The interaction of proteins with hydroxyapatite. II. Role of acidic and basic groups, *Anal. Biochem.* 136 (1984) 433-439.

26. H. Uludag, D. D'Augusta, J. Golden, Li J, G. Timony, R. Riedel, J.M. Wozney, Implantation of recombinant human bone morphogenetic proteins with biomaterial carriers: A correlation between protein pharmacokinetics and osteoinduction in the rat ectopic model, *J. Biomed. Mater. Res.* 50 (2000) 227-238.

CHAPTER IV

ASSESSING THE BONE MINERAL AFFINITY OF FETUIN-BISPHOSPHONATE CONJUGATES *IN VIVO*.

INTRODUCTION

The need to induce the regeneration of bone, be it locally or systemically, is a challenge that physicians currently face. Numerous growth factors have been identified that can elicit bone deposition *de novo* upon their parenteral administration (**1**). Due to the detrimental effects induced by growth factors at extra-skeletal sites, however, a means of targeting these proteins to bone is essential so as to circumvent these effects while concurrently taking advantage of their innate osteogenic properties. By virtue of their high affinity for bone mineral (i.e. hydroxyapatite, HA), the conjugation of bisphosphonates onto such growth factors is thought to be a feasible means of increasing their affinity for HA. Indeed, the conjugation of 1-amino-1,1-diphosphonate methane (aminoBP) directly onto a protein's lysine amino acid residues using succinimidyl-4-(N-maleimidomethyl)-cyclohexane-1-carboxylate (SMCC) has successfully enhanced the bone mineral affinity of several model proteins including bovine serum albumin (**2, 3**), lysozyme (**3**), and fetuin (**4, 5**) *in vitro*. In fact, aminoBP conjugation has been shown to enhance bovine serum albumin and lysozyme targeting to bone by up to 7.5-fold upon parenteral administration of radiolabeled conjugates (**3**).

As a method to circumvent any potential loss of protein bioactivity elicited by the direct chemical modification of its lysine amino acid residues, a second conjugation scheme was designed to conjugate aminoBPs onto a glycoprotein's carbohydrate moieties using 4-(maleimidomethyl)cyclohexane-1-carboxyl-hydrazide (MMCCH) (**4**). This approach takes advantage of the fact that the carbohydrate moieties of several osteogenic growth factors, such as bone morphogenetic protein-2, do not play an integral role in their osteogenicity (as evidenced through the bioactivity of the prokaryotically-expressed, non-

glycoslyated forms of these proteins, **6**). The aminoBP-fetuin conjugates prepared using the carbohydrate-attached conjugates appeared to have a higher affinity than the lysine-attached conjugates (**4**). To better understand the influence of aminoBP-fetuin conjugate characteristics, a subsequent study investigated the effect of modulating tether length on conjugate bone mineral affinity. Here, aminoBPs conjugated onto fetuin via shorter tethers resulted in a superior affinity for mineralized matrices both *in vitro* and *in vivo* than conjugates prepared using longer tethers (**5**). It was postulated that the differences in binding affinity may have been due to: (i) fetuin's amino acids facilitating aminoBP-mediated conjugate binding; (ii) shorter crosslinkers allowing aminoBPs to be physically closer together resulting in the potentiation of aminoBP binding; and/or (iii) steric hindrance elicited by the coiled, and thus relatively bulky, longer tethers adversely affecting aminoBP capacity to bind to HA (**5**).

This particular study was performed to characterize the SMCC-linked and MMCCH-linked aminoBP-fetuin conjugate targeting to bone *in vivo*. Conjugates were iodinated and administered through either intraperitoneal (IP) or intravenous (IV) injection. Initially, the retention of these conjugates to a commercially-available coralline hydroxyapatite matrix (i.e. Pro-Osteon®) was assessed *in vitro* as well as *in vivo*. The results of this study highlight both the potential as well as the limitations associated with the approach of conjugating bisphosphonates onto proteins as a means of imparting bone affinity *in vivo*.

MATERIALS AND METHODS

Materials

Bovine fetuin (lot #59H7616), 2-iminothiolane (2-IT), bovine adult serum, trichloroacetic acid (TCA), and 1,3,4,6-tetrachloro-3α,6α-diphenylglycouril (TCDG), and 3-(4-hydroxyphenyl)propionic acid N-hydroxysuccinimide ester (Bolton Hunter reagent) were obtained from Sigma Aldrich (St. Louis, MO). The succinimidyl-4-(N-maleimidomethyl)cyclohexane-1-carboxylate (SMCC), and 4-(maleimidomethyl) cyclohexane-1-carboxyl-hydrazide (MMCCH) crosslinkers were acquired from Molecular Biosciences (Boulder, CO). Pre-cast 4-20% LongLife polyacrylamide gels were from Gradipore (Frenchs Forest, NSW, Australia). The $Na^{125}I$ (in 0.1 M NaOH) was obtained from Perkin Elmer (Wellesley, MA). 0.9% NaCl was from Baxter Corporation (Toronto, ON, Canada). The dimethylsulfoxide (DMSO) and N,N-dimethylformamide (DMF) were from Caledon Laboratories (Georgetown, ON). The Spectra/Por dialysis tubing with MW cutoff of 12-14,000 Da was acquired from Spectrum Laboratories (Rancho Dominguez, CA). The preparation of HA, 1-amino-1,1-diphosphonate methane, 0.1 M phosphate buffer (pH 7.4), 0.1 M carbonate buffer (pH 10) and 0.1 M acetate buffer (pH 4.5) have been previously described (**2, 4**). The SDS-glycine sample buffer for electrophoresis was prepared as previously described (**4**). The SDS-PAGE running buffer was prepared by the addition of 2.9% (w/v) Trizma Base, 14.4% (w/v) glycine, and 1.0% (w/v) SDS in deionized water. The SDS-PAGE low molecular weight standard was from BioRad (Richmond, CA). Metofane® (methoxyflurane), an inhalational anaesthetic, was obtained from Janssen Inc. (Toronto, ON, Canada). The Pro-Osteon 200HA® implants, which are coralline hydroxyapatite discs (10 mm in diameter x 4 mm in thickness) with

porous three-dimensional micro-architecture similar to that of cortical bone (7), were kindly donated by Interpore Cross International (Irvine, CA). Pre-sterilized Helistat® absorbable collagen sponges were from Integra Life Sciences (Plainsboro, NJ).

AminoBP Conjugation onto Fetuin:

AminoBP conjugations onto fetuin were performed according to previously published procedures (4). To conjugate aminoBP to the lysine groups of fetuin using SMCC, fetuin (15 mg/ml in 0.1 M phosphate buffer) was incubated for 2.5 h with 10 mM of SMCC (dissolved as 0.15 M in DMF). Separately, aminoBP was thiolated by incubating equal volumes of aminoBP (80 mM in 0.1 M phosphate buffer) and 2-IT solutions (40 mM in, 0.1 mM phosphate buffer) for 2.5 h. The product from this reaction was then directly added to SMCC-reacted fetuin in equal volumes for 1.5 h. All reactions were performed at room temperature. The removal of unreacted reagents (i.e. SMCC, aminoBP, and thiolated aminoBP) was through extensive dialysis against 0.1 M carbonate buffer (x 3) and dH_2O (x 2).

To conjugate aminoBP to the carbohydrate groups of fetuin using MMCCH, the oxidation of adjacent hydroxyl groups on fetuin's carbohydrate moieties were first oxidized through the use of 4 mM of $NaIO_4$ (in 0.1 M acetate buffer). Following a 2.5 h incubation, the samples were extensively dialyzed against dH_2O and 0.1 M acetate buffer. The oxidized fetuin was incubated with 10 mM MMCCH (dissolved as 0.15 M in DMF) for 2.5 h, thiolated aminoBP, which had been prepared as described above, was added to the MMCCH-reacted fetuin at equal volumes. This reaction was allowed to proceed for 1.5 h. All reactions were performed at room temperature. The unreacted reagents (i.e.

MMCCH, aminoBP, and thiolated aminoBP) were removed through extensive dialysis. All aminoBP-fetuin conjugates were stored at 4 °C.

Conjugation Efficiency

Protein concentrations were determined using the Bradford Protein Assay (**8**) as follows: a 50 µl sample was added to 1 ml of the protein reagent, which consisted of 0.01% (w/v) Coomassie Blue R-250, 4.7% (w/v) ethanol, and 8.5% (w/v) phosphoric acid. The sample's absorbance was subsequently determined at 595 nm. A phosphate assay, which was modified from the procedure by Ames (**9**), was used to determine aminoBP concentration of the samples (**2**). The aminoBP concentrations of the fetuin samples were used in combination with the protein concentration to yield the number of aminoBPs conjugated onto fetuin as a mol:mol ratio. The exact number of aminoBPs conjugated per protein used in each study is stated in the Results section. Where indicated, unmodified fetuin and oxidized fetuin (without aminoBP conjugation were used as a control for the SMCC and the MMCCH conjugates.

Assessment of Mineral Affinity *In Vitro*

Preparation of Radioiodinated Proteins: HA binding by the proteins was assessed by using ^{125}I-labeled proteins. The proteins used were labeled through one of two radiolabeling techniques. The *TCDG* technique, which resulted in the attachment of ^{125}I onto the tyrosine and histidine residues, was as follows. In microcentrifuge tubes previously coated with TCDG (200 µl of 20 µg/ml TCDG in choloroform), 100 µg of protein was added to 50 µl of 0.1 M phosphate buffer (pH 7.4), and 20 µl of 0.01 mCi

$Na^{125}I$ (in 0.1 M NaOH). The samples were incubated for 20 minutes, and dialyzed against 0.05 M phosphate buffer (3x). Conversely, the *Bolton-Hunter* technique, which resulted in the attachment of ^{125}I onto the lysine residues, was as follows. In microcentrifuge tubes previously coated with TCDG (as above), 50 µl of 50 mg/ml Bolton-Hunter reagent (in DMSO) was added to 50 µl 0.1 M phosphate buffer and 20 µl of 0.01 mCi $Na^{125}I$ (in 0.1 M NaOH). After 2 min, 100 µl of DMF and 200 µl of benzene were added to extract the labeled Bolton-Hunter reagent into an organic phase, which was isolated and dried under a stream of air. 100 µg of protein solution (diluted in ice-cold 0.1 M borate buffer (pH 8.5)) was added to the microcentrifuge tubes containing the labeled Bolton-Hunter reagent. The reaction was allowed to continue for 2 h on ice. Unreacted reagents (i.e. free ^{125}I or ^{125}I –Bolton-Hunter reagent) was separated from the radiolabeled protein via dialysis against 0.05 M phosphate buffer. After precipitating an aliquot of the samples with 20% TCA, it was confirmed that all iodinated samples contained <5% free ^{125}I.

To further ensure the quality of the radiolabeled conjugates, 10 µg aliquots of non-radiolabeled as well as 10^6 cpm of radiolabeled protein samples were mixed separately with an SDS-glycine sample buffer and loaded onto a 4-20% Tris-HCl polyacrylamide gel. The samples were run at 150 V for 1.5 h in an SDS-glycine running buffer. The halves of the gel containing the hot and cold protein samples were separated. The half of the gel containing the cold protein samples was stained overnight using a Coomassie Blue R-250 (0.1% w/v Coomassie Blue R-250 in 10% v/v methanol and 10% v/v acetic acid), destained (against a solution of 40% v/v methanol and 10% v/v acetic acid) and scanned on a flat-bed scanner. The half containing the hot proteins, on the other

hand, was exposed to x-ray film (XOMAT™, Kodak) for 30 min, and the film was subsequently scanned on a flat-bed scanner.

HA-Based Matrix Binding In Vitro: Radiolabeled proteins were added to cold protein to give a radioactive count of ~10^6 cpm at 0.1 mg/ml protein concentration. Along with 175 µl of 50% bovine adult serum (diluted with 0.9% saline), 5 mg of HA was added the microcentrifuge tubes. After periodical shaking over a 3 h period, the samples were centrifuged. The supernatant was collected and the pellet, consisting of HA, was washed with 50% bovine adult serum, and re-centrifuged. This washing procedure was then repeated twice more and the collected supernatant from each of these steps was subsequently counted separately by a γ-counter (Wallac Wizard 1470, Turku, Finland). HA affinity, expressed as percentage HA binding, was calculated as follows: 100% x (counts in HA pellet) ÷ { (counts in HA pellet) + (counts in supernatants) }. As all binding was assessed in duplicate, the mean ± standard deviation was reported. The *in vitro* HA affinity of all proteins used in this study were assessed.

The *in vitro* affinity of the proteins to the mineral matrix used for implantation (i.e. Pro-Osteon®) was also determined. A 50 µl aliquot, containing 2.5 x 10^5 cpm of radiolabeled conjugate along with 0.1 mg/ml cold protein, was initially applied to each autoclaved Pro-Osteon® disc as well as to each 1 cm^2 Helistat® sponge. Following a 10 min-incubation, the matrices (n = 3 Pro-Osteon® discs per group, n = 2 Helistat® sponges per group) were washed thoroughly (5x) using 50% bovine adult serum in saline. The supernatants collected from each of the washes, along with the matrices, were quantified

separately using a γ-counter. The affinity that the conjugates exhibited for the implants was calculated using the "HA affinity" formula described above.

Assessment of Mineral Affinity *In Vivo*

Two month-old female Sprague-Dawley rats were purchased from Charles River Laboratories (Quebec City, PQ). Rats were acclimated until 3-4 months of age under standard laboratory conditions (23°C, 12 h of light/day) prior to the beginning of each study. While maintained in pairs, rats were provided standard commercial rat chow and tap water *ad libitum*. All procedures involving the rats were approved by the Animal Welfare Committee at the University of Alberta (Edmonton, Alberta).

HA-Based Matrix Binding In Vivo: To assess conjugate affinity to an HA-based matrix *in vivo*, Pro-Osteon® discs, which were prepared as described above, were implanted subcutaneously. The initial counts in the implant were determined before implantation. Once rats were anaesthetized with Metofane®, two Pro-Osteon® discs were implanted into bilateral ventral pouches in each rat (2 rats per group). Three days following implantation, the rats were killed by CO_2 asphyxiation. At necropsy, the implants and thyroid were harvested from each animal. The radioactivity associated with the thyroid and excised implants was quantified separately using a γ-counter. The degree of protein retention in the implants, expressed as a percentage of the initial dose, was calculated as follows: 100% x { (initial counts in implant) – (final counts in implant) } ÷ (initial counts in implant).

Assessment of Bone Targeting Upon Parenteral Administration

The studies performed to assess bone targeting of proteins are summarized in **Table 4-1**. In Study 1, 300 µl of radiolabeled solution (containing ~10^6 cpm of hot protein, and 0.1 mg/ml cold protein diluted in 0.9% saline) was administered intraperitonealy (IP) into each animal. To accurately assess the total dose administered, the radioactivity associated with 300 µl aliquot of each of radiolabeled protein solution was assessed in duplicate using a γ-counter prior to injection. The values obtained were averaged and referred to as the initial dose administered. Twenty-four hours after injection, all animals were killed via CO_2 asphyxiation. At necropsy, a sample of blood was obtained via cardiac puncture and weighed. The bilateral femora, bilateral tibiae, bilateral kidneys, spleen, sternum, and a section of liver, which was weighed, were harvested. The radioactivity associated with each tissue sample was determined separately using a γ-counter. All values (% injected dose) were reported as mean ± standard deviation (n = 3 for spleen, sternum and liver; and n = 6 for femora, tibiae, and kidneys). The liver samples were normalized by dividing the counts of the excised tissue by its weight. Consequently, the reported values for these samples are in % dose/g. On the other hand, the volume of the blood was calculated by dividing the weight of the sample by the density of rat blood (i.e. 1.05 g/ml, **10**). As the blood samples were subsequently normalized by dividing the counts by the volume of blood obtained, the reported values for these samples are in % dose/ml.

To determine the TCA-precipitable counts in serum, a ~ 500 µl aliquot from each blood sample was centrifuged for 5 min to separate the serum from the red blood cells (RBCs). 1000 µl of 20% TCA was then added to the isolated serum fractions. Once re-centrifuged for 5 min, the supernatant, which represented the TCA-soluble radioactive

fraction, was isolated from the pellet. The radioactive counts in the supernatant, and pellet, along with the RBCs were determined separately using a γ-counter. The percentage of radioactivity in the serum was determined by using the following formula: 100 x { (counts in the supernatant) / (counts in the supernatant + counts in the pellet + counts in RBCs) }. The percentage of TCA-soluble radioactivity in the serum was determined by using the following formula: 100 x { (counts in supernatant) / (counts in the supernatant + counts in the pellet) }.

Studies 2-4 subsequently assessed conjugate targeting to bone upon IV injection. With the exception of the route of administration used, nearly all details for these experiments are similar to the procedures used in Study 1. 300 μl of re-labeled protein sample was administered to each animal through tail vein injections. The localization of the SMCC-linked aminoBP-fetuin conjugate was assessed 24 h (Study 2) as well as 6 h and 48 h post-IV administration (Study 3). Additionally, Study 3 determined the amount of radioactivity in the urine. For this, the animals were immediately placed into metabolic cages following conjugate administration. The urine collected from each animal was weighed; and the radioactivity in each sample was quantified using a γ-counter. The percentage of TCA-soluble radioactivity in the urine was determined by taking a ~300 μl aliquot of urine and adding it to 200 μl of bovine adult serum and 1000 μl of 20% TCA. After centrifugation, the counts within the pellet and supernatant were quantified separately. The animals destined for sacrifice at 6 h were replaced in the metabolic cages by those destined for 48 h sacrifice. Urine collected at the 24 h and 48 h time points were analyzed as above. Study 4 determined the localization of the MMCCH-linked aminoBP-

fetuin conjugate 72 h and 144 h post-IV administration. All details for this experiment are described above.

Statistics

Differences in protein binding, retention and targeting between proteins (in the in vitro, in vivo matrix studies; as well as Studies 1 and 2) were assessed using Tukey post-hoc comparison ($p < 0.05$, S-PLUS 2000 Professional, Release 2, Insightful Corp., Seattle, WA.). Comparisons between fetuin and either the SMCC-linked (Study 3) or the MMCCH-linked (Study 4) aminoBP-fetuin conjugate groups were determined using student's *t*-test ($p < 0.05$, two-sided).

RESULTS

Assessment of Mineralized Matrix Affinity

The conjugates that had been prepared using SMCC and MMCCH contained 11.0 and 9.0 aminoBPs per fetuin, respectively. Gel electrophoresis was performed to ensure that the process of radioiodination did not inadvertently cause protein fragmentation (**Figure 4-1**). The autoradiographic bands produced by the radiolabeled proteins were in line with the bands visualized by the Coomassie blue-stained, unradiolabeled proteins. As no bands representing smaller molecular weight fragments were observed, radiolabeling the proteins using the TCDG method did not lead to the fragmentation of fetuin, oxidized fetuin, or aminoBP-fetuin conjugates. There were no bands corresponding to the presence of larger molecular weight species as well, suggesting a lack of protein-protein aggregation under electrophoresis conditions.

The conjugates' propensity to bind to bone mineral was assessed by an HA binding assay. In 50% adult bovine serum, SMCC- and MMCCH-conjugation gave a 4.1- and 2.4-fold better HA binding over unmodified fetuin and oxidized fetuin, respectively. Under similar experimental conditions, the capacity of the same proteins to bind to Pro-Osteon® was subsequently assessed *in vitro*. In parallel to the HA binding results, the aminoBP-SMCC-fetuin bound 2.4-fold more tenaciously to the Pro-Osteon® discs than fetuin, while the MMCCH-linked aminoBP-fetuin conjugate bound 1.3-fold higher than oxidized fetuin (**Figure 4-2A**). To assess conjugate affinity for a non-mineralized matrix, binding to collagenous Helistat® was assessed *in vitro* (**Figure 4-2A**). Although no statistically significant differences were observed among protein binding to Helistat®, the capacity of all proteins to bind to Helistat® was significantly lower than their ability to bind to Pro-Osteon® (**Figure 4-2A**).

Conjugate retention to both the Pro-Osteon® and Helistat® matrices was subsequently determined *in vivo*. Twenty-four hours after transplantation, the SMCC- and MMCCH-linked aminoBP-fetuin conjugate retention to the Pro-Osteon® discs was 1.6- and 1.5- times higher than fetuin, respectively (**Figure 4-2B**). With Helistat®, protein retention was significantly lower than that observed with Pro-Osteon®. While there were no differences between fetuin, oxidized fetuin and the MMCCH-linked aminoBP-fetuin conjugate retention to Helistat®, a significant decrease in the SMCC conjugate retention was observed relative to fetuin. No statistically significant inter-group differences were observed in the amount of radioactivity recovered in the thyroid for either Helistat® (0.17 ± 0.06% of administered dose) or Pro-Osteon® (0.28 ± 0.09 of administered dose). Further analysis of the binding data revealed a statistically significant linear correlation

between the *in vitro* and *in vivo* protein binding to Helistat® (**Figure 4-2C**, $r^2 = 0.8956$, $p < 0.05$) as well as to Pro-Osteon® (**Figure 4-2D**, $r^2 = 0.9214$, $p < 0.025$).

Assessment of Bone Targeting Upon Parenteral Administration

AminoBP-fetuin conjugate targeting to bone was initially assessed upon IP administration. The SMCC-linked and MMCCH-linked aminoBP-fetuin conjugates used for this experiment contained 6.1 and 7.1 aminoBPs per fetuin, respectively. Relative to an average HA binding of 10.4 ± 0.4% and 17.4 ± 0.2% for the unmodified and oxidized fetuin, respectively, the SMCC-linked and MMCCH-linked conjugates had an HA binding of 52.1 ± 3.7% and 50.7 ± 4.0%, respectively. Once their affinity for HA had been established *in vitro*, the radiolabeled-protein biodistribution was assessed 24 h following IP administration (**Figure 4-3**). With the exception of the spleen, conjugate targeting to all organs analyzed, including osseous tissues (i.e. femora, tibiae and sternum), was significantly lower than either fetuin or oxidized fetuin. A significant increase in the amount of TCA-soluble radioactivity in the serum was observed for aminoBP-fetuin conjugates relative to their controls ($p<0.05$).

The propensity of the aminoBP-fetuin conjugates to target to bone was subsequently determined following IV administration. This study was performed with the same conjugates as used in the IP injection study. Twenty-four hours following IV administration, the delivery of oxidized fetuin was significantly higher in all osseous tissues assessed (**Figure 4-4**). Conjugate targeting to the tibiae or sternum was not significantly different than the unmodified fetuin. Their distribution, however, was significantly lower in the kidneys, liver, spleen and blood relative to that of fetuin

($p<0.0125$). The TCA-soluble radioactivity in the blood was significantly higher in aminoBP-fetuin conjugate groups ($p<0.05$).

Next, bone targeting was assessed at shorter (6 h) as well as longer (48 h) time points following IV administration. The distribution of fetuin and the SMCC-linked aminoBP-fetuin conjugate were determined 6 h and 48 h post-IV administration. Only the SMCC-linked aminoBP-fetuin conjugate, which was the same preparation as above, was used in this study. Although fetuin localization was significantly higher ($p<0.0125$) in the kidneys 6 h after administration, differences in the biodistribution between fetuin and SMCC-conjugates were not significant in any other organs assessed (**Figure 4-5A**). In addition, no significant differences were observed between the percentage of the original dose administered recovered from the thyroid of the fetuin group (8.1 ± 1.1%) and that of the SMCC conjugate group (9.4 ± 2.6%). Forty-eight h post-administration, the concentration of fetuin was significantly higher in the femora, tibiae, kidneys and blood than that of the SMCC conjugate. SMCC conjugate localization in the spleen was higher than that of fetuin (**Figure 4-5B**). No differences were found in the localization of radioactivity in the thyroid of the fetuin group (8.3 ± 1.3%) and that of the SMCC-linked aminoBP-fetuin conjugate group (8.8 ± 3.2%). Likewise, no differences were observed in urinary parameters (i.e. % dose recovered, and TCA-soluble radioactivity in the urine) between the two groups at any of the time points assessed (**Table 4-2**). Although there were no inter-group differences in TCA-soluble radioactivity in the blood at 48 h, the levels in the SMCC conjugate group were significantly higher than fetuin at the 6 h time point.

The distribution of fetuin and the MMCCH-linked aminoBP-fetuin conjugates, which had been radiolabeled with the Bolton-Hunter chemistry, was assessed 72 h and 144 h post-IV administration. The conjugation efficiency of the MMCCH conjugate used in this experiment was 4.1 aminoBPs per fetuin. The *in vitro* HA binding of the ^{125}I-labeled fetuin, oxidized fetuin, and MMCCH conjugate was 47.33 ± 3.2%, 47.8 ± 0.7%, and 62.4 ± 2.8%, respectively. Seventy-two h post-IV administration, there were no differences between fetuin and conjugate localization to the femora, tibiae, sternum, spleen, and blood (**Figure 4-6A**). Increased conjugate localization was observed in the liver, while increased concentrations of fetuin were observed in the kidneys. Levels of radioactivity were significantly greater ($p < 0.05$) in the thyroid of the fetuin group (2.8 ± 0.8%) than of the MMCCH-linked aminoBP-fetuin conjugate group (1.0 ± 0.4%). Following the same trends at the 72 h sacrifice time point, no statistically significant differences were observed in protein localization to the femora, tibiae, sternum, or blood 144 h after administration (**Figure 4-6B**). In addition to the differences in the liver and kidneys observed at the 72 h time point, a significant difference in protein localization in the spleen was observed at the 144 h time point. No differences were found in the thyroid of the fetuin and MMCCH conjugate groups (1.0 ± 0.1% and 1.2 ± 0.2%, respectively), the percentage of dose recovered in the urine, the percentage of radioactivity in serum and the percentage of TCA-soluble radioactivity in serum (**Table 4-3**).

DISCUSSION

Conjugation of aminoBP onto glycoproteins, through the use of either the SMCC or the MMCCH chemistry, was designed to enhance their bone mineral affinity. Detailed

characterization of these conjugates performed in previous studies suggested that their affinity for various HA-based matrices increased in a manner proportional to the extent of aminoBPs conjugated onto them (**4**). This study was undertaken to evaluate the *in vivo* bone affinity of aminoBP-fetuin conjugates prepared using both the SMCC- and MMCCH-based reactions. The conjugates' binding and retention to Pro-Osteon® was determined prior to assessing their capacity to target to bone upon parenteral administration. Proteins with high affinity for mineralized matrices are expected to be beneficial in two aspects: (i) improved protein retention to mineralized implants; and (ii) enhanced targeting of proteins to bone upon parenteral administration.

Assessment of Mineralized Matrix Affinity: Due to the problems associated with the use of biologically-derived grafts in the repair of large osseous defects, the utilization of synthetic mineralized matrices is becoming increasingly more prevalent. To improve the osteoconductivity as well as the osteoinductivity (and thus the osseointegration) of HA-based implants, numerous studies have examined the effects of implant treatment with an osteogenic growth factor. For example, the treatment of a porous ceramic HA matrix with recombinant human bone morphogenetic-2 (rhBMP-2) prior to implantation significantly improved implant performance over non-treated groups in a calvarial implant model in rabbit (**11**). Similarly, the treatment of: (i) biphasic ceramic HA/tricalcium phosphate implants with rhBMP-2 in a spinal fusion model in sheep (**12**); and (ii) HA-coated titanium rods with recombinant human transforming growth factor-β_2 in a canine implantation model (**13**) enhanced radiological and histological indices of osseointegration over control groups. Recently, a correlation was demonstrated between

an osteogenic protein's osteoinductivity and its retention onto various matrices *in vivo* (**14**). In light of these observations, it was postulated that conjugation of aminoBP onto proteins may enhance protein retention to HA-based/coated matrices, and thus further improve the performance of growth factor-treated HA implants.

To this end, the capacity of both the MMCCH-linked and SMCC-linked aminoBP-fetuin conjugates to bind to a Pro-Osteon® was assessed *in vitro* as well as *in vivo*. Pro-Osteon® was used in this study because of its utilization in various clinical applications (**7**). As expected, conjugation of aminoBP through the use of either chemistry resulted in a significant increase in fetuin's capacity to bind and be retained to Pro-Osteon® implants (**Figure 4-2**). An initial concern in these studies was the impact that aminoBP conjugation would have on protein solubility. Through the use of BMP-2, Uludag *et al.* demonstrated that chemical modification of a protein may alter its physiological solubility (**14**). This is significant as an increase in BMP-2's inherent solubility, as a result of a modification, resulted in rapid protein loss from various implants irrespective of the physicochemical nature of the implant, which included Helistat® and Osteograf/N® (an HA-based matrix). Based on these results, a causal relationship between a protein's solubility and its rate of release from implants was established (**14**). Given that conjugation of aminoBP onto fetuin through the use of either the SMCC or MMCCH approach may alter the glycoprotein's solubility, conjugate binding and retention to Helistat®, a non-mineral containing matrix, was consequently determined as a control. Protein retention to Helistat® suggests neither the process of oxidation nor conjugation via the SMCC- or the MMCCH-based chemistries significantly affected fetuin's inherent solubility. As such, changes in solubility were considered

negligible in influencing conjugate retention in Pro-Osteon®; thus the increase in conjugate retention to this matrix was due to aminoBP conjugation. Plotting both protein binding to Helistat® as well as Pro-Osteon® *in vitro* versus *in vivo* revealed a statistically significant correlation ($p < 0.05$, and $p < 0.025$, respectively). All together, these results suggest that the conjugation of aminoBP onto fetuin through the use of either chemistry is appropriate for enhancing the glycoprotein's affinity and retention to an HA-based matrix *in vivo*. Furthermore, the results indicate that the *in vitro* experimental set-up described in this study may be used to accurately predict the retention of proteins to either Helistat® or Pro-Osteon® *in vivo*. Given that aminoBP conjugation onto fetuin was shown to increase protein retention in an implantation model, systemic conjugate targeting to bone was subsequently assessed.

Bone Targeting Upon Parenteral Administration: Conjugate targeting to bone was attempted using IP as well as IV routes of administration. Conjugation of aminoBP using either chemistry did not result in the targeting of fetuin to bone. With the exception of spleen, levels of radioactivity in all of the tissues assessed were significantly less in the conjugate-treated groups than that of control fetuin upon IP injection. Increased levels of TCA-soluble radioactivity in the serum of the IP-injected aminoBP-fetuin conjugates suggested that either disassociation of the radiolabel from the conjugates or degradation of the conjugates into low molecular weight species *in vivo* (**15**) may be responsible for the observed trends. Additionally, these results may also be due to: (i) poor conjugate uptake by the lymphatic system from the peritoneal cavity resulting in decreased systemic

exposure (16); (ii) metabolism by the reticuloendothelial system (namely the spleen); or (iii) a combination of these mechanisms.

To address the possibility of poor lymphatic uptake from the peritoneum, conjugate targeting to bone was assessed upon IV administration (**Figure 4-4**). Similar to the trends observed upon IP injection, levels of conjugate-associated radioactivity were lower than either fetuin or oxidized fetuin in the majority of tissues analyzed. Here, the results initially suggested that the oxidation of fetuin enhanced its affinity for osseous tissues (as levels of radioactivity in the femora, tibiae, and sternum were significantly greater in the oxidized fetuin group). Because levels of oxidized fetuin were significantly higher in the blood, these results should be interpreted with caution as this phenomenon may simply be due an increase in the oxidized glycoprotein's systemic bioavailability. Given that the IV route of administration ensured that the initial systemic exposure of each of the glycoproteins assessed was identical, the possibility of poor lymphatic uptake into systemic circulation was eliminated as a cause for the lack of conjugate targeting to bone. The observed increased TCA-soluble radioactivity in the blood of the aminoBP-fetuin conjugate-treated groups (both the SMCC and MMCCH conjugates) suggested that conjugate catabolism and/or radiolabel disociation from the conjugates had occured. To differentiate between these two possibilites, urine was collected in subsequent experiments following the IV administration of the proteins. No significant differences between fetuin and the conjugate groups were found in any of the urinary parameters assessed (i.e. % dose recovered in the urine, and TCA-soluble radioactivity in urine) in these studies. Because the TCA-soluble radioactivity in the serum was generally significantly higher in the conjugate-treated groups, while both the urinary parameters as

well as the amount of radioactivity in recovered in the thyroid were the same among fetuin and conjugate groups, the radioactivity quantified in the serum was likely the products of protein metabolism and not dissociated ^{125}I.

Radiolabeling is the most convenient method of assessing protein pharmacokinetics. As oxidative radiolabeling via the TCDG method has been shown to alter the biochemical properties of several proteins (**17-21**), it was thought that iodination using this technique may be a reason for negating the aminoBP-fetuin's inherent affinity to bone once administered parenterally. The Bolton-Hunter technique was chosen as an alternate means of radiolabeling as this method had not adversely altered the biochemical properties of IgM (**18**), IgG1 (**19**); and placental insulin receptors (**20**) while the TCDG method had. Interestingly, labeling with the Bolton-Hunter technique resulted in a ~ 3-fold increase in fetuin's as well as oxidized fetuin's capacity to bind to HA in 50% bovine serum as compared to TCDG-labeled samples. The reason(s) for increased *in vitro* HA binding was not known. As above, no differences between the Bolton-Hunter-radiolabeled fetuin and MMCCH-linked aminoBP-fetuin conjugate were found in their capacity to target to bone 72 and 144 h following IV administration. Using fetuin as a reference, levels of the MMCCH conjugate was significantly higher in the spleen as well as the liver at 144 h. Although no differences were found in any of the urinary or serum parameters between the two groups, these data suggest that the spleen may play an integral role in the degradation of the conjugates. Consequently, the radiolabeling technique employed did not affect the conjugates' incapacity to target to bone.

Taken together, these data suggest that neither SMCC- nor MMCCH-linked aminoBP conjugation enhanced fetuin targeting to bone. These observations were

unexpected as SMCC-mediated aminoBP conjugation enhanced the bone targeting of bovine serum albumin and lysozyme upon intravenous and subcutaneous administration in normal as well as ovariectomized rats (3). Given the increase in protein degradation of the conjugates, the presence of aminoBP may have increased fetuin's susceptibility to splenic and/or hepatic degradation. Based on these observations, the capacity of aminoBP-mediated bone targeting appears to be protein-specific. Because these albumin and lysozyme conjugates contained 11.0 and 3.9 aminoBPs/protein, respectively, the extent of aminoBP conjugation onto fetuin (i.e. between 4-7 aminoBPs/fetuin) was not likely the reason for the lack of bone targeting in these studies. As unmodified fetuin is 48.4 kDa, while albumin and lysozyme are 66 and 14 kDa, respectively, the glycoprotein's size was not likely an issue. Exploring fetuin's innate physiological and physicochemical properties may offer some insight into explaining the inability of aminoBP conjugation to target fetuin to bone.

The negative charges of fetuin's β-sheet in its cystatin-like domain D1 imparts an ability to bind to basic calcium phosphate (BCP) (22). Through its ability to bind to BCP, it is thought that the formation of 30-150 nm colloidal "calciprotein particles" consisting of up to 100 molecules of fetuin bound to apatitic microcrystals enables fetuin to delay the growth of these calcium microcrystals and facilitates their mobilization and subsequent removal from circulation via the hepatic and splenic phagocytes in the reticuloendothelial system (22). Corroborating its ability to prevent the precipitation of calcium and phosphate *in vitro* (22-24), fetuin has been shown to be an integral component in mitigating aberrant mineralization *in vivo* (25-28). As the aminoBP-fetuin conjugates used in these studies have a higher capacity to bind to HA than unmodified

fetuin (**4**, **5**), it was postulated that these fetuin conjugates may be more efficient in forming "calciprotein particles"-like complexes *in vivo* than either fetuin or oxidized fetuin. This may serve to explain the conjugates' increased susceptibity to the liver and spleen; and the significant decrease in the blood levels of the aminoBP-fetuin conjugate groups relative to fetuin (**Figures 4-4** and **4-5**) at shorter time points (i.e. < 48 h) following administration. That other conjugates (i.e. lysozyme and albumin) were successfully targeted to bone suggests that interaction of circulating microapatitic crystals does not occur to a significant degree with these bisphosphonate-protein conjugates.

Futher insights into the inablility of aminoBP to target fetuin to bone may be drawn from the findings of Hirabayashi *et al.* (**29**, **30**). In exploring the pharmacokinetics of a diclofenac-BP conjugate, it was shown that the amount of conjugate recovered in skeletal tissue increased as the duration of intravenous infusion increased from 0 (i.e. bolus injection) to 0.5 h. Lengthening the rate of infusion was also associated with an decrease in the amount of diclofenac-BP conjugate recovered in the liver and spleen (**29**). In a related study, it was found that increasing the dose of a diclofenac-BP conjugate administered IV actually decreased the degree of skeletal targeting while increasing the conjuguate's accumulation in the liver and spleen (**30**). To account for these observations, it was postulated that at high serum concentrations, the BP-diclofenac conjugate formed a complex with serum calcium, which upon precipitation, accumulated in both the liver and spleen. Consequently, by either decreasing the amount of conjugate administered or by lengthening the duration of administration, the serum concentration of the diclofenac-BP conjugate remained below the point at which calcium-diclofenac-BP precipitation occurs; thus resulting in increased bioavailability and increased skeletal targeting (**29**, **30**). Given

that IP and IV administration resulted in a similar conjugate biodistribution, decreasing the rate of aminoBP-fetuin conjugate infusion is not likely to influence the degree of conjugate targeting to bone. It was conceivably possible, however, that the dose of aminoBP-fetuin conjugates administered was simply too high to observe bone targeting. The dose of protein administered in these studies, however, was comparable to that used to achieve bone targeting in Uludag *et al.* (**4**) and significantly less than fetuin's endogenous serum concentrations of 2.5-4.5 mg/ml (**31**). Thus, the protein concentration of the dose administered in this study (i.e. 0.1 mg/ml) was not a likely factor in preventing conjugate targeting to bone. Future studies should be performed to assess the effects of modulating the dose of conjugate administered on bone targeting.

CONCLUSIONS

AminoBP conjugation enhanced fetuin's affinity for HA *in vitro*. Similarly, conjugation of aminoBP onto fetuin did increase the glycoprotein's retention to an HA-based matrix in an ectopic rat model. These results suggest that this approach may be feasible to enhance the retention, and thus possible the biological effect, of osteogenic proteins when implanted with an HA-based matrix *in vivo*. Upon parenteral administration, however, no discernable differences were found between either of the SMCC-linked or the MMCCH-linked conjugates' ability to target to osseous tissues. Despite the increase in conjugate binding and retention to an HA-based matrix *in vivo*, these data suggested that aminoBP conjugation may increase fetuin's susceptibility to the reticuloendothelial system (liver and spleen). As this was unlike other proteins previously targeted to bone, the capacity of aminoBP-conjugation to enhance protein targeting to

bone upon parenteral administration was determined to be protein-specific. Thus, future studies should be conducted to elucidate which proteins are appropriate for bisphosphonate-based targeting.

Table 4-1: Study Summary of Conjugate Targeting upon Parenteral Administration

Study	Group Number	Route of Administration	No. of Rats per Group	Proteins Injected	Radiolabeling Technique	Sacrifice Time Points
1	1	IP	1 *	Fetuin	TCDG	24 h
	2	IP	3	SMCC-conjugate	TCDG	24 h
	3	IP	2 *	Oxidized Fetuin	TCDG	24 h
	4	IP	2 *	MMCCH-conjugate	TCDG	24 h
2	1	IV	3	Fetuin	TCDG	24 h
	2	IV	3	SMCC-conjugate	TCDG	24 h
	3	IV	3	Oxidized Fetuin	TCDG	24 h
	4	IV	3	MMCCH- conjugate	TCDG	24 h
3	1	IV	3	Fetuin	TCDG	6 h
	2	IV	3	Fetuin	TCDG	48 h
	3	IV	3	SMCC-conjugate	TCDG	6 h
	4	IV	3	SMCC-conjugate	TCDG	48 h
4	1	IV	3	Fetuin	Bolton-Hunter	72 h
	2	IV	3	Fetuin	Bolton-Hunter	144 h
	3	IV	3	MMCCH-conjugate	Bolton-Hunter	72 h
	4	IV	3	MMCCH-conjugate	Bolton-Hunter	144 h

* Although 3 rats per group were typically used, some rats were eliminated due to inadvertent administration to the gastrointestinal tract.

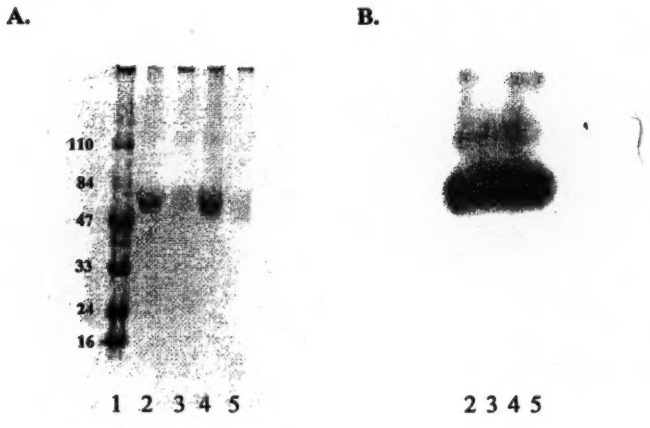

Figure 4-1: Gel electrophoresis of unlabeled (A) and radiolabeled proteins (B). The samples were initially run on SDS-PAGE and subsequently visualized via Coomassie staining (A) or autoradiography (B), respectively. Lanes contain the following samples: 1. molecular weight standard (kDa); 2. fetuin; 3. aminoBP-SMCC-fetuin conjugate, 4. oxidized fetuin; 5. aminoBP-MMCCH-fetuin conjugate.

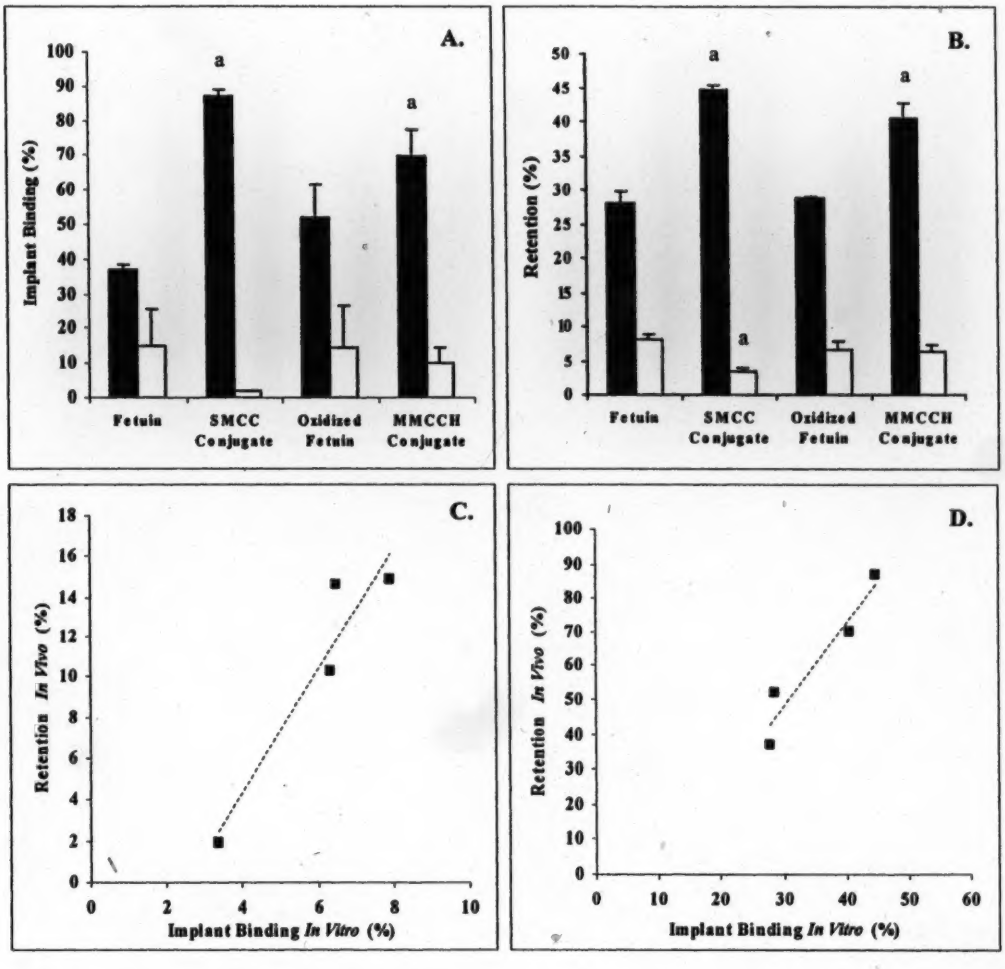

Figure 4-2: Conjugate binding to Pro-Osteon (black bars) and Helistat (white bars) was determined in 50% adult bovine serum *in vitro* (**A**) as well as *in vivo* (**B**). A linear correlation was observed between protein binding *in vitro* and protein retention *in vivo* in both Helistat (**C**, $r^2 = 0.8956$, $p < 0.05$) as well as Pro-Osteon (**D**, $r^2 = 0.9214$, $p < 0.025$). [a] $p < 0.0125$. Note the difference in scale for **C** and **D**.

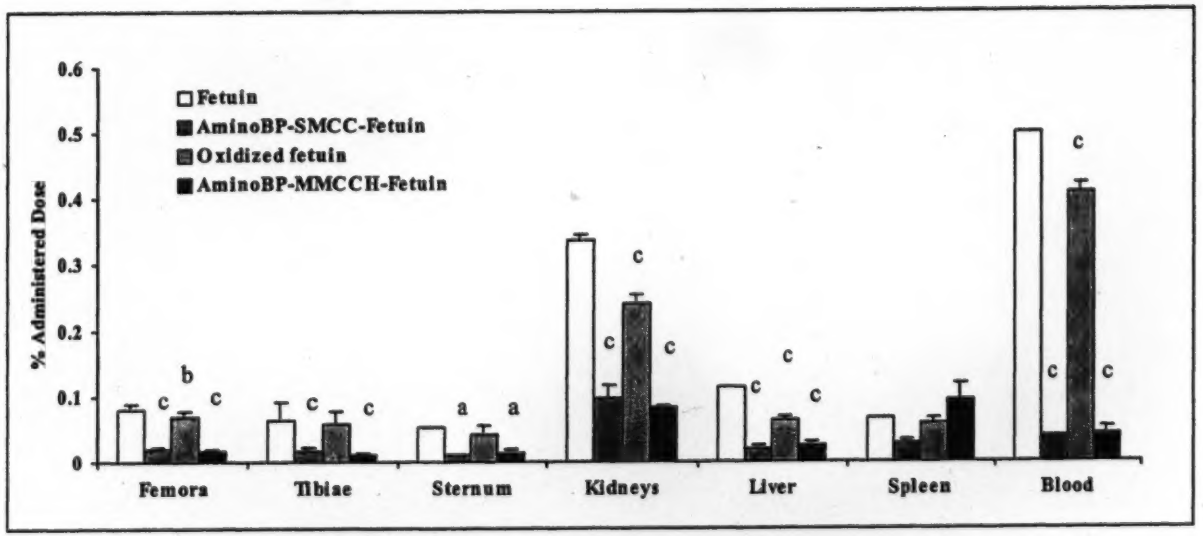

Group	TCA-Soluble Radioactivity in Serum (%)
Unmodified Fetuin	5.3
AminoBP-Fetuin (SMCC)	29.3 ± 4.6 [a]
Oxidized Fetuin	4.5 ± 0.7
AminoBP-Fetuin (MMCCH)	30.6 ± 5.9 [a]

Figure 4-3: The biodistribution of the aminoBP-SMCC-fetuin and the aminoBP-MMCCH-fetuin conjugates and their respective controls 24 h after IP administration. The amount of radioactive counts for each site was normalized by the average dose administered per animal. The % administered dose to liver and blood was further normalized by the weight of the tissue and by the volume obtained, respectively. Listed in the table is a summary of the TCA-soluble fraction in the serum. [a] $p < 0.05$; [b] $p < 0.025$; [c] $p < 0.0125$ *vs*. fetuin group.

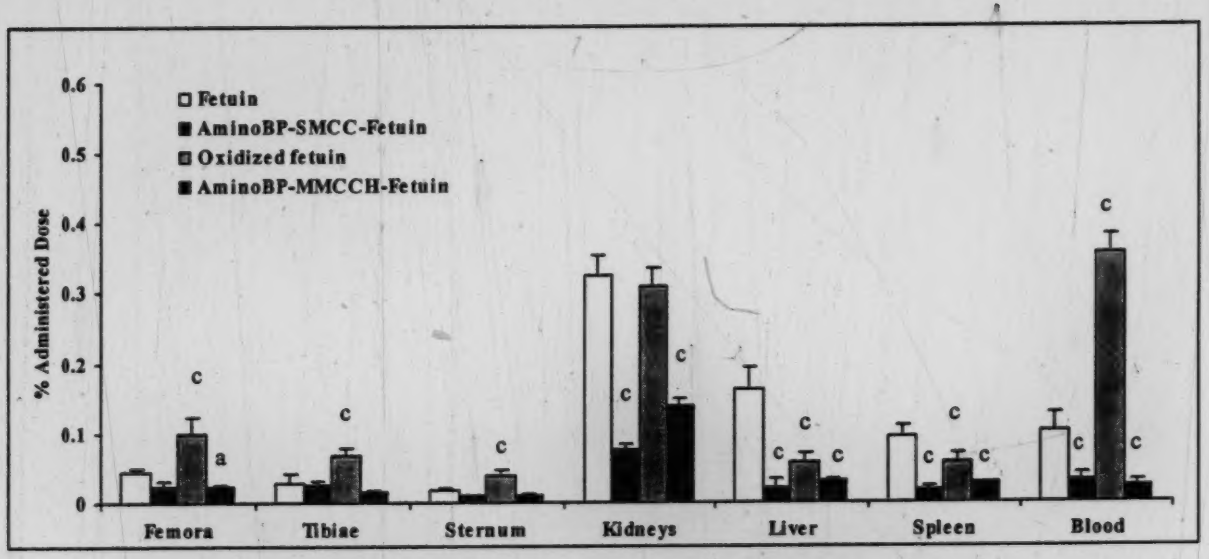

Group	TCA-Soluble Radioactivity in Blood (%)
Unmodified Fetuin	9.3 ± 3.6
AminoBP-Fetuin (SMCC)	23.35 ± 1.9 [c]
Oxidized Fetuin	3.45 ± 0.9
AminoBP-Fetuin (MMCCH)	23.6 ± 1.9 [c]

Figure 4-4: The biodistribution of the aminoBP-SMCC-fetuin and the aminoBP-MMCCH-fetuin conjugates and their respective controls 24 h after IV administration. The amount of radioactivity (i.e. counts) for each site was normalized by the average dose administered per animal. The % administered dose to liver and blood was further normalized by the weight of the tissue and by the volume obtained, respectively. Listed in the table is a summary of the TCA-soluble fraction in the blood. [a] $p < 0.05$; [b] $p < 0.025$ *vs.* fetuin group.

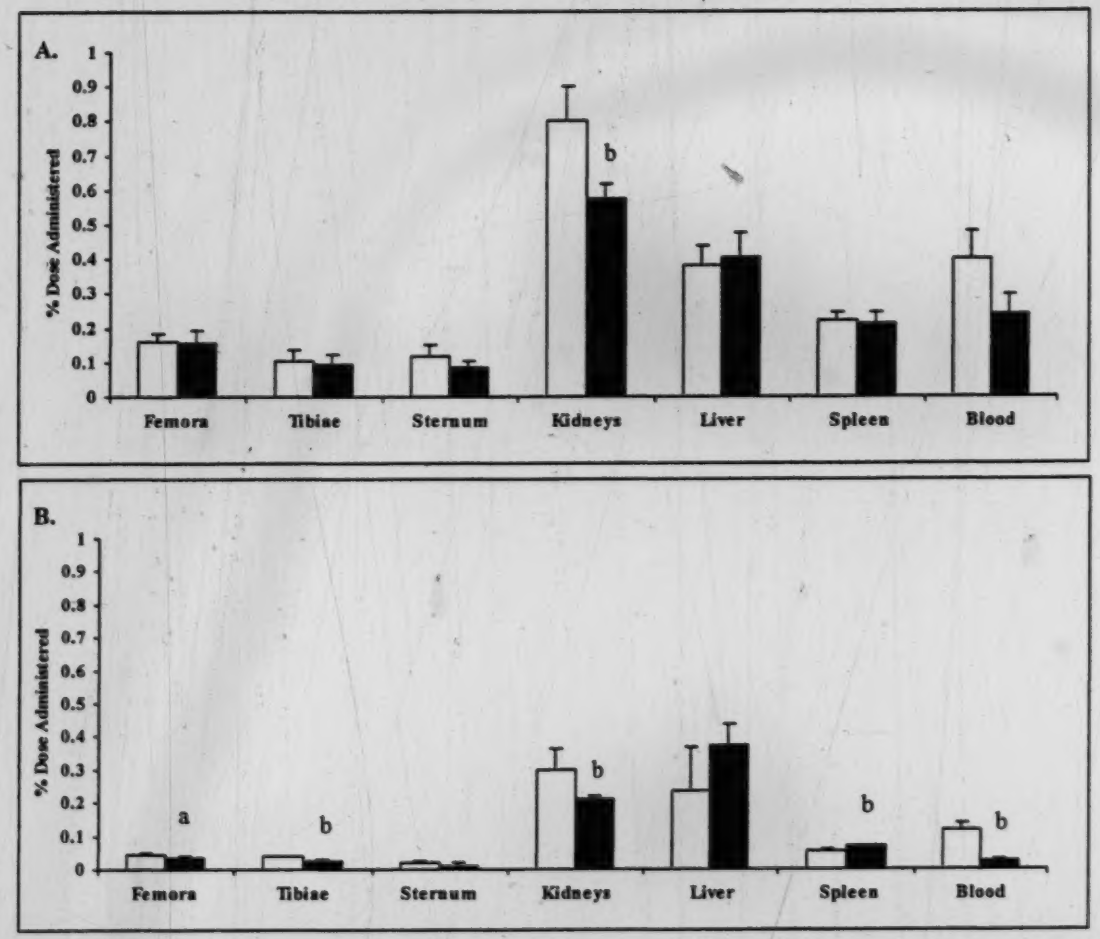

Figure 4-5: The biodistribution of the SMCC-conjugates (dark bars) and fetuin (white bars) 6 h **(A)** and 48 h **(B)** after IV administration. The amount of radioactivity (i.e. counts) for each site was normalized by the average dose administered per animal. The % administered dose to liver and blood was further normalized by the weight of the tissue and by the volume obtained, respectively. [a] $p < 0.05$; [b] $p < 0.025$; [c] $p < 0.0125$ *vs.* fetuin group.

Table 4-2: Urinary and Blood Analysis 6, 24 and 48 h post-IV administration.

Group	6 h			24 h		48 h		
	Dose Recovered in Urine (%)	TCA-Soluble Radioactivity in Urine (%)	TCA-Soluble Radioactivity in Blood (%)	Dose Recovered in Urine (%)	TCA-Soluble Radioactivity in Urine (%)	Dose Recovered in Urine (%)	TCA-Soluble Radioactivity in Urine (%)	TCA-Soluble Radioactivity in Blood (%)
Unmodified Fetuin	33.5 ± 1.0	90.4 ± 1.1	11.7 ± 1.7	14.8 ± 7.0	89.0 ± 0.8	3.8 ± 1.1	90.0 ± 2.1	2.69 ± 3.3
AminoBP-Fetuin (SMCC)	17.2 ± 18.8	89.7 ± 1.3	57.2 ± 6.6 [a]	19.0 ± 2.6	89.5 ± 0.8	2.0 ± 0.8	88.3 ± 2.2	8.7 ± 12.7

[a] $p < 0.05$ *vs.* fetuin group.

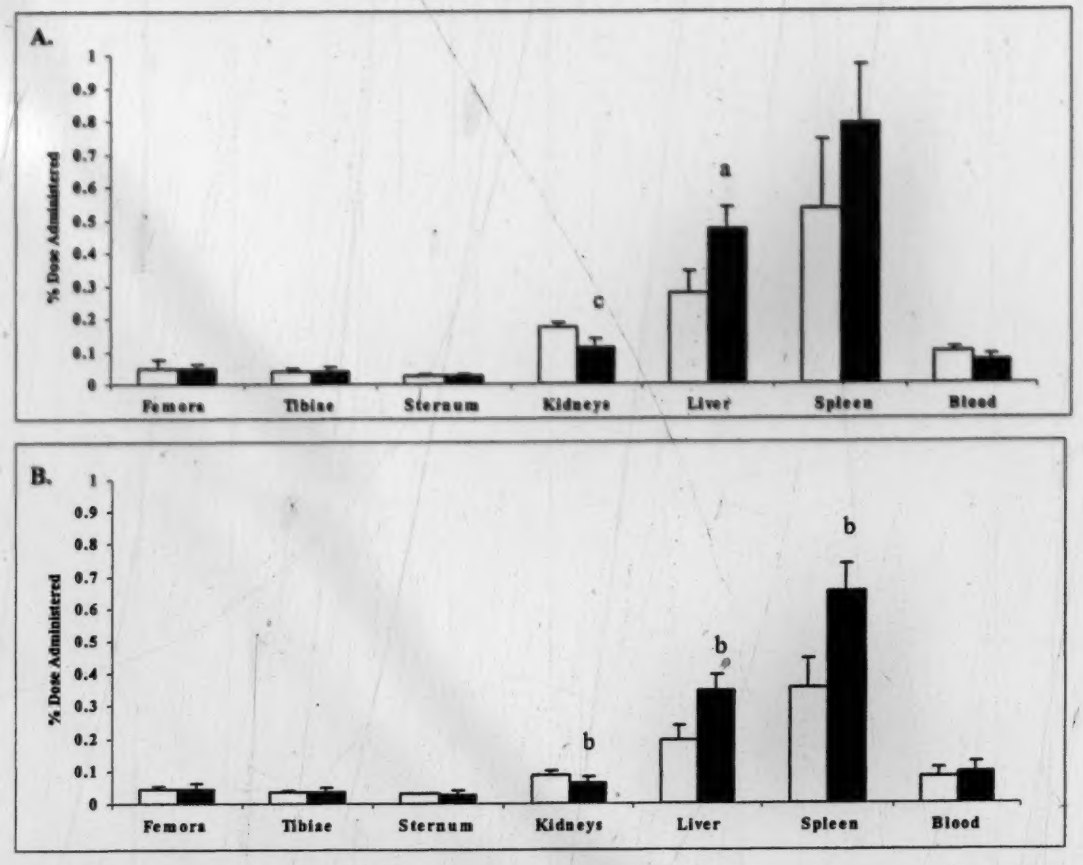

Figure 4-6: The biodistribution of the MMCCH-conjugates (dark bars) and fetuin (white bars) 72 h **(A)** and 144 h **(B)** after IV administration. The amount of radioactivity (i.e. counts) for each site was normalized by the average dose administered per animal. The % administered dose to liver and blood was further normalized by the weight of the tissue and by the volume obtained, respectively. [a] $p < 0.05$; [b] $p < 0.025$; [c] $p < 0.0125$ *vs.* fetuin group.

Table 4-3: Urinary and Blood Analysis 72 and 144 h post-IV administration.

Group	72 h			144 h		
	Dose Recovered in Urine (%)	^{125}I in Serum (%)	TCA-Soluble Radioactivity in Serum (%)	Dose Recovered in Urine (%)	^{125}I in Serum (%)	TCA-Soluble Radioactivity in Serum (%)
Unmodified Fetuin	28.9 ± 4.6	71.5 ± 4.8	5.5 ± 3.5	3.2 ± 1.4	62.0 ± 2.7	13.2 ± 4.4
AminoBP-Fetuin (MMCCH)	25.1 ± 5.2	82.0 ± 5.7	15.8 ± 10.4	2.4 ± 0.5	64.2 ± 3.0	10.4 ± 3.9

REFERENCES

1. S.A. Gittens, H. Uludag, Growth factor delivery for bone tissue engineering, *J. Drug Target.* 9(2001) 407-429.

2. H. Uludag, N. Kousinioris, T. Gao, D. Kantoci, Bisphosphonate conjugation to proteins as a means to impart bone affinity, *Biotechnol. Prog.* 16 (2000) 258-267.

3. H. Uludag, J. Yang, Targeting systemically administered proteins to bone by bisphosphonate conjugation, *Biotechnol. Prog.* 18 (2002) 604-11.

4. S.A. Gittens, J.R. Matyas, R.F. Zernicke, H. Uludag, Imparting bone affinity to glycoproteins through the conjugation of bisphosphonates, *Pharm. Res.* 20 (2003) 978-987.

5. S.A. Gittens, P.I. Kitov, J.R. Matyas, R. Loebenberg, H. Uludag, Impact of tether length on 2the bone mineral affinity of protein-bisphosphonate conjugates, *Pharm. Res.* 21 (2004) 608-616.

6. K. Bessho, Y. Konishi, S. Kaihara, K. Fujimura, Y. Okubo, and T. Iizuka. Bone induction by Escherichia coli -derived recombinant human bone morphogenetic protein-2 compared with Chinese hamster ovary cell-derived recombinant human bone morphogenetic protein-2, *Br. J. Oral. Maxillofac. Surg.* 38 (2000) 645-649.

7. J.S. Thalgott, Z. Klezl, M. Timlin, J.M, Giuffre, Anterior lumbar interbody fusion with processed sea coral (coralline hydroxyapatite) as part of a circumferential fusion, *Spine.* 27 (2002) E518-E525.

8. M.M. Bradford, A rapid and sensitive method for the quantitation of microgram quantities of protein utilizing the principle of protein-dye binding, *Anal. Biochem.* 72 (1976) 248-254 .

9. B.N. Ames, Assay of inorganic phosphate, total phosphate, and phosphatases. In E.F. Neufield, and V. Ginsburg (eds.), *Methods in Enzymology, Volume VIII, Complex Carbohydrates*, Academic Press, New York, (1966) pp. 115-117.

10. S.A. Anderson, S.K. Song, J.J. Ackerman, R.S. Hotchkiss, Sepsis increases intracellular free calcium in brain, *J. Neurochem.* 72 (1999) 2617-2620.

11. J.A. Koempel, B.S. Patt, K. O'Grady, J. Wozney, D.M. Toriumi, The effect of recombinant human bone morphogenetic protein-2 on the integration of porous hydroxyapatite implants with bone, *J. Biomed. Mater. Res.* 41 (1998) 359-363.

12. S.D. Boden, G.J. Martin Jr., M.A. Morone, J.L. Ugbo, P.A. Moskovitz, Posterolateral lumbar intertransverse process spine arthrodesis with recombinant human bone morphogenetic protein 2/hydroxyapatite-tricalcium phosphate after laminectomy in the nonhuman primate, *Spine.* 24 (1999) 1179-1185.

13. D.R. Sumner, T.M. Turner, R.M. Urban, R.M. Leven, M. Hawkins, E.H. Nichols, J.M. McPherson, J.O. Galante, Locally delivered rhTGF-beta2 enhances bone ingrowth and bone regeneration at local and remote sites of skeletal injury, *J. Orthop. Res.* 19 (2001) 85-94.

14. H. Uludag, D. D'Augusta, J. Golden, J. Li, G. Timony, R. Riedel, J.M. Wozney, Implantation of recombinant human bone morphogenetic proteins with biomaterial carriers: A correlation between protein pharmacokinetics and osteoinduction in the rat ectopic model, *J. Biomed. Mater Res.* 50 (2000) 227-238.

15. S. Yokota, T. Uchida, S. Kokubo, K. Aoyama, S. Fukushima, K. Nozaki, T. Takahashi, R. Fujimoto, R. Sonohara, M. Yoshida, S. Higuchi, S. Yokohama, T. Sonobe, Release of recombinant human bone morphogenetic protein 2 from a newly developed carrier, *Int. J. Pharm.* 251 (2003) 57-66.

16. M.F. Flessner, R.L. Dedrick, J.S. Schultz, Exchange of macromolecules between peritoneal cavity and plasma, *Am. J. Physiol.* 248 (1985) H15-H25.

17. G.L. Mayers, J. Klostergaard, The use of protein A in solid-phase binding assays: a comparison of four radioiodination techniques, *J. Immunol. Methods*. 57 (1983) 235-246.

18. E. Vigorito, A. Robles, H. Balter, A. Nappa, F. Goni, [125I]IgM (KAU) human monoclonal cold agglutinin: labelling and studies on its biological activity, *Appl. Radiat. Isot.* 46 (1995) 975-979.

19. D.F. Hayes, M.A. Noska, D.W. Kufe, M.R. Zalutsky, Effect of radioiodination on the binding of monoclonal antibody DF3 to breast carcinoma cells, *Int. J. Rad. Appl. Instrum. B.* 15 (1988) 235-241.

20. S. Ganguly, Iodination-induced alterations in biochemical properties of human placental insulin receptor, *FEBS Lett.* 224 (1987) 198-200.

21. G. Vaidyanathan, M.R. Zalutsky, Protein radiohalogenation: observations on the design of N-succinimidyl ester acylation agents, *Bioconjug. Chem.* 1 (1990) 269-273.

22. A. Heiss, A. DuChesne, B. Denecke, J. Grotzinger, K. Yamamoto, T. Renne, W. Jahnen-Dechent, Structural basis of calcification inhibition by alpha 2-HS glycoprotein/fetuin-A. Formation of colloidal calciprotein particles, *J. Biol. Chem.* 278 (2003) 13333-13341.

23. T. Schinke, C. Amendt, A. Trindl, O. Poschke, W. Muller-Esterl, W. Jahnen-Dechent, The serum protein alpha2-HS glycoprotein/fetuin inhibits apatite

formation in vitro and in mineralizing calvaria cells. A possible role in mineralization and calcium homeostasis, *J. Biol. Chem.* 271 (1996) 20789-20796.

24. P.A. Price, J.E. Lim, The inhibition of calcium phosphate precipitation by fetuin is accompanied by the formation of a fetuin-mineral complex, *J. Biol. Chem.* 278 (2003) 22144-22152.

25. W. Jahnen-Dechent, C. Schafer, A. Heiss, J. Grotzinger, Systemic inhibition of spontaneous calcification by the serum protein alpha 2-HS glycoprotein/fetuin, Z. *Kardiol.* 90 (2001) 47-56.

26. P.A. Price, M.K. Williamson, T.M. Nguyen, T.N. Than, Serum levels of the fetuin-mineral complex correlate with artery calcification in the rat, *J. Biol. Chem.* 279 (2004) 1594-600.

27. M. Ketteler, P. Bongartz, R. Westenfeld, J.E. Wildberger, A.H. Mahnken, R. Bohm, T. Metzger, C. Wanner, W. Jahnen-Dechent, J. Floege, Association of low fetuin-A (AHSG) concentrations in serum with cardiovascular mortality in patients on dialysis: a cross-sectional study, *Lancet.* 361 (2003) 827-833.

28. C. Schafer, A. Heiss, A. Schwarz, R. Westenfeld, M. Ketteler, J. Floege, W. Muller-Esterl, T. Schinke, W. Jahnen-Dechent, The serum protein alpha 2-Heremans-Schmid glycoprotein/fetuin-A is a systemically acting inhibitor of ectopic calcification, *J. Clin. Invest.* 112 (2003) 357-366.

29. H. Hirabayashi, T. Sawamoto, J. Fujisaki, Y. Tokunaga, S. Kimura, T. Hata, Relationship between physicochemical and osteotropic properties of bisphosphonic derivatives: rational design for osteotropic drug delivery system (ODDS), *Pharm. Res.* 18 (2001) 646-651.

30. H. Hirabayashi, T. Takahashi, J. Fujisaki, T. Masunaga, S. Sato, J. Hiroi, Y. Tokunaga, S. Kimura, T. Hata, Bone-specific delivery and sustained release of diclofenac, a non-steroidal anti-inflammatory drug, via bisphosphonic prodrug based on the Osteotropic Drug Delivery System (ODDS), *J. Control. Release.* 70 (2001) 183-191.

31. J.A. Kazi, O. Nakamura, T. Ohnishi, N. Arakaki, T. Kajihara, S. Nakagawa, Y. Daikuhara, Changes with age of the rat fetuin concentration in serum and its mRNA expression, *J. Biochem.* 124 (1998) 179-186.

CHAPTER V

IMPARTING BONE MINERAL AFFINITY TO OSTEOGENIC PROTEINS THROUGH HEPARIN-BISPHOSPHONATE CONJUGATES[1].

[1] The contents of this chapter have been previously published in: Gittens SA, Bagnall K, Matyas JR, Loebenberg R, and Uludağ H. Imparting Bone Affinity to Osteogenic Proteins through the Use of Heparin-Bisphosphonate Conjugates. *J. Control. Release* (2004) 98(5): 255-268.

INTRODUCTION

Much attention has recently been given to the emerging prospect of using osteogenic growth factors to elicit the systemic regeneration of bone upon their parenteral administration (reviewed in **1**). Because of their pleiotropic nature, however, these proteins have been shown to mediate numerous extra-skeletal side effects that currently preclude them from being used clinically for indications such as osteoporosis. For example, the systemic administration of basic fibroblast growth factor (bFGF) resulted in non-specific distribution leading to the development of anemia as well as pathological changes to the kidneys (e.g. glomerular lesions) in various animal models (**2, 3**). Bone morphogenetic protein (BMP)-2, on the other hand, has been shown to elicit undesirable heterotropic bone formation away from sites of administration (**4**). To circumvent the generation of such adverse effects, these growth factors must be targeted to osseous tissues, whereby they can stimulate bone formation through bone cell proliferation and differentiation (**1**) with minimal distribution to other sites.

In response to the inherent need to deliver these osteogenic growth factors to skeletal tissue, we are currently pursuing the strategy of modifying proteins with bisphosphonates, so that the exceptionally high affinity that these pyrophosphate analogs have for the mineral component of bone (i.e. hydroxyapatite, HA) will be imparted onto the proteins. In fact, it has already been shown that the conjugation of 1-amino-1,1-diphosphonate methane (aminoBP) directly onto bovine serum albumin (**5-7**), lysozyme (**7**), and fetuin (**8, 9**) increased these proteins' affinity for bone and/or mineralized biomaterial matrices both *in vitro* and *in vivo*. One of the primary concerns with this approach, however, is the effect that direct aminoBP conjugation will have on protein

bioactivity. A review of the literature suggests that the way in which chemical modifications will affect a given protein's bioactivity is protein-specific. For example, moderate chemical modifications of bFGF's lysine groups (via biotinylation) (**10**) or its cysteine groups (via carboxymethylation) (**11**) does not appear to affect its bioactivity *in vitro*; although excessive biotinylation (**10**) or site directed mutagenesis of specific lysine groups (K to Q) diminishes bFGF's bioactivity (**12**). On the other hand, the influence of chemical modification on BMP-2's bioactivity *in vivo* appeared to be dependent on the chemistry used to biotinylate the protein itself (**13**). It is expected that various osteogenic proteins may be chosen to be targeted to bone, and that 3-10 aminoBP moieties per protein are expected to be required to yield sufficient protein targeting upon systemic administration. Consequently, the chemical conjugation of BPs onto a given osteogenic protein may inadvertently alter its tertiary structure, ultimately culminating in the potential loss of the protein's bioactivity.

Consequently, a drug delivery system was developed that could effectively enhance the bone mineral affinity of osteogenic growth factors without the need to chemically modify protein. In delineating an appropriate approach to achieve this goal, heparin, an ubiquitously-found, anionic glycosaminoglycan typically associated with its anti-coagulant activity (**14**), was chosen as the foundation of our delivery system due to its inherently high affinity for various proteins, including basic fibroblast growth factor (bFGF) (**14-16**), bone morphogenetic protein (BMP)-2 (**17, 18**) acidic fibroblast growth factor (**14**), BMP-4 (**18**), BMP-7 (**19, 20**) vascular endothelial growth factor (**16**), platelet-derived growth factor (**16**) and transforming growth factor-β_1 and β_2 (**16, 21**). It was postulated that by conjugating aminoBP directly onto heparin, a mineral affinity

would be imparted onto glycosaminoglycan. Providing that the process of conjugation does not compromise heparin's affinity for the aforementioned bone-regulating proteins, the corollary effect of combining the aminoBP-heparin conjugate with these cytokines should be a corresponding increase in their affinity for bone mineral. In its very essence, the premise behind this approach is that heparin, engineered to have a high affinity for bone, will serve as a drug delivery system that can ultimately target heparin-binding proteins to bone to achieve a therapeutic response following its parenteral, systemic administration.

Accordingly, this study was performed to: (i) determine the feasibility of conjugating aminoBP onto heparin through the use of 4-(maleimidomethyl)cyclohexane-1-carboxyl-hydrazide; (ii) assess the aminoBP-heparin conjugates' affinity for HA affinity *in vitro*; and (iii) establish the capacity of these conjugates to increase the affinity of both bFGF and BMP-2 to bone mineral. Both bFGF and BMP-2 were chosen as model heparin-binding, osteogenic proteins in this study because of their availability and ability to elicit the regeneration of bone *in vivo* (1). A novel approach is introduced that is engineered to enhance the affinity of osteogenic cytokines to bone without the previous prerequisite of directly modifying these bioactive proteins.

MATERIALS AND METHODS

Materials:

The compound 4-(maleimidomethyl)cyclohexane-1-carboxyl-hydrazide (MMCCH) was acquired from Molecular Biosciences (Boulder, CO). Heparin (sodium salt isolated from porcine intestinal mucosa; lot 082K1498), 2-iminothiolane (2-IT),

bovine adult serum, sodium periodate ($NaIO_4$), trichloroacetic acid (TCA), 1,3,4,6-tetrachloro-3α,6α-diphenylglycouril (TCDG) were obtained from Sigma Aldrich (St. Louis, MO). $Na^{125}I$ (in 0.1M NaOH) was obtained from Perkin Elmer (Wellesley, MA), while toluidine blue O and hexanes were acquired from Fisher Scientific (Fairlawn, NJ). Saline (0.9% NaCl) was obtained from Baxter Corporation (Toronto, ON). The NAP-10 columns used were obtained from Amersham Pharmacia Biotech (Baie d'Urfé, QC). 2,4-dinitrophenylhydrazine (DNP) was from Kodak (Rochester, NY). N,N-dimethylformamide (DMF) was from Caledon Laboratories (Georgetown, ON). The Spectra/Por dialysis tubing with MW cutoff of 12-14,000 Da was acquired from Spectrum Laboratories (Rancho Dominguez, CA). The phosphate (pH 7.4), and 0.1 M carbonate (pH 10) buffers were prepared as described by Uludağ *et al.* (**5**), whereas the 0.1 M sodium acetate buffer was prepared as described by Chamow *et al.* (**22**). The buffer used to facilitate the interaction between bFGF and BMP-2 with heparin, referred to as Kamei's buffer, was prepared according to Kamei *et al.* (**23**). Briefly, NaCl and KCl were added to 10 mM phosphate buffer to yield a final concentration of 138 mM and 2.7 mM, respectively. The glycine buffer used was prepared by adjusting the pH of 0.1 M glycine to 3 using 0.1 M HCl. Basic fibroblast growth factor (bFGF, lot number: 000172) was obtained from BD Biosciences (Bedford, MA) while bone morphogenetic protein-2 (BMP-2) was purchased from Dr. W. Sebald (Universität Würzburg, Würzburg, Germany). The hydroxyapatite (HA) and aminoBP were prepared as described in Uludağ *et al.* (**5**).

AminoBP Conjugation onto Heparin (*Figure 5-1*):

Initially, the vicinal diol groups within heparin's unsulfated glucuronic and iduronic acid residues **(24)** were selectively oxidized **(8, 22)** by treating heparin (25 mg/ml in 0.1 M acetate buffer) with 25 mM of $NaIO_4$. Following a 2.5 h incubation, the process of oxidation was terminated by extensive dialysis against dH_2O and subsequently against 0.1 M acetate buffer. The oxidized heparin was then reacted for 2.5 h with 25 mM MMCCH (stock solution dissolved as 150 mM in DMF), a heterobifunctional crosslinker whose nucleophilic hydrazine and electrophilic maleimide moieties react with aldehyde and -SH groups, respectively. Separately, aminoBP was thiolated by incubating equal volumes of aminoBP (80 mM in 0.1 M phosphate buffer) with 2-IT solution (40 mM in 0.1 mM phosphate buffer) for 2.5 h. The product from this reaction was then added directly to MMCCH-reacted heparin in equal volumes for 2.5 h. To remove the unreacted reagents (i.e. aminoBP, 2-IT, thiolated aminoBP, and crosslinker) the conjugates were thoroughly dialyzed against 0.2 M carbonate buffer (x3) and deionized water (x2).

Analysis of the Conjugates:

Heparin Assay **(25)**: A 100 µl heparin-containing sample was added to 400 µl of 0.2% NaCl and 600 µl of heparin reagent (0.05% toluidine blue in 0.01 N HCl and 0.2% NaCl). Following the addition of 1000 µl of hexanes, the sample was shaken and the absorbance of the aqueous layer was determined at 630 nm. Serially diluted heparin reconstituted in dH_2O was used for the calibration curve.

DNP Assay for Aldehydes **(27)**: A 50 µl aliquot of oxidized heparin was added to 2.5 ml of 0.2 mM DNP (in 1 M HCl) and incubated for 1 h at 37 °C. The absorbance of the

samples was determined at 370 nm. Serially diluted formaldehyde (in dH_2O) was used for the calibration curve. Once the aldehyde and heparin concentrations were quantified, the number of aldehyde groups per heparin was calculated (mol:mol ratio).

Phosphate Assay: The phosphate assay was modified from the original procedure of Ames (27) and has been described previously (5). A calibration curve consisting of known concentrations of aminoBP dissolved in dH_2O was utilized. The phosphate concentrations generated were used in combination with the results from the heparin assay to yield the number of aminoBPs conjugated onto heparin (mol:mol ratio).

Assessment of Conjugate Affinity to Hydroxyapatite:

Hydroxyapatite Binding: The details of the hydroxyapatite (HA) binding assay have been described previously (5, 8). Briefly, an aliquot of heparin sample (~60 μg) was added to a microcentrifuge tube containing 5 mg of HA with 150 mM phosphate buffer (pH 7.4). The molarity of this phosphate buffer had previously been determined to provide the optimal conditions for differentiating HA binding between the conjugate and unmodified heparin. After being shaken for 2.5 h at room temperature, the samples were centrifuged and the heparin concentration in the supernatant was subsequently determined using the previously described Heparin assay. HA affinity (expressed as %binding) was calculated as follows: 100% x {(heparin concentration without HA) – (heparin concentration with HA)} ÷ (heparin concentration without HA). As all binding was assessed in duplicate, the average values were reported.

Assessment of bFGF and BMP-2 Affinity to HA:

Protein Iodination: The binding was assessed by using ^{125}I-labeled proteins. In tubes previously coated with TCDG (200 µl of 20 µg/ml TCDG in choloroform), 10 µg of either bFGF or BMP-2, both of which had been reconstituted to a concentration of 0.2 µg/µl, was added to 30 µl of 0.1 M phosphate buffer (pH 7.4), and 20 µl of 0.01 mCi of Na^{125}I (in 0.1 M NaOH). After reacting for 20 minutes, free ^{125}I was separated from the radiolabeled protein by elution on a NAP-10 column with 0.1 M phosphate buffer (pH 7.4), and 0.1 M glycine buffer (pH 3) for bFGF and BMP-2, respectively. It was assumed that the amount of protein recovered following elution was 100%. Once an aliquot of the samples was precipitated with 20% trichloroacetic acid, it was confirmed that the radioiodinated proteins contained <5% free ^{125}I.

HA Binding Assay: Assuming 100% recovery after NAP-column filtration, 5.5 pmol of either bFGF or BMP-2 was added to 550 pmol of heparin sample in Kamei's buffer containing 1.5% bovine adult serum to ensure a 100:1 (mol:mol) ratio between heparin and protein. After a 1 min incubation at 23 °C, 50 µl aliquots of the protein-heparin mixture were added to 1.5 ml microcentrifuge tubes containing 5 mg of HA and 200 µl of binding buffer consisting of either 0.25 M or 0.5 M phosphate buffer. As such, the final phosphate concentrations used in these experiments were 200 mM and 400 mM respectively. In some experiments, the effects of modulating either the phosphate buffer concentration, or the ratio of protein to heparin was assessed. After periodical shaking over a 2.5 h period, the samples were subsequently centrifuged to obtain an HA pellet. The supernatant was collected and the pellet, consisting of HA, was washed

with the binding buffer and re-centrifuged. This washing procedure was then repeated twice more and the collected supernatant from each of these steps was subsequently measured separately. Quantification of the radioactivity was determined using a γ-counter (Wallac Wizard 1470, Turku, Finland). HA affinity, expressed as %HA binding, was calculated as follows: 100% x (counts in HA) ÷ {(counts in HA) + (counts in supernatants)}. As all binding was assessed in duplicate, the average values were reported. Each experiment presented was repeated twice (n=2).

Statistical Analysis:

bFGF and BMP-2 binding to HA was compared in the presence as well as the absence of unmodified heparin using a student's *t*-test. The reported *p*-value from this method of analysis is two-sided; $p < 0.05$). Analysis of growth factor binding to HA alone or in the presence of unmodified heparin, oxidized heparin, or aminoBP-heparin conjugates was assessed using Tukey post-hoc comparison ($p < 0.05$). Statistical analysis was performed by S-PLUS Student Ed. 6.0 (Insightful Corp, Seattle, WA).

RESULTS

AminoBP-Conjugation onto Heparin:

Due to the inherent paucity in the number of aldehyde groups found in heparin, the glycosaminoglycan was initially oxidized using $NaIO_4$ prior to conjugating aminoBP onto the heparin. As a means of validating this procedure, the effect of modulating the concentration of $NaIO_4$ on the subsequent number of aldehyde moieties introduced onto heparin was determined. As the concentration of $NaIO_4$ used to oxidize heparin increased, a corresponding concentration-dependent increase in the number of aldehyde groups

introduced onto the heparin was observed (**Figure 5-2A**). It was found that the product from this process of oxidation was stable at 4°C for at least a month (data not shown). In proportion to the degree of oxidation, an increase in the number of aminoBPs subsequently conjugated onto heparin was observed when the concentration of MMCCH and thiolated aminoBP (30 mM and 40 mM, respectively) were kept constant (**Figure 5-2B**). Under the experimental conditions, not all aldehyde groups introduced onto heparin were used for conjugation; however, the number of aldehyde groups per molecule of heparin correlated strongly to the number of aminoBP conjugated onto heparin (r^2 = 0.9726; $p < 0.001$; **Figure 5-2C**).

The effect of modulating MMCCH and thiolated aminoBP concentrations on the conjugation efficiency was subsequently assessed. Similar to the concentration-dependent trends observed with the $NaIO_4$ experiments, the number of aminoBPs conjugated onto heparin increased in a manner proportional to the concentration of thiolated aminoBP and crosslinker used (data not shown). The maximal number of aminoBPs conjugated onto heparin in these studies was 7.2 aminoBPs/heparin. On average, the control samples (i.e. non-oxidized heparin that had either been reacted with thiolated aminoBP or MMCCH alone or oxidized heparin that had either been reacted with thiolated aminoBP or MMCCH alone) had < 1.8 aminoBPs/heparin suggesting some degree of aminoBP retention after dialysis. Cumulatively, these data suggest that the MMCCH chemistry applied is appropriate for the conjugation of aminoBP onto heparin.

HA Affinity of the Amino-BP-Heparin Conjugates:

Using the same samples that had been synthesized in the previous experiments, an HA binding assay was used to assess whether the process of conjugation enhanced the bone mineral affinity of heparin. As can be seen in **Figure 5-3**, the conjugates' capacity to bind to HA increased as the number of aminoBPs conjugated onto heparin also increased. While an average HA binding of 26% was observed for the control samples, a maximum binding of 62% (under the experimental conditions) was achieved when ~ 7 aminoBPs were conjugated per heparin. It should also be noted that neither the extent of heparin oxidation nor the extent of maleimide groups conjugated per heparin affected its innate ability to bind to HA under the experimental conditions used. All together, these results confirmed that the covalently attached aminoBPs were indeed responsible for the heparin conjugates' affinity for HA.

HA Affinity of bFGF and BMP-2 with the Amino-BP-Heparin Conjugates:

Given the *in vitro* mineral affinity of the aminoBP-heparin conjugates, the propensity of these conjugates to enhance the affinity of bFGF and BMP-2 to HA was subsequently determined. Prior to doing so, however, the mineral affinities of ^{125}I-labeled bFGF and BMP-2 were assessed as a baseline. In comparison to an inherent bFGF binding of 17.5 ± 0.3% and 16.2 ± 2.4% in 200mM and 400mM phosphate buffers, respectively, the addition of unmodified stock heparin decreased bFGF's inherent affinity for HA; albeit non-significantly (**Figure 5-4**). Relative to an inherent BMP-2 binding of 61.4 ± 2.1% and 40.6 ± 0.8% in 200mM and 400mM phosphate buffer, respectively, addition of heparin decreased BMP-2's affinity for HA by ~18% and ~4% in 200 mM

(**Figure 5-4A**) and 400 mM phosphate buffers (**Figure 5-4B**), respectively. When bFGF and BMP-2 binding to HA was assessed in the presence of aminoBP-heparin conjugates (with varying numbers of conjugated aminoBPs per heparin), the binding of both bFGF and BMP-2 increased in a manner proportional to the number of aminoBPs conjugated onto heparin. In 200 mM phosphate buffer (**Figure 5-5A**), the addition of heparin containing 2.6 aminoBPs/heparin increased the affinity of both bFGF and BMP-2 for HA by ~52% and ~9%, respectively; while an increase of ~38% and ~25% was observed in 400 mM phosphate buffer (**Figure 5-5B**), respectively. These differences were relative to growth factor binding to HA in the absence of heparin at 200 mM and 400 mM phosphate buffer (as observed in **Figure 5-4**). The ability of both BMP-2 and bFGF to bind to HA correlated linearly to the heparin-conjugates' ability to bind to HA, but the extent to which the heparin-conjugates enhanced the growth factors' affinity was protein-specific ($r^2 = 0.8244, p < 0.01$ for bFGF; $r^2 = 0.9393, p < 0.0025$ for BMP-2; **Figure 5-6**).

To further elucidate the capacity of the heparin conjugates to enhance the affinity of bFGF and BMP-2 to bone mineral, HA binding was assessed over a wider range of phosphate concentrations. The extent of both bFGF and BMP-2 binding to HA was inversely proportional to the concentration of phosphate used in the binding medium (**Figures 5-7A** and **5-7B**, respectively). Irrespective of the presence of either heparin, oxidized heparin, or conjugated heparin, maximum HA binding of ~90% for bFGF was observed at 0 mM phosphate buffer. The presence of heparin did not significantly influence bFGF's capacity to bind to HA at any of the phosphate buffer concentrations assessed (i.e. 0 mM, 200 mM, 300 mM and 400 mM phosphate) except at 100 mM phosphate (Tukey post-hoc). Oxidized heparin increased bFGF binding to HA also at 100

mM phosphate buffer. bFGF binding to HA, however, was distinctly higher in the presence of the aminoBP-heparin conjugate over the other groups in all cases where phosphate buffer concentrations increased the binding medium's stringency. A similar trend was observed with respect to the influence of the aminoBP-heparin conjugate on BMP-2's affinity to HA; as binding to HA was increased in aminoBP-conjugate presence at all phosphate buffer concentrations. As observed in previous experiments (**Figure 5-4**), the addition of stock heparin significantly diminished BMP-2's affinity for HA between 200 mM and 400 mM phosphate concentrations.

Using conjugates consisting of 2 aminoBPs/heparin, the effect of modulating the heparin:protein ratio was also assessed in 400 mM phosphate buffer. Increasing the ratio of unmodified heparin:protein did not affect either bFGF's or BMP-2's affinity for HA (**Figure 5-8A** and **5-8B**, respectively). Increasing the amount of aminoBP-heparin conjugate:protein, however, resulted in an increase in both of the proteins' affinity for HA in a concentration-dependent manner.

DISCUSSION

In this study, a novel means of enhancing the bone mineral affinity of two osteogenic growth factors, namely bFGF and BMP-2, through the use of an aminoBP-heparin conjugate has been described. Although the conjugation of aminoBP directly onto various proteins has previously been shown to enhance their affinity for bone *in vivo* (**6-8, 9**), the described aminoBP-heparin conjugates are intended to serve as a drug delivery vehicle to enhance an osteogenic protein's bone affinity while circumventing any potential loss in the protein's bioactivity as a result of chemically modifying it

directly through BP conjugation. The foundation for this particular approach is based on heparin's inherent capacity to bind to various growth factors via electrostatic interactions between its negatively-charged sulfate groups and the proteins' positively-amino acid residues (typically arranged as one of a number of specific consensus sequences that orient themselves as defined structural elements) (**28**). An additional benefit to the use of heparin in this drug delivery system is its ability to increase growth factor stability (i.e. biological half-life). This was evidenced by the combination of heparin with: (i) TGF-β for the enhancement of extracellular matrix synthesis both *in vitro* and *in vivo* (**29**); (ii) aFGF for the potentiation of neurite outgrowth *in vitro* (**30**); and (iii) bFGF for the prevention of undesirable non-enzymatic glycosylation (**31**), and for increased cell proliferation *in vitro* (**32**).

In the results presented, the use of the MMCCH-based chemistry facilitated the conjugation of up to 7 aminoBPs per molecule of heparin. This enhanced heparin's affinity for HA by over two-fold (from an average baseline of 26% binding to a maximum of 62% binding in the experimental condition used). Given that the extent of heparin binding to HA was proportional the number of aminoBPs conjugated onto it (**Figure 5-3**), these results indicated that the conjugated aminoBPs were indeed responsible for imparting the bone mineral affinity onto the glycosaminoglycan. Similarly, the results also indicated that the propensity of the aminoBP-heparin conjugates to enhance the affinity of either bFGF or BMP-2 was dependent on the number of aminoBPs conjugated onto heparin (**Figure 5-5**). These particular observations are noteworthy as they suggest that: (i) the aminoBP-heparin conjugates formed a complex with the growth factors (illustrating that the process of conjugation did

not compromise heparin's property); and (ii) the conjugates' high bone mineral affinity was imparted onto the proteins. The former finding was similar to the results reported by Ishihara *et al.*, where it was shown that the process of oxidizing heparin with 100 mM sodium periodate did not adversely affect the glycosaminoglycan's ability to interact with bFGF, vascular endothelial growth factor, and hepatocyte growth factor (**33**). Although a relatively conservative concentration of 25 mM sodium periodate was used to yield aldehyde groups at the C2 and C3 positions of heparin's unsulfated glucuronic and iduronic acid residues (**25**), potential products of degradation from this process of oxidation were not assessed in these studies due to the fact that: (i) basic conditions were not used after the process of oxidation to lead to the fragmentation of heparin (**24, 34**); and (ii) any low-molecular-weight fractions of heparin that may have been generated were removed during dialysis (as the MW cut-off of the dialysis tubing used was 12-14 kDa). The propensity of both BMP-2 and bFGF to bind to HA correlated linearly to the ability of the heparin-conjugates to bind to HA; however, the extent to which the heparin-conjugates enhanced the growth factors' affinity was protein-specific (**Figure 5-6**). This suggests that either the protein's inherent physicochemical properties (such as its size, number of charged amino acid residues, etc.) affected the manner in which the aminoBP-heparin conjugates enhanced the protein's mineral affinity.

By emulating nature's approach to sequestering heparin-binding proteins in the extracellular matrix, heparin has been used by others as an integral component in numerous drug delivery systems (**35**). The majority of these systems are only appropriate for the local delivery of growth factors. A novel approach, termed by Park et al. "antibody-targeted, triggered, electrically modified prodrug-type strategy", however, may

potentially be used for systemic targeting (**36**). Here, heparin is conjugated onto an antibody and allowed to interact electrostatically with an enzyme that has been modified through the conjugation of a cationic poly(Arg)$_7$ peptide (**36**). Once targeted to a desired site by the antibody component, the enzyme is subsequently displaced, and thus activated, from the heparin moiety by the administration of protamine, a protein which binds to heparin more tenaciously than most other cationic species (**36**). Consequently, it is hypothesized that the administration of a similar trigger mechanism may be used to modulate an osteogenic protein's release from the described aminoBP-heparin conjugate bound to bone mineral. This will be attempted in future studies.

It has recently been observed that the tether length between the protein and aminoBP directly influenced the degree to which aminoBP-glycoprotein conjugates bound to HA *in vitro* and to a coralline hydroxyapatite matrix *in vivo*. Other studies have shown that the binding of bFGF onto heparin is sensitive to the physicochemical properties of heparin itself (i.e. its length and sulfation pattern) (**37, 38**). To optimize the ability of the aminoBP-heparin conjugates to target bFGF and BMP-2 to bone, the effect of modulating crosslinker length as well as the use of low-molecular weight heparin will be determined in the future. As aminoBP conjugation directly onto a model protein (i.e. albumin) enhanced its retention when administered intra-osseously (6) as well as increased its localization and subsequent retention to bone (i.e. femora, tibiae, sternum) when administered intravenously and subcutaneously (7), a similar biodistribution is expected when bFGF and BMP-2 are administered in combination with the described aminoBP-heparin delivery system under similar experimental conditions *in vivo*. Because increased osteogenic growth factor retention corresponded to increased osteogenic

bioactivity *in vivo* (**39**), it is expected that increased protein retention to mineralized tissues, irrespective of whether administered locally or systemically, will enhance the capacity of these osteogenic growth factors to elicit the regeneration of bone.

Consequently, further studies also will be conducted to determine the ability of the system described to target bFGF and BMP-2 to skeletal tissues upon parenteral, systemic administration as well as its ability to enhance the affinity of these proteins to bone when administered locally and to HA-containing biomaterial matrices *in vivo*. The latter studies will determine the ability of this drug delivery system to address the goal within the field of bone tissue engineering, and ultimately orthopaedic surgery, to elicit both local and systemic bone regeneration for clinical indications ranging from fracture repair to osteoporosis.

It should be noted that the particular approach used to develop this drug delivery system should not be limited to heparin. As aforementioned, it was previously shown that the conjugation of aminoBP onto the carbohydrate moieties of fetuin, enhances the glycoprotein's affinity for mineral matrices both *in vitro* (**8**) and *in vivo* (unpublished data). As numerous glycoproteins have been shown to bind to various osteogenic proteins, they can theoretically be used to target these proteins to bone upon BP conjugation onto their carbohydrate groups. Examples of glycoproteins that can be used for this application include: fetuin, which binds to members of the transforming growth factor-β (TGF-β) family, including TGF-β_1, TGF-β_2, BMP-2, BMP-4 and BMP-6 (**40**); gremlin, which binds to BMP-2 (**41**); noggin (**42**), cerberus (**43**) and chordin (**44**), which have each been shown to bind to BMP-4; and insulin-like growth factor binding proteins, which bind to insulin-like growth factor (**45**).

CONCLUSIONS

This study has demonstrated the feasibility of conjugation aminoBP onto heparin. This was shown to increase the affinity of the glycosaminoglycan for the primary mineral component of bone, HA, *in vitro*. The number of aminoBPs conjugated onto heparin can be modulated to yield the desired conjugation efficiency by modulating the concentration of the reacting reagents. Further analysis revealed that this process of conjugation did not compromise heparin's innate affinity for either bFGF or BMP-2 as the aminoBP-heparin conjugates enhanced the propensity of these growth factors to bind to HA *in vitro* in an aminoBP/heparin-dependent manner. All together, these results describe a novel drug delivery system that enhances the affinity of bFGF and BMP-2 to bone mineral.

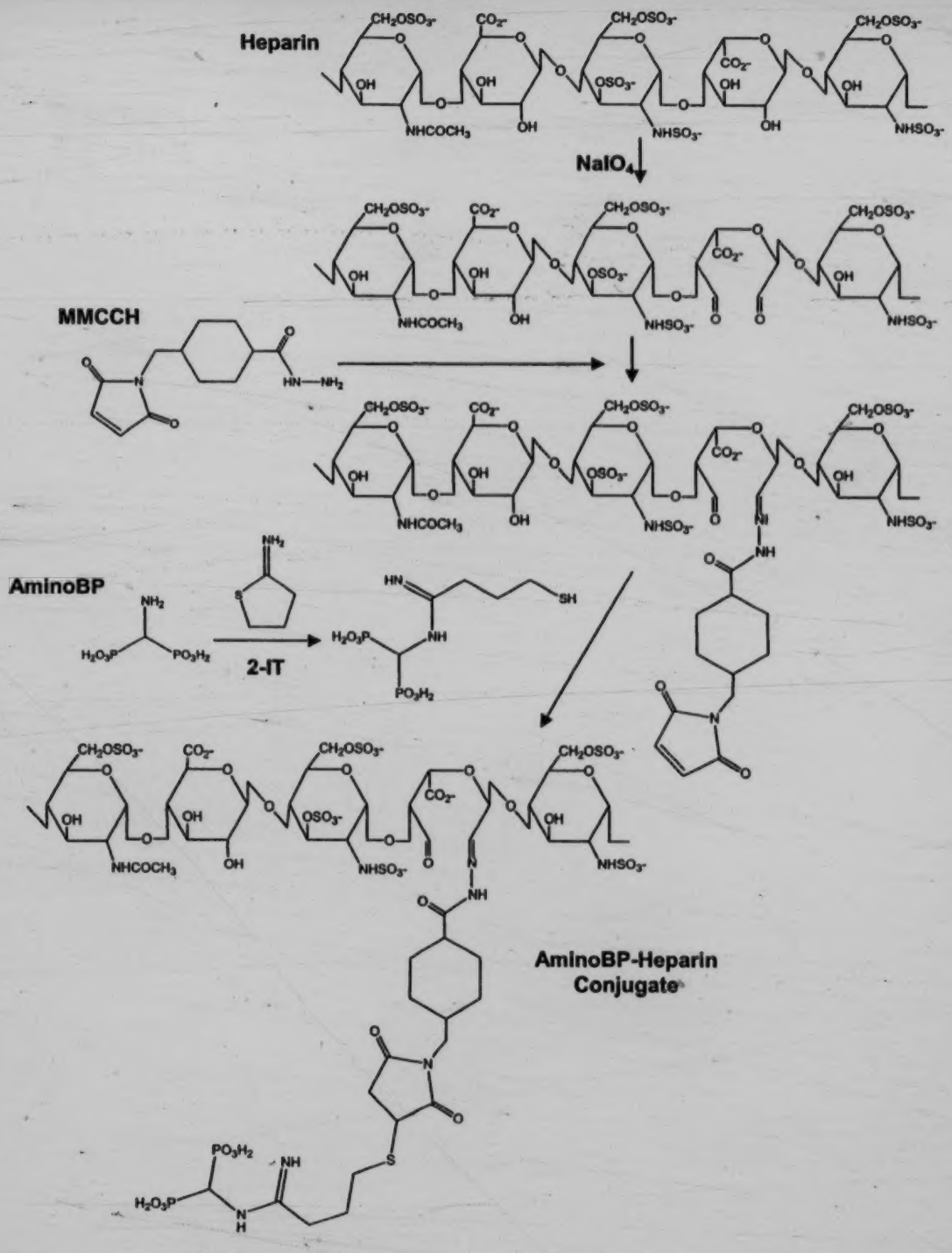

Figure 5-1: A schematic representation of the chemistry used to conjugate aminoBP onto heparin through the use of MMCCH.

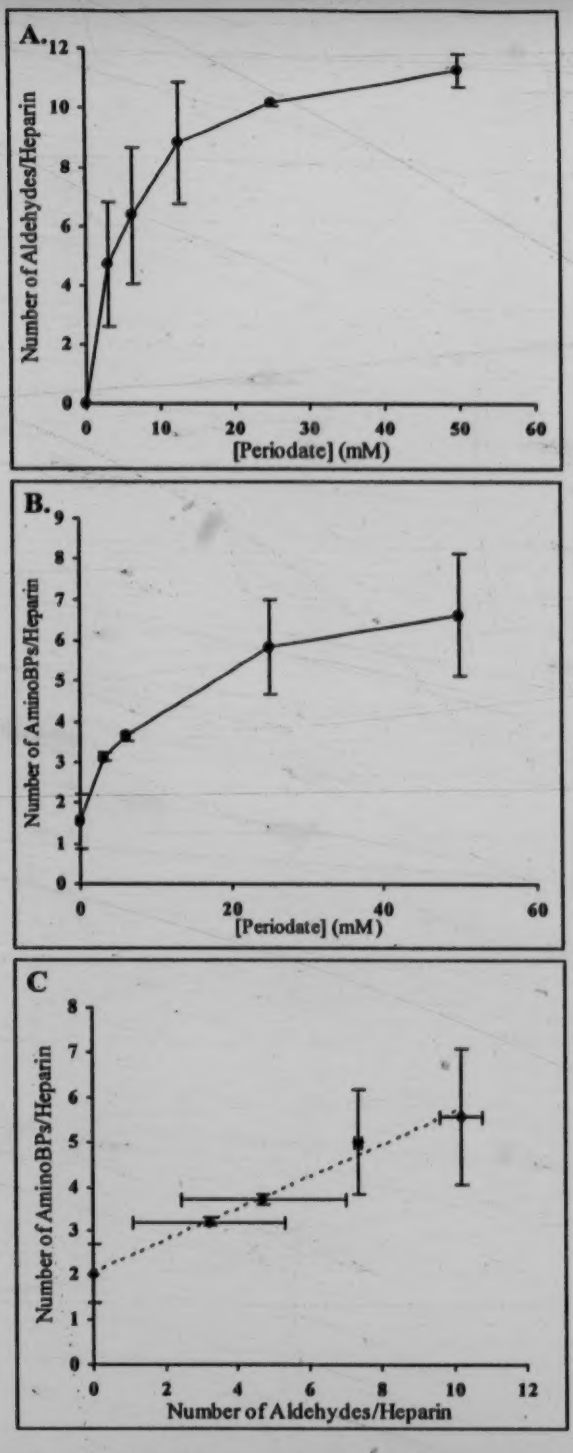

Figure 5-2: The effects of modulating the concentration of $NaIO_4$ on the number of aldehydes (**A**) and aminoBPs (**B**) introduced onto heparin. Although both MMCCH and thiolated aminoBP were used in excess, not all aldehydes were utilized during the process of conjugation. However, there was a linear correlation between the number of aldehydes per heparin and aminoBPs conjugated per heparin ($r^2 = 0.9726$, **C**)

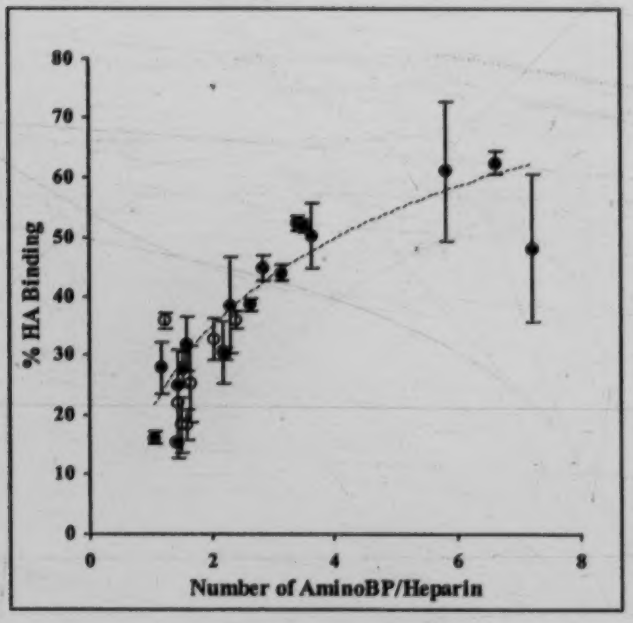

Figure 5-3: The correlation between the number of aminoBPs conjugated per heparin and HA binding. The samples used were either controls (○, refer to text), or the aminoBP-heparin conjugates (●). Binding to HA was assessed in 150 mM phosphate buffer medium.

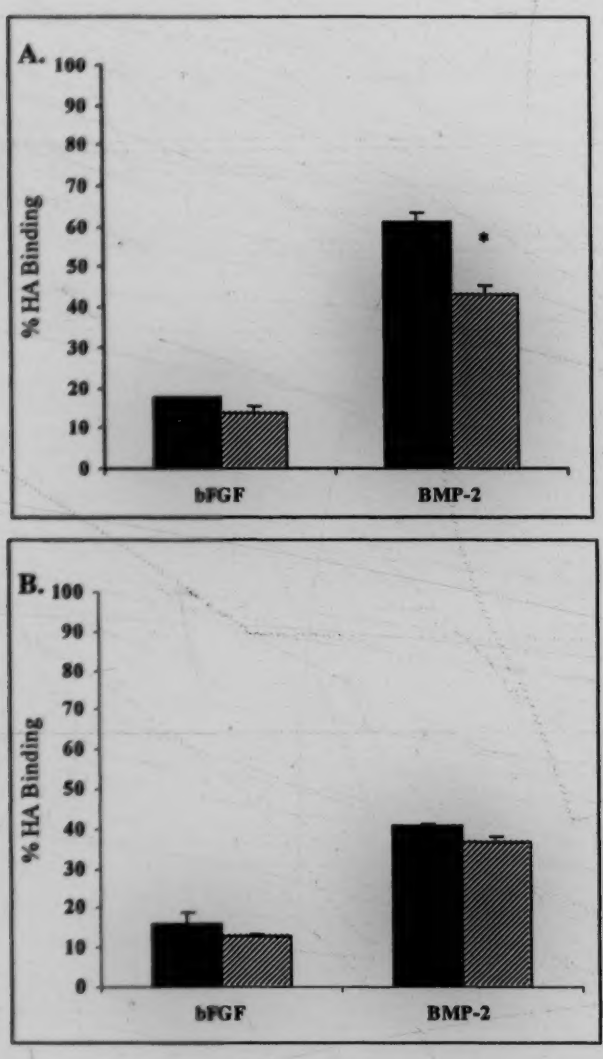

Figure 5-4: The capacity of bFGF and BMP-2 to bind to HA in the absence (solid bars) and presence of unmodified heparin (hashed bars) in either 200 mM (**A**) or 400 mM (**B**) phosphate buffer binding medium. Note that bFGF binding to HA was not significantly influenced by the presence of heparin, whereas BMP-2 binding was reduced by the presence of heparin in 200 mM phosphate buffer in a statistically significant manner (*, $p < 0.05$ vs. BMP-2 alone).

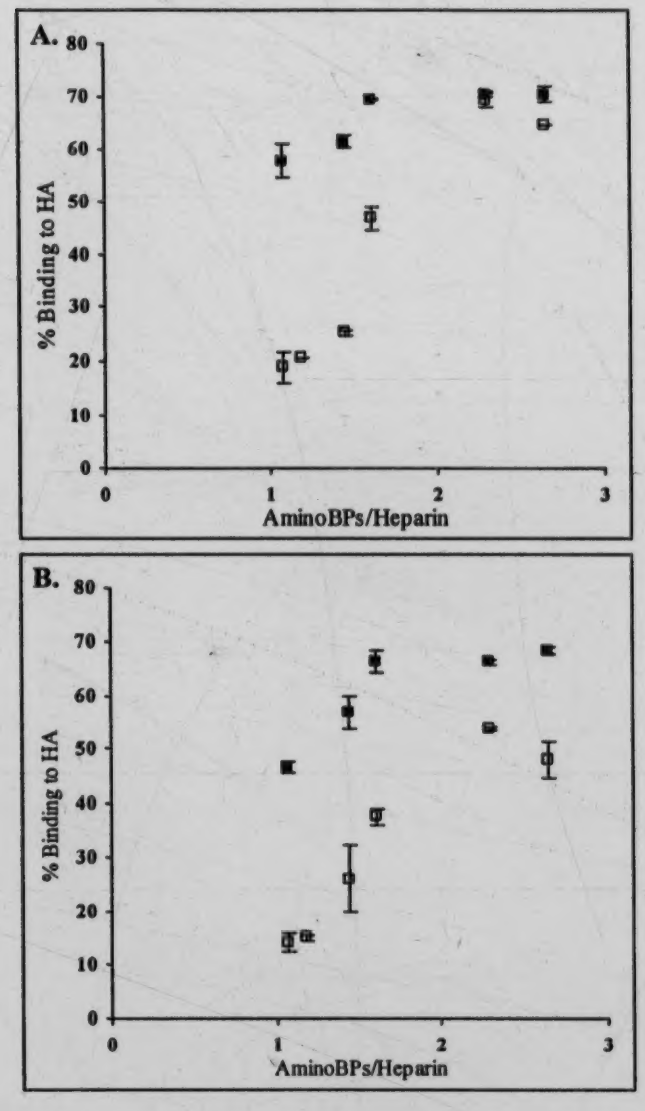

Figure 5-5: The effect of increasing the number of aminoBPs/heparin on the conjugates' capacity to enhance the affinity of bFGF (□) and BMP-2 (■) in either 200 mM (**A**) or 400 mM (**B**) phosphate buffer binding medium. A clear increase in bFGF and BMP-2 binding to HA was evident as the number of aminoBPs/heparin increased; albeit the increase seen in the latter protein was considerably less in magnitude.

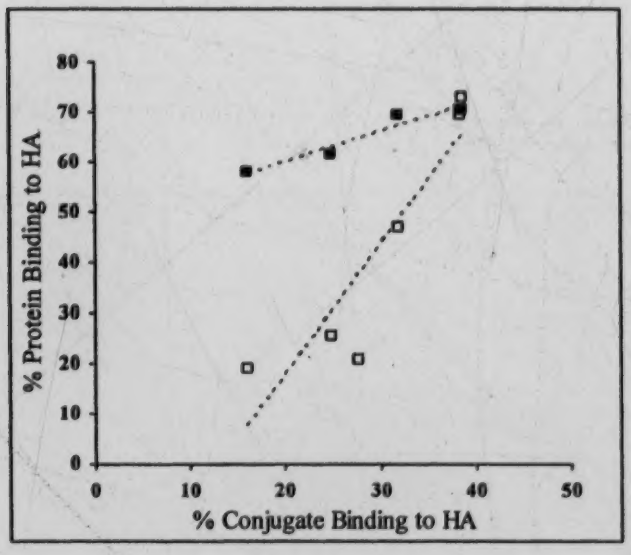

Figure 5-6: The correlation between the aminoBP-heparin conjugates' capacity to bind to HA in 150 mM phosphate buffer and their ability to enhance the affinity of bFGF (□, $r^2 = 0.8244$) and BMP-2 (■, $r^2 = 0.9393$) to HA in 200 mM phosphate buffer. Note that two separate data points overlap one another at the crest of the BMP-2 curve.

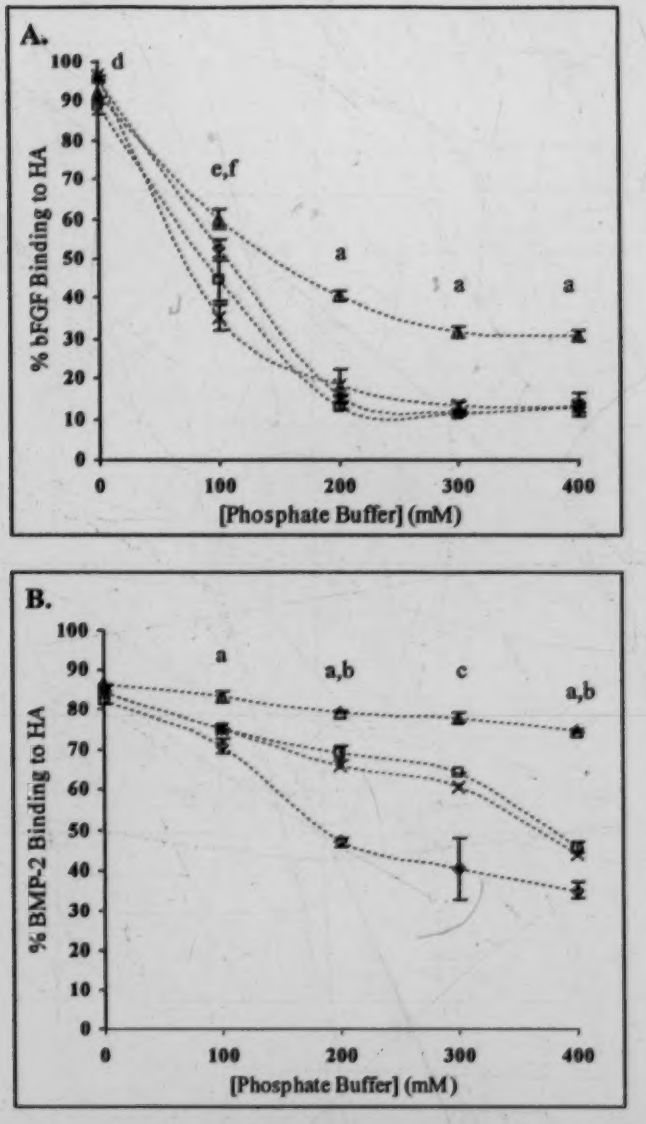

Figure 5-7: The effect of modulating phosphate buffer concentrations on bFGF's (**A**) and BMP-2's (**B**) ability to bind to HA. Protein binding was assessed without any heparin (X), with unmodified heparin (◊), oxidized heparin (□), and aminoBP-heparin conjugate (Δ). As was evident in the case of both proteins, only the aminoBP-heparin conjugate significantly increased in HA binding at higher phosphate buffer concentrations. The conjugate was different from all other groups. [a] aminoBP-heparin conjugate significantly different from remaining groups. [b] unmodified heparin significantly different from remaining groups. [c] unmodified heparin significantly different from aminoBP-heparin. [d] growth factor alone significantly different from oxidized. [e] growth factor alone significantly different from aminoBP-heparin and unmodified heparin. [f] aminoBP-heparin significantly different from oxidized heparin.

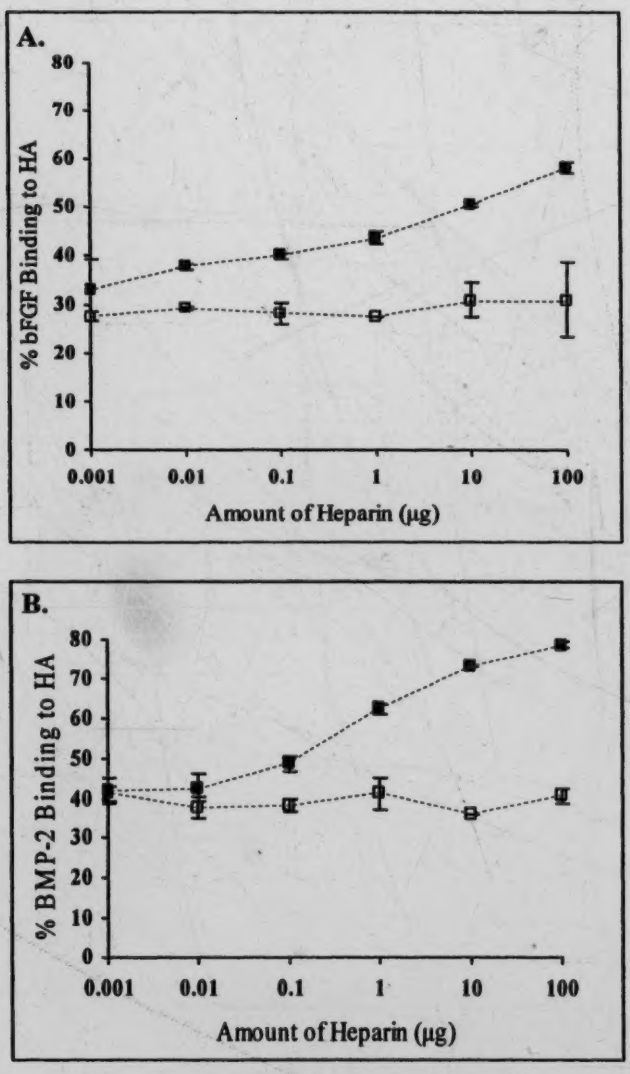

Figure 5-8: Modulating the ratio of aminoBP-heparin conjugate (■) and unmodified heparin (□) to either bFGF (**A**) or BMP-2 (**B**) in 200 mM phosphate buffer. The amount of protein was kept constant (at 0.1 µg) and the amount of aminoBP-conjugate varied. In these experimental conditions, the % HA binding of bFGF and BMP-2 alone was ~27% and ~38%, respectively. With both proteins, HA binding increased as the amount of aminoBP-heparin present increased.

REFERENCES

1. S.A. Gittens, H. Uludag, Growth factor delivery for bone tissue engineering, *J. Drug Target.* 9 (2001) 407-429.

2. G. Mazue, F. Bertolero, L. Garofano, M. Brughera, P. Carminati, Experience with the preclinical assessment of basic fibroblast growth factor (bFGF), *Toxicol. Lett.* 64-65 (1992) 329-338.

3. G. Mazue, A.J. Newman, G. Scampini, Della P. Torre, G.C. Hard, M.J. Iatropoulos, G.M. Williams, S.M. Bagnasco, The histopathology of kidney changes in rats and monkeys following intravenous administration of massive doses of FCE 26184, human basic fibroblast growth factor, *Toxicol. Pathol.* 21 (1993) 490-501.

4. A. Valentin-Opran, J. Wozney, C. Csimma, L. Lilly, G.E. Riedel, Clinical evaluation of recombinant human bone morphogenetic protein-2, *Clin. Orthop.* 395 (2002) 110-120.

5. H. Uludag, N. Kousinioris, T. Gao, D. Kantoci, Bisphosphonate conjugation to proteins as a means to impart bone affinity, *Biotechnol. Prog.* 16 (2000) 258-267.

6. H. Uludag, T. Gao, G.R. Wohl, D. Kantoci, R.F. Zernicke, Bone affinity of a bisphosphonate-conjugated protein in vivo, *Biotechnol. Prog.* 16 (2000) 1115-1118.

7. H. Uludag, J. Yang, Targeting systemically administered proteins to bone by bisphosphonate conjugation, *Biotechnol. Prog.* 18 (2002) 604-611.

8. S.A. Gittens, J.R. Matyas, R.F. Zernicke, H. Uludag, Imparting bone affinity to glycoproteins through the conjugation of bisphosphonates, *Pharm. Res.* 20 (2003) 978-987.

9. S.A. Gittens, P.I. Kitov, J.R. Matyas, R. Lobenberg, H. Uludag, Impact of tether length on bone mineral affinity of protein-bisphosphonate conjugates, *Pharm. Res.* 21 (2004) 608-616.

10. I. Pieri, D. Barritault, Biotinylated basic fibroblast growth factor is biologically active, *Anal. Biochem.* 195 (1991) 214-219.

11. P. Caccia, G. Nitti, O. Cletini, P. Pucci, M. Ruoppolo, F. Bertolero, B. Valsasina, F. Roletto, C. Cristiani, G. Cauet, P. Sarmientos, A. Malorni, G. Marino, Stabilization of recombinant human basic fibroblast growth factor by chemical modifications of cysteine residues, *Eur. J. Biochem.* 204 (1992) 649-655.

12. L.Y. Li, M. Safran, D. Aviezer, P. Bohlen, A.P. Seddon, A. Yayon, Diminished heparin binding of a basic fibroblast growth factor mutant is associated with reduced receptor binding, mitogenesis, plasminogen activator induction, and in vitro angiogenesis, *Biochem.* 33 (1994) 10999-11007.

13. H. Uludag, J. Golden, R. Palmer, J.M. Wozney, Biotinated bone morphogenetic protein-2: In vivo and in vitro activity, *Biotechnol. Bioeng.* 65 (1999) 668-672.

14. A.D. DiGabriele, I. Lax, D.I. Chen, C.M. Svahn, M. Jaye, J. Schlessinger, W.A. Hendrickson, Structure of a heparin-linked biologically active dimer of fibroblast growth factor, *Nature.* 393 (1998) 812-817.

15. R. Raman, G. Venkataraman, S. Ernst, V. Sasisekharan, R. Sasisekharan, Structural specificity of heparin binding in the fibroblast growth factor family of proteins, *Proc. Natl. Acad. Sci. U S A.* 100 (2003) 2357-2362.

16. R. Lever, C.P. Page, Novel drug development opportunities for heparin, *Nat. Rev. Drug Discov.* 1 (2002) 140-148.

17. R. Ruppert, E. Hoffmann, W. Sebald, Human bone morphogenetic protein 2 contains a heparin-binding site which modifies its biological activity, *Eur. J. Biochem.* 237 (1996) 295-302.

18. T. Takada, T. Katagiri, M. Ifuku, N. Morimura, M. Kobayashi, K. Hasegawa, A. Ogamo, R. Kamijo, Sulfated polysaccharides enhance the biological activities of bone morphogenetic proteins, *J. Biol. Chem.* 278 (2003) 43229-43235.

19. S. Vukicevic, V. Latin, P. Chen, R. Batorsky, A.H. Reddi, T.K. Sampath, Localization of osteogenic protein-1 (bone morphogenetic protein-7) during human embryonic development: high affinity binding to basement membranes, *Biochem. Biophys. Res. Commun.* 198 (1994) 693-700.

20. Irie, H. Habuchi, K. Kimata, Y. Sanai, Heparan sulfate is required for bone morphogenetic protein-7 signaling, *Biochem. Biophys. Res. Commun.* 308 (2003) 858-865.

21. M. Lyon, G. Rushton, J.T. Gallagher, The interaction of the transforming growth factor-betas with heparin/heparan sulfate is isoform-specific, *J. Biol. Chem.* 272 (1997) 18000-18006.

22. S.M. Chamow, T.P. Kogan, D.H. Peers, R.C. Hastings, R.A. Byrn, A. Ashkenazi, Conjugation of soluble CD4 without loss of biological activity via a novel carbohydrate-directed cross-linking reagent, *J. Biol. Chem.* 267 (1992) 15916-15922.

23. K. Kamei, X. Wu, X. Xu, K. Minami, N.T. Huy, R. Takano, H. Kato, S. Hara, The analysis of heparin-protein interactions using evanescent wave biosensor with regioselectively desulfated heparins as the ligands, *Anal. Biochem.* 295 (2001) 203-213.

24. T. Islam, M. Butler, S.A. Sikkander, T. Toida, R.J. Linhardt, Further evidence that periodate cleavage of heparin occurs primarily through the antithrombin binding site, *Carbohydr. Res.* 337 (2002) 2239-2243.

25. F.C. MacIntosh, A colorimetric method for the standardization of heparin preparations, *Biochem.* 35 (1956) 776-782.

26. R. Fields, H.B. Dixon, Micro method for determination of reactive carbonyl groups in proteins and peptides, using 2,4-dinitrophenylhydrazine, *Biochem. J.* 121 (1971) 587-589.

27. B.N. Ames, Assay of inorganic phosphate, total phosphate, and phosphatases, in E.F. Neufield, V. Ginsburg (eds.), Methods in Enzymology, Volume VIII, Complex Carbohydrates, Academic Press, New York, 1966, pp. 115-117.

28. I. Capila, R.J. Linhardt, Heparin-protein interactions, *Angew. Chem. Int. Ed. Engl.* 41 (2002) 391-412.

29. J.A. Schroeder-Tefft, H. Bentz, T.D. Estridge, Collagen and heparin matrices for growth factor delivery, *J. Control. Release.* 49 (1997) 291-298.

30. D.H. Damon, R.R. Lobb, P.A. D'Amore, J.A. Wagner, Heparin potentiates the action of acidic fibroblast growth factor by prolonging its biological half-life, *J. Cell. Physiol.* 138 (1989) 221-226.

31. N.N. Nissen, R. Shankar, R.L. Gamelli, A. Singh, L.A. DiPietro, Heparin and heparan sulphate protect basic fibroblast growth factor from non-enzymic glycosylation, *Biochem. J.* 338 (1999) 637-642.

32. Sommer, D.B. Rifkin, Interaction of heparin with human basic fibroblast growth factor: protection of the angiogenic protein from proteolytic degradation by a glycosaminoglycan, *J. Cell. Physiol.* 138 (1989) 215-220.

33. M. Ishihara, K. Ono, K. Ishikawa, H. Hattori, Y. Saito, H. Yura, T. Akaike, Y. Ozeki, S. Tanaka, H. Mochizuki, A. Kurita, Enhanced ability of heparin-carrying polystyrene (HCPS) to bind to heparin-binding growth factors and to inhibit growth factor-induced endothelial cell growth, *J. Biochem.* 127 (2000) 797-803.

34. K. Ono, M. Ishihara, K. Ishikawa, Y. Ozeki, H. Deguchi, M. Sato, H. Hashimoto, Y. Saito, H. Yura, A. Kurita, T. Maehara, Periodate-treated, non-anticoagulant heparin-carrying polystyrene (NAC-HCPS) affects angiogenesis and inhibits subcutaneous induced tumour growth and metastasis to the lung, *Br. J. Cancer.* 86 (2002) 1803-1812.

35. S.E. Sakiyama-Elbert, J.A. Hubbell, Functional Biomaterials: Design of Novel Biomaterials, *Annu. Rev. Mater. Res.* 31 (2001) 183-201.

36. Y.J. Park, J.F. Liang, H. Song, Y.T. Li, S. Naik, V.C. Yang, ATTEMPTS: a heparin/protamine-based triggered release system for the delivery of enzyme drugs without associated side-effects, *Adv. Drug. Deliv. Rev.* 55 (2003) 251-265.

37. D.A. Pye, R.R. Vives, P. Hyde, J.T. Gallagher, Regulation of FGF-1 mitogenic activity by heparan sulfate oligosaccharides is dependent on specific structural features: differential requirements for the modulation of FGF-1 and FGF-2, *Glycobiology.* 10 (2000) 1183-1192.

38. M. Delehedde, M. Lyon, J.T. Gallagher, P.S. Rudland, D.G Fernig, Fibroblast growth factor-2 binds to small heparin-derived oligosaccharides and stimulates a sustained phosphorylation of p42/44 mitogen-activated protein kinase and proliferation of rat mammary fibroblasts, *Biochem. J.* 366 (2002) 235-244.

39. H. Uludag, D. D'Augusta, J. Golden, J. Li, G. Timony, R. Riedel, J.M. Wozney, Implantation of recombinant human bone morphogenetic proteins with biomaterial carriers: A correlation between protein pharmacokinetics and osteoinduction in the rat ectopic model, J. Biomed. Mater. Res. 50 (2000) 227-238.

40. M. Demetriou, C. Binkert, B. Sukhu, H.C. Tenenbaum, J.W. Dennis, Fetuin/alpha2-HS glycoprotein is a transforming growth factor-beta type II receptor mimic and cytokine antagonist, *J. Biol. Chem.* 271 (1996) 12755-12761.

41. D.R. Hsu, A.N. Economides, X. Wang, P.M. Eimon, R.M. Harland, The Xenopus dorsalizing factor Gremlin identifies a novel family of secreted proteins that antagonize BMP activities, *Mol. Cell.* 1 (1998) 673-683.

42. L.B. Zimmerman, J.M. De Jesus-Escobar, R.M. Harland, The Spemann organizer signal noggin binds and inactivates bone morphogenetic protein 4, *Cell.* 86 (1996) 599-606.

43. S. Piccolo, E. Agius, L. Leyns, S. Bhattacharyya, H. Grunz, T. Bouwmeester, E.M. De Robertis, The head inducer Cerberus is a multifunctional antagonist of Nodal, BMP and Wnt signals, *Nature.* 397 (1999) 707-710.

44. S. Piccolo, E. Agius, B. Lu, S. Goodman, L. Dale, E.M. De Robertis, Cleavage of Chordin by Xolloid metalloprotease suggests a role for proteolytic processing in the regulation of Spemann organizer activity, *Cell.* 91 (1997) 407-416.

45. S.M. Firth, R.C Baxter, Cellular actions of the insulin-like growth factor binding proteins, *Endocr. Rev.* 23 (2002) 824-854.

CHAPTER VI

SYSTEMIC BONE FORMATION WITH WEEKLY PTH ADMINISTRATION IN OVARIECTOMIZED RATS[1].

[1] The contents of this chapter have been previously published in: Gittens SA, Wohl GR, Zernicke RF, Matyas JR, Morley P and Uludağ H. Systemic Bone Formation with Weekly PTH Administration in Ovariectomized Rats. *Journal of Pharmacy and Pharmaceutical Sciences*, (2004) 7(1): 27-37.

INTRODUCTION

The continuous administration of the amino-terminal fragment (1-34) of parathyroid hormone (PTH (1-34)) has been shown to elicit a catabolic effect on skeletal tissue. Intermittent administration of PTH (1-34), however, has been shown to promote the deposition of new bone (**1-3**). Although the biochemical pathways responsible for mediating these divergent responses have yet to be fully elucidated (**2**), the anabolic effects of PTH (1-34) has been observed in normal rats (**4-7**) as well as the rats rendered osteopenic by neurectomy (**8**), tail-suspension, (**8-10**), aging (**11-17**), streptozotocin-induced diabetes (**18**), and orchidectomy (**19**). Since the ovariectomized (OVX) rat is one of two animal models mandated by the US Food and Drug Administration for the preclinical assessment of agents designed to treat osteoporosis (**20**), much of the literature concerning the effects of PTH (1-34) administration on systemic bone regeneration has been based on this particular model. As assessed through x-ray absorptiometry, histomorphometry, micro-computed tomography (μCT), and various other techniques, the preponderance of the evidence provided by studies using this particular animal model suggests that the daily, parenteral administration of PTH (1-34) resulted in an anabolic effect on the surfaces of both trabecular and cortical bone (**21-24**). The predominant corollary associated with PTH (1-34) administration is not only the regeneration of mineralized tissue on the axial and appendicular skeleton, but an improvement in bone architecture in terms of increased connectivity, trabecular thickness, etc. It has been shown that the culmination of these effects is an enhancement in bone biomechanical performance (**25, 26**).

Despite these encouraging results, recent reports suggest that long-term administration of the synthetic PTH (1-34) was associated with some detrimental side effects (**27, 28**). For example, Sato *et al.* reported that the daily administration of as little of 8 μg/kg PTH (1-34) for 1 year in OVX rats led to an 11% increase in brittleness (i.e. ultimate displacement) of diaphyseal cortical bone and a 48% reduction in diaphyseal marrow space (**27**). In addition to these adverse skeletal effects, exogenous PTH therapy has been associated with hypercalcemia both in animal studies, as well as in clinical studies (**29**). Besides the hypercalcemia, transient headaches, nausea and arthralgia were also reported with clinical PTH (1-34) administration (**29**).

It was thought, therefore, that a reduction in the dosing frequency could serve as a means of circumventing some of these adverse effects. Consequently, the aim of this was to investigate the anabolic response elicited by low dose PTH (1-34) administered weekly. The doses selected in this study, as well as the administration duration was considerably lower than the other studies reported in the literature. It was our desire to determine whether such a restricted dosing regimen would have had any systemic effects on skeletal tissues.

MATERIALS and METHODS

Animal Care

Twenty seven, 2 month-old, commercially ovariectomized, female Sprague-Dawley rats were purchased from Charles River Laboratories (Quebec City, PQ). Rats were acclimated until 9 months of age under standard laboratory conditions (23°C, 12 h of light/day) prior to the beginning of the study. While maintained in pairs in sterilized

cages, rats were provided standard commercial rat chow and tap water (*ad libitum*). All procedures involving the rats were approved by the Animal Welfare Committee at the University of Alberta (Edmonton, Alberta).

Experimental Design

Rats were weighed and assigned randomly into 4 groups. Rats in the initial baseline control group (n = 6) were killed at the beginning of the study just prior to the onset of the treatment protocols. For 4 weeks, the remaining 3 groups (n = 7 per group) received subcutaneous injections once per week of either vehicle (acidified saline), a low PTH (1-34) dose (10 μg/kg per injection), or a high PTH (1-34) dose (80 μg/kg per injection). Eight days after the final injection rats were killed via asphyxiation using a CO_2 chamber and weighed. At autopsy, the uterus was excised and weighed to confirm systemic depletion of estrogen. Bone tissues including both femora, tibiae, and a portion of the lumbar spine (L1-L4), were harvested at time of euthanasia, fixed immediately in 70% ethanol, and stored at -20°C.

The delivery vehicle used consisted of saline (0.9 % NaCl; Baxter Corporation, Toronto, ON) acidified to 0.01 mM HCl. The synthetic hPTH (1-34) (lot #: NO5129A1, American Peptide Company, Sunnyvale, CA) was diluted in the delivery vehicle just prior to weekly injections.

Bone Analysis

Femur Length: Using a vernier caliper (reading error ± 0.01mm, Mituyomo, Japan), femoral bone length was assessed as the distance between the proximal and distal femoral growth plates - a measure of femoral diaphyseal length.

Mineral Ash Content: Mineral ash content was determined by ashing 1-cm long segments of tibia from the proximal tibial growth plate to the mid-diaphysis (**30**). Samples were defatted in acetone and then dried for 24 hr at 100°C. The dry samples were weighed in air (dry bone mass), and then rehydrated in distilled water for 24 hr under vacuum and weighed underwater (wet bone mass). The samples were then ashed at 800°C for 24 hr and weighed (mineral ash mass). Archimedes' Principle was used to determine bone density (ρ, g/cm^3) and volume (cm^3). Ash content was calculated as a measure of mineral ash mass per dry bone mass (ash content, %), and mineral ash mass per bone volume (ash density, g/cm^3).

Femoral Bone Mineral Density (BMD): Femoral BMD (g/cm^2) was measured by dual-energy X-ray absorptiometry (DEXA; Piximus Mouse Densitometer, GE Medical Systems Canada, Ottawa, ON). BMD, calculated by dividing bone mineral content (g) by the projected bone area (cm^2), was assessed for the total femur as well as for three equivalent femoral subregions: the proximal third, central third, and distal third of each femur.

Trabecular Bone Architectural Properties: To elucidate the anabolic effects of weekly PTH (1-34) administration, structural parameters of the trabecular bone within the femoral neck were evaluated through μCT. Architectural changes in the trabecular bone of the rat femoral neck and L3 vertebrae were specifically analyzed (Skyscan 1072 X-ray Microtomograph, Skyscan, Aartselaar, Belgium). All bone samples were scanned at 100 kV/98 μA. The proximal femurs were scanned at an isometric resolution of 11.46 μm/pixel and 11.46μm slice thickness, and the L3 vertebra were scanned at an isometric resolution of 14.89 μm/pixel with 14.89 slice thickness. Reconstruction of the original scan data was performed using a cone-beam algorithm (31) into two-dimensional 1024 X 1024, 8-bit, 256 grayscale bitmap image slices. For the femoral neck, identically sized cylindrical volumes of interest (VOI) were sampled from bitmap images stacks to include trabecular bone regions and exclude cortical bone within each femoral neck data set. Each VOI of femoral neck trabecular bone was centered within the femoral neck about the narrowest region, approximately 2 mm distal to the femoral head growth plate, and was oriented parallel to the axis of the femoral neck. Likewise, ellipsoid VOI were sampled from each L3 bitmap data set to include only trabecular bone within the vertebral centrum. The axis of the L3 cylindrical VOI was aligned along the cranial–caudal axis of the vertebral centrum. Digital segmentation of the bone from air/marrow tissues was performed by global thresholding. The global threshold for each sample data set was determined by selecting a local minimum in the frequency plot of bitmap pixel greylevels for the sample (32). The VOI were then reconstructed in three dimensions (ANT, Skyscan, Aartselaar, Belgium), and measures of bone volume fraction (BV/TV),

bone surface fraction (BS/BV), and trabecular thickness (Tb.Th.). Trabecular number was calculated separately (3-D Calculator v0.9, Skyscan, Belgium)

Cortical Bone Cross-section (XSA): Cortical bone cross-sectional areal properties were measured by analyzing single μCT bitmap cross-sectional image slices of the rat femoral necks. The BITMAP images were sampled in a plane perpendicular to the femoral neck axis at the narrowest portion of the femoral neck. Each slice was analyzed using custom software (MATLAB, ver.6.0.0.88, rel.12, The Mathworks, Inc., Natick, MA) for measures of femoral neck cross-sectional area (XSA), and moments of area about the horizontal (Ixx) and vertical axes (Iyy) for the whole bone and separately for the cortical bone and trabecular bone. XSA measures were also calculated for the area within the periosteal envelope (i.e., femoral neck XSA enveloped by the periosteal perimeter including all bone and myeloid spaces), and the endosteal envelope (i.e., the XSA enveloped by the endosteal perimeter including trabecular bone and marrow spaces).

Statistical Analysis

Unless otherwise noted, all values are expressed as mean ± standard deviation. Rat body masses were compared between the onset and end of treatment within each animal using student's paired *t*-test (SPSS for Windows 11.0.1, SPSS Inc., Chicago, IL). For comparisons of all other variables among treatment groups, significant main effects were tested by multivariate analysis (generalized linear model). Where main effects were significant ($p < 0.05$), treatment groups were compared using Tukey post-hoc comparison

($p < 0.05$). To test whether or not either rat body mass or uterine mass had a confounding effect on bone properties, all data were also compared by multivariate analysis with rat body mass and uterine mass as covariates.

RESULTS

Measures of femoral BMD and tibial ash content were not obtained for the baseline (pre-treatment) group. All other measures (μCT based bone properties, rat body mass, and uterine mass) were compared among all treatment groups including the baseline group.

Body Mass, Uterine Mass, and Femoral Diaphyseal Length

Body mass did not differ among the treatment groups either at the onset of the treatment protocols (9 months, $p = 0.537$), or at temination (4 week into treatment, $p = 0.193$). There was no significant change in body mass over the 4 wk treatment interval. Ovariectomy was confirmed by reduced uterine masses of the rats at sacrifice (0.15±0.08 g, n = 27; historical data from our lab indicated uterine mass of ~0.9 g for the age-matched normal rats). There were no differences in uterine mass among the treatment groups. A comparison of the groups with rat body mass and uterine mass as covariates found that neither parameter had any significant interaction on ash content, bone mineral density, or bone architectural properties. The femoral diaphyseal lengths did not differ significantly ($p = 0.185$) among the baseline group (34.4 ± 1.0 mm), the vehicle group (34.5 ± 1.2 mm), the low-dose PTH (1-34) group (35.7 ± 0.7 mm), or the high-dose PTH (1-34) group (34.9 ± 1.0 mm).

Tibial Ash Content

To assess changes elicited by weekly PTH (1-34) administration on the bone mineral content, segments of the proximal tibia were ashed. Weekly treatment of 10 μg/kg PTH (1-34) resulted in significant increases in both ash content (2.7%) and ash density (5.8%) compared to the vehicle-treated group (**Figure 6-1**). In addition, an increase of 2.9% in tibial bone density was observed in the 10 μg/kg PTH–treated group compared to the vehicle–treated group. Slight increases in the same parameters were observed in high-dose PTH group, but these values were not significantly different than the vehicle-treated controls.

Femoral Bone Mineral Density

Weekly administration of low-dose PTH led to a significant ($p<0.0125$) increase of 15.6% in total femoral BMD over the vehicle-treated controls (**Figure 6-2**). Weekly low-dose PTH also led to a significant increase of 8.9% in BMD over the high-dose PTH group. Both the proximal and the mid-diaphyseal regions of the femur exhibited similar, statistically significant increases in the 10 μg/kg–treated group over the vehicle and high-dose PTH groups. Although a similar trend was observed in the distal region of the femur, these differences were not statistically significant ($p = 0.222$).

Architecture of Trabecular Bone within the Femoral Neck:

As summarized in **Figure 6-3**, treatment by vehicle alone had no appreciable effects on femoral neck trabecular bone architectural properties compared to baseline control. Weekly low-dose PTH (1-34) treatment did result in significant increases in

BV/TV and Tb.Th ($p < 0.0125$) in the femoral neck over all other groups including baseline. BS/BV, on the other hand, was significantly *reduced* in the femoral necks of 10 μg/kg–treated animals compared to all other groups. Despite a significant reduction in Tb.N in the 10 μg/kg–treated group over baseline group ($p < 0.05$), no other statistically significant differences were found for either Tb.N or Tb.Sp among the 3 study groups. Altogether, these data suggest that a net anabolic effect had been elicited by the weekly administration of 10 μg/kg PTH (1-34) on the trabecular bone within the femoral neck.

Femoral Neck Bone Cross Sectional Area (XSA)

Total XSA of the femoral neck was significantly larger in the 10 μg/kg–treated group compared to all other groups (**Figure 6-4**). When XSA area was evaluated separately as cortical and trabecular regions, the statistically significant increase was found for the cortical, but not the trabecular bone. Specifically, the 10 μg/kg cortical XSA was significantly greater than the cortical XSA in all other test groups ($p < 0.0125$). Further analysis revealed that PTH treatment with 10 μg/kg significantly increased the XSA area within the periosteal envelope compared to treatment by vehicle alone (**data not shown**). Though XSA within the endosteal envelope tended to decrease in all treated groups compared to baseline, there were no significant differences among the groups (**data not shown**). A significant increase of 13% ($p < 0.05$) in the area of the periosteal envelope was found between the 10 μg/kg PTH (1-34)-treated group over the vehicle–treated group. Despite a 17% reduction in the 10 μg/kg PTH (1-34)– compared to vehicle–treated group, changes in the area of the endosteal surfaces were not significant among any of the groups. The culmination of these data suggested that the weekly

administration of 10 μg/kg PTH (1-34) influenced the cortical bone within the femoral neck in an anabolic manner.

The second moments of area, namely the distribution of bone about the horizontal (anterior–posterior) and vertical (inferior–superior) axes (Ixx and Iyy, respectively), through the femoral neck cross section are illustrated in **Figure 6-4**. Despite a similar trend to total XSA for both Ixx and Iyy, only the difference in total Iyy between the 10 μg/kg– and vehicle–treated groups reached significance among all of the second moments of area values. The ratio of Ixx/Iyy was also compared among the treatment groups to determine if PTH therapy preferentially influenced bone apposition in one direction over the other about the femoral neck axes. Changes in Iyy were proportional to those seen in Ixx, and there were no differences among the groups in the ratio of Ixx/Iyy ($p = 0.22$ for total bone cross-section Ixx/Iyy). The observed PTH-mediated apposition of cortical bone mass about the femoral neck was symmetrical about both the anterior–posterior and inferior–superior axes.

Architecture of Trabecular Bone within the Third Lumbar Vertebra

Analysis of the trabecular bone within the L3 revealed that BV/TV of the 10 μg/kg–treated group was greater than that of both the vehicle– and 80 μg/kg–treated groups, but not statistically different than the baseline group (**Figure 6-5**). Tb.Th was significantly increased while BS/BV was significantly decreased for the 10 μg/kg–treated group relative to the other groups including the baseline. No statistically significant differences in Tb.N and Tb.Sp were found among the three study groups. As in the

femoral neck these data suggested that the weekly administration of 10 μg/kg PTH (1-34) had a net anabolic effect on the trabecular bone within the L3 region.

DISCUSSION

Given the few studies that have investigated the anabolic response elicited by PTH administration at a lower dosing frequency than the traditional daily regimen, we elected to investigate the anabolic response elicited by weekly administration. In the current study, PTH (1-34) therapy significantly increased cortical bone mass in the femoral neck, and trabecular bone mass in both the femoral neck and lumbar vertebrae (L3) in the OVX rat model of osteopenia. The PTH (1-34) therapy did not significantly influence femoral diaphyseal length, uterus or animal mass. These observations were consistent with other studies that have reported no difference in these parameters in response to PTH (1-34)-treatment in OVX rats (**26, 33**).

Total as well as regional (i.e. proximal and central) increases in femoral BMD suggested that cortical bone apposition was increased by the weekly administration of 10 μg/kg PTH (1-34). Site-specific analysis revealed that PTH therapy significantly increased the periosteal envelope in this study. Though some previous studies have reported that PTH therapy exerts its effects primarily on the endosteal surface (**21, 23, 33**), others have found significant increases at both the endosteal and periosteal surfaces (**25, 34**). Preferential endosteal bone apposition was demonstrated in studies with daily injection schedules, while periosteal bone apposition were found primarily with weekly injections (**34**, current study), with exception of Sato *et al.* (**25**) in which 9 month OVX rats were dosed daily with either 8 μg/kg or 40 μg/kg PTH (1-34). A comparison of

periosteal and endosteal measures suggested that the discrepancy in the envelope specific actions of PTH therapy was most likely due to the dose and frequency of PTH (1-34) administration (**34**). For example, bone formation rate (BFR) at the *endosteal* surface of the rat tibia increased proportionally over OVX by daily PTH (1-34) dose at 8 μg/kg dose (+32%) and 40 μg/kg dose (+122%) (**25**). In comparison, *periosteal* BFR was increased dramatically by daily 8 μg/kg dose (+193%), but the increase in BFR above this initial jump was relatively small with the 40 μg/kg dose (+243%) (**25**). Furthermore, though osteoclast numbers were not increased by a weekly dose of 10 μg/kg PTH (1-34), a higher weekly dose (90 μg/kg) caused significant increases in endosteal osteoclast number and osteoclast surface ratio (**34**). We speculate that the endosteal cell populations may have had greater capacity to respond to the higher frequency and larger doses of PTH in studies utilizing daily PTH dose regimens.

In the current study, the distribution of cortical bone apposition about the axis of the femoral neck did not appear to favor any one direction over another (e.g., vertical vs. horizontal). Preferential bone apposition about the cortex can improve the bone's resistance to bending about one axis. For example, though age related human osteopenia reduces bone mass, continued periosteal apposition (and endosteal absorption) in the ulna of older women helps to preserve structural bone strength (**35**). Further, a bone's response to altered mechanical loading can cause preferential bone apposition about the bone cortex (**36**). Though the current study did not address this hypothesis specifically, bone apposition may similarly be enhanced preferentially in one direction over another by exogenous therapies that that are amplified by the bone's inherent mechanical milieu. Both Ixx and Iyy, however, demonstrated similar trends to bone XSA with PTH–

mediated increases compared to baseline. Thus, over the 4-week treatment duration, the PTH (1-34) anabolic effects were relatively uniform around the entire OVX rat femoral neck cross-section, and did not appear to have preferential apposition that might improve femoral neck structural properties in any particular direction over the vehicle–treated or baseline animals. Previous work with the combined insult of OVX and hindlimb–unloading in rats demonstrated that the absence of mechanical loading did not alter PTH efficacy on osteoblast number or cortical bone formation in the rat tibia (**37**).

The analysis of the periosteal and endosteal envelopes in mid-femoral neck cross-sections suggested that increments in bone mass were due primarily to increases in cortical bone rather than trabecular bone. As observed in the total bone cross-sectional area, the cortical bone XSA was significantly greater in the 10 μg/kg-treated femoral neck than all other groups, but there were no significant differences among the groups in trabecular bone mass within the endosteal envelope. Using this method of analysis, however, trabecular bone measures were inherently more sensitive than cortical measures to inter–animal biological variance, perturbations in the location of the analyzed cross-section, as well as the orientation of the plane of the cross-section. In contrast, structural analysis of the μCT-generated data identified several indices of trabecular bone architecture that demonstrated PTH (1-34) anabolic effects on the trabecular bone in both the femoral neck and the lumbar (L3) vertebra. The three dimensional volumes of interest within the endosteal surface along the length of the femoral neck were less sensitive to site–specific variance within individual femurs, and were more representative. As found in previous studies (**21**, **22**), the increase in trabecular bone volume fraction with PTH therapy was primarily due to increased trabecular thickness,

and not an increase in trabecular number. Given that Tb.Th. was inversely proportional to BS/BV, the significant increases found in Tb.Th. were consequently reflected in a significant reduction in BS/BV in both the femoral neck and L3 (when comparing baseline and vehicle-treated to 10 μg/kg PTH (1-34) treated rats). Since the treatment of the OVX rats by vehicle resulted in no significant changes in the quantified architectural indices compared to baseline control animals, the significant increases in bone properties in the 10 μg/kg animals compared to both baseline and vehicle treated animals suggested that the PTH (1-34) therapy did not simply prevent bone loss, but rather had a net anabolic effect on the rat bone mass in just four doses over the 4 week treatment protocol. Consequently, these results were strongly indicative of a PTH-mediated appreciation in the structural integrity of trabecular bone. Such anabolic changes have previously been shown to correspond to an increase in bone biomechanical performance (**34**).

Weekly administration of 10 μg/kg of PTH (1-34) has previously been shown by Okimoto *et al.* to effectively increase bone accretion after 3 and 6 month therapies (for a total dose of 120 and 340 μg/kg, respectively) in the OVX Wistar rat model as measured by bone mineral density, mechanical and histomorphometric parameters (**34**). These findings are in agreement with the current study. Okimoto *et al.* also found that 90 μg/kg led to a similar anabolic effect. In contrast to the findings by Okimoto *et al.*, however, in the current study neither cortical nor trabecular bone mass was augmented by the 80 μg/kg/wk dose of PTH (1-34) at the selected anatomical locations in the OVX rat skeleton. One or more of the following differences between these two studies may account for this observation: Firstly, we used Sprague Dawley rats, whereas the Okimoto *et al.* utilized Wistar rats. Secondly, the rats in this study were allowed to develop

osteopenia for 7 months, longer than the 3 months utilized by Okimoto *et al.* The severely compromised trabecular bone tissue in the current study would be less responsive to the PTH (1-34) effects. Finally, the treatment period in our study (4 weeks) was shorter than the duration (3 months) used by Okimoto *et al.* and may not have allowed sufficient time for new bone deposition. Nevertheless, these factors did not influence the low dose (10 μg/kg) response, so that the anabolic effects of the PTH (1-34) were observed at distinct anatomical sites.

Another possible explanation for the apparently ineffective 80 μg/kg in the current study might have been a dose–related effect. As discussed previously, a 90 μg/kg dose caused a significant increase in endosteal osteoclast numbers and osteoclast surface ratio (Oc.S/BS) (**34**). In the same study, cessation of the 90 μg/kg dose resulted in a dramatic bone loss after 3 months with BMD returning to the levels seen in vehicle–treated animals, while rats treated at 10 μg/kg retained bone mass after the cessation of PTH (1-34) (**34**). Another study also demonstrated poor bone retention following the cessation of daily injections of 80 μg/kg PTH (1-34) in male Sprague Dawley rats (**5**). Compared to vehicle–treated animals, 12 daily injections of 80 μg/kg PTH (1-34) resulted in a significant increase (111%) in osteoblast surface ratio (Ob.S/BS), as well as Oc.S/BS, and a significant increase in BV/TV (60%). Other treatment groups included rats treated with PTH for 12 days, followed by vehicle (i.e., withdrawal from PTH therapy) for either 4 or 12 more days. In the 4-day withdrawal group, the cessation of PTH treatment resulted in a 73% reduction in Ob.S/BS and a dramatic, 254% increase in the Oc.S/BS. This rapid effect on the osseous cell populations suggested a shift in bone remodeling favoring the resorption of bone, which after 12 day of withdrawal resulted in

a reduction in BV/TV, Tb.Th and Tb.N to levels that were similar to vehicle-treated animals (5). Given that 8 days were allowed to pass between the final injections and study termination in the current study, the histological response associated with the discontinuation of high doses of PTH (as observed by others) may have been responsible for the loss of any bone accrued by the administration of the 4 weekly doses of 80 μg/kg PTH (1-34).

There are no other reports, to our knowledge, that describe the stimulation of systemic bone growth using a total dose of PTH (1-34) as low as 40 μg/kg (10 μg/kg/week x 4 week). When 1, 5, and 25 μg/kg of rat PTH (1-34) were administered for 28 days (for a total of 28, 140 and 700 μg/kg, respectively), several dynamic indices of bone formation in trabecular bone from the proximal tibial metaphysis were significantly increased at all doses (38). Despite the increases in histomorphometric bone formation indices, the daily 1 μg/kg rat PTH (1-34) therapy (28 μg/kg) did not produce significant improvements in bone mass over daily vehicle–treated animals. The difference between the two studies may have been a combination of the increased dose (12 μg/kg over the 4 week study duration), and the frequency (daily vs. weekly). At 1 μg/kg/day, the significant histomorphological indices suggested a slower effect on net bone anabolism that may have generated increased bone mass over a study duration longer than 4 weeks (38). The comparison of these data with the current study suggested that these low doses, 28-40 μg/kg over 4 weeks, may be close to the threshold for effective dose for bone mass accretion in the OVX rat model.

In conclusion, weekly administration of 10 μg/kg of PTH (1-34) led to a systemic, anabolic response on both skeletal architecture and mineral content, and thus, our results suggests that reducing dosing frequency may serve as means of circumventing some of the aforementioned adverse effects associated with the daily PTH (1-34) administration. To our knowledge, the total administered dose of 40 μg/kg of PTH (1-34) represents one of the lowest doses ever to elicit an effective net anabolic response in an OVX rat model. An additional study is planned to investigate the potential anabolic effects of weekly, low doses of PTH (1-34) over a longer duration. It will be important to determine whether such an augmentation of skeletal tissue will be stable following the discontinuation of therapy.

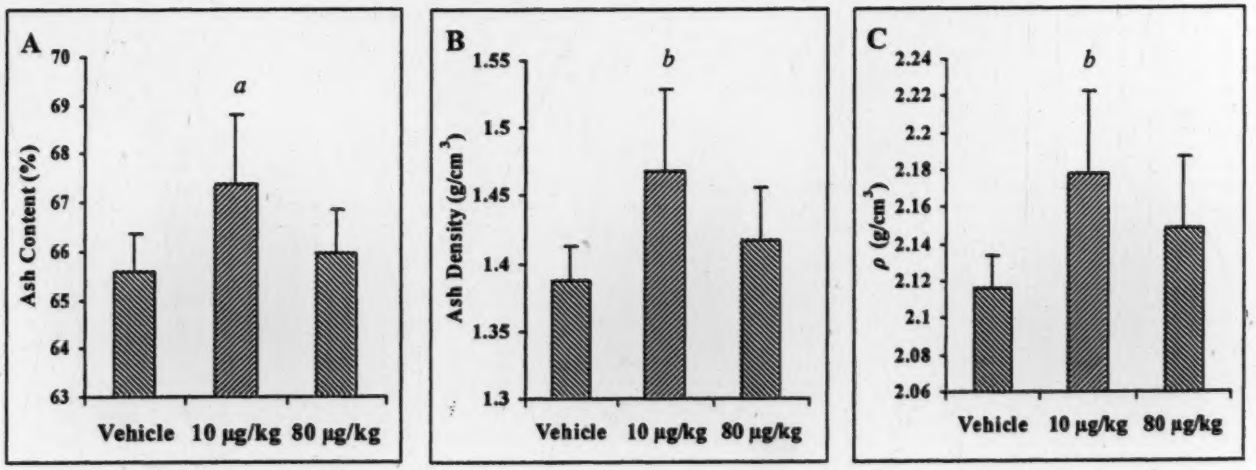

Figure 6-1: The effects of weekly PTH (1-34) administration on bone mineral content in the tibia. Tibial ash content is presented as a function of either dry weight (**A**), or volume (**B**). Bone density of the segmented samples was also determined (**C**). In all cases, the weekly administration of 10 ug/kg PTH (1-34) led to a statistically significant increase over the vehicle-treated group. [a] $p<0.025$ *vs.* vehicle–treated group. [b] $p<0.0125$ *vs.* vehicle–treated group.

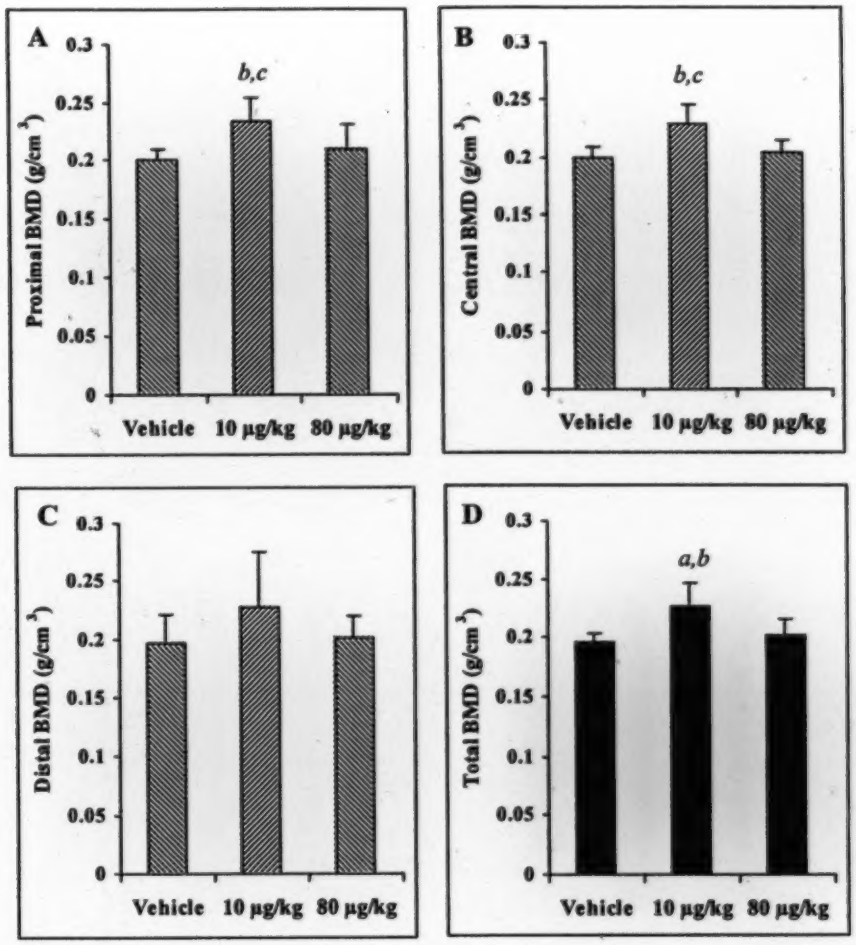

Figure 6-2: The effects of weekly PTH (1-34) administration on bone mineral density within the proximal (**A**), central (**B**), and distal (**C**) regions as well as the total (**D**) femur. In all of the selected regions, except distal, a significant increase in the 10 µg/kg–treated group was observed over that of the vehicle- and 80 µg/kg-treated groups. [a] *p<0.05 vs.* 80 µg/kg–treated group. [b] *p<0.025 vs.* vehicle–treated group. [c] *p<0.025 vs.* 10 µg/kg – treated group.

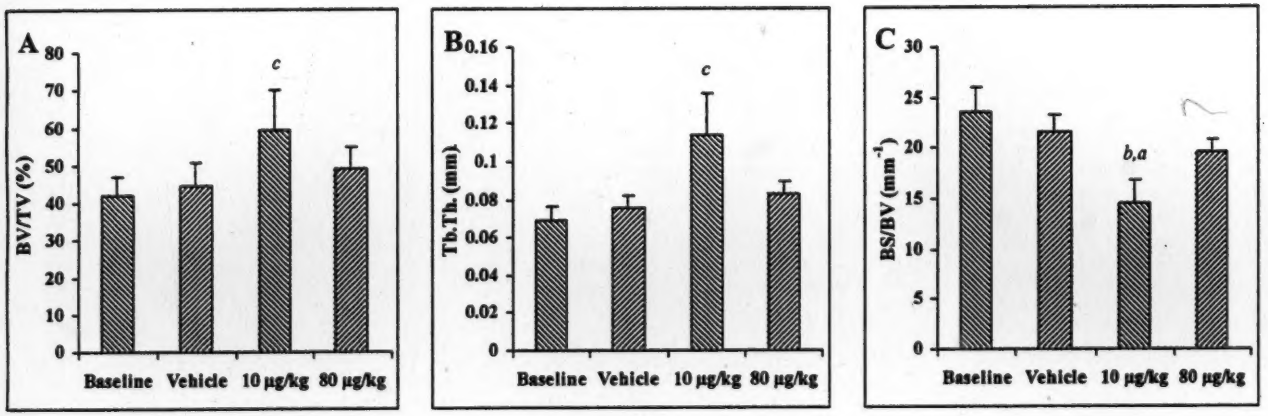

Trabecular Spacing (Tb.Sp.) and Trabecular Number (Tb.N.) of the Femoral Neck.

Group	Tb.Sp. (mm)	Tb.N. (mm^{-1})
Baseline	0.11 ± 0.02	5.93 ± 0.43[a]
Vehicle	0.12 ± 0.03	5.71 ± 0.52
10 µg/kg	0.09 ± 0.03	5.09 ± 0.40
80 µg/kg	0.10 ± 0.03	5.76 ± 0.34

Figure 6-3: The effect of weekly PTH (1-34) administration on structural parameters BV/TV (**A**), Tb.Th (**B**) and BS/TV (**C**), of the trabecular bone within the femoral neck. Listed in the table is a summary of all of the architectural parameters generated for this region. [a] *p<0.05 vs.* 80 µg/kg–treated group. [b] *p<0.0125 vs.* vehicle and 80 µg/kg–treated groups and . [c] *p<0.0125 vs.* all other groups.

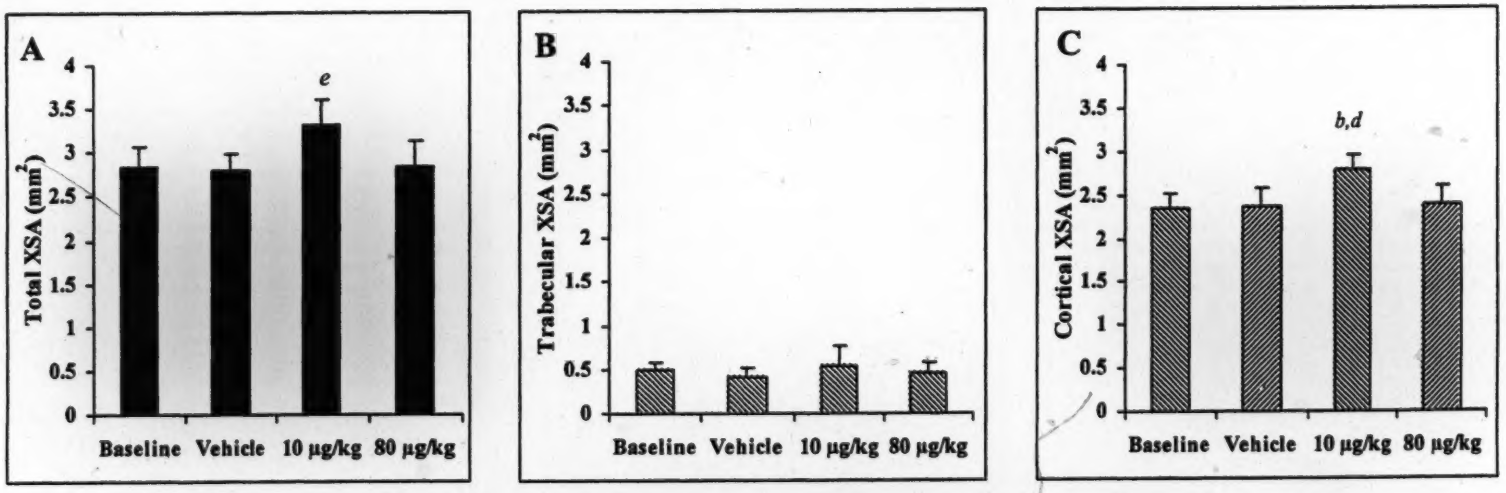

Cross Sectional Moments of Inertia and Envelopes for Femoral Neck.

Group	Total Ixx (mm^4)	Total Iyy (mm^4)	Total Ixx/Iyy	Tb. Ixx (mm^4)	Tb. Iyy (mm^4)	Ct. Ixx (mm^4)	Ct. Iyy (mm^4)	Per. Env. (mm^2)	Endo. Env. (mm^2)
Baseline	1.05 ± 0.22	0.71 ± 0.08	1.46 ± 0.21	0.06 ± 0.02	0.03 ± 0.01	0.99 ± 0.20	0.68 ± 0.07	3.32 ± 0.27	0.97 ± 0.15
Vehicle	1.02 ± 0.21	0.64 ± 0.15	1.59 ± 0.10	0.04 ± 0.01	0.02 ± 0.01	0.98 ± 0.21	0.62 ± 0.15	3.21 ± 0.38	0.77 ± 0.22
10 µg/kg	1.22 ± 0.32	0.91 ± 0.21[c]	1.34 ± 0.21	0.05 ± 0.04	0.04 ± 0.05	1.18 ± 0.29	0.87 ± 0.18[c]	3.64 ± 0.46[a]	0.80 ± 0.33
80 µg/kg	0.96 ± 0.12	0.71 ± 0.18	1.40 ± 0.26	0.04 ± 0.02	0.03 ± 0.01	0.92 ± 0.11	0.68 ± 0.17	3.23 ± 0.27	0.80 ± 0.14

Figure 6-4: The effect of weekly PTH (1-34) administration on total (**A**), trabecular (**B**) and cortical (**C**) XSA within the femoral neck. Summarized in the table are the second moments of area about the horizontal and vertical axes (Iyy and Ixx, respectively) for total, trabecular (Tb.) and cortical (Ct.) XSA as well as the areas of the periosteal and endosteal envelopes (Endo.Env. and Per.Env., respectively). [a] *$p<0.05$ vs.* vehicle–treated group. [b] *$p<0.05$ vs.* 80 µg/kg–treated group. [c] *$p<0.025$ vs.* vehicle–treated group. [d] *$p<0.0125$ vs.* baseline and vehicle–treated groups. [e] *$p<0.0125$ vs.* all other groups.

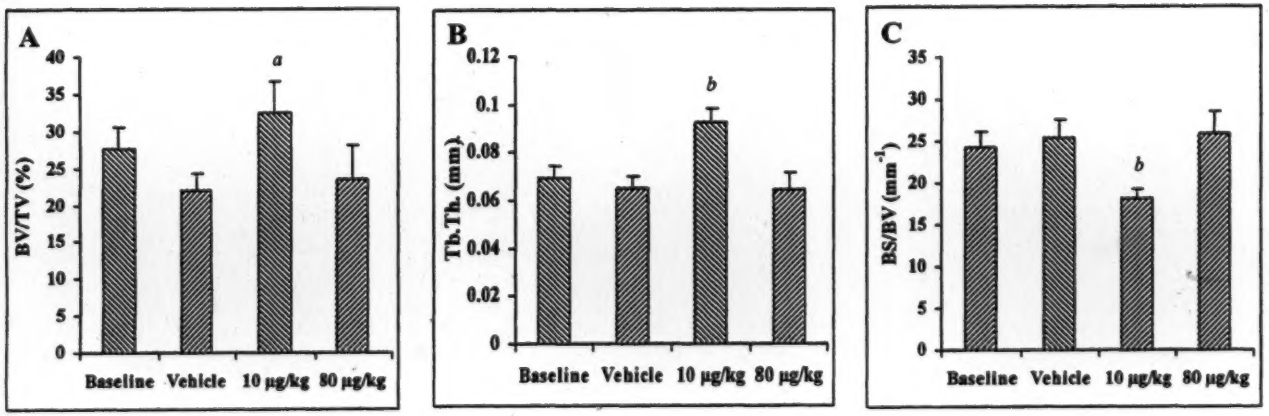

Trabecular Spacing (Tb.Sp.) and Trabecular Number (Tb.N.) of Third Lumbar Vertebra.

Group	Tb.Sp. (mm)	Tb.N. (mm^{-1})
Baseline	0.20 ± 0.04	4.00 ± 0.38
Vehicle	0.27 ± 0.03	3.32 ± 0.20
10 µg/kg	0.21 ± 0.04	3.51 ± 0.34
80 µg/kg	0.22 ± 0.04	3.80 ± 0.49

Figure 6-5: The effect of weekly PTH (1-34) administration on the structural parameters BV/TV (**A**), Tb.Th (**B**), and BS/TV (**C**), of trabecular bone within the third lumbar vertebra. The table summarizes all of the architectural parameters generated of the trabecular bone from the L3. [a] *p<0.0125 vs.* vehicle and 80 µg/kg–treated groups. [b] *p<0.0125 vs.* all other groups.

REFERENCES

1. T. Uzawa, M. Hori, S. Ejiri, H, Ozawa Comparison of the effects of intermittent and continuous administration of human parathyroid hormone (1-34) on rat bone. *Bone.* 16 (1995) 477-484.

2. S. Lotinun, J.D. Sibonga, R.T. Turner, Differential effects of intermittent and continuous administration of parathyroid hormone on bone histomorphometry and gene expression, *Endocrine.* 17 (2002) 29-36.

3. V. Shen, R. Birchman, D.D. Wu, R. Lindsay, Skeletal effects of parathyroid hormone infusion in ovariectomized rats with or without estrogen repletion, *J. Bone Min. Res.* 15 (2000) 740-746.

4. J.M. Hock, J. Fonseca, M. Gunness-Hey, B.E. Kemp, T.J. Martin, Comparison of the anabolic effects of synthetic parathyroid hormone-related protein (PTHrP) 1-34 and PTH 1-34 on bone in rats, *Endocrinol.* 125 (1989) 2022-2027.

5. M. Gunness-Hey, J.M. Hock, Loss of the anabolic effect of parathyroid hormone on bone after discontinuation of hormone in rats, *Bone.* 10 (1989) 447-452.

6. H. Oxlund, C. Ejersted, T.T. Andreassen, O. Torring, M.H. Nilsson, Parathyroid hormone (1-34) and (1-84) stimulate cortical bone formation both from periosteum and endosteum, *Calcif. Tissue Int.* 53 (1993) 394-399.

7. M. Gunness-Hey, J.M. Hock, Increased trabecular bone mass in rats treated with human synthetic parathyroid hormone, *Metab. Bone. Dis. Relat. Res.* 5 (1984) 177-181.

8. I. Moriyama, J. Iwamoto, T. Takeda, Y. Toyama, Comparative effects of intermittent administration of human parathyroid hormone (1-34) on trabecular and cortical bone loss in tail-suspended and sciatic neurectomized young rats, *J. Orthop. Sci.* 7 (2002) 379-385.

9. B.P. Halloran, D.D. Bikle, J. Harris, S. Tanner, T. Curren, E. Morey-Holton, Regional responsiveness of the tibia to intermittent administration of parathyroid hormone as affected by skeletal unloading, *J. Bone Miner. Res.* 12 (1997) 1068-1074.

10. T. Ogawa, H. Yamagiwa, T. Hayami, Z. Liu, K.Y. Huang, K. Tokunaga, T. Murai, N. Endo, Human PTH (1-34) induces longitudinal bone growth in rats, *J. Bone Miner. Metab.* 20 (2002) 83-90.

11. H. Oxlund, M. Dalstra, C. Ejersted, T.T. Andreassen, Parathyroid hormone induces formation of new trabecular bone with substantial mechanical strength at a site where it had disappeared in old rats, *Eur. J. Endocrinol.* 146 (2002) 431-438.

12. C. Ejersted, T.T. Andreassen, M.H. Nilsson, H. Oxlund, Human parathyroid hormone (1-34) increases bone formation and strength of cortical bone in aged rats, *Eur. J. Endocrinol.* 130 (1994) 201-207.

13. C. Ejersted, T.T. Andreassen, E.M. Hauge, F. Melsen, H. Oxlund, Parathyroid hormone (1-34) increases vertebral bone mass, compressive strength, and quality in old rats, *Bone.* 17 (1995) 507-511.

14. C. Ejersted, T.T. Andreassen, H. Oxlund, P.H. Jorgensen, B. Bak, J. Haggblad, O. Torring, M.H. Nilsson, Human parathyroid hormone (1-34) and (1-84) increase the mechanical strength and thickness of cortical bone in rats, *J. Bone Miner. Res.* 8 (1993) 1097-1101.

15. C. Ejersted, H. Oxlund, T.T. Andreassen, Bisphosphonate maintains parathyroid hormone (1-34)-induced cortical bone mass and mechanical strength in old rats, *Calcif. Tissue Int.* 62 (1998) 316-322.

16. H.A. Simmons, C.M. Pirie, D.D. Thompson, H.Z. Ke, Parathyroid hormone (1-34) increased total body bone mass in aged female rats, *J. Pharmacol. Exp. Ther.* 286 (1998) 341-344.

17. B.H. Mitlak, D.C. Williams, H.U. Bryant, D.C. Paul, R.M. Neer, Intermittent administration of bovine PTH-(1-34) increases serum 1,25-dihydroxyvitamin D concentrations and spinal bone density in senile (23 month) rats, *J. Bone Miner. Res.* 7 (1992) 479-484.

18. T. Tsuchida, K. Sato, N. Miyakoshi, T. Abe, T. Kudo, Y. Tamura, Y. Kasukawa, K. Suzuki, Histomorphometric evaluation of the recovering effect of human parathyroid hormone (1-34) on bone structure and turnover in streptozotocin-induced diabetic rats, *Calcif. Tissue Int.* 66 (2000) 229-233.

19. J.M. Hock, I. Gera, J. Fonseca, L.G. Raisz, Human parathyroid hormone-(1-34) increases bone mass in ovariectomized and orchidectomized rats, *Endocrinology.* 122 (1988) 2899-2904.

19. D.D. Thompson, H.A. Simmons, C.M. Pirie, H.Z. Ze, FDA guidelines and animal models for osteoporosis, *Bone.* 16 (1995) 157-161.

20. P. Morley, J.F. Whitfield, G.E. Willick, Parathyroid hormone: an anabolic treatment for osteoporosis, *Curr. Pharm. Des.* 7 (2001) 671-687.

22. D.W. Dempster, F. Cosman, M. Parisien, V. Shen, R. Lindsay, Anabolic actions of parathyroid hormone on bone, *Endocr. Rev.* 14 (1993) 690-709.

23. M. Li, T.J. Wronski, Response of femoral neck to estrogen depletion and parathyroid hormone in aged rats, *Bone.* 16 (1995) 551-557.

24. M. Kneissel, A. Boyde, J.A. Gasser, Bone tissue and its mineralization in aged estrogen-depleted rats after long-term intermittent treatment with parathyroid hormone (PTH) analog SDZ PTS 893 or human PTH(1-34), *Bone*. 28 (2001) 237-250.

25. M. Sato, G.Q. Zeng, C.H. Turner, Biosynthetic human parathyroid hormone (1-34) effects on bone quality in aged ovariectomized rats, *Endocrinology*. 138 (1997) 4330-4337.

26. H. Oxlund, M. Dalstra, C. Ejersted, T.T. Andreassen, Parathyroid hormone induces formation of new cancellous bone with substantial mechanical strength at a site where it had disappeared in old rats, *Eur. J. Endocrinol*. 146 (2002) 431-438.

27. J.L. Vahle, M. Sato, G.G. Long, J.K. Young, P.C. Francis, J.A. Engelhardt, M.S. Westmore, Y. Linda, J.B. Nold, Skeletal changes in rats given daily subcutaneous injections of recombinant human parathyroid hormone (1-34) for 2 years and relevance to human safety, *Toxicol. Pathol*. 30 (2002) 312-321.

28. M. Sato, Y.L. Ma, J.M. Hock, M.S. Westmore, J. Vahle, A. Villanueva, C.H. Turner, Skeletal efficacy with parathyroid hormone in rats was not entirely beneficial with long-term treatment, *J. Pharmacol. Exp. Ther*. 302 (2002) 304-313.

29. C. Crandall, Parathyroid hormone for treatment of osteoporosis, *Arch. Intern. Med*. 162 (2002) 2297-2309.

30. S. Bain, N.S. Ramamurthy, T. Impeduglia, S. Scolman, L.M. Golub, Rubin C, Tetracycline prevents trabecular bone loss and maintains near-normal rates of bone formation in streptozotocin diabetic rats, *Bone*. 21 (1997) 147-153.

31. L.A. Feldkamp, L.C. Davis, J.W. Kress, Practical cone-beam algorithm. *J. Opt. Soc. Am. –A1* (1984) 612-619.

32. C.A. Glaseby, An Analysis of Histogram-Based Thresholding Algorithms, *CVGIP: Graphical Models and Image Processing.* 55 (1993) 532-537.

33. L. Mosekilde, L. Tornvig, J.S. Thomsen, P.B. Orhii, M.J. Banu, D.N. Kalu, Parathyroid hormone and growth hormone have additive or synergetic effect when used as intervention treatment in ovariectomized rats with established osteopenia, *Bone.* 26 (2000) 643-651.

34. N. Okimoto, H. Tsurukami, Y. Okazaki, S. Nishida, A. Sakai, H. Ohnishi, M. Hori, K. Yasukawa, T. Nakamura, Effects of a weekly injection of human parathyroid hormone (1-34) and withdrawal on bone mass, strength, and turnover in mature ovariectomized rats, *Bone.* 22 (1998) 523-531.

35. M.L. Bouxsein, K.H. Myburgh, M.C. van der Meulen, E. Lindenberger, R. Marcus, Age-related differences in cross-sectional geometry of the forearm bones in healthy women, *Calcif. Tissue Int.* 54 (1994) 113-118.

36. S. Judex, T.S. Gross, R.F. Zernicke, Strain gradients correlate with sites of exercise-induced bone-forming surfaces in the adult skeleton, *J. Bone. Min. Res.* 12 (1997) 1737-1745.

37. R.T. Turner, G.L. Evans, J.M. Cavolina, B. Halloran, E. Morey-Holton, Programmed administration of parathyroid hormone increases bone formation and reduces bone loss in hindlimb-unloaded ovariectomized rats, *Endocrinology.* 139 (1998) 4086-4091.

38. J. Fox, M.A. Miller, G.B. Stroup, E.F. Nemeth, S.C. Miller, Plasma levels of parathyroid hormone that induce anabolic effects in bone of ovariectomized rats can be achieved by stimulation of endogenous hormone secretion, *Bone.* 21 (1997) 163-169.

CHAPTER VII

SYSTEMIC ADMINISTRATION OF VASCULAR ENDOTHELIAL GROWTH FACTOR AND BASIC FIBROBLAST GROWTH FACTOR IN OVARIECTOMIZED RATS.

INTRODUCTION

The potent anabolic effects of basic fibroblast growth factor (bFGF) on the skeletal tissue of ovariectomized (OVX) rats have been well-documented (**1-11**). Culminating in the stimulation of endocortical and cancellous bone formation in this animal model, bFGF increases osteoblast number and osteoblast-synthesized osteoid; while concurrently decreases osteoclast number (**6-10**). Not only does bFGF exert its effects on pre-existing bone, its parenteral administration elicits the formation of osteoid spicules *de novo* in myeloid cavities (**9-11**). All together, the effects that bFGF elicit upon parenteral administration reflect its endogenous role as an anabolic modulator in the formation and regulation of skeletal tissue (**12-14**).

Like bFGF, mounting evidence suggests that vascular endothelial growth factor (VEGF) is integral in the development (**15-20**), maintenance (**21, 22**), and repair of bone (**23, 24**). Abrogation of VEGF activity through the administration of anti-VEGF antibodies during skeletogenesis inhibited metaphyseal blood vessel invasion, and led to the expansion of the hypertrophic chondrocyte zone, and aberrant formation of trabecular bone (**15**). Similarly, mice genetically-manipulated to only express the $VEGF_{120}$ isoform not only exhibited randomly arranged bone vasculature but also a decreased osteoblast activity and chondrocyte maturation resulting in a reduction in both the mineralization and size of endochondral and intramembranous bone (**16, 17**). Not only are VEGF and its receptors expressed on both osteoblasts and osteoclasts (**21, 25**), but vertebral VEGF concentrations correlated to changes bone mineral density in glucocorticoid-induced osteopenic Göttingen minipigs (**21**). These results suggested that VEGF is an important autocrine and/or paracrine factor during the process of bone remodeling; and lend support to Parfitt's hypothesis that endothelial cells belonging to basic multicellular units

involved in bone remodeling are integral in coupling bone resorption with formation (**21, 26**).

Despite the evidence implicating VEGF in numerous skeletal processes, the effects of parenteral VEGF administration on skeletal tissue have never been assessed in an OVX animal model. Thus, the primary purpose of this study was to evaluate any potential effects that VEGF may elicit on bone upon subcutaneous or intravenous administration. It was also the goal of this study to determine whether growth factor-mediated responses were affected by the route in which they were administered. Because the anabolic effects of bFGF have been well-established in the OVX rat model, VEGF-mediated changes to bone were compared to those induced by the administration of bFGF.

MATERIALS AND METHODS

Animal Care

Forty, 60 day-old, female Sprague-Dawley rats, which had been commercially ovariectomized, as well as 8 age-matched, sham-operated rats were purchased from Charles River Laboratories (Quebec City, PQ). Throughout the course of the study, the rats were maintained in pairs in standard laboratory conditions (23°C, 12 h of light/day). Rats were provided standard commercial rat chow and tap water (*ad libitum*). All procedures involving the use of rats were approved by the Animal Welfare Committee at the University of Alberta (Edmonton, Alberta).

Experimental Design

All animals used were weighed and ear-tagged five days prior to the beginning of the experiment when rats were 5 months of age (3 months post-surgery). At this time, a small aliquot of blood was also collected through the tail vein. While the sham-operated rats were assigned to group 1, all ovariectomized rats were assigned randomly into 5 groups. For a total of one week, all the rats received daily intravenous (IV) or subcutaneous (SC) injections of saline, VEGF (80 μg/kg body weight per injection), or bFGF (80 μg/kg body weight per injection). The groups were as follows:

Group	Animal Operation	No. of Animals	Treatment Administered	Route of Administration
1	Sham	8	Saline	IV
2	OVX	8	Saline	IV
3	OVX	8	bFGF	SC
4	OVX	8	bFGF	IV
5	OVX	8	VEGF	SC
6	OVX	8	VEGF	IV

One week after the final injection, rats were killed via asphyxiation using a CO_2 chamber and weighed. At necropsy, the uterus was excised and weighed; and an aliquot of blood was obtained via cardiac puncture. Bone tissues, including both femora, tibiae, and a portion of the lumbar spine (L1-L4), were harvested, fixed immediately in 70% ethanol, and stored at -20°C.

The delivery vehicle used consisted of saline (0.9% NaCl; Baxter Corporation, Toronto, ON). The rh-bFGF and rh-VEGF (lot numbers: AU470021 and II120021,

respectively; National Cancer Institute Biological Resources Branch, Rockville, MD) were diluted in the 0.9% saline just prior to the beginning of injections. IV injections were made into the tail vein. All injections were carried out by members of the technical staff from the Health Sciences Laboratory Animal Services at the University of Alberta.

Serum Biochemical Analysis

Serum phosphorus (mg/dL), calcium (mg/dL), and alkaline phosphatase (ALP, U/L) concentrations were quantified using the ammonium molybdate, o-cresolphthalein complexone, and p-nitrophenyl phosphate methods, respectively, as per the manufacturer's instructions (Sigma Aldrich, St. Louis, MO).

Bone Analysis

Mineral Ash Content: The mineral ash content was determined by ashing 1-cm long segments of tibia from the proximal tibial growth plate to the mid-diaphysis (27). Samples were defatted in acetone and then dried for 24 hr at 100°C. The dry samples were weighed in air (dry bone mass), rehydrated in distilled water for 24 hr under vacuum, weighed underwater (wet bone mass), ashed at 800°C for 24 hr and finally weighed (mineral ash mass). Archimedes principle was used to determine bone density (ρ, g/cm^3) and volume (cm^3). Ash content was calculated as a measure of mineral ash mass per dry bone mass (ash content, %), and mineral ash mass per bone volume (ash density, g/cm^3).

Femoral and Tibial Bone Mineral Density: The bone mineral density (BMD) of all right-side tibiae and femora harvested were determined using dual energy x-ray absorptiometry (DEXA, Enhanced Vision Systems Corp., London, Ontario). BMD (g/cm^2) was calculated by dividing bone mineral content (g) by projected bone area (cm^2).

Architecture of Trabecular Bone within the Distal Femoral Metaphysis: Growth factor-mediated morphological changes in trabecular bone were evaluated using micro-computed tomography (μCT). Specifically, the distal end of the rat femurs was scanned at 100 kV/100 μAmp using a Skyscan 1072 X-ray microtomograph (Skyscan, Aartselaar, Belgium). The acquired tiff images were then reconstructed 2D using the "Volumetric-Reconstruction for SkyScan Micro-CT Instruments" program (version 2.2, Skyscan, Aartselaar, Belguim). The number of 2D slices to be analyzed in each sample was normalized by taking 2.881% of the entire length of the femur as determined using a Mitutoyo absolute digitamatic caliper (reading error ± 0.01 mm, Mitutoyo Corporation, Japan). This ensured that approximately 100 slices (or given that each slice = 10 μm, approx. 1.0 mm) of metaphyseal bone was analyzed. The volume of interest used was the region between the slice where the growth plate was no longer evident in the metaphysis (identified manually), up to the pre-determined number of proximal slices. Using the "Analyze" program (version 4.0, Mayo Foundation for Medical Education and Research, Rochester, Mn), the selected slices were then median filtered. The trabecular core within the medulla was segmented from the cortical bone by manually outlining the cortical-trabecular bone interface; and the volume of the segmented tissue (i.e. medullar area including the trabecular bone, known as the tissue volume, TV; mm^3) was subsequently

determined. The segmented trabecular bone was then reconstructed 3-dimensionally using a universal threshold (see **APPENDIX B**) with the "3D-Creator" program (version 2.2d, Skyscan, Aartselaar, Belgium). Bone volume (BV; mm^3), bone surface fraction (BS/BV; mm^{-1}), degree of anisotropy (DA), structure model index (SMI), and mean trabecular thickness (Tb.Th; μm) were then determined. The following morphometric indices were calculated: bone volume fraction (BV/TV; %; [100 x (BV/TV)]); trabecular number (Tb.N; mm^{-1}; ([(BV/TV)/100]/ (Tb.Th x 1000)) and trabecular separation (Tb.Sp; mm; (1/(Tb.N)- (Tb.Th/1000)) (**14**).

Statistical Analysis

Unless stated otherwise, all values stated are expressed as the mean ± standard deviation. Rat body masses, serum calcium and phosphorus concentrations were compared between the onset and end of treatment for each animal using student's paired *t*-test. Differences in uterine weight of the sham-operated versus the ovariectomized rats were assessed using student's *t*-test. The *p* values reported for all *t*-tests are two-sided. Statistically significant inter-group differences found within the serum biochemical, mineral ashing, DEXA and μCT data were identified using one-way analysis of variance (ANOVA) followed by Tukey post-hoc multiple comparison test. All statistical analysis was performed using S-PLUS student edition 6.0 (Insightful Corp, Seattle, WA). *p* values less than 0.05 were considered statistically significant.

RESULTS

Although the administration of bFGF and VEGF was generally well-tolerated, the delivery of VEGF through the tail-vein injection led to local vascular congestion at the site of administration.

Body and Uterine Mass

With the exception of the bFGF–SC-treated group, rat body mass from each of OVX treatment groups was significantly higher than the sham-operated group at the onset of the experiment ($p < 0.05$, **Table 7-1**). At necropsy, however, no differences in rat body mass were found between any of the groups. Despite a generalized decrease in individual body masses over the course of the study, these changes were not statistically significant ($p = 0.117$). Relative to the uterine weights of the sham-operated rats (0.900 ± 0.257 g, n = 8), the estrogen-depleted status of all OVX animals used was confirmed by the significant reduction in the average uterine mass (0.151 ± 0.076 g, n = 40, $p < 0.001$).

Serum Biochemical Analysis

In comparison to the sham-operated group, serum calcium concentrations from each of the OVX groups were significantly lower at baseline as well as at necropsy ($p < 0.05$, **Table 7-1**). Following treatment, serum calcium was significantly higher in each of the OVX groups than at the onset of the study. While there were no differences in serum phosphorus concentrations between any of the groups at the onset of treatment, the bFGF-IV- and VEGF-SC-treated groups were significantly lower than the OVX control group. Apart from the bFGF-IV-treated group, serum phosphorus concentrations for all

groups were significantly higher following therapy than before. Although no inter-group differences in serum ALP concentrations were evident at either study's onset or completion, a significant decrease of 43.5 % (on average) in ALP activity was observed in all groups between baseline concentrations and those at necropsy.

Mineral Ash Content

To assess changes elicited by daily growth factor administration on bone mineral content, segments of the proximal tibia were ashed. No statistically significant differences between treatment groups were observed in bone density (**Figure 7-1A**). Similarly, no inter-group differences were found in the ash content as either a function of dry weight (**Figure 7-1B**) or volume (**Figure 7-1C**). In all three of the parameters assessed, however, the vehicle-treated OVX group was consistently the lowest among the groups.

Femoral and Tibial Bone Mineral Density

Femoral and tibial BMD of the sham-operated group was 0.233 ± 0.012 g/cm^2, and 0.212 ± 0.018 g/cm^2, respectively; while that of the vehicle-treated OVX group was 0.200 ± 0.008 g/cm^2, and 0.182 ± 0.009 g/cm^2, respectively (**Figure 7-2**). This represents a statistically significant decrease of 14.3% ($p = 6.1 \times 10^{-6}$) and 14.4% ($p = 4.3 \times 10^{-4}$), respectively. Irrespective of the route of delivery, neither the administration of bFGF nor VEGF elicited any changes in the BMD. In comparison to other OVX groups, however, femoral and tibial BMD for the bFGF-treated groups were slightly higher; while those of the VEGF-IV treated group were among the lowest.

Architecture of Trabecular Bone within the Distal Femoral Metaphysis

As summarized in **Table 7-2**, structural parameters of the trabecular bone in the distal femur were evaluated using μCT. Among the morphometric parameters assessed, significant differences were observed in Tb.N, BV/TV, and SMI between the sham and each of the OVX groups. Tb.Th and BS/BV were significantly lower in the VEGF-treated groups relative to the sham-operated group. Apart from an increase in DA in the VEGF-IV-treated group, there were no statistically significant differences in any of the architectural parameters assessed between the vehicle-treated OVX group and the growth factor-treated OVX groups. Although not statistically significant, treatment of VEGF either IV or SC resulted in a decrease in Tb.Th (14.5 %, and 16.8 %, respectively), Tb.N (34.5 %, and 30.5%, respectively), and BV/TV (44.5 %, and 36.7%, respectively) as well as an increase of BS/BV (25.0%, and 26.9 %, respectively) relative to vehicle-treated OVX rats.

DISCUSSION

No studies to date have investigated the response elicited by parenteral administration of VEGF on bone in an OVX rat model. Consequently, it was the goal of this study to characterize these effects and to compare them to the effects mediated by the administration of bFGF. The results presented here suggested that neither the administration of VEGF nor bFGF elicited a significant effect on the bones assessed from the appendicular skeleton—irrespective of the route of administration used.

Consistent with a previous study examining the effects of exogenous bFGF administration on OVX rats (**9**), treatment with either bFGF or VEGF did not significantly affect individual body weight. Additionally, treatment with either growth factor did not influence uterus weight. Similar to previous observations with bFGF-treated (100 μg/kg/day for 7 days) OVX rats (**9**), the administration of either bFGF or VEGF did not affect serum calcium concentrations. On the other hand, serum phosphorus concentrations following the administration of bFGF IV, as well as VEGF SC were significantly decreased. These observations are in line with the hypophosphatemia elicited by the administration of bFGF IV, albeit at a much higher dose (i.e. 200 μg/kg/day for either 7 or 14 days) (**9**). It should be noted that baseline phosphorus concentrations reported in this study (9.28-13.00 mg/dL for sham and OVX rats) were significantly higher than those reported in other studies (6.2-6.7 mg/dL (**6**), and 5.8-9.1 mg/dL (**9**)) using similarly aged, OVX Sprague-Dawley rats. The reasons for this decrease, as well as that in serum ALP concentrations are not known.

As assessed using DEXA, the ovariectomization of the animals used in this study led to a significant decrease in BMD as compared to the sham-operated animals. These observations were corroborated by various bone architectural parameters (i.e. Tb.N, BV/TV, and SMI) determined using μCT. The changes mediated by the depletion of systemic estrogens on BMD and morphometric indices confirm that the OVX rats used were indeed osteopenic and are consistent with other studies that have evaluated the effects of ovariectomy on rat skeletal tissues using these techniques (**28-30**).

Irrespective of route of administration, the administration of either 80 μg/kg/day bFGF or VEGF did not elicit a statistically significant change in any of the bone

parameters assessed. That the administration of bFGF did not increase any of the parameters assessed was unexpected as previous studies examining the effects of exogenous bFGF administration in OVX rats have demonstrated that bFGF elicits an anabolic response on both cortical as well as trabecular bone in both the appendicular and axial skeleton. The lowest dose used among these studies (i.e. 100 μg/kg/day for 7 days administered IV) significantly increased osteoid volume, increased osteoblast surface, decreased osteoclast surface (**9**), and increased cortical bone width (**11**). Although the frequency and duration of administration were identical, the dose administered in these studies (i.e. 100 μg/kg/day) was 25% higher than that used in this study (**9, 11**). Perhaps a threshold in the local, skeletal concentration of bFGF must be surpassed to successfully stimulate the formation of bone. No studies to date have characterized a dose-response relationship for bFGF using an OVX rat model. As reported by Pun *et al.*, bFGF's ability to promote the differentiation of bone mesenchymal stem cells into osteoblasts was significantly attenuated in fatty (yellow) marrow in comparison to hematopoietic (red) marrow (**8**). Because the extent of fatty marrow is age-related (**31**), not only was the age, but the species, weight and OVX status of the animals used in this study were similar to those used in the aforementioned studies evaluating the effects of 100 μg/kg/day bFGF (**9, 11**). Thus, marrow-mediated mitigation of bFGF's effects was not likely responsible for the lack of bFGF-induced bone formation in the present study. Despite having been acquired from a reputable source, assays to determine the bioactivity of bFGF and VEGF *in vitro* were not performed prior to their utilization *in vivo*. Given the increase in local vascular congestion at the site of VEGF administration, however, protein bioactivity was not likely an issue (for VEGF at least). Although Nakamura *et al.* successfully used

DEXA to confirm the statistically significant increase in BMD elicited by the administration of 100 μg/kg/day bFGF for 7 days on the femur of 6 week-old male rats (32), while Lane et al. used μCT to evaluate the morphological changes elicited by the administration of 1000 μg/kg/day bFGF for 7 days, it remains possible that the anabolic effects administered by bFGF in this study were simply not detected by any of the methods of quantification used (i.e. mineral ashing, DEXA and μCT). Histomorphometry, the most prevalent analytical technique used to study the effects of exogenous bFGF on bone formation *in vivo*, was not used in this study.

Despite the lack of bFGF-mediated bone formation upon parenteral administration, treatment of VEGF, however, resulted in a (statistically non-significant) decrease in Tb.Th, Tb.N, and BV/TV and an increase of BS/BV relative to the vehicle-treated OVX group. A similar trend was also observed in both the femoral and tibial BMD of the VEGF-IV-treated group. Together, these data suggest that the administration of VEGF may have exacerbated the bone loss associated with the development of osteopenia in the OVX rats. Given VEGF's ability to serve as a chemoattractant for osteoclasts (33, 34) as well as enhance osteoclast activity and survival *in vitro* (35), these observations support the findings made by Kodama et al., who found that VEGF could substitute macrophage colony-stimulating factor in enhancing osteoclast differentiation and activity in osteopetrotic (*op/op*) mice (36). Relative to sham-operated controls, ovariectomy of these *op/op* mice led to the upregulation of VEGF mRNA expression in bone tissue as well as an increase in serum concentrations of VEGF. This increase in VEGF corresponded to an increase in osteoclast number and survival which was abrogated by the administration of 17β-estradiol, VEGF neutralizing antibody or a

soluble VEGF receptor 1-Fc chimera (37). Further studies should be done to elucidate the effects of VEGF administration on bone in an OVX animal model. Repeating the present study using a larger sample size (to improve the statistical strength), as well as higher doses of both bFGF and VEGF (to accentuate the effects elicited by growth factor administration) should afford some insight into the relationship between VEGF and the development of osteopenia. The results generated from such a study would help clarify VEGF's role in the pathogenesis of osteoporosis; and may provide the rationale for pursuing the development of VEGF-modulating agents that may attenuate the progression of this disease.

CONCLUSIONS

Administration of either bFGF or VEGF, through either an IV or SC route of administration, did not elicit a significant response on skeletal architecture or bone mineral content. This was the first study to attempt to examine the effects of exogenous VEGF administration in an OVX animal model. Given that the results presented herein were inconclusive, the study should be repeated to assess the effects of VEGF on bone in an OVX rat model of osteopenia.

Table 7-1: Body and Uterus Weight, and Serum Biochemical Analysis of Bone Formation Parameters.

	Sham Vehicle IV	OVX Vehicle IV	OVX FGF-2 SC	OVX FGF-2 IV	OVX VEGF SC	OVX VEGF IV
Body Weight before (g)	305 ± 18	340 ± 23[a]	338 ± 23	351 ± 19[a]	342 ± 22[a]	346 ± 25[a]
Body Weight After (g)	306 ± 19	334 ± 33	335 ± 21	334 ± 17	337 ± 21	327 ± 26
Uterus Weight (g)	0.90 ± 0.26	0.14 ± 0.063[a]	0.22 ± 0.10[a]	0.11 ± 0.05[a]	0.16 ± 0.06[a]	0.12 ± 0.06[a]
Serum [Ca] before (mg/dL)	11.43 ± 0.61	9.02± 0.40[a]	9.29 ±0.47[a]	9.34 ± 0.31[a]	9.30 ± 0.38[a]	9.10 ± 0.52[a]
Serum [Ca] after (mg/dL)	11.80 ± 0.66	10.89 ± 0.60[a,c]	10.55 ± 0.39[a,c]	10.93 ± 0.64[a,c]	10.89 ± 0.57[a,c]	10.51 ± 0.53[a,c]
Serum [P] before (mg/dL)	10.85 ± 1.18	10.71 ± 0.49	11.03 ± 1.57	11.07 ± 1.00	10.48 ± 0.84	10.88 ± 0.72
Serum [P] after (mg/dL)	13.08 ± 1.07[d]	14.29 ± 0.88[c]	12.88± 0.90[c]	11.48 ± 1.66[b]	11.69 ± 0.80[b,c]	13.12 ± 0.94[c]
Serum [ALP] before (U/L)	2.43 ± 0.61	2.09± 0.61	2.26 ± 0.67	2.27± 0.51	2.50 ± 0.53	2.10 ± 0.56
Serum [ALP] after (U/L)	1.34 ± 0.15[c]	1.52 ± 0.37[c]	1.57 ± 0.56[c]	1.18 ± 0.32[c]	1.09± 0.28[c]	1.00 ± 0.31[c]

[a] = statistically significant difference ($p < 0.05$) as compared to sham vehicle IV group
[b] = statistically significant difference ($p < 0.05$) as compared to OVX vehicle IV group
[c] = statistically significant difference ($p < 0.05$) as compared to *before* group

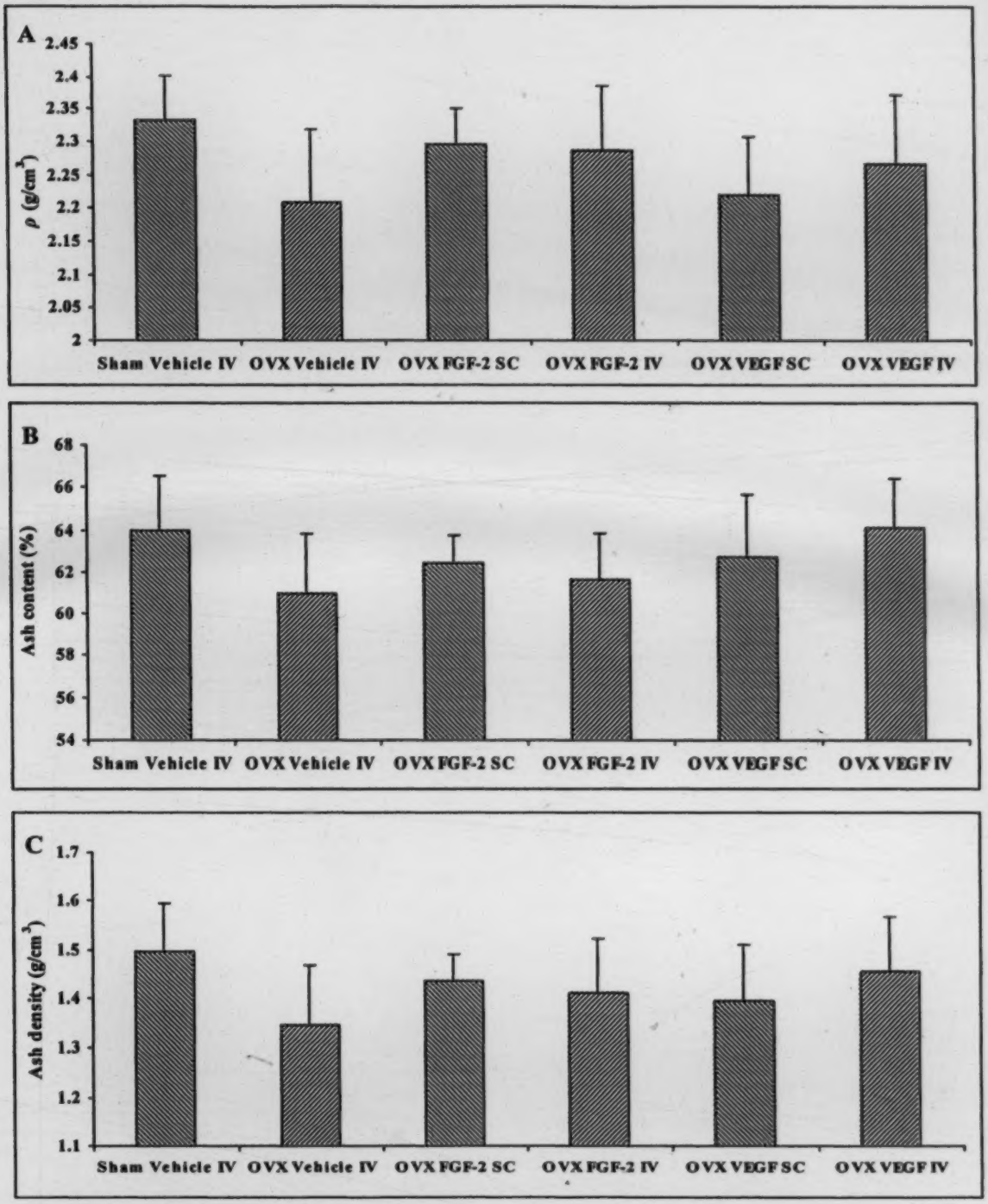

Figure 7-1: Determining the effects of growth factor administration on the density (A), ash content as a function of the dry weight (B) and ash content as a function of the volume of the proximal metaphyseal/diaphyseal region of the tibia. No statistically significant inter-group differences ($p > 0.05$) are observed.

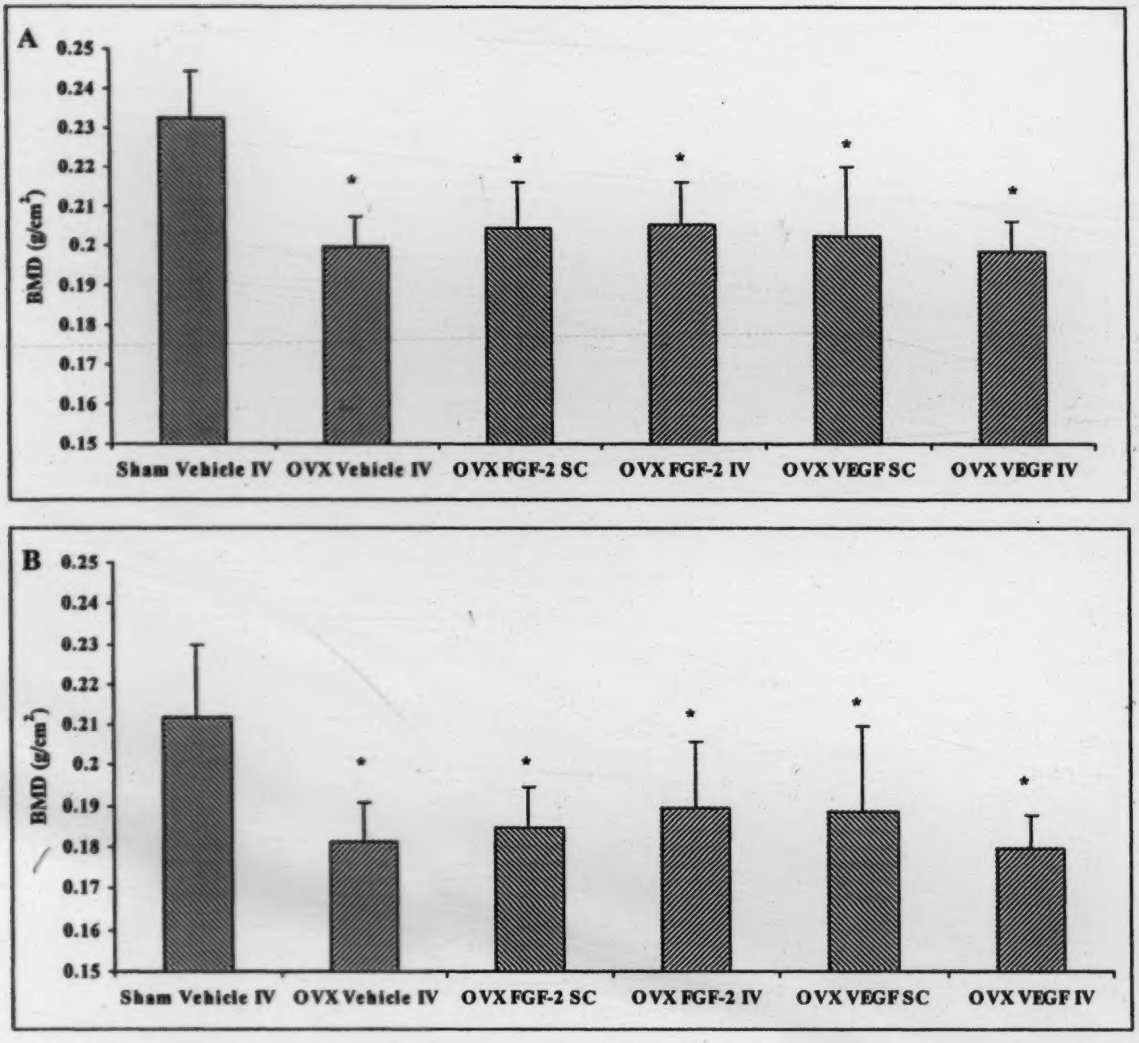

Figure 7-2: The effect of daily bFGF or VEGF administration on femoral (A) and tibial bone mineral density (BMD). Although administration of growth-factor does not elicit any statistically signifcant differences, the BMD of the sham-operated group was significantly higher than each of the OVX groups assessed. (* $p < 0.05$ vs. sham-vehicle group)

Table 7-2: 3-dimensional morphometric parameters from μCT of the distal femora of OVX rats administered vehicle, bFGF, or VEGF.

	Sham Vehicle IV	OVX Vehicle IV	OVX FGF-2 SC	OVX FGF-2 IV	OVX VEGF SC	OVX VEGF IV
Tb.Th	52.51 ± 5.20	46.79 ± 3.79	45.71 ± 7.70	44.24 ± 8.67	38.93 ± 10.23[a]	39.97 ± 4.31[a]
Tb.N	3.23 ± 0.58	0.70 ± 0.35[a]	0.68 ± 0.36[a]	0.55 ± 0.29[a]	0.48 ± 0.35[a]	0.46 ± 0.31[a]
Tb.Sp	0.27 ± 0.07	2.09 ± 1.76	2.07 ± 1.82	2.30 ± 1.23	3.18 ± 2.18[a]	2.44 ± 1.41
BS/BV	58.18 ± 7.61	71.26 ± 8.34	73.31 ± 11.29	76.11 ± 19.94	90.44 ± 20.24[a]	89.01 ± 9.63[a]
TV	8.51 ± 0.75	8.14 ± 1.53	8.06 ± 0.73	7.72 ± 0.84	8.91 ± 1.40	7.78 ± 0.93
BV/TV	17.23 ± 4.38	3.31 ± 1.76[a]	3.12 ± 1.90[a]	2.51 ± 1.37[a]	2.10 ± 1.69[a]	1.84 ± 1.37[a]
DA	0.26 ± 0.02	0.29 ± 0.06	0.31 ± 0.02	0.33 ± 0.03[a]	0.34 ± 0.03[a]	0.36 ± 0.05[a,b]
SMI	2.13 ± 0.22	2.52 ± 0.11[a]	2.40 ± 0.19[a]	2.48 ± 0.13[a]	2.56 ± 0.15[a]	2.44 ± 0.13[a]

[a] = statistically significant difference ($p < 0.05$) when compared to sham vehicle IV group
[b] = statistically significant difference ($p < 0.05$) when compared to OVX vehicle IV group

REFERENCES

1. U.T. Iwaniec, L. Mosekilde, N.G. Mitova-Caneva, J.S. Thomsen, T.J. Wronski, Sequential treatment with basic fibroblast growth factor and PTH is more efficacious than treatment with PTH alone for increasing vertebral bone mass and strength in osteopenic ovariectomized rats, *Endocrinology*. 143 (2002) 2515-2526.

2. N.E. Lane, J. Kumer, W. Yao, T. Breunig, T. Wronski, G. Modin, J.H. Kinney, Basic fibroblast growth factor forms new trabeculae that physically connect with pre-existing trabeculae, and this new bone is maintained with an anti-resorptive agent and enhanced with an anabolic agent in an osteopenic rat model, *Osteoporos. Int.* 14 (2003) 374-382.

3. H. Nagai, R. Tsukuda, H. Yamasaki, H. Mayahara, Systemic injection of FGF-2 stimulates endocortical bone modelling in SAMP6, a murine model of low turnover osteopenia, *J. Vet. Med. Sci.* 61 (1999) 869-875.

4. H. Mayahara, T. Ito, H. Nagai, H. Miyajima, R. Tsukuda, S. Taketomi, J. Mizoguchi, K. Kato, In vivo stimulation of endosteal bone formation by basic fibroblast growth factor in rats, *Growth Factors*. 9 (1993) 73-80.

5. N.E. Lane, W. Yao, J.H. Kinney, G. Modin, M. Balooch, T.J. Wronski. Both hPTH(1-34) and bFGF increase trabecular bone mass in osteopenic rats but they have different effects on trabecular bone architecture, *J. Bone Miner. Res.* 18 (2003) 2105-2115.

6. T.J. Wronski, A.M. Ratkus, J.S. Thomsen, Q. Vulcan, L. Mosekilde, Sequential treatment with basic fibroblast growth factor and parathyroid hormone restores lost cancellous bone mass and strength in the proximal tibia of aged ovariectomized rats, *J. Bone Miner. Res.* 16 (2001) 1399-1407.

7. R.A. Power, U.T. Iwaniec, T.J. Wronski, Changes in gene expression associated with the bone anabolic effects of basic fibroblast growth factor in aged ovariectomized rats, *Bone*. 31 (2002) 143-148.

8. S. Pun, R.L. Dearden, A.M. Ratkus, H. Liang, T.J. Wronski, Decreased bone anabolic effect of basic fibroblast growth factor at fatty marrow sites in ovariectomized rats, *Bone*. 28 (2001) 220-226.

9. H. Liang, S. Pun, T.J. Wronski, Bone anabolic effects of basic fibroblast growth factor in ovariectomized rats, *Endocrinology*. 140 (1999) 5780-5788.

10. U.T. Iwaniec, K.A. Magee, N.G. Mitova-Caneva, T.J. Wronski, Bone anabolic effects of subcutaneous treatment with basic fibroblast growth factor alone and in combination with estrogen in osteopenic ovariectomized rats, *Bone*. 33 (2003) 380-386.

11. S. Pun, C.L. Florio, T.J. Wronski, Anabolic effects of basic fibroblast growth factor in the tibial diaphysis of ovariectomized rats, *Bone*. 27 (2000) 197-202.

12. K. Yu, J. Xu, Z. Liu, D. Sosic, J. Shao, E.N. Olson, D.A. Towler, D.M. Ornitz, Conditional inactivation of FGF receptor 2 reveals an essential role for FGF signaling in the regulation of osteoblast function and bone growth, *Development*. 130 (2003) 3063-3074.

13. P.J. Marie, Fibroblast growth factor signaling controlling osteoblast differentiation, *Gene*. 316 (2003) 23-32.

14. A. Montero, Y. Okada, M. Tomita, M. Ito, H. Tsurukami, T. Nakamura, T. Doetschman, J.D. Coffin, M.M. Hurley, Disruption of the fibroblast growth

factor-2 gene results in decreased bone mass and bone formation, *J. Clin. Invest.* 105 (2000) 1085-1093.

15. H.P. Gerber, T.H. Vu, A.M. Ryan, J. Kowalski, Z. Werb, N. Ferrara, VEGF couples hypertrophic cartilage remodeling, ossification and angiogenesis during endochondral bone formation, *Nat. Med.* 5 (1999) 623-628.

16. E. Zelzer, W. McLean, Y.S. Ng, N. Fukai, A.M. Reginato, S. Lovejoy, P.A. D'Amore, B.R. Olsen, Skeletal defects in VEGF(120/120) mice reveal multiple roles for VEGF in skeletogenesis. *Development.* 129 (2002) 1893-1904.

17. C. Maes, P. Carmeliet, K. Moermans, I. Stockmans, N. Smets, D. Collen, R. Bouillon, G. Carmeliet, Impaired angiogenesis and endochondral bone formation in mice lacking the vascular endothelial growth factor isoforms VEGF164 and VEGF188, *Mech. Dev.* 111 (2002) 61-73.

18. A.M. Ryan, D.B. Eppler, K.E. Hagler, R.H. Bruner, P.J. Thomford, R.L. Hall, G.M. Shopp, C.A. O'Neill, Preclinical safety evaluation of rhuMAbVEGF, an antiangiogenic humanized monoclonal antibody, *Toxicol Pathol.* 27 (1999) 78-86.

19. M. Ichigatani, T. Saga, K. Yamaki, M. Yoshizuka, Appearance of vascular endothelial growth factor (VEGF) in femoral head in the growing rat, *Histol Histopathol.* 16 (2001) 463-468.

20. A. Horner, S. Bord, A.W. Kelsall, N. Coleman, J.E. Compston, Tie2 ligands angiopoietin-1 and angiopoietin-2 are coexpressed with vascular endothelial cell growth factor in growing human bone, *Bone.* 28 (2001) 65-71.

21. T. Pufe, K.E. Scholz-Ahrens, A.T. Franke, W. Petersen, R. Mentlein, D. Varoga, B. Tillmann, J. Schrezenmeir, C.C. Gluer, The role of vascular endothelial growth

factor in glucocorticoid-induced bone loss: evaluation in a minipig model, *Bone.* 33 (2003) 869-876.

22. S. Mekraldi, M.H. Lafage-Proust, S. Bloomfield, C. Alexandre, L. Vico, Changes in vasoactive factors associated with altered vessel morphology in the tibial metaphysis during ovariectomy-induced bone loss in rats, *Bone.* 32 (2003) 630-641.

23. J. Street, M. Bao, L. deGuzman, S. Bunting, F.V. Peale Jr., N. Ferrara, H. Steinmetz, J. Hoeffel, J.L. Cleland, A. Daugherty, N. van Bruggen, H.P. Redmond, R.A. Carano, E.H. Filvaroff, Vascular endothelial growth factor stimulates bone repair by promoting angiogenesis and bone turnover, *Proc. Natl. Acad. Sci. U S A.* 99 (2002) 9656-9661.

24. T. Pufe, B. Wildemann, W. Petersen, R. Mentlein, M. Raschke, G. Schmidmaier, Quantitative measurement of the splice variants 120 and 164 of the angiogenic peptide vascular endothelial growth factor in the time flow of fracture healing: a study in the rat, *Cell Tissue Res.* 309 (2002) 387-392.

25. J. Tombran-Tink, C.J. Barnstable, Osteoblasts and osteoclasts express PEDF, VEGF-A isoforms, and VEGF receptors: possible mediators of angiogenesis and matrix remodeling in the bone, *Biochem. Biophys. Res. Commun.* 316 (2004) 573-579.

26. A.M. Parfitt, The mechanism of coupling: A role for the vasculature, *Bone.* 26 (2000) 319-323.

27. S. Bain, N.S. Ramamurthy, T. Impeduglia, S. Scolman, L.M. Golub, Rubin C, Tetracycline prevents trabecular bone loss and maintains near-normal rates of bone formation in streptozotocin diabetic rats, *Bone.* 21 (1997) 147-153.

28. J. Yang, S.M. Pham, D.L. Crabbe, High-resolution Micro-CT evaluation of mid- to long-term effects of estrogen deficiency on rat trabecular bone, *Acad. Radiol.* 10 (2003) 1153-1158.

29. A. Laib, J.L. Kumer, S. Majumdar, N.E. Lane,The temporal changes of trabecular architecture in ovariectomized rats assessed by MicroCT, *Osteoporos. Int.* 12 (2001) 936-941.

30. P. Ammann, R. Rizzoli, D. Slosman, J.P. Bonjour, Sequential and precise in vivo measurement of bone mineral density in rats using dual-energy x-ray absorptiometry, *J. Bone Miner. Res.* 7 (1992) 311-316.

31. A.C. Maurin, P.M. Chavassieux, E. Vericel, P.J. Meunier, Role of polyunsaturated fatty acids in the inhibitory effect of human adipocytes on osteoblastic proliferation, *Bone.* 31 (2002) 260-266.

32. T. Nakamura, K. Hanada, M. Tamura, T. Shibanushi, H. Nigi, M. Tagawa, S. Fukumoto, T. Matsumoto, Stimulation of endosteal bone formation by systemic injections of recombinant basic fibroblast growth factor in rats, *Endocrinology.* 136 (1995) 1276-1284.

33. M.T. Engsig, Q.J. Chen, T.H. Vu, A.C. Pedersen, B. Therkidsen, L.R. Lund, K. Henriksen, T. Lenhard, N.T. Foged, Z. Werb, J.M. Delaisse, Matrix metalloproteinase 9 and vascular endothelial growth factor are essential for osteoclast recruitment into developing long bones, *J. Cell. Biol.* 151 (2000) 879-889.

34. K. Henriksen, M. Karsdal, J.M. Delaisse, M.T. Engsig, RANKL and vascular endothelial growth factor (VEGF) induce osteoclast chemotaxis through an ERK1/2-dependent mechanism, *J. Biol. Chem.* 278 (2003) 48745-48753.

35. M. Nakagawa, T. Kaneda, T. Arakawa, S. Morita, T. Sato, T. Yomada, K. Hanada, M. Kumegawa, Y. Hakeda, Vascular endothelial growth factor (VEGF) directly enhances osteoclastic bone resorption and survival of mature osteoclasts, *FEBS Lett.* (2000) 473(2):161-4.

36. S. Niida, M. Kaku, H. Amano, H. Yoshida, H. Kataoka, S. Nishikawa, K. Tanne, N. Maeda, S. Nishikawa, H. Kodama, Vascular endothelial growth factor can substitute for macrophage colony-stimulating factor in the support of osteoclastic bone resorption, *J. Exp. Med.* 190 (1999) 293-298.

37. I. Kodama, S. Niida, M. Sanada, Y. Yoshiko, M. Tsuda, N. Maeda, K. Ohama, Estrogen regulates the production of VEGF for osteoclast formation and activity in op/op mice, *J. Bone Miner. Res.* 19 (2004) 200-206.

GENERAL DISCUSSION & FUTURE STUDIES

The work presented in this dissertation has contributed to the development of bisphosphonate (BP)-mediated protein targeting to bone as well improved our understanding of the effects of parathyroid hormone (1-34) [PTH(1-34)] administration elicit on the skeletal tissues of ovariectomized rats. Moreover, it also represents the foundation for numerous additional studies to further expand upon our knowledge in the fields of drug targeting and bone tissue engineering.

Based on their high affinity for bone mineral, it was initially postulated that BP conjugation would confer an increase in protein affinity for bone; thus resulting in a corresponding increase in protein targeting to skeletal tissue, and a corollary decrease in in extra-skeletal distribution upon systemic administration. Due to the BP-mediated increase in targeting efficiency, it was also expected that a similar biological effect could be elicited by using a reduced dose relative to unmodified protein. Ultimately, a reduction in the side-effects produced upon drug administration is expected due to the decrease in the dose administered and non-skeletal distribution. In addition to enabling protein targeting, BP conjugation is also expected to improve protein retention at the site of localization (i.e. bone mineral). This is thought to improve drug efficacy-- as a correlation was recently demonstrated between an osteogenic protein's retention (i.e. mean residence time) at the site of application and its osteoinductivity *in vivo* (1). Alll together, the conjugation of BPs onto proteins is expected to afford spatial (i.e. targeting) and temporal (i.e. retention) properties, both of which should culminate in increased protein performance.

Initially, conjugation of 1-amino-1,1-diphosphonate methane (aminoBP) directly onto a protein's lysine amino acid residues through the use of an SMCC-based chemistry

was proposed by Uludag *et al.* (2). Due to the distinct possibility that this particular approach may alter the protein's pharmacophore and thus its inherent bioactivity, a novel method of conjugating aminoBP onto the carbohydrate moieties of glycoproteins was described in **CHAPTER II**. Given the aminoBP-dependent increase in fetuin's affinity for hydroxyapatite (HA) *in vitro*, the capacity of both the SMCC- and MMCCH-based fetuin conjugates to localize to bone was determined *in vivo*. While aminoBP conjugation increased the relative affinity of both lysozyme and bovine serum albumin to bone upon parenteral administration in previous studies (3), aminoBP conjugation (using either chemistry) did not do so for bovine fetuin **(CHAPTER IV)**. This lack of aminoBP-mediated targeting may be due to several reasons including the aminoBP-fetuin conjugates forming "calciprotein particles" (4) resulting in their increased susceptibity to the liver and spleen relative to unmodifed fetuin, and/or an increase in susceptibity to asialoglycoprotein receptor-mediated hepatic uptake of the fetuin conjugate. Regardless, it is now believed that the success of aminoBP-mediated protein targeting is thought to be protein-specific. To elucidate this possibility, further characterization of other aminoBP-proteins will most likely be required *in vivo*. For this a library of aminoBP-protein conjugates should be developed based on protein physicochemical properties (e.g. size, isoelectric point, state of glycosylation and/or lipidation) to assess which of these properties affect BP-mediated conjugate binding. This may enable the identification of several parameters that will predict the suitability of BP-conjugation to target a given protein to bone.

As another means to potentially predict the binding capacity of conjugates, **CHAPTER III** introduces the concept of *in silico* characterization. In this study, only the

conjugate pendant ligand could be simulated using Molecular Dynamics (MD). Using this software, a proportional relationship was identified between the capacity of the conjugates to bind to HA and the maximal probability/radial density of their pendent ligand. The latter parameter being inversely proportional to tether length. By increasing the capacity of the existing computational system, MD simulations of an entire BP-protein conjugate may facilitate the investigation of various issues including: the effects that charged amino acid moieties adjacent to a linkage site on BP-mediated HA binding; and the effects of modulating the spatial orientation of conjugated BPs on HA binding. Future MD studies should also introduce virtual HA surfaces to further assess conjugate-HA binding *in silico*, as well as enable simulations of conjugate binding to HA in the presence of ions and other proteins that may affect conjugate binding. These studies serve as the foundation for developing a theoretical approach to predicting the biodistribution of conjugates *in vivo*.

To optimize conjugate affinity for bone mineral, other BPs apart from aminoBP should also be considered. As they contain primary amine groups, alendronate and pamidronate are suitable candidates to undergo either SMCC- or MMCCH-based BP conjugation. In addition, novel, multimeric bisphosphonate moieties, such as di(bisphosphonate), tetra(bisphosphonate), and octa(bisphosphonate), should also be considered. By virtue of their dense phosphonate densities, conjugation with these BPs should theoretically improve protein affinity for HA over current aminoBP conjugates. Ideally, the use of such ligands should reduce the total number of conjugated BPs to impart sufficient bone mineral affinity onto a protein—resulting in a decrease in the likelihood of adversely affecting protein bioactivity upon BP conjugation.

As aminoBPs have only been conjugated onto model proteins (e.g. albumin, fetuin, lysozyme), BP conjugation onto biologically-active, osteogenic proteins should be done to determine whether these proteins are suitable for aminoBP conjugation. Suitable candidates include basic fibroblast growth factor (bFGF) and members of the bone morphogenetic protein (BMP) family such as BMP-2, BMP-4, and BMP-7. Pharmacokinetic and subsequent pharmacodynamic studies will determine whether BP conjugation can improve an osteogenic protein's therapeutic window by eliciting an anabolic response in bone without increasing the incidence of side effects associated with its parenteral administration. Additional studies should also assess the feasibility of using osteogenic growth factor conjugates in an animal model for fracture repair. This would help to elucidate whether BP conjugation can mediate an increase in protein retention at the site of injury; and whether this increase in retention would enable osteogenic protein conjugates to enhance the endogenous process of fracture repair.

The study described in **CHAPTER V** introduces the concept of conjugating BPs onto a drug carrier, such as heparin, to develop a drug delivery system that can enhance the bone mineral affinity of osteogenic growth factors without modifying the growth factor directly. A potential concerns associated with the use of this heparin-based drug delivery system is the anti-coagulating effects that the modified heparin may elicit upon parenteral administration. Before assessing this possibility, however, it is imperative to establish: (i) whether aminoBP modification affects heparin's inherent ability to bind to anti-thrombin III; (ii) the optimal ratio of aminoBP-heparin-conjugate:bFGF for efficient protein targeting/retention *in vivo*; and (iii) the dose of bFGF (once co-administered with the aminoBP-heparin conjugate) required for an anabolic response in rats. Prior to even

conducting these particular experiments, further studies need to be conducted to determine whether this system is capable of increasing the retention of heparin-binding osteogenic growth factors to HA-based implants both *in vitro*, as well as in an implantation animal model (as was used in **CHAPTER IV**). Based on these findings, the capacity of this drug delivery system to increase growth factor targeting to bone should be assessed upon parenteral administration. As above, the effects of modulating tether length, and the use of other bisphosphonates should also be determined to facilitate optimization of this system. The development of other potential growth factor delivery systems (e.g. conjugation of BP onto an antibody for a specific osteogenic protein) should also be considered.

Despite the numerous benefits that would be afforded by protein targeting via direct BP conjugation or the heparin-BP drug delivery system, however, several general considerations must be taken into account (e.g. (i) conjugate immunogenicity; (ii) conjugate targeting to calcified, non-boney tissues; (iii) effect of disease state on conjugate targeting). As is true for the administration of most exogenous proteins, a primary concern associated with the administration of BP-modified proteins is the immunological response they may elicit *in vivo*. Although a multitude of factors affect a protein's immunogenicity (e.g. route of administration, frequency of administration, an individual's genetic background, disease state, etc.), it is generally thought that the more divergent an exogenous protein is from its endogenous counterpart, the more of an immunogenic response it will likely mediate (**5**). Thus, it is expected that the conjugation of BPs onto a given protein may subsequently result in an increase in its immunogenicity, which may not only affect its pharmacokinetics but also its pharmacodynamic properties

(i.e. osteogenic activity). It is likely, however, that the possible incidence of allergic/immunological side-effects associated with conjugate administration will have to be noted not only on a protein-to-protein basis, but also on a subject-to-subject basis.

For indications requiring the systemic administration of BP-based conjugates (e.g. osteoporosis), disease state was initially expected to influence both protein targeting and retention; as the increase in bone remodeling frequency associated in post-menopausal osteoporosis, for example, provides an increase in the amount of exposed hydroxyapatite (HA) surface for BP interactions. While this should afford improved protein targeting, retention may be adversely affected by the increase in remodeling (as release of BPs, and thus possibly BP-protein conjugates, from the mineralized extracellular matrix of bone is thought to be dependent on bone turnover (**6**)). As demonstrated in Uludag *et al.* (**3**), however, no differences were seen between the targeting efficiency of bovine serum albumin-BP conjugates when administered intravenously in either normal or ovariectomized rats. Further studies will have to be conducted to determine the effect of various disease states on conjugate targeting and retention.

The possibility of targeting to calcified, non-boney tissues, such as calcified collagenous tissues, as well as calcified tissues associated with the pathogenesis of atherosclerotic (fibrotic) calcification, medial artery calcification, cardiac valve calcification, and calciphylaxis (**8**) is an additional consideration relating to the use of BP-targeted proteins. As with all of the issues associated with BP targeting, further studies, which will specifically address these concerns, will be required to elucidate their significance.

As described in **CHAPTER VI**, weekly administration of low dose PTH (1-34) elicited an anabolic response in the skeletal tissue of OVX animals. Given the potential benefit shown with the weekly administration of PTH (1-34), additionally studies should be conducted to directly compare the effects modulating the dosing schedule (e.g. daily vs. weekly administration) on the anabolic effects this hormone elicits on bone. Such studies may have implications on the current dosing regimen of PTH (1-34) to osteopenic/osteoporotic individuals. Although the administration of PTH (1-34) is well-tolerated in humans (as side effects include nausea, headache, and transient hypercalcemia) (**9**), this peptide could still be a suitable candidate for BP-conjugation. Its targeting to bone may not only reduce the incidents of the listed side effects, but may also reduce the dose required to exhibit an anabolic effect. Because of the significant cost of treatment with PTH (1-34) for post-menopausal osteoporosis (**9**), a reduction in total drug administered may also result in a substantial cost savings.

The study presented in **CHAPTER VII** was the first to examine the effects of parenteral vascular endothelial growth factor (VEGF) administration on systemic bone regeneration. As these results were inconclusive, the study should be repeated using larger sample sizes, as well as higher doses of growth factor. Such a study would help clarify VEGF's role in the pathogenesis of osteoporosis; and may provide the rationale for pursuing the development of VEGF-modulating agents that may attenuate or even reverse the progression of this disease. Much like PTH (1-34), these proteinacious drugs may also be suitable candidates for BP-mediated targeting.

REFERENCES

1. H. Uludag, D. D'Augusta, J. Golden, J. Li, G. Timony, R. Riedel, J.M. Wozney, Implantation of recombinant human bone morphogenetic proteins with biomaterial carriers: A correlation between protein pharmacokinetics and osteoinduction in the rat ectopic model, *J. Biomed. Mater Res.* 50 (2000) 227-238.

2. H. Uludag, N. Kousinioris, T. Gao, D. Kantoci, Bisphosphonate conjugation to proteins as a means to impart bone affinity, *Biotechnol. Prog.* 16 (2000) 258-267.

3. H. Uludag, J. Yang, Targeting systemically administered proteins to bone by bisphosphonate conjugation, *Biotechnol. Prog.* 18 (2002) 604-611.

4. A. Heiss, A. DuChesne, B. Denecke, J. Grotzinger, K. Yamamoto, T. Renne, W. Jahnen-Dechent, Structural basis of calcification inhibition by alpha 2-HS glycoprotein/fetuin-A. Formation of colloidal calciprotein particles, *J. Biol. Chem.* 278 (2003) 13333-13341.

5. Structural basis of calcification inhibition by alpha 2-HS glycoprotein/fetuin-A. Formation of colloidal calciprotein particles, *J. Biol. Chem.* 278 (2003) 13333-13341.

6. H. Schellekens, Immunogenicity of therapeutic proteins: clinical implications and future prospects, *Clin. Ther.* 24 (2002) 1720-1740.

7. H. Hirabayashi, J. Fujisaki, Bone-specific drug delivery systems: approaches via chemical modification of bone-seeking agents, *Clin. Pharmacokinet.* 42 (2003) 1319-1330.

8. R. Vattikuti, D.A Towler, Osteogenic regulation of vascular calcification: an early perspective, *Am. J. Physiol. Endocrinol. Metab.* 286 (2004) E686-E696.

9. K.A. Cappuzzo, J.C. Delafuente, Teriparatide for severe osteoporosis, *Ann. Pharmacother.* 38 (2004) 294-302.

APPENDICES

APPENDIX A

Protein-Based Therapeutic Agents that Can Potentially Be Targeted for Diseases Affecting Bone

In addition to osteoporosis, targeting proteins to bone may be a suitable approach in the treatment of numerous other skeletal diseases. Despite being characterized by complex etiologies (1), the underlying basis of most of these disorders can be traced to aberrant behavior of cellular components residing in the skeletal system. The cells include the heterogeneous population of multipotent cells in bone marrow, as well as the specialized bone-forming osteoblast cells and bone-resorbing osteoclast cells. To normalize aberrant cell activity, potential therapeutic strategies revolve around modulating the pathogenic activity directly (e.g., inhibiting enzymatic activity directly responsible for osteolytic activity) or attenuating the pathological stimulus involved in eliciting the untoward behavior (e.g., regulatory molecules giving rise to osteolytic cells). Proteins are ideal therapeutic agents for alleviating such cellular behaviour since these activities are readily modulated by protein-based endogenous signaling mechanisms. The metabolism and excretion of proteins can also be performed by endogenous pathways responsible for protein catabolism, unlike synthetic entities whose transformation and bodily accumulation are not readily predictable. However, a significant drawback of the utilization of proteins in a therapeutic capacity is that their cellular receptors are typically found ubiquitously in more than one physiological system. Consequently, administration of a given protein is likely to act on several tissues at once.

Major diseases that affect bone tissue are osteoporosis, multiple myeloma, bone metastasis, and rheumatoid arthritis. Summarized in **Tables A-1** to **A-3** are protein-based therapeutic options for these diseases. The potential of the proteins listed were identified

based on data from *in vitro* cell culture systems, preclinical animal models, and clinical settings. Despite the inherent complexity associated with the biochemical cascade(s) responsible for disease pathogenesis, the administration of a single protein resulted in a significant benefit in the indicated system. The proteins can exert their effects directly, antagonize the undesired activity of a pathogenic protein[1] (and thus the underlying pathogenic cascade), or elicit a cellular response that counters the effects of the disease. As it is rationalized that the administration of these proteins will *primarily* result in the modulation of cellular activity, it is expected that each of these strategies will culminate in the normalization of the disease. Therefore, the proteins can be classified as "disease-modifying proteinaceous drugs" (DMPDs). In certain instances, DMPD administration may lead to reversal of disease, while in others, administration will simply attenuate the progression of disease. As BP-mediated targeting is designed primarily for the extracellular targeting of proteins to skeletal tissue, intracellular protein targets, although potentially viable options, have not been considered in this summary.

A. Osteoporosis

To circumvent the imminent dangers associated with the compromized skeletal integrity, there are two distinct strategies that may be employed to restore the balance between osteoclast and osteoblast activity: a reduction in osteoclast activity or an elevation of osteoblast activity. Both strategies have previously been employed to attenuate the progression of the disease. While osteoprotegerin (8-13) and calcitonin (14-16) and have

[1] As identified as "Anti-X" in the table, means of attenuating a pathogenic protein's activity include administration of: (i) an antibody specific for the protein (i.e. a neutralizing antibody); (ii) an antibody specific for the protein's receptor; (iii) a soluble form of the protein's receptor; (iv) a protein's endogenous inhibitor; or (v) a classic antagonist to block its receptor.

sucessfully been used to inhibit osteoclast activity, several hormones and growth factors were capable of enhancing bone formation in some capacity by inducing osteoblast proliferation, differentiation, and/or stimulating osteoblast activity. As indicated in **Table 1-1**, the anabolic approach is promising in that the DMPDs may offer an avenue to restore the lost bone, and possibly the "normal" micro-architecture (as in the case of PTH 1-34), to levels equivalent to those seen prior to the onset of osteoporosis. Anti-resorptive agents will be also beneficial for situations where excessive resorption affects the bone tissues, such as the glucocorticoid-induced osteoporosis, Paget's disease and osteoarthritis. Many of the osteogenic proteins listed in **Table 1-1** would also be appropriate for enhancing the endogenous process of fracture repair by increasing the amount of bone deposited, while reducing healing time, as well as the incidence of non-union. In this case, local administration of BP-conjugates at the site of fracture would increase the mean residence time of the osteogenic conjugates; which would ulitmately result in augment their biological effect **(2)**.

B. Multiple Myeloma

Affecting 15,000 new patients a year in the US, multiple myeloma (MM) is an incurable disease of malignant differentiated B lymphocytes localized exclusively in bone marrow **(3,4)**. In addition to renal failure and compromised immune system, this neoplasia is clinically characterized by the presence of osteolytic lesions, and bone fractures due to excessive osteolytic activity **(3)**. Given that MM cells are responsible for expressing chemokines believed to induce osteoclast-mediated bony lesions, the majority of the interventional strategies involved directly inhibiting their activity **(Table A-1)**. The

anabolic proteins insulin-like growth factor (IGF)-1 and several BMP's (see **Table 1-1**) were shown to mitigate MM cell activity, so that these DMPDs may also serve to promote the regeneration of bone tissue in addition to directly ameliorating the MM.

C. Bone Metastasis

Depending on the aggressiveness of the primary tumor, advanced cases of breast and prostate neoplasms almost invariably metastasize to bone (**38**). Although traditional dogma suggests that the former neoplasm typically induces formation of osteolytic lesions while the latter neoplasms typically yield osteosclerotic lesions, recent evidence suggests that the preponderance of bone metastasis is both osteolytic and osteosclerotic in nature (**38**). Preclinical studies investigating the effects of a particular DMPD, however, have only used animal models of bone metastasis that were exclusively either osteolytic or osteosclerotic in nature (**Table A-2**). Nevertheless, the reported therapies were effective in abrogating the effects of metastasis on the overall integrity of bone. Targeting anti-neoplastic agents to bone, however, is not expected to treat the underlying cause of disease. Consequently, efforts to eradicate the primary extra-skeletal tumor need to be addressed in this strategy.

D. Rheumatoid Arthritis

Being a chronic immuno-inflammatory disease, rheumatoid arthritis (RA) culminates in destruction of cartilage and subchondral bone, and affects up to 1% of the population in the industrialized world (**55**). Given the significant progress made in elucidating the biochemical cascade involved in mediating the pathogenesis of RA, numerous proteins

have been potential targets against the progression of disease (**Table A-3**). The majority of the DMPDs target cytokines that mediate the aberrant inflammation process. Several of these DMPD have been approved by regulatory bodies for RA treatment and these include infliximab and adalimumab, anti-TNF-α monoclonal antibodies, as well as etanercept, a fusion protein containing the ligand-binding portion of the TNF-α receptor (**107**). Because the inflammation process is significantly elevated at disease sites, as compared to the rest of the body, these agents readily exhibit a beneficial effect without targeting the DMPD to bone sites. Bone targeting is expected to further improve the efficacious dose for the clinically available agents by elevating the local joint concentration of the drug at a given administration dose. If the effects of a protein at non-diseased sites are not acceptable for clinical application, bone targeting will enable clinical entry by eliminating these unacceptable side effects due to reduced distribution to extra-skeletal sites.

Table A-1. Protein-Based Therapeutic Agents for Treatment of Multiple Myeloma

Protein	Rationale	Reference
Anti-IGF-1 Ab	IGF-1 is involved in the growth, trafficking, and survival of MM cells *in vitro*. This activity was completely inhibited by an anti-IGF-1 receptor antibody.	5
TRAIL/Apo2L	While sparing normal cells, TRAIL/Apo2L induces caspase-mediated myeloma cell apoptosis *in vitro* and *in vivo*.	6-8
Anti-VEGF Ab	VEGF induced proliferation and migration of MM cells *in vitro*. This activity was diminished with an anti-VEGF antibody.	9-13
Anti-TNF-α Ab	TNF-α, an osteoclastic cytokine, was shown to promote the growth and survival of MM cells through the up-regulation of IL-6 synthesis. Administration of TNF-α neutralizing antibodies decreased the survival of human myeloma cell lines *in vitro*.	14,15
OPG	OPG administration clinically to patients with myeloma bone disease resulted in a dramatic decrease in biochemical markers of bone turnover due to a reduction in the formation of osteoclasts.	16-24
Anti-MIP-1α Ab	The expression of MIP-1α, an osteoclastogenic chemokine, was upregulated in MM cells. Administration of anti-MIP-1α antibodies reduced the number of osteolytic lesions in an *in vivo* murine model of MM.	25-31
Anti-$\alpha_4\beta_1$ integrin Ab	$\alpha_4\beta_1$ integrins expressed on MM cells interacts with and promotes development of osteoclasts. Administration of anti-$\alpha_4\beta_1$ antibodies suppressed myeloma cell-mediated formation and activity of osteoclasts generated in co-cultures of myeloma and bone marrow cells *in vitro*.	32,33
BMP-2	BMP-2 induced apoptosis in both primary human MM cells and numerous MM cell lines *in vitro*.	34,35
BMP-4	BMP-4 inhibited cell proliferation and survival in several MM cell lines *in vitro*.	36,37
BMP-5-BMP-7	BMPs decreased cell proliferation and induced apoptosis in primary human myeloma cell *in vitro*.	37

Abbreviations: Antibody (Ab); Apo2 Ligand (Apo2L); Bone Morphogenetic Protein (BMP); Insulin-like Growth Factor (IGF) –1; Interleukin (IL); Macrophage Inflammatory Protein (MIP); Osteoprotegerin (OPG); Tumor Necrosis Factor-Related Apoptosis-Inducing Ligand (TRAIL); Tumor Necrosis Factor (TNF); Vascular Cell Adhesion Molecule (VCAM); Vascular Endothelial Growth Factor (VEGF).

Table A-2. Protein-Based Therapeutic Agents for Treatment of Bone Metastasis

Protein	Rationale	Reference
Angiostatin	Angiostatin inhibited breast cancer-induced osteolysis by hindering osteoclast activity *in vitro* and *in vivo*.	39
Anti-PTHrP Ab	PTHrP produced from breast cancer metastasis promoted osteoclastic bone resorption. Antibodies to PTHrP lowered the number of metastastic tumor area, as well as the size/number of osteolytic lesions in animal models of breast and lung metastasis.	40-42
Anti-TGF-β Receptor	In a vicious cycle, osteoclast-derived TGF-β perpetuates the expression of tumor-derived PTHrP. In a murine model of breast cancer metastasis, administration of breast cancer cells, in which TGF-β type II receptor had been knocked out, resulted in smaller tumor foci and less cortical and trabecular bone destruction than constitutively-expressing TGF-β type II receptor.	43-45
OPG	Osteoblast RANKL expression is required for osteoclast-mediated bone resorption. By eradicating tumor-associated osteoclasts, OPG administration the decreased size and number of osteolytic lesions in a murine model of breast cancer metastasis.	34, 46-49
Anti-PDGF Ab	Increased tumor-expression of PDGF in breast cancer patients was associated with metastasis and poor prognosis clinically. Neutralization of its activity by an antibody decreased new bone formation *in vitro* and osteosclerotic lesions an animal model of breast cancer metastasis.	50
Anti-Endothelin-1	Endothelin-1, an osteoblastic mitogen, was implicated in osteosclerotic lesions associated with prostate cancer. Antagonism of its receptor (ET_A) by BQ-123, a cyclic peptide, inhibited osteoblast proliferation and new bone formation induced by breast cancer cells in a murine calvaria *in vitro* assay.	51-53
Anti-VEGFR Ab	Promoting angiogenesis and vessel permeability, VEGF was associated with tumor survival and metastasis. Administration of anti-VEGFR-2 antibody in a murine model of prostate cancer metastasis inhibited the growth of osteosclerotic lesions.	54

Abbreviations: Antibody (Ab); Endothelin A Receptor (ET_A); Osteoprotegerin (OPG); Parathyroid Hormone-Related Protein (PTHrP); Platelet Derived Growth Factor (PDGF); Receptor Activator of Nuclear Factor KappaB (RANK); Receptor Activator of Nuclear Factor KappaB Ligand (RANKL); Transforming Growth Factor (TGF) –β; Tumor Necrosis Factor-Related Apoptosis-Inducing Ligand (TRAIL); Vascular Endothelial Growth Factor (VEGF); VEGF Receptor (VEGFR).

Table A-3. Protein-Based Therapeutic Agents for Treatment of Rheumatoid Arthritis

Protein	Rationale	Reference
OPG	Imbalance in the RANK/RANKL/OPG signaling pathway leads to characteristic peri-articular skeletal erosions associated with RA. Administration of OPG led to the preservation of bone and cartilage in several animal models of RA.	56-60
Anti-bFGF Ab	bFGF is believed to play a role in the progression of RA since it can stimulate osteoclastogenesis *in vitro*. Anti-bFGF antibodies inhibited osteoclastogenesis *in vitro* and lowered bone and joint destruction in an animal model of RA.	61, 62
Anti-VEGF Ab or VEGFR	VEGF-induced angiogenesis plays an integral role in the pathogenesis of RA. Parenteral administration of an anti-VEGF antibody or soluble VEGFR-1 was shown to prevent the erosion bone and cartilage in murine animal models of RA.	63-65
Anti-TNF-α Ab or TNFR	TNF-α plays an integral in regulation of inflammatory cytokines involved in the pathogenesis of RA. Several anti-TNF-α antibodies and soluble TNF-α receptors are approved for patient use (e.g. infliximab, etanercept and adalimumab) or are in various stages of clinical trials for treatment of RA.	66-72
IL-1 Receptor	IL-1 is a pro-inflammatory cytokines shown to play a critical role in pathogenesis of arthritis. Bone and cartilage destruction was attenuated by an anti IL-1 antibody. Anakinra, a recombinant form of an endogenous IL-1 receptor antagonist, is available for clinical use.	68,69,73-75
IL-4	IL-4 is an anti-inflammatory cytokine that inhibits the synthesis of pro-inflammatory cytokines. Systemic administration of IL-4 decreased bone and cartilage destruction associated with RA.	76-78
IL-6 Receptor	Although synovial levels of IL-6 correspond directly to disease activity and joint damage, its precise role in the pathogenesis of RA remains controversial. Several clinical trials have suggested significant improvements of RA with soluble IL-6R administration.	79-82
Soluble gp130	Recent evidence suggests that IL-6 bound to soluble IL-6R may actually be responsible for eliciting the effects previously attributed to IL-6. Administration of IL-6R's natural antagonist, soluble gp130, inhibited the RA progression in a murine model of arthritis.	82
IL-10	IL-10 is a pleiotropic cytokine that suppresses the expression of pro-inflammatory IL-1 and TNF-α. Intraperitoneal administration of IL-10 suppressed RA progression in a murine model (especially when administered in combination with either IL-4 or anti-TNF-α antibodies).	78, 83
IL-11	Although chondrocyte-derived IL-11 stimulates osteoclast activity, it also up-regulates expression TIMPs while down-regulating production of nitric oxide and expression of MIP-α. Administration of IL-11 reduced extent of joint destruction in a murine RA model.	84
Anti-IL-12 Ab	IL-12 promotes Th1 T-cell-mediated immunological responses as well as up-regulates the expression of interferon-γ. Administration of anti-IL-12 antibody decreased paw thickness as well as the clinical score of disease severity (synergistically with anti-TNF-α antibody administration) in murine models of RA.	71,85
Anti-IL-17 or	Through modulating RANKL expression, IL-17 enhances osteoclastogenesis and bone erosion *in vivo*.	86,87

IL-17R	Administration of either soluble IL-17 receptor or anti-IL-17 antibody to RA bone explants from patients inhibited the destruction of bone *in vitro*.	
Anti-IL-18 Ab	IL-18 up-regulates production of pro-inflammatory cytokines and cyclooxygenase-2 expression. It's inhibition via the administration of either anti-IL-18 antibody or recombinant human IL-18 binding protein decreased inflammation and cartilage degradation *in vivo*.	**88-90**
Anti-PECAM-1 Ab	PECAM-1 plays a role in the migration of leukocytes to inflamed synovium. Administration of anti-PECAM antibodies prevented joint destruction in a murine model of RA.	**91**
Anti-ICAM-1 Ab	ICAM-1 facilitates leukocyte extravasation into the synovium. Therapy with an anti-ICAM-1 antibody improved the clinical outcome of the disease.	**92-94**
Endostatin	The inhibition of pannus formation and bone destruction was observed upon the administration of endostatin, an anti-angiogenic cytokine, in murine models of RA.	**95,96**

Abbreviations: Antibody (Ab); Basic Fibroblast Growth Factor (bFGF); Glycoprotein 130 (gp130); Intercellular Adhesion Molecule (ICAM); Interleukin (IL); Osteoprotegerin (OPG); Platelet Endothelial Cell Adhesion Molecule (PECAM); Receptor Activator of Nuclear Factor KappaB (RANK); Receptor Activator of Nuclear Factor KappaB Ligand (RANKL); Tissue Inhibitors of Metalloproteinases (TIMPs); Tumor Necrosis Factor-Related Apoptosis-Inducing Ligand (TRAIL); Tumor Necrosis Factor (TNF); TNF Receptor (TNFR); Vascular Cell Adhesion Molecule (VCAM); Vascular Endothelial Growth Factor (VEGF); VEGF Receptor (VEGFR).

References

1. S.A. Gittens, H. Uludag, Growth factor delivery for bone tissue engineering, *J. Drug Targeting.* 9 (2001) 407-429.

2. H. Uludag, D. D'Augusta, J. Golden, J. Li, G. Timony, R. Riedel, J.M. Wozney. Implantation of recombinant human bone morphogenetic proteins with biomaterial carriers: A correlation between protein pharmacokinetics and osteoinduction in the rat ectopic model. *J. Biomed. Mater. Res.* 50 (2000) 227-238.

3. G.D. Roodman, Role of the bone marrow microenvironment in multiple myeloma, *J Bone Miner Res.* 17 (2002) 1921-1925.

4. T. Hideshima, P. Richardson, K.C. Anderson, Novel therapeutic approaches for multiple myeloma, *Immunol. Rev.* 194 (2003) 164-176.

5. N.L. Ge, S. Rudikoff, Insulin-like growth factor I is a dual effector of multiple myeloma cell growth, *Blood.* 96 (2000) 2856-2861.

6. N. Mitsiades, C.S. Mitsiades, V. Poulaki, K.C. Anderson, S.P. Treon, Intracellular regulation of tumor necrosis factor-related apoptosis-inducing ligand-induced apoptosis in human multiple myeloma cells, *Blood.* 99 (2002) 2162-2171.

7. C.S. Mitsiades, S.P. Treon, N. Mitsiades, Y. Shima, P. Richardson, R. Schlossman, T. Hideshima, K.C. Anderson, TRAIL/Apo2L ligand selectively induces apoptosis and overcomes drug resistance in multiple myeloma: therapeutic applications, *Blood.* 98 (2001) 795-804.

8. C.M. Shipman, P.I. Croucher, Osteoprotegerin is a soluble decoy receptor for tumor necrosis factor-related apoptosis-inducing ligand/Apo2 ligand and can

function as a paracrine survival factor for human myeloma cells, *Cancer Res.* 63 (2003) 912-916.

9. T. Wrobel, G. Mazur, P. Surowiak, P. Dziecedilgiel, L. Usnarska-Zubkiewicz, K. Kuliczkowski, Increased expression of vascular endothelial growth factor in bone marrow of multiple myeloma patients, *Eur. J. Intern. Med.* 14 (2003) 98-100.

10. K. Podar, Y.T. Tai, F.E. Davies, S. Lentzsch, M. Sattler, T. Hideshima, B.K. Lin, D. Gupta, Y. Shima, D. Chauhan, C. Mitsiades, N. Raje, P. Richardson, K.C. Anderson, Vascular endothelial growth factor triggers signaling cascades mediating multiple myeloma cell growth and migration, *Blood.* 98 (2001) 428-435.

11. R. Ria, A.M. Roccaro, F. Merchionne, A. Vacca, F. Dammacco, D. Ribatti, Vascular endothelial growth factor and its receptors in multiple myeloma, *Leukemia.* 17 (2003) 1961-1916.

12. S. Kumar, T.E. Witzig, M. Timm, J. Haug, L. Wellik, R. Fonseca, P.R. Greipp, S.V. Rajkumar, Expression of VEGF and its receptors by myeloma cells, *Leukemia.* 17 (2003) 2025-2031.

13. Vacca, R. Ria, D. Ribatti, F. Semeraro, V. Djonov, F. Di Raimondo, F. Dammacco, A paracrine loop in the vascular endothelial growth factor pathway triggers tumor angiogenesis and growth in multiple myeloma, *Haematologica.* 88 (2003) 176-185.

14. T. Hideshima, D. Chauhan, R. Schlossman, P. Richardson, K.C. Anderson, The role of tumor necrosis factor alpha in the pathophysiology of human multiple myeloma: therapeutic applications, *Oncogene.* 20 (2001) 4519-4527.

15. M. Jourdan, K. Tarte, E. Legouffe, J. Brochier, J.F. Rossi, B. Klein, Tumor necrosis factor is a survival and proliferation factor for human myeloma cells, *Eur. Cytokine Netw.* 10 (1999) 65-70.

16. P.M. Doran, R.T. Turner, D. Chen, S.M. Facteau, J.M. Ludvigson, S. Khosla, B.L. Riggs, S.J. Russell, Native osteoprotegerin gene transfer inhibits the development of murine osteolytic bone disease induced by tumor xenografts, *Exp. Hematol.* 32 (2004) 351-359.

17. O. Sezer, U. Heider, I. Zavrski, C.A. Kuhne, L.C. Hofbauer, RANK ligand and osteoprotegerin in myeloma bone disease, *Blood.* 101 (2003) 2094-2098.

18. K. Vanderkerken, E. De Leenheer, C. Shipman, K. Asosingh, A. Willems, B. Van Camp, P. Croucher, Recombinant osteoprotegerin decreases tumor burden and increases survival in a murine model of multiple myeloma, *Cancer Res.* 63 (2003) 287-289.

19. U. Heider, C. Langelotz, C. Jakob, I. Zavrski, C. Fleissner, J. Eucker, K. Possinger, L.C. Hofbauer, O. Sezer, Expression of receptor activator of nuclear factor kappaB ligand on bone marrow plasma cells correlates with osteolytic bone disease in patients with multiple myeloma, *Clin. Cancer Res.* 9 (2003) 1436-1440.

20. A.N. Farrugia, G.J. Atkins, L.B. To, B. Pan, N. Horvath, P. Kostakis, D.M. Findlay, P. Bardy, A.C. Zannettino, Receptor activator of nuclear factor-kappaB ligand expression by human myeloma cells mediates osteoclast formation in vitro and correlates with bone destruction in vivo, *Cancer Res.* 63 (2003) 5438-5445.

21. H. Libouban, M.F. Moreau, M.F. Basle, R. Bataille, D. Chappard, Increased bone remodeling due to ovariectomy dramatically increases tumoral growth in the 5T2 multiple myeloma mouse model, *Bone.* 33 (2003) 283-292.

22. E.M. Sordillo, R.N. Pearse, RANK-Fc: a therapeutic antagonist for RANK-L in myeloma, *Cancer*. 97 (2003) 802-812.

23. C. Seidel, O. Hjertner, N. Abildgaard, L. Heickendorff, M. Hjorth, J. Westin, J.L. Nielsen, H. Hjorth-Hansen, A. Waage, A. Sundan, M. Borset, Nordic Myeloma Study Group, Serum osteoprotegerin levels are reduced in patients with multiple myeloma with lytic bone disease, *Blood*. 98 (2001) 2269-2271.

24. J.J. Body, P. Greipp, R.E. Coleman, T. Facon, F. Geurs, J.P. Fermand, J.L. Harousseau, A. Lipton, X. Mariette, C.D. Williams, A. Nakanishi, D. Holloway, S.W. Martin, C.R. Dunstan, P.J. Bekker, A phase I study of AMGN-0007, a recombinant osteoprotegerin construct, in patients with multiple myeloma or breast carcinoma related bone metastases, *Cancer*. 97 (2003) 887-892.

25. B.O. Oyajobi, G.R. Mundy, Receptor activator of NF-kappaB ligand, macrophage inflammatory protein-1alpha, and the proteasome: novel therapeutic targets in myeloma, *Cancer*. 97 (2003) 813-817.

26. B.O. Oyajobi, G. Franchin, P.J. Williams, D. Pulkrabek, A. Gupta, S. Munoz, B. Grubbs, M. Zhao, D. Chen, B. Sherry, G.R. Mundy, Dual effects of macrophage inflammatory protein-1alpha on osteolysis and tumor burden in the murine 5TGM1 model of myeloma bone disease, *Blood*. 102 (2003) 311-319.

27. J.H. Han, S.J. Choi, N. Kurihara, M. Koide, Y. Oba, G.D. Roodman, Macrophage inflammatory protein-1alpha is an osteoclastogenic factor in myeloma that is independent of receptor activator of nuclear factor kappaB ligand, *Blood*. 97 (2001) 3349-3353.

28. E. Terpos, M. Politou, R. Szydlo, J.M. Goldman, J.F. Apperley, A. Rahemtulla, Serum levels of macrophage inflammatory protein-1 alpha (MIP-1alpha) correlate

with the extent of bone disease and survival in patients with multiple myeloma, *Br. J. Haematol.* 123 (2003) 106-109.

29. S. Uneda, H. Hata, F. Matsuno, N. Harada, Y. Mitsuya, F. Kawano, H. Mitsuya, Macrophage inflammatory protein-1 alpha is produced by human multiple myeloma (MM) cells and its expression correlates with bone lesions in patients with MM, *Br. J. Haematol.* 120 (2003) 53-55.

30. M. Abe, K. Hiura, J. Wilde, K. Moriyama, T. Hashimoto, S. Ozaki, S. Wakatsuki, M. Kosaka, S. Kido, D. Inoue, T. Matsumoto, Role for macrophage inflammatory protein (MIP)-1alpha and MIP-1beta in the development of osteolytic lesions in multiple myeloma, *Blood.* 100 (2002) 2195-2202.

31. S.J. Choi, Y. Oba, Y. Gazitt, M. Alsina, J. Cruz, J. Anderson, G.D. Roodman, Antisense inhibition of macrophage inflammatory protein 1-alpha blocks bone destruction in a model of myeloma bone disease. *J. Clin. Invest.* 108 (2001) 1833-1841.

32. Y.T. Tai, K. Podar, L. Catley, Y.H. Tseng, M. Akiyama, R. Shringarpure, R. Burger, T. Hideshima, D. Chauhan, N. Mitsiades, P. Richardson, N.C. Munshi, C.R. Kahn, C. Mitsiades, K.C. Anderson. Insulin-like growth factor-1 induces adhesion and migration in human multiple myeloma cells via activation of beta1-integrin and phosphatidylinositol 3'-kinase/AKT signaling. *Cancer Res.* 63 (2003) 5850-5858.

33. T. Michigami, N. Shimizu, P.J. Williams, M. Niewolna, S.L. Dallas, G.R. Mundy, T. Yoneda, Cell-cell contact between marrow stromal cells and myeloma cells via VCAM-1 and alpha(4)beta(1)-integrin enhances production of osteoclast-stimulating activity, *Blood.* 96 (2000) 1953-1960.

34. C. Kawamura, M. Kizaki, Y. Ikeda, Bone morphogenetic protein (BMP)-2 induces apoptosis in human myeloma cells, *Leuk. Lymphoma*. 43 (2002) 635-639.

35. C. Kawamura, M. Kizaki, K. Yamato, H. Uchida, Y. Fukuchi, Y. Hattori, T. Koseki, T. Nishihara, Y. Ikeda, Bone morphogenetic protein-2 induces apoptosis in human myeloma cells with modulation of STAT3, *Blood*. 96 (2000) 2005-2011.

36. O. Hjertner, H. Hjorth-Hansen, M. Borset, C. Seidel, A. Waage, A. Sundan, Bone morphogenetic protein-4 inhibits proliferation and induces apoptosis of multiple myeloma cells, *Blood*. 97 (2001) 516-522.

37. Baade Ro T, Utne Holt R, Brenne AT, Hjorth-Hansen H, Waage A, Hjertner O, Sundan A, Borset M.Bone morphogenetic protein-5, -6 and -7 inhibit growth and induce apoptosis in human myeloma cells. *Oncogene*. (2003) 1-9.

38. G.R. Mundy, Metastasis to bone: causes, consequences and therapeutic opportunities, *Nat. Rev. Cancer*. 2 (2002) 584-593.

39. O. Peyruchaud, C.M. Serre, R. NicAmhlaoibh, P. Fournier, P. Clezardin, Angiostatin inhibits bone metastasis formation in nude mice through a direct anti-osteoclastic activity, *J. Biol. Chem*. 278: 45826-45832.

40. T.A. Guise, J.J. Yin, S.D. Taylor, Y. Kumagai, M. Dallas, B.F. Boyce, T. Yoneda, G.R. Mundy, Evidence for a causal role of parathyroid hormone-related protein in the pathogenesis of human breast cancer-mediated osteolysis, *J. Clin. Invest*. 98 (1996) 1544-1549.

41. S.M. Kakonen, K.S. Selander, J.M. Chirgwin, J.J. Yin, S. Burns, W.A. Rankin, B.G. Grubbs, M. Dallas, Y. Cui, T.A. Guise, Transforming growth factor-beta stimulates parathyroid hormone-related protein and osteolytic metastases via

Smad and mitogen-activated protein kinase signaling pathways, *J. Biol. Chem.* 277 (2002) 24571-24578.

42. H. Iguchi, S. Tanaka, Y. Ozawa, T. Kashiwakuma, T. Kimura, T. Hiraga, H. Ozawa, A. Kono, An experimental model of bone metastasis by human lung cancer cells: the role of parathyroid hormone-related protein in bone metastasis, *Cancer Res.* 56 (1996) 4040-4043.

43. R.S. Muraoka, N. Dumont, C.A. Ritter, T.C. Dugger, D.M. Brantley, J. Chen, E. Easterly, L.R. Roebuck, S. Ryan, P.J. Gotwals, V. Koteliansky, C.L. Arteaga, Blockade of TGF-beta inhibits mammary tumor cell viability, migration, and metastases, *J. Clin. Invest.* 109 (2002) 1551-1559.

44. Y.A. Yang, O. Dukhanina, B. Tang, M. Mamura, J.J. Letterio, J. MacGregor, S.C. Patel, S. Khozin, Z.Y. Liu, J. Green, M.R. Anver, G. Merlino, L.M. Wakefield, Lifetime exposure to a soluble TGF-beta antagonist protects mice against metastasis without adverse side effects, *J. Clin. Invest.* 109 (2002) 1607-1615.

45. J.J. Yin, K. Selander, J.M. Chirgwin, M. Dallas, B.G. Grubbs, R. Wieser, J. Massague, G.R. Mundy, T.A. Guise, TGF-beta signaling blockade inhibits PTHrP secretion by breast cancer cells and bone metastases development, *J. Clin. Invest.* 103 (1999) 197-206.

46. S. Kitazawa, R. Kitazawa, RANK ligand is a prerequisite for cancer-associated osteolytic lesions, *J. Pathol.* 198 (2002) 228-236.

47. B.O. Oyajobi, D.M. Anderson, K. Traianedes, P.J. Williams, T. Yoneda, G.R. Mundy, Therapeutic efficacy of a soluble receptor activator of nuclear factor kappaB-IgG Fc fusion protein in suppressing bone resorption and hypercalcemia in a model of humoral hypercalcemia of malignancy, *Cancer Res.* 61 (2001) 2572-2578.

48. S. Morony, C. Capparelli, I. Sarosi, D.L. Lacey, C.R. Dunstan, P.J Kostenuik, Osteoprotegerin inhibits osteolysis and decreases skeletal tumor burden in syngeneic and nude mouse models of experimental bone metastasis, *Cancer Res.* 61 (2001) 4432-4436.

49. C. Capparelli, P.J. Kostenuik, S. Morony, C. Starnes, B. Weimann, G. Van, S. Scully, M. Qi, D.L. Lacey, C.R. Dunstan, Osteoprotegerin prevents and reverses hypercalcemia in a murine model of humoral hypercalcemia of malignancy, *Cancer Res.* 60 (2000) 783-787.

50. H. Uehara, S.J. Kim, T. Karashima, D.L. Shepherd, D. Fan, R. Tsan, J.J. Killion, C. Logothetis, P. Mathew, I.J. Fidler, Effects of blocking platelet-derived growth factor-receptor signaling in a mouse model of experimental prostate cancer bone metastases, *J. Natl. Cancer Inst.* 95 (2003) 458-470.

51. E.S. Kopetz, J.B. Nelson, M.A. Carducci, Endothelin-1 as a target for therapeutic intervention in prostate cancer, *Invest. New Drugs*. 20 (2002) 173-182.

52. T.A. Guise, J.J. Yin, K.S. Mohammad, Role of endothelin-1 in osteoblastic bone metastases, *Cancer*. 97 (2003) 779-784.

53. J.J. Yin, K.S. Mohammad, S.M. Kakonen, S. Harris, J.R. Wu-Wong, J.L. Wessale, R.J. Padley, I.R. Garrett, J.M. Chirgwin, T.A. Guise, A causal role for endothelin-1 in the pathogenesis of osteoblastic bone metastases, *Proc. Natl. Acad. Sci. U. S. A.* 100 (2003) 10954-10599.

54. P. Sweeney, T. Karashima, S.J. Kim, D. Kedar, B. Mian, S. Huang, C. Baker, Z. Fan, D.J. Hicklin, C.A. Pettaway, C.P. Dinney, Anti-vascular endothelial growth factor receptor 2 antibody reduces tumorigenicity and metastasis in orthotopic prostate cancer xenografts via induction of endothelial cell apoptosis and

reduction of endothelial cell matrix metalloproteinase type 9 production, *Clin. Cancer Res.* 8 (2002) 2714-2724.

55. J.S. Smolen, G. Steiner, Therapeutic strategies for rheumatoid arthritis, *Nat. Rev. Drug. Discov.* 2 (2003) 473-488.

56. Y.Y. Kong, U. Feige, I. Sarosi, B. Bolon, A. Tafuri, S. Morony, C. Capparelli, J. Li, R. Elliott, S. McCabe, T. Wong, G. Campagnuolo, E. Moran, E.R. Bogoch, G. Van, L.T. Nguyen, P.S. Ohashi, D.L. Lacey, E. Fish, W.J. Boyle, J.M. Penninger, Activated T cells regulate bone loss and joint destruction in adjuvant arthritis through osteoprotegerin ligand, *Nature*. 402 (1999) 304-309.

57. E. Romas, N.A. Sims, D.K. Hards, M. Lindsay, J.W. Quinn, P.F. Ryan, C.R. Dunstan, T.J. Martin, M.T. Gillespie, Osteoprotegerin reduces osteoclast numbers and prevents bone erosion in collagen-induced arthritis, *Am. J. Pathol.* 161 (2002) 1419-1427.

58. G. Campagnuolo, B. Bolon, U. Feige, Kinetics of bone protection by recombinant osteoprotegerin therapy in Lewis rats with adjuvant arthritis, *Arthritis Rheum.* 46 (2002) 1926-1936.

59. B. Bolon, G. Campagnuolo, U. Feige, Duration of bone protection by a single osteoprotegerin injection in rats with adjuvant-induced arthritis, *Cell. Mol. Life Sci.* 59 (2002) 1569-1576.

60. G. Schett, K. Redlich, S. Hayer, J. Zwerina, B. Bolon, C. Dunstan, B. Gortz, A. Schulz, H. Bergmeister, G. Kollias, G. Steiner, J.S. Smolen, Osteoprotegerin protects against generalized bone loss in tumor necrosis factor-transgenic mice, *Arthritis Rheum.* 48 (2003) 2042-2051.

61. N. Manabe, H. Oda, K. Nakamura, Y. Kuga, S. Uchida, H. Kawaguchi, Involvement of fibroblast growth factor-2 in joint destruction of rheumatoid arthritis patients, *Rheumatology*. 38 (1999) 714-720.

62. Yamashita, Y. Yonemitsu, S. Okano, K. Nakagawa, Y. Nakashima, T. Irisa, Y. Iwamoto, Y. Nagai, M. Hasegawa, K. Sueishi, Fibroblast growth factor-2 determines severity of joint disease in adjuvant-induced arthritis in rats, *J. Immunol*. 168 (2002) 450-457.

63. H. Sone, Y. Kawakami, M. Sakauchi, Y. Nakamura, A. Takahashi, H. Shimano, Y. Okuda, T. Segawa, H. Suzuki, N. Yamada, Neutralization of vascular endothelial growth factor prevents collagen-induced arthritis and ameliorates established disease in mice, *Biochem. Biophys. Res. Commun*. 281 (2001) 562-568.

64. J. Miotla, R. Maciewicz, J. Kendrew, M. Feldmann, E. Paleolog., Treatment with soluble VEGF receptor reduces disease severity in murine collagen-induced arthritis, *Lab. Invest*. 80 (2000) 1195-1205.

65. D.M. Gerlag, E. Borges, P.P. Tak, H.M. Ellerby, D.E. Bredesen, R. Pasqualini, E. Ruoslahti, G.S. Firestein, Suppression of murine collagen-induced arthritis by targeted apoptosis of synovial neovasculature, *Arthritis Res*. 3 (2001) 357-361.

66. T.R. Mikuls, A.L. Weaver, Lessons learned in the use of tumor necrosis factor-alpha inhibitors in the treatment of rheumatoid arthritis, *Curr. Rheumatol. Rep*. 5 (2003) 270-277.

67. M. Feldmann, R.N. Maini, TNF defined as a therapeutic target for rheumatoid arthritis and other autoimmune diseases, *Nat. Med*. 9 (2003) 1245-1250.

68. L.H. Calabrese, Molecular differences in anticytokine therapies, *Clin. Exp. Rheumatol.* 21(2003) 241-248.

69. S.A. Paget, Efficacy of anakinra in bone: comparison to other biologics, *Adv. Ther.* 19 (2002) 27-39.

70. A.J. Schuerwegh, J.F. Van Offel, W.J. Stevens, C.H. Bridts, L.S. De Clerck, Influence of therapy with chimeric monoclonal tumour necrosis factor-alpha antibodies on intracellular cytokine profiles of T lymphocytes and monocytes in rheumatoid arthritis patients, *Rheumatology.* 42 (2003) 541-548.

71. D.M. Butler, A.M. Malfait, R.N. Maini, F.M. Brennan, M. Feldmann, Anti-IL-12 and anti-TNF antibodies synergistically suppress the progression of murine collagen-induced arthritis, *Eur. J. Immunol.* 29 (1999) 2205-2212.

72. U. Feige, Y.L. Hu, J. Gasser, G. Campagnuolo, L. Munyakazi, B. Bolon. Anti-interleukin-1 and anti-tumor necrosis factor-alpha synergistically inhibit adjuvant arthritis in Lewis rats. *Cell. Mol. Life Sci.* 57 (2000) 1457-1470.

73. L.A. Joosten, M.M. Helsen, T. Saxne, F.A. van De Loo, D. Heinegard, W.B. van Den Berg, IL-1 alpha beta blockade prevents cartilage and bone destruction in murine type II collagen-induced arthritis, whereas TNF-alpha blockade only ameliorates joint inflammation, *J. Immunol.* 163 (1999) 5049-5055.

74. W.B. van den Berg, L.A. Joosten, M. Helsen, F.A. van de Loo, Amelioration of established murine collagen-induced arthritis with anti-IL-1 treatment, *Clin. Exp. Immunol.* 95 (1994) 237-243.

75. S.B. Abramson, A. Amin, Blocking the effects of IL-1 in rheumatoid arthritis protects bone and cartilage, *Rheumatology.* 41 (2002) 972-980.

76. L.A. Joosten, E. Lubberts, M.M. Helsen, T. Saxne, C.J. Coenen-de Roo, D. Heinegard, W.B. van den Berg, Protection against cartilage and bone destruction by systemic interleukin-4 treatment in established murine type II collagen-induced arthritis, *Arthritis Res.* 1 (1999) 81-91.

77. L.K. Myers, B. Tang, J.M. Stuart, A.H. Kang, The role of IL-4 in regulation of murine collagen-induced arthritis, *Clin. Immunol.* 102 (2002) 185-191.

78. L.A. Joosten, E. Lubberts, P. Durez, M.M. Helsen, M.J. Jacobs, M. Goldman, W.B. van den Berg, Role of interleukin-4 and interleukin-10 in murine collagen-induced arthritis. Protective effect of interleukin-4 and interleukin-10 treatment on cartilage destruction, *Arthritis Rheum.* 40 (1997) 249-260.

79. N. Nishimoto, K. Yoshizaki, K. Maeda, T. Kuritani, H. Deguchi, B. Sato, N. Imai, M. Suemura, T. Kakehi, N. Takagi, T. Kishimoto, Toxicity, pharmacokinetics, and dose-finding study of repetitive treatment with the humanized anti-interleukin 6 receptor antibody MRA in rheumatoid arthritis. Phase I/II clinical study, *J. Rheumatol.* 30 (2003) 1426-1435.

80. E.H. Choy, D.A. Isenberg, T. Garrood, S. Farrow, Y. Ioannou, H. Bird, N. Cheung, B. Williams, B. Hazleman, R. Price, K. Yoshizaki, N. Nishimoto, T. Kishimoto, G.S. Panayi, Therapeutic benefit of blocking interleukin-6 activity with an anti-interleukin-6 receptor monoclonal antibody in rheumatoid arthritis: a randomized, double-blind, placebo-controlled, dose-escalation trial, *Arthritis Rheum.* 46: (2002) 3143-3150.

81. E. Choy, Interleukin 6 receptor as a target for the treatment of rheumatoid arthritis, *Ann. Rheum. Dis.* 62 (2003) II68-II69.

82. M.A. Nowell, P.J. Richards, S. Horiuchi, N. Yamamoto, S. Rose-John, N. Topley, A.S. Williams, S.A. Jones, Soluble IL-6 receptor governs IL-6 activity in

experimental arthritis: blockade of arthritis severity by soluble glycoprotein 130, *J. Immunol.* 171 (2003) 3202-3209.

83. M. Walmsley, P.D. Katsikis, E. Abney, S. Parry, R.O. Williams, R.N. Maini, M. Feldmann, Interleukin-10 inhibition of the progression of established collagen-induced arthritis, *Arthritis Rheum.* 39 (1996) 495-503.

84. M. Walmsley, D.M. Butler, L. Marinova-Mutafchieva, M. Feldmann, An anti-inflammatory role for interleukin-11 in established murine collagen-induced arthritis, *Immunol.* 95 (1998) 31-37.

85. A.M. Malfait, D.M. Butler, D.H. Presky, R.N. Maini, F.M. Brennan, M. Feldmann, Blockade of IL-12 during the induction of collagen-induced arthritis (CIA) markedly attenuates the severity of the arthritis, *Clin. Exp. Immunol.* 111 (1998) 377-383.

86. M. Chabaud, E. Lubberts, L. Joosten, W. van Den Berg, P. Miossec, IL-17 derived from juxta-articular bone and synovium contributes to joint degradation in rheumatoid arthritis, *Arthritis Res.* 3 (2001) 168-177.

87. E. Lubberts, L. van den Bersselaar, B. Oppers-Walgreen, P. Schwarzenberger, C.J. Coenen-de Roo, J.K. Kolls, L.A. Joosten, W.B. van den Berg, IL-17 promotes bone erosion in murine collagen-induced arthritis through loss of the receptor activator of NF-kappa B ligand/osteoprotegerin balance, *J. Immunol.* 170 (2003) 2655-2662.

88. S. Holmes, J.A. Abrahamson, N. Al-Mahdi, S.S. Abdel-Meguid, Y.S. Ho, Characterization of the in vitro and in vivo activity of monoclonal antibodies to human IL-18, *Hybrid.* 19 (2000) 363-337.

89. C. Plater-Zyberk, L.A. Joosten, M.M. Helsen, P. Sattonnet-Roche, C. Siegfried, S. Alouani, F.A. van De Loo, P. Graber, S. Aloni, R. Cirillo, E. Lubberts, C.A. Dinarello, W.B. van Den Berg, Y. Chvatchko, Therapeutic effect of neutralizing endogenous IL-18 activity in the collagen-induced model of arthritis, *J. Clin. Invest.* 108 (2001) 1825-1832.

90. L.A. Joosten, F.A. van De Loo, E. Lubberts, M.M. Helsen, M.G. Netea, J.W. van Der Meer, C.A. Dinarello, W.B. van Den Berg, An IFN-gamma-independent proinflammatory role of IL-18 in murine streptococcal cell wall arthritis, *J. Immunol.* 165 (2000) 6553-6558.

91. J. Ishikaw, Y. Okada, I.N. Bird, B. Jasani, J.H. Spragg, T. Yamada, Use of anti-platelet-endothelial cell adhesion molecule-1 antibody in the control of disease progression in established collagen-induced arthritis in DBA/1J mice, *Jpn. J. Pharmacol.* 88 (2002) 332-340.

92. A.F. Kavanaugh, L.S. Davis, R.I. Jain, L.A. Nichols, S.H. Norris, P.E. Lipsky, A phase I/II open label study of the safety and efficacy of an anti-ICAM-1 (intercellular adhesion molecule-1; CD54) monoclonal antibody in early rheumatoid arthritis, *J. Rheumatol.* 23 (1996) 1338-1344.

93. J. Vuorte, P.J. Lindsberg, M. Kaste, S. Meri, S.E. Jansson, R. Rothlein, H. Repo, Anti-ICAM-1 monoclonal antibody R6.5 (Enlimomab) promotes activation of neutrophils in whole blood, *J. Immunol.* 162 (1999) 2353-2357.

94. A.F. Kavanaugh, L.S. Davis, L.A. Nichols, S.H. Norris, R. Rothlein, L.A. Scharschmidt, P.E. Lipsky, Treatment of refractory rheumatoid arthritis with a monoclonal antibody to intercellular adhesion molecule 1, *Arth. Rheum.* 37 (1994) 992-999.

95. D. Kurosaka, K. Yoshida, J. Yasuda, T. Yokoyama, I. Kingetsu, N. Yamaguchi, K. Joh, M. Matsushima, S. Saito, A. Yamada, Inhibition of arthritis by systemic administration of endostatin in passive murine collagen induced arthritis, *Ann. Rheum. Dis.* 62 (2003) 677-679.

96. H. Matsuno, K. Yudoh, M. Uzuki, F. Nakazawa, T. Sawai, N. Yamaguchi, B.R. Olsen, T. Kimura, Treatment with the angiogenesis inhibitor endostatin: a novel therapy in rheumatoid arthritis, *J. Rheumatol.* 29 (2002) 890-895.

APPENDIX B

Modulating Threshold on Architectural Parameter Quantification of Trabecular Bone.

To assess the effects of modulating threshold on the analysis of the trabecular bone from distal femoral metaphysis, a sample from the sham-operated group as well as one from the OVX-treated groups were randomly selected. Bone volume (BV; mm^3), bone surface area (BS; mm^2), bone surface area / bone volume (BS/BV; mm^{-1}), degree of anisotropy (DA), structure model index (SMI) were assessed as above.

A. Effect of Threshold on Osteopenic Bone

The osteopenic bone sample was reconstructed using numerous threshold values ranging from 190, the point were the samples are barely visible, up to 237. **Figure B-1** illustrates the effects of increasing the threshold on various architectural parameters from a sample of trabecular bone from an ovariectomized rat. The filled data points represent 3D reconstructions of the osteopenic bone sample that do not include any outlying cortical bone. The hollow points represent the reconstructions where cortical bone surrounding the trabcular bone began to manifest itself (at a threshold of 221). This was an artifact generated from the process of segmenting the cortical bone from the trabecular bone (to be reconstructed and analyzed).

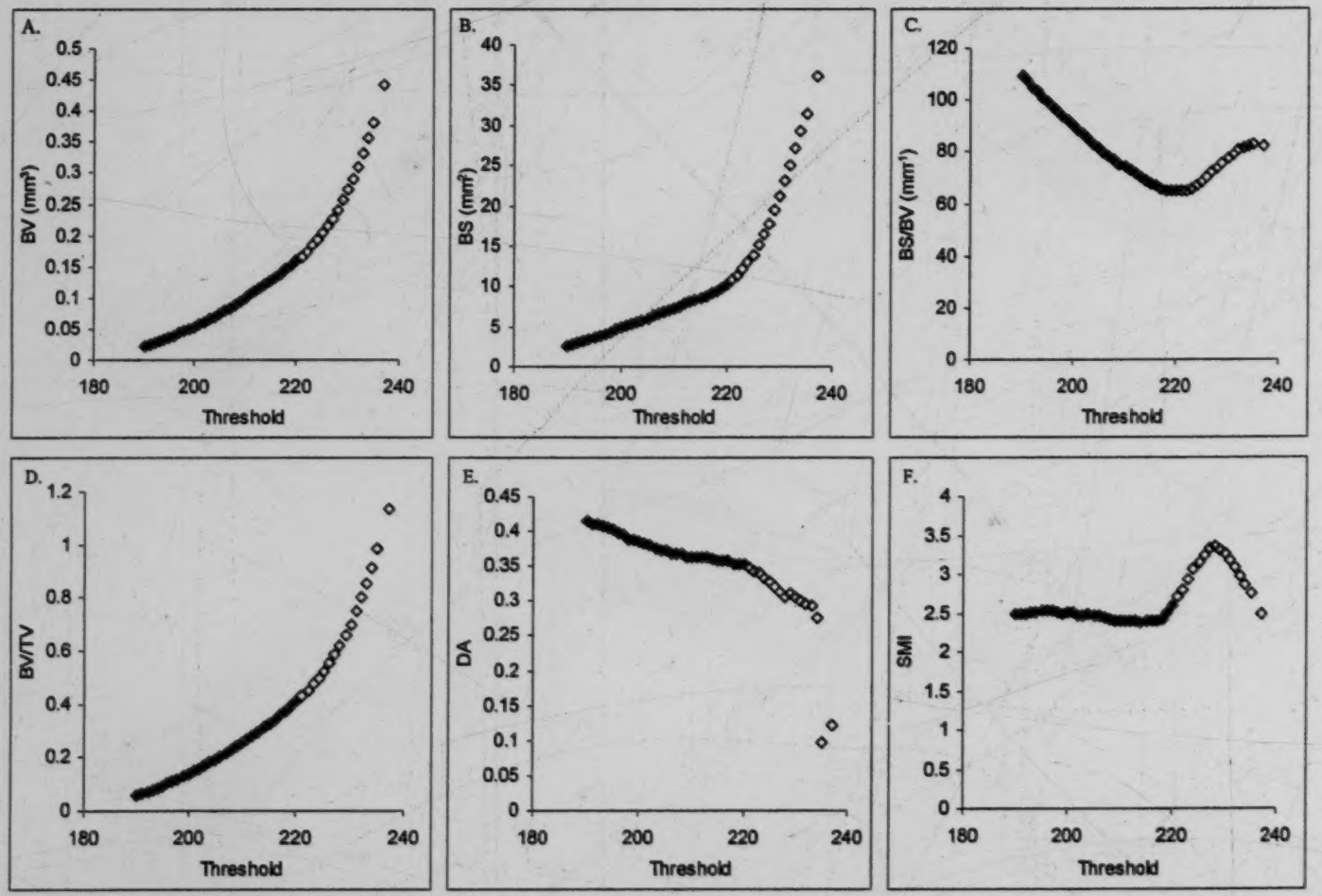

Figure B-1: The effects of increasing the threshold on BV (A), BS (B), BS/BV (C), BV/TV (D), DA (E), and SMI (F) on a bone sample from an ovariectomized rat

Initially, BV, BS, and BV/TV in the osteopenic sample appear to rise in a quasi-linear fashion whereas BS/BV and DA decrease in a similar fashion. These particular trends remain valid until the cortical bone surrounding the medullar volume of interest begins to manifest itself in the 3D-reconstructions generated at higher threshold values. The anomalous presence of cortical bone was expected to skew the morphometric analysis of the trabecular bone.

B. Effect of Threshold on Normal Bone

The threshold values used for the analysis of the sham-operated (normal) sample ranged from 190 to 228. **Figure B-2** illustrates the effects of increasing the threshold on various architectural parameters from a sample of trabecular bone from a sham-operated rat.

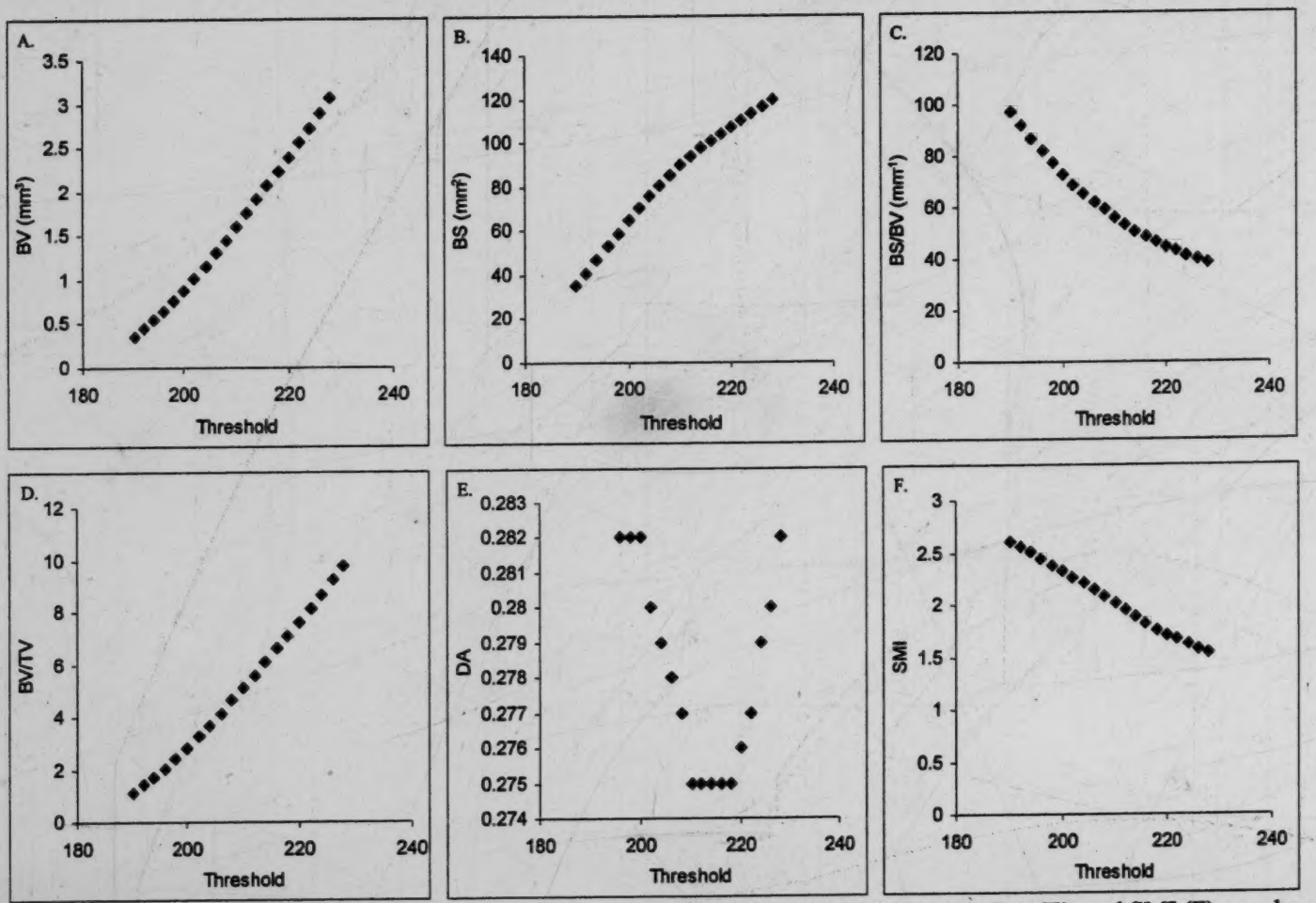

Figure B-2: The effects of increasing the threshold on BV (A), BS (B), BS/BV (C), BV/TV (D), DA (E), and SMI (F) on a bone sample from a sham-operated rat

With the sole exception of DA, which appears to be marginally, yet unpredictably, influenced by threshold, the observed trends initially seen in the osteopenic sample extend themselves for the sample from the sham-operated rat. (Unlike the osteopenic sample, it should be noted that no cortical bone was inadvertently captured during the segmentation of trabecular bone from this bone sample.)

C. Comparing the Effect of Threshold on Normal and Osteopenic Bone

To compare the effects of modulating threshold on the various morphometric parameters of the osteopenic and normal bone samples, the threshold values used were limited to ensure that the relationship was linear. **Figure B-3** illustrates these effects on the osteopenic and sham-operated bone samples.

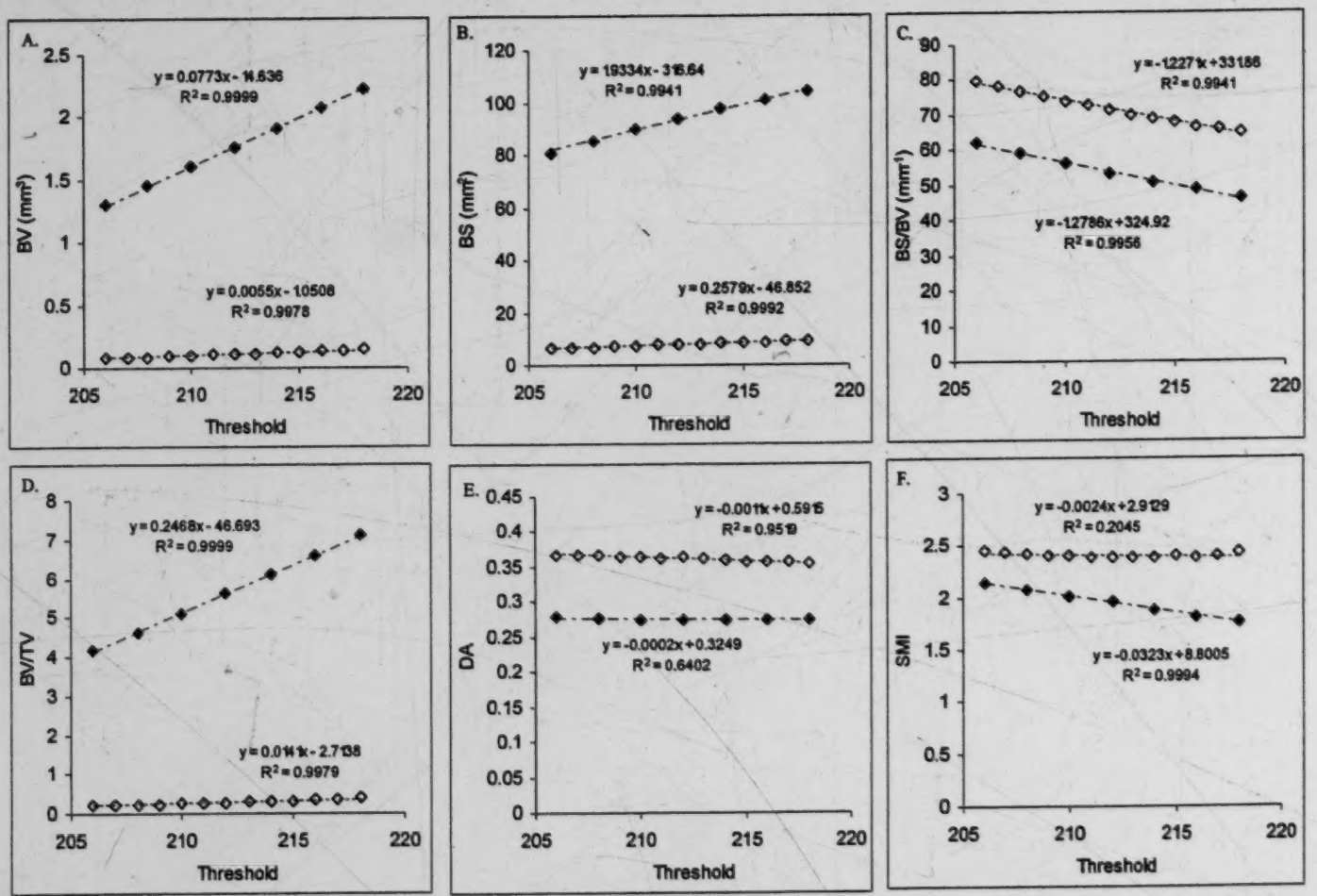

Figure B-3: Comparing the effects of modulating threshold on BV (A), BS (B), BS/BV (C), BV/TV (D), DA (E), and SMI (F) on bone samples from a sham-operated rat (filled points) and an ovariectomized rat (hollow points).

A *t*-test for parallelism was used as a means to evaluate whether any statistically significant differences existed in the way in which threshold affected the normal and osteopenic bone samples. Apart from BS/BV and DA, there appears to be a significant discrepancy ($p < 0.01$) between the manner in which threshold affects the 3D parameters between the normal and osteopenic bone samples. These data suggest that the effects mediated by increasing threshold are not uniform and that normal (non-osteopenic) samples are more sensitive to changes in threshold than osteopenic samples.

D. Analysis of the Data Using a Threshold of 214 and Subsequent Comparison to Results Generated Using a Threshold of 211

To elucidate the effects of modulating threshold on the quantification of trabecular architectural parameters, the μCT data from the "VEGF vs. bFGF" study was re-analyzed using a threshold of 214 (instead of 211 that was initially used). The parameters compared included: Tb.Th; BV; BS; BS/BV; BV/TV; DA; and SMI. All of the inter-group relationships identified using a threshold of 211 (**Table 7-2**) were found using a threshold of 214 (**data not shown**). The Tb.Th for the sham-operated and the VEGF-SC group, however, was not significant at a threshold of 214. Based on these results, it was concluded that choice of threshold to be applied universally when determining the various μCT architectural parameters had a nominal impact on the outcome of the data generated (providing that the chosen threshold was relatively reasonable).